



**A GEOCHEMICAL INVESTIGATION OF THE WATER AND SEDIMENTS  
OF  
BARBER'S PAN  
NORTH WEST PROVINCE**

**OLIVER KNESL**

B.Sc. (Wits)

B.Sc. (Hons) (Wildlife Management) (Pret.)

Submitted in partial fulfilment of the requirements of the degree of

**MASTER OF SCIENCE**

in the

Department of Geological Sciences

Faculty of Science

University of Cape Town

January 1996

The copyright of this thesis vests in the author. No quotation from it or information derived from it is to be published without full acknowledgement of the source. The thesis is to be used for private study or non-commercial research purposes only.

Published by the University of Cape Town (UCT) in terms of the non-exclusive license granted to UCT by the author.

## ACKNOWLEDGEMENTS

I would like to sincerely thank and acknowledge the help and support of the following people and organisations:

Associate Professor James Willis and Dr. Martin Fey my two supervisors. Thank you for the enormous time and effort expended on your part in turning what was a rookie ecologist into a fledgling environmental geochemist. The countless hours spent in both your offices discussing the intricacies of geochemistry in general, as well as the application of geochemical principles to the unravelling of the complex chemistry of pan environments, will be fondly remembered and sorely missed. Thank you both.

Associate Professor James Willis for taking the photographs used in this thesis.

Dr. Jenny Day, Department of Zoology, University of Cape Town, for providing me with substantial amounts of literature on saline systems in general and for introducing me to and providing me with a copy of "Wetzels' book". Your help and advice was also much appreciated.

Miss Heather Dodds, for diving out the core samples from Barber's Pan and for help and advice with laboratory work.

Dr. John Rogers, Department of Geological Sciences, University of Cape Town, for advice on the particle-size analyses and general aspects of lacustrine sedimentation.

Mr. Peter Holmes, Department of Environmental and Geographical Sciences, University of Cape Town, for useful discussions on pan geomorphology.

Mr. Patrick Sias for invaluable assistance with the HPIC analyses and Mr. Ernest Stout for introducing me the fine art of briquette making.

Mr. Peter Meyer for help with the particle-size analyses.

Mrs. Shereen Govender and Mr. Andreas Späth for help with the making of fusion discs and in carrying out the XRFS analyses, and Mr. Bruce Cairns for cutting the cores.

Mrs. Antoinette Upton for help in the laboratory and Mrs. Barbara Joron for help with digitizing.

Mr. Jan Schutte, Geohydrological Division, Department of Water Affairs and Forestry (DWAF), for making available the Barber's Pan data from the DWAF database.

Mr. Gustav Englebrecht, Warden, Barber's Pan Nature Reserve for his kindness and willingness to help during the sampling phase of the project. Baie dankie Gustav !!

The Computing Centre for Water Research (CCWR) at the University of Natal, Pietermaritzburg, for access to MINTEQA2 software.

The Department of Sea Fisheries for the loan of the Grant YSI 2000 probe.

EMATEK Division of the C.S.I.R., Stellenbosch, for the loan of the Van Veen Grab.

North West Province Environmental Conservation for the loan of a Geographical Positioning System (GPS) and for giving me time off to complete my M.Sc.

The Department of Mining Engineering, University of the Witwatersrand, for granting me access to their computer facilities.

Messrs. Lewis "Luigi" McCaffrey and Tom Nowiki for general help and advice.

My classmates; Nico Bez., Philippa Huntsman, Ollie Paul, Frank Schwegler, Trevor Harroway, Pierre Rousseau and Tom Demmer for giving our room character and helping to make 1995 a memorable (or perhaps notorious) year.

The other staff and postgraduate students at the Department of Geological Sciences, University of Cape Town.

James Willis (Jnr) for introducing me to Action Cricket.

Mom and Dad for their usual unflagging support.

Bronwyn, for always being there when I need her most.

## TABLE OF CONTENTS

ACKNOWLEDGEMENTS	i
LIST OF FIGURES	vi
LIST OF TABLES	x
GLOSSARY	xi
SUMMARY	xii
1. INTRODUCTION	1
1.1 Objectives of the study	3
1.2 The study area	4
1.2.1 Physiography	4
1.2.2 Geology and soils	5
1.2.3 Climate	5
1.2.4 Vegetation	8
2. GEOMORPHOLOGICAL AND GEOCHEMICAL CHARACTERISTICS OF PANS AND ATHALASSIC SALINE LAKES – WITH SPECIAL REFERENCE TO SOUTH AFRICA	9
2.1 Introduction	9
2.2 Geomorphological studies on pans	9
2.2.1 General characteristics of pans	9
2.2.2 Models of pan development	10
2.3 Sediments and sedimentary processes in pans and saline lakes	14
2.3.1 Saline lake deposits	14
2.3.1.1 Depositional processes and characteristics of pan sediments	16
2.3.1.2 South African pan sediments	24
2.3.1.3 Saline lake sediments	25
2.4 Water chemistry of athalassic saline waters	29
2.4.1 Water composition of saline lakes	29
2.4.2 Water chemistry of southern African inland saline lakes	32
2.4.3 The evolution of saline lake waters	33
2.4.4 Mineral solubility equilibria	40
2.5 Nutrient status of athalassic saline lakes	43
2.5.1 Essential elements	43
2.5.2 Nutrient dynamics	45
2.5.3 Phosphorus	45
2.5.4 Nitrogen	47
2.5.5 Other nutrients	47
2.6 Conclusions	48
3. THE AQUEOUS CHEMISTRY OF BARBER'S PAN	50
3.1 Introduction	50
3.2 Water sampling and analysis	51
3.2.1 Sample collection	51
3.2.2 Water analyses	51
3.2.2.1 On-site determinations	51
3.2.2.2 Laboratory analyses	52
3.2.2.2.1 Electrical conductivity (EC) and pH	52
3.2.2.2.2 Alkalinity	53
3.2.2.2.3 Anions	53

3.2.2.2.4	Phosphate	54
3.2.2.2.5	Total elemental concentrations	54
3.2.2.2.6	Silicon	54
3.2.2.2.7	Prediction of chemical speciation and saturation indices (S.I.)	55
3.2.3	Department of Water Affairs and Forestry (DWAF) database	56
3.3	Results and discussion of water analyses	56
3.3.1	On-site determinations	56
3.3.2	Laboratory analyses	57
3.3.2.1	Electrical conductivity (EC)	57
3.3.2.2	pH	62
3.3.2.3	Alkalinity	63
3.3.2.4	Ion dominance in Barber's Pan	64
3.3.2.5	Chemical speciation modelling	67
3.3.2.5.1	Charge balance	68
3.3.2.5.2	Calcium	68
3.3.2.5.3	Magnesium	71
3.3.2.5.4	Sodium, potassium and chloride	71
3.3.2.5.5	Iron	72
3.3.2.5.6	Manganese	73
3.3.2.5.7	Carbonate/bicarbonate	73
3.3.2.5.8	Sulphate	73
3.3.2.5.9	Phosphorus	74
3.3.2.5.10	Silicon	75
3.3.2.5.11	Lead	76
3.3.2.5.12	Zinc, copper and nickel	77
3.3.2.5.13	Aluminium	78
3.3.2.5.14	Fluorine	78
3.3.2.6	Mineral solubility equilibria	78
3.3.3	The evaporative concentration of Barber's Pan	86
3.3.4	Solute behaviour during the evaporative concentration of Barber's Pan	91
3.3.5	The nutrient and pollutant status of Barber's Pan	100
3.3.5.1	Nutrients in Barber's Pan	100
3.3.5.1.1	Cations	100
3.3.5.1.2	Anions	101
3.3.5.1.3	Nitrogen	102
3.3.5.1.4	Phosphorus	103
3.3.5.1.5	Iron and manganese	106
3.3.5.1.6	Other micronutrients	107
3.3.5.1.7	Sulphur	107
3.3.5.1.8	Silicon	108
3.3.5.2	Pollutants in Barber's Pan	108
3.3.5.2.1	TDS, EC and pH	109
3.3.5.2.2	Lead	112
3.3.5.2.3	Nickel	113
3.3.5.2.4	Aluminium	114
3.3.5.2.5	Iron	114
3.3.5.2.6	Chloride	114
3.3.5.2.7	Potassium	115
3.3.5.2.8	Phosphorus	115

3.3.5.2.9	General discussion with regard to the status of pollutants in the pan . . . . .	115
3.4	Conclusions . . . . .	116
4.	THE GEOCHEMISTRY OF BARBER'S PAN SEDIMENTS . . . . .	119
4.1	Introduction . . . . .	119
4.2	Sediment sampling and analysis . . . . .	120
4.2.1	Sampling . . . . .	120
4.2.1.1	Barber's Pan . . . . .	121
4.2.1.2	Leeupan . . . . .	124
4.2.1.3	Harts River inlet . . . . .	124
4.3	Sediment analyses . . . . .	124
4.3.1	Organic carbon . . . . .	124
4.3.2	Carbonate . . . . .	124
4.3.3	Clay mineralogy . . . . .	125
4.3.4	Extractable phosphate . . . . .	125
4.3.5	X-ray fluorescence spectrometry (XRFS) . . . . .	126
4.3.6	Particle-size distribution: pipette method . . . . .	127
4.4	Results and discussion of sediment analyses . . . . .	127
4.4.1	Particle-size analysis . . . . .	127
4.4.2	Clay mineralogy . . . . .	129
4.4.2.1	Untreated samples . . . . .	129
4.4.2.1.1	Harts River sediment . . . . .	130
4.4.2.1.2	Barber's Pan sediments . . . . .	130
4.4.2.1.3	Leeupan sediment . . . . .	132
4.4.2.2	Treated samples . . . . .	134
4.4.2.2.1	Mg-saturation and glyceration . . . . .	135
4.4.2.2.2	K-saturation and heat treatment . . . . .	138
4.4.2.3	General discussion of Barber's Pan clay mineralogy . . . . .	139
4.4.3	Chemical composition of the sediments . . . . .	142
4.4.4	Chemistry of the core sample . . . . .	150
4.4.5	Sedimentation rates in Barber's Pan . . . . .	156
4.4.6	Phosphate-sediment interactions . . . . .	157
4.5	Conclusions . . . . .	161
5.	CONCLUSIONS AND RECOMMENDATIONS . . . . .	163
6.	REFERENCES . . . . .	168
7.	APPENDICES . . . . .	183
7.1	APPENDIX 1: On-site water analyses . . . . .	183
7.2	APPENDIX 2: Calculation of concentration factor for Barber's Pan . . . . .	184
7.3	APPENDIX 3: Department of Water Affairs and Forestry database ( $\text{NO}_3^-$ + $\text{NO}_2^-$ as N and $\text{PO}_4^{3-}$ as P. All values in Mg/L unless stated otherwise). . . . .	185
7.4	APPENDIX 4: An example of a MINTEQA2 print out . . . . .	192
7.5	APPENDIX 5: Total elemental concentrations for the sediment samples determined by x-ray fluorescence spectrometry . . . . .	200
7.6	APPENDIX 6: Results of organic carbon and carbonate determinations in the sediment samples . . . . .	205

7.7 APPENDIX 7:	Correlation matrix for XRFS grab sample data. Only significant correlations are tabulated (figures in bold: $P < 0.0001$ ; underlined: $P < 0.001$ ; normal font: $P < .01$ . In all cases $n = 13$ ). . . . .	206
7.8 APPENDIX 8:	Instrumental parameters and data quality for routine major and trace element determinations by WDXRFS. . . . .	207

## LIST OF FIGURES

<b>Figure 1:</b>	The approximate location of Barber's Pan within the Republic of South Africa . . . . .	2
<b>Figure 2:</b>	Schematic map of Barber's Pan and surrounds . . . . .	2
<b>Figure 3:</b>	Views of Barber's Pan showing its situation in an area lacking marked physiographic features . . . . .	6
<b>Figure 4:</b>	The Harts River inlet . . . . .	7
<b>Figure 5:</b>	Leeupan, an active, deflationary pan neighbouring Barber's Pan . . . . .	7
<b>Figure 6:</b>	A model of pan development (From Goudie and Wells, 1995) . . . . .	11
<b>Figure 7:</b>	Idealized diagram of depositional subenvironments which can occur in arid zone playa (pan) basins (after Hardie <i>et al.</i> , 1978; from Thomas and Shaw, 1989) . . . . .	19
<b>Figure 8:</b>	A model of the saline pan cycle (from Lowenstein and Hardie, 1985) . . . . .	21
<b>Figure 9:</b>	Map showing the concentric arrangement of evaporative salts in the Saline Valley Playa, California (After Hardie <i>et al.</i> , 1978) . . . . .	24
<b>Figure 10:</b>	The calculated evolution of typical Sierra Nevada spring water at constant temperature in equilibrium with the atmosphere (After Garrels and Mackenzie, 1967; from Hammer, 1986) . . . . .	34
<b>Figure 11:</b>	Flow diagram for the geochemical evolution of closed lake basin brines (After Eugster and Hardie, 1978; from Hammer, 1986) . . . . .	36
<b>Figure 12:</b>	Schematic plots of individual solute content versus the degree of overall solution concentrations, illustrating the characteristic effect of specific mechanisms on changes in chemical composition (from Eugster and Jones, 1979) . . . . .	38
<b>Figure 13:</b>	Schematic representation of mechanisms that control aqueous concentration of elements (from Rai and Kittrick, 1989) . . . . .	41
<b>Figure 14:</b>	A map of the study area showing sites where bulk pan water samples and Grant/YSI 3800 probe readings were taken . . . . .	52
<b>Figure 15:</b>	The Grant/YSI 3800 Water Quality Logging System used for on-site determinations of EC, pH, temperature, and salinity . . . . .	53
<b>Figure 16:</b>	The solubility of amorphous silica and aluminium hydroxide as a function of pH at 25 °C (from Mason and Moore, 1982) . . . . .	63

<b>Figure 17:</b>	Piper trilinear diagram showing hydrochemical facies (from Ward, 1975) . . . . .	66
<b>Figure 18:</b>	A Piper diagram representation the average bulk water composition of Barber's Pan . . . . .	67
<b>Figure 19:</b>	Stability – diagram for palygorskite – smectite system in Barber's Pan, using the stability boundaries of Elprince <i>et al.</i> , 1979) . . . . .	82
<b>Figure 20:</b>	A solubility diagram for hydroxyapatite and fluorapatite – fluorite (after Lindsay, 1979) . . . . .	84
<b>Figure 21:</b>	The ratio of $Cl^{-}:(Cl^{-} + SO_4^{2-})$ plotted against TDS for Barber's pan . . . . .	89
<b>Figure 22:</b>	A plot of the concentration of Na against Cl for Barber's Pan water over the period 1982 – 1988 . . . . .	92
<b>Figure 23:</b>	A plot of the Na/Cl ratio against Cl concentration for Barber's Pan water over the period 1982 – 1988 . . . . .	93
<b>Figure 24:</b>	A plot of bicarbonate alkalinity against Cl concentration for Barber's Pan water over the period 1982 – 1988 . . . . .	93
<b>Figure 25:</b>	A plot of Ca against Cl concentration for Barber's Pan water over the period 1982 – 1988 . . . . .	94
<b>Figure 26:</b>	A plot of Mg against Cl concentration for Barber's Pan water over the period 1982 – 1988 . . . . .	95
<b>Figure 27:</b>	A plot of K against Cl concentration for Barber's Pan water over the period 1982 – 1988 . . . . .	96
<b>Figure 28:</b>	A plot of $SO_4$ against Cl concentration for Barber's Pan water over the period 1982 – 1988 . . . . .	97
<b>Figure 29:</b>	A plot of F against Cl concentration for Barber's Pan water over the period 1982 – 1988 . . . . .	98
<b>Figure 30:</b>	A plot of Si against Cl concentration for Barber's Pan water over the period 1982 – 1988 . . . . .	99
<b>Figure 31:</b>	Change in TDS over time in Barber's Pan . . . . .	111
<b>Figure 32:</b>	A map of the study area showing sites where pan grab and core samples were taken . . . . .	121
<b>Figure 33:</b>	The Van Veen Grab used for sediment sample collection in Barber's Pan. The grab ready to be lowered to the sediment and being emptied after sample collection . . . . .	122

<b>Figure 34:</b>	The diver preparing to take a core sample from Barber's Pan using a 0.50m PVC hand-corer . . . . .	123
<b>Figure 35:</b>	A grab sample being taken from Leeupan using a shovel. A lunette associated with Leeupan can be seen in the background . . . . .	123
<b>Figure 36:</b>	X-ray diffractogram of Na-saturated clay fractions extracted from Barber's Pan sediment sample no. 4, Leeupan upper and lower sediment samples and the Harts River sediment sample. Peak locations are shown for calcite (Ca), dolomite (Do), kaolinite (Kt), the mica group minerals (Mi) and quartz (Qz) . . . . .	130
<b>Figure 37:</b>	X-ray diffractogram of Na-saturated clay fractions extracted from Barber's Pan sediment samples no. 7, 8, 9 and 10. Peak locations are shown for calcite (Ca), kaolinite (Kt), the mica group minerals (Mi) and quartz (Qz) . . . . .	131
<b>Figure 38:</b>	X-ray diffractogram of Na-saturated clay fractions extracted from Barber's Pan sediment samples no. 2, 5, 16 and 17. Peak locations are shown for calcite (Ca), kaolinite (Kt), the mica group minerals (Mi) and quartz (Qz) . . . . .	131
<b>Figure 39:</b>	Dolomite layer in Leeupan . . . . .	133
<b>Figure 40:</b>	X-ray diffractograms of Harts River sediment and Barber's Pan sediment sample no. 7 clay fraction pretreated by K-saturation and heating or by Mg-saturation and glycerol solvation. Peak locations are shown for kaolinite (Kt), the mica group minerals (Mi) and quartz (Qz) . . . . .	136
<b>Figure 41:</b>	X-ray diffractograms of Barber's Pan sediment sample nos. 8 and 16 clay fraction pretreated by K-saturation and heating or by Mg-saturation and glycerol solvation. Peak locations are shown for kaolinite (Kt), the mica group minerals (Mi) and quartz (Qz) . . . . .	137
<b>Figure 42:</b>	Amygdales at the edge of Barber's Pan . . . . .	141
<b>Figure 43:</b>	Plots of the relationships between K and Rb, Al <sub>2</sub> O <sub>3</sub> and Fe <sub>2</sub> O <sub>3</sub> , Al <sub>2</sub> O <sub>3</sub> and organic carbon and Al <sub>2</sub> O <sub>3</sub> and MnO in the Barber's Pan, Harts River and Leeupan sediments . . . . .	144
<b>Figure 44:</b>	Plots of the relationships between Al <sub>2</sub> O <sub>3</sub> and Cr, Al <sub>2</sub> O <sub>3</sub> and Ni, Al <sub>2</sub> O <sub>3</sub> and Cu and Al <sub>2</sub> O <sub>3</sub> and Zn in the Barber's Pan, Harts River and Leeupan sediments . . . . .	146
<b>Figure 45:</b>	Plot of the relationship between Ca and Sr in the Barber's Pan, Harts River and Leeupan sediments . . . . .	147
<b>Figure 46:</b>	Plots of the relationships between Fe <sub>2</sub> O <sub>3</sub> and V and Fe <sub>2</sub> O <sub>3</sub> and Ni in the Barber's Pan, Harts River and Leeupan sediments . . . . .	149

<b>Figure 47:</b>	A plot of the concentrations of Pb, Cu, Ni and Zn with increasing depth in the core sample from Barber's Pan . . . . .	151
<b>Figure 48:</b>	A plot of the concentrations of Cr, Zr, Rb and V with increasing depth in the core sample from Barber's Pan . . . . .	151
<b>Figure 49:</b>	A plot of the concentrations of CaO, MgO, Al <sub>2</sub> O <sub>3</sub> and Fe <sub>2</sub> O <sub>3</sub> with increasing depth in the core sample from Barber's Pan . . . . .	152
<b>Figure 50:</b>	Breakdown of clay flakes and the removal of finer material by deflation from the surface of Leeupan . . . . .	154
<b>Figure 51:</b>	A plot of the concentrations of Co, Zn, Cu, Ni and V against Al <sub>2</sub> O <sub>3</sub> showing their relationship in the core sample from Barber's Pan . . . . .	155
<b>Figure 52:</b>	A plot of the K against Rb showing their relationship in the core sample from Barber's Pan . . . . .	156

## LIST OF TABLES

<b>Table 1:</b>	Processes influencing sedimentation in saline lakes (from Hammer, 1986) . .	17
<b>Table 2:</b>	Previously recorded chemical subtypes (multiple anion dominance) of athalassic saline lake waters (adapted from Hammer, 1986) . . . . .	31
<b>Table 3:</b>	Analysis of Barber's Pan bulk pan water (duplicate water samples from the same sampling location are denoted x and y) . . . . .	58
<b>Table 4:</b>	Analysis of Barber's Pan sediment supernatant . . . . .	60
<b>Table 5:</b>	Analysis of Barber's Pan sediment interstitial water . . . . .	61
<b>Table 6:</b>	The average concentration of the major ionic constituents of Barber's Pan bulk pan water . . . . .	65
<b>Table 7:</b>	Chemical species predicted by MINTEQA2 as likely to be present in bulk pan water sample no. 5 . . . . .	69
<b>Table 8:</b>	Chemical species predicted by MINTEQA2 as likely to be present in interstitial pan water sample no. 5 . . . . .	70
<b>Table 9:</b>	Mg/Ca ratios for several water samples from Barber's Pan . . . . .	80
<b>Table 10:</b>	MINTEQA2 calculated saturation indices for selected minerals possibly occurring in Barber's Pan. Positive values indicate supersaturation; negative values indicate undersaturation . . . . .	83
<b>Table 11:</b>	Comparison of the Si concentrations ( $\text{mg}\cdot\text{dm}^{-3}$ ) determined by the colorimetric blue silicomolybdous acid procedure of Weaver <i>et al.</i> (1968) with those determined by ICP–AES . . . . .	87
<b>Table 12:</b>	A comparison of water quality variables determined for the bulk pan water in Barber's Pan with recommended maximum levels for a number of possible water uses . . . . .	110
<b>Table 13:</b>	Proportions of sand and mud determined in core sample 4, grab samples 4 and 7 and the Harts River sediment sample . . . . .	128
<b>Table 14:</b>	The $\text{CaO}/\text{CO}_2$ and $\text{MgO}/\text{CO}_2$ ratios for the sediments sampled . . . . .	143
<b>Table 15:</b>	Concentrations of extractable phosphorus in the Barber's Pan, Leeupan and Harts River sediment samples (extraction was by means of the AMBIC method of Van der Merwe <i>et al.</i> [1984]) . . . . .	158

## GLOSSARY

- Athalassic saline lakes – Lakes which have had no connection to the sea in geologically Recent times, or have been evaporated to dryness after having been flooded by marine waters and subsequently reflooded.
- Benthos – The assemblage of organisms associated with the solid-liquid interface in aquatic systems.
- Endorheic system – Closed systems lacking surface outflow.
- Epiphytic algae – Algae growing on macrophytic surfaces.
- Eutrophic lakes – Lakes with high nutrient concentrations and high organic production.
- Hypolimnetic – Associated with the hypolimnion.
- Hypolimnion – The deepest stratum of water in a stratified lake.
- Littoral zone – The interface between the land of a drainage basin and the open water of lakes.
- Macrophyte (aquatic) – Macroscopic forms of aquatic vegetation, encompassing macroalgae, mosses, ferns and true angiosperms.
- Meromictic lakes – Lakes that do not undergo complete circulation, the primary water mass not mixing with a lower portion.
- Mixolimnion – The upper stratum of water in a meromictic lake that periodically undergoes circulation.
- Monimolimnion – The deeper stratum of water (underlying the mixolimnion) in a meromictic lake that is perennially isolated.
- Pelagial zone – The free open water in a lake, separable from the bottom of the lake basin and the littoral zone.
- Plankton – The assemblage of plants and animals with limited or no powers of locomotion suspended in a water-body.

## SUMMARY

*Pans comprise a large proportion of southern African wetlands and yet remain poorly classified. Very little data is available on the aqueous chemistry of southern African saline systems, and with the exception of a few publications dealing, in part, with the soil and associated materials of pan floors and margins, soil and sediment information on pans is similarly limited.*

*Barber's Pan is a shallow, alkaline lake situated in the North West Province of South Africa. It is a unique system in several respects, but is considered most valuable from the aspect of bird conservation, since it is perennial in an area characterized by shallow, seasonally filled pans. Its perennial state is the consequence of anthropogenic intervention in the early part of this century which resulted in the diversion of the Harts River back along its fossil course. The biogeographical importance of Barber's Pan is emphasised by its designation as the only RAMSAR site in the North West Province.*

*The overall objective of this study was to provide a geochemical characterization of Barber's Pan. This was approached by reviewing pertinent literature on the origin and geochemical characteristics of pans and saline lakes through an investigation of the water and sediments of Barber's Pan. The study focused on four aspects of the pan geochemistry, namely: the levels of certain nutrients and potential pollutants in the pan; gaining an understanding of the dynamics of phosphorus, as well as other nutrients, in the pan; geochemically characterizing the sediments; and investigating the impact of evaporative concentration of the pan water on the overall geochemistry of the system. Comparative investigations were carried out on the sediments of the Harts River diversion and Leeupan, a neighbouring, actively deflational, ephemeral pan.*

*Water samples were collected at various points in a transect across the pan. Sediment supernatant and interstitial waters were obtained from sediment samples by decanting and centrifugation, respectively. The electrical conductivity, pH and alkalinity of the water samples were determined by standard methods, total elemental concentrations by inductively coupled plasma – atomic emission spectrometry and anion concentrations by high performance ion chromatography. Additionally Si and  $\text{PO}_4^{3-}$  concentrations were determined colorimetrically. Water analyses carried out by the Department of Water Affairs and Forestry (DWAF) over the last 15 years were also examined. The geochemical equilibrium speciation model MINTQA2 was used to model speciation interactions and mineral solubility equilibria in the pan water.*

*Grab sediment samples were taken in Barber's Pan, Leeupan and the Harts River (both of which were dry at the time of sampling). Core samples were also taken from Barber's Pan by means of a hand corer. The total elemental concentrations of these samples were determined by means of x-ray fluorescence spectrometry and their clay mineralogy by x-ray diffraction. Standard methods were used to determine particle-size distributions, organic carbon and carbonate concentrations. The extractable phosphorus content of the pan and river samples was determined using the AMBIC method.*

*The bulk pan water is well mixed, having a very uniform composition throughout. The water can be described as being very alkaline and subsaline and with  $\text{Na}^+$  and  $\text{Cl}^-$  as the dominant ions.  $\text{HCO}_3^-$  is also abundant. The pan water is unusual in that Mg concentrations dominate over those of Ca. The interstitial waters are also very homogeneous, but contain higher concentrations of most solutes determined than the bulk pan water. Exceptions to this are Al*

and  $\text{SO}_4^{3-}$ , both concentrations decreasing in the interstitial water. The decrease in Al is attributed to the decreased pH of the interstitial waters (on average 1 pH unit lower than that of the bulk pan water) lowering its solubility.  $\text{SO}_4^{2-}$  concentrations are thought to be lower in the interstitial waters as a consequence of the reduction of  $\text{SO}_4^{2-}$  by bacteria in the sediments producing  $\text{H}_2\text{S}$  and metal sulphides in the superficial sediments of the pan. The lower pH of the interstitial water is a consequence of the reduction of  $\text{SO}_4^{2-}$ .  $\text{PO}_4^{3-}$  and Si concentrations were particularly enriched in the interstitial waters relative to the bulk pan water. Depletion of Si in the bulk pan water was attributed to the activities of diatoms and the precipitation of silicate minerals. The enrichment of the  $\text{PO}_4^{3-}$  in the interstitial waters relative to the surface waters was attributed to an oxidized microzone preventing its release into the bulk water column. The pan sediments can, therefore, be seen to be acting as a sink for phosphorus.

Chemical speciation modelling using the thermodynamic equilibrium model MINTEQA2 predicted the predominance of carbonate and hydroxide species. Carbonate and hydroxide species were dominant in the speciation interactions despite the overall dominance of Na and Cl, which were predicted as occurring in the form of free ions.

MINTEQA2 predicted that the waters were supersaturated with respect to a number of calcium minerals that could occur under the given conditions. These included calcite, dolomite, hydroxyapatite and fluorapatite. Precipitation of these minerals could scavenge other ions, trace metals (e.g. Pb) in particular, from solution. Phosphate solubility was governed by the minerals fluorapatite and hydroxyapatite. The precipitation of these minerals would contribute significantly to the removal of  $\text{PO}_4^{3-}$  from the bulk pan water to the sediments.

Examination of the DWAf data together with modelled outputs of mineral solubility equilibria suggested that brine evolution in Barber's Pan followed the fate of the path III inflow water described in Eugster and Hardies' (1978) model of brine evolution. The ratio of Mg/Ca in the bulk pan water increased with evaporative concentration.

During evaporative concentration Na and Cl behaved as conservative solutes.  $\text{HCO}_3^-$  was gradually removed from solution with increasing evaporation. Ca levels remained approximately constant during evaporative concentration, suggesting a constant rate of removal. The Mg/Ca ratio, however, increased with evaporative concentration. Mg and K showed a gradual decline in concentration with evaporation. A plot of  $\text{SO}_4$  concentration against Cl indicated that  $\text{SO}_4$  also declined gradually with evaporation. The calculation of a concentration factor for  $\text{SO}_4$  relative to Cl in the bulk pan water indicated that it had only increased 5x as compared to the 13x increase of Cl. The presence of iron sulphides in the sediments was also noted as was the evolution of  $\text{H}_2\text{S}$ , showing that sulphur was being removed from solution. F initially behaved in a conservative fashion increasing until a point of saturation after which it was rapidly depleted. Si showed conservative behaviour during evaporative concentration.

Mn and Fe appeared to be the only nutrients that may be limiting to productivity in the pan at certain times of the year.  $\text{PO}_4^{3-}$  levels recorded in the bulk pan water were high enough to suggest that the pan was at the very least mesotrophic. The very high  $\text{PO}_4^{3-}$  levels in the interstitial waters are likely to be for the most part unavailable to the pan biota as a consequence of the oxidized microzone at the sediment surface interface. Wind probably plays an important role in the nutrient dynamics of the pan by resuspending the sediment and

*deepening the oxidized microzone. The possibility of seasonal eutrophication associated with periodically high numbers of avifauna must still be investigated.*

*On the basis of the water quality variables determined, the pan water appears to be largely unpolluted. Only Pb and Ni appear to have unusually high concentrations and the potential source of these pollutants needs further investigation. With natural baseline levels of potential pollutants in the pan not having been determined in the past, it is difficult to make interpretations as to the significance of current levels. The main significance of the data presented is, therefore, that it provides a benchmark against which the results of future monitoring activities can be compared. The subsaline nature of the pan water may confer to the pan biota a certain degree of resistance against pollution.*

*The sediments of Barber's Pan were found to consist predominantly of mud-sized particles (< 0.053mm). The shallower sediments on the pan fringe were found to contain a greater proportion of sand-sized (> 0.053mm) particles than the deeper, central sediments. Wind and wave action is likely to be responsible for the removal of finer clay-sized material from the edge to the central sediments. The clay mineralogy of Barber's Pan can be described as interstratified chloritic-smectitic material with mica, kaolinite, quartz and calcite also present. The same clay minerals were identified in the Harts River sediment with the exception of calcite which was not present. The Leeupan sediment had two distinct components. An upper layer which closely resembled that of Barber's Pan and a lower layer consisting predominantly of dolomite. A microbially mediated process may be responsible for the formation of the dolomite layer. Traces of sepiolite and palygorskite could also be present in the clay fractions of all the sediments sampled.*

*The carbonate content of the Barber's Pan sediments was high and the deeper, central sediments contained substantial quantities of organic matter. Elemental associations in the sediments analyzed appeared to conform to well documented patterns. Trace elements were associated predominantly with  $Al_2O_3$ ,  $Fe_2O_3$  and organic matter. CaO was associated with carbonates and MnO with the mud fraction. Calcrete was observed in one of the edge sediments of Barber's Pan. In Leeupan, a substantial amount of the MgO was associated with the dolomite layer. Al was thought to be concentrated in the clay minerals and Fe in the oxidates. Adsorption of trace elements by the clay minerals and organic matter accounts for the correlation observed between these three components. Adsorption and coprecipitation of trace elements by iron oxides probably accounts for the correlation between  $Fe_2O_3$  and the trace elements.  $SiO_2$  and Zr were associated with resistant minerals like quartz and zircon and showed elevated concentrations in the shallow edge sediments, which were found to have a greater proportion of sand-sized particles.*

*The core sample analyzed showed an interesting trend of changing chemical composition with depth. Most elements increased in concentration with depth until the deepest portion, at which point their concentrations showed a sharp decrease. In contrast, MgO, CaO and  $SiO_2$  concentrations increased sharply at the deepest portion of the core. This was accompanied by an increase in the proportion of the sand-sized fraction. Two possible explanations for this trend were invoked. It could either be attributed to the sampling, storage, transport and preparation procedures, or it could represent the sediments that had accumulated on top of a calcareous layer formed when the pan was last completely desiccated. In the latter case, aeolian deflation could account for the removal of finer mud-sized material (increasing the proportion of sand-sized particles) and the precipitation of carbonates during evaporative concentration would account for the calcareous layer. A further series of longer cores are, however, required to make conclusive deductions as to the present sedimentation rates in the*

*pan and the effect of the Smuts diversion on these rates. The superficial sediments of Leeupan and central, superficial sediments of Barber's Pan were found to be enriched in extractable phosphorus. In Barber's Pan the oxidation of the superficial layers of the sediments through perturbation by wind action is, however, likely to make this pool of phosphorus largely unavailable to the pan biota by trapping it beneath an oxidized microzone.*

# 1. INTRODUCTION

Barber's Pan (26° 35' S; 25° 35' E) is a shallow, alkaline lake situated in the North West Province of South Africa approximately 17 km north–east of the town of Delareyville (Fig. 1). It forms part of a provincial nature reserve, 3118 ha in extent, of which the pan makes up 1750 ha (at the high–water mark). Milstein (1975) noted that it is unique in several respects, being most valuable from the aspect of bird conservation since it is perennial in an area characterized by shallow, seasonally filled, pans. Its biogeographical importance was confirmed when it received RAMSAR<sup>1</sup> designation as a Wetland of International Importance on the 13th March 1975.

Barber's Pan lies near the commencement of the fossil course of the Harts River, which can be traced northward for a further 45 km. Von Backström (1963) suggests that Barber's Pan was formed as a result of the impeded drainage of an old tributary of the Harts with wind playing an important part. He notes that strong and persistent winds from the north prevail throughout the autumn and early summer months, carrying fine limestone from the floors of the great pans which are dry, except after good rains. This material has deposited against the southern flanks of the channel, where it gradually built up the low hills that impeded the drainage and caused the formation of the pan. Although adjoining the floodplain of the Harts River, the pan did not receive water along the fossil course (except during peak floods) because of the natural limestone obstruction which caused the water to flow past Schweizer–Reneke and on to the Vaal (Milstein, 1975) (Figs. 2 and 14).

This changed in 1918 when General J.C. Smuts constructed a stone wall blocking the flow of the river, and removed the surface limestone obstruction thereby diverting the Harts river into its fossil course. The first subsequent flood bypassed a sluice intended to control it, and commenced enlarging the fossil course into Barber's Pan (Milstein, 1975). Since this diversion Barber's Pan has never dried up and can now be considered to be a perennial pan.

---

<sup>1</sup> Convention on Wetlands of International Importance Especially as Waterfowl Habitat, 2 February 1971 (Ramsar, Iran).

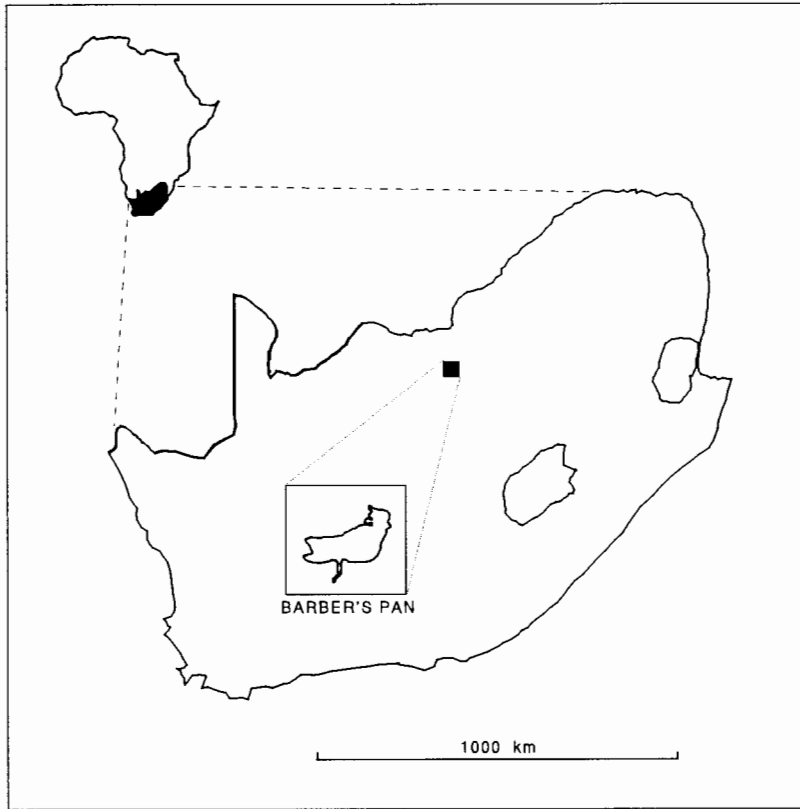


**Figure 1:** The approximate location of Barber's Pan within the Republic of South Africa.

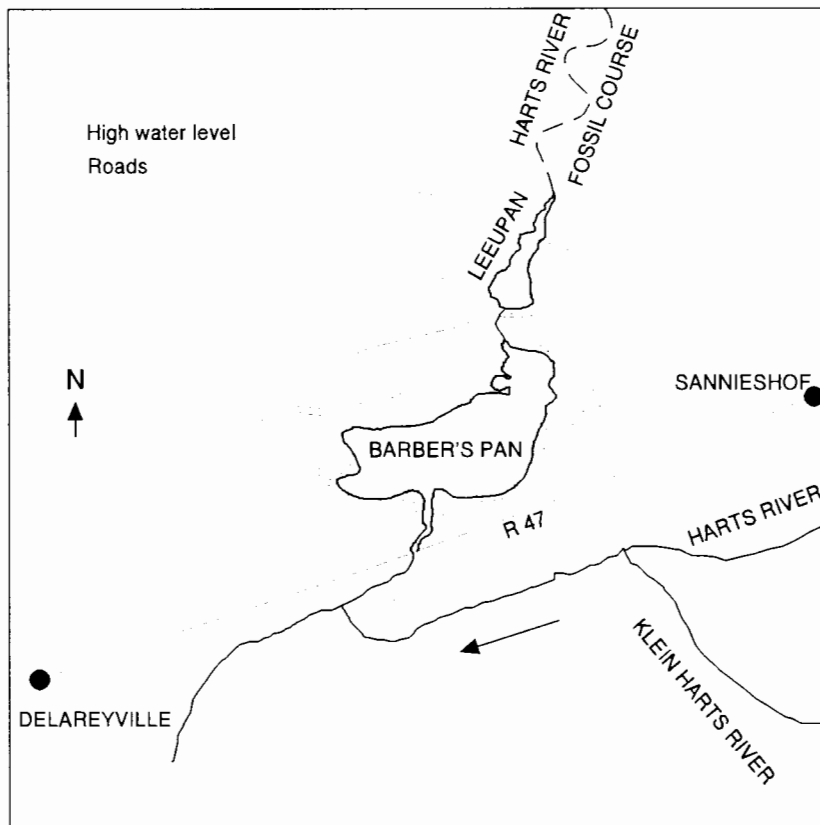


**Figure 2:** Schematic map of Barber's Pan and surrounds.

With Barber's Pan having been anthropogenically converted into a perennial pan, fine limestone is no longer being blown out of the pan during the dry season. Additionally, strong winds in spring often bring severe dust storms from the surrounding cultivated lands, and it is likely that silt is also being brought in via the Harts river inlet. The pan may thus be gradually silting up.

Milstein (1975) recorded that limnologists considered Barberspan to be potentially the least contaminated large body of water in the then Transvaal Province. Increasing anthropogenic influences on the pan were, however, already being noted by Farkas (1962).

Combrinck (1966) found phosphate ion concentrations in the pan to be low and Milstein (1975) proposed that phosphate may act as a limiting nutrient having a serious affect on the secondary productivity of fish and birds. He further suggested that iron may be a limiting factor for plant growth at certain times of the year (apparently made less available by the pan limestone).

### **1.1 Objectives of the study**

The objectives of this study were to review the pertinent literature on the origin and geochemical characteristics of pans and to conduct an investigation of the water and sediments of Barber's Pan to address three specific questions:

- i) In the past it was stated that the pan was one of the least contaminated, large bodies of water in the then Transvaal Province. Is this statement still valid ?
- ii) How do the prevailing chemical conditions within the pan influence the distribution and bioavailability of phosphate ( $\text{PO}_4^{3-}$ ) in the pan ?
- iii) Anthropogenic intervention in 1918 changed Barber's Pan from an intermittently dry, wind-blown pan to a shallow, perennial lake. Can any effects of this change be detected in the pan's sediments, and what implications do they hold for the pan's future ?

Additionally, the effects of evaporative concentration on the water composition of the pan was investigated through the determination of mineral solubility equilibria and the characterization of the behaviour of major solutes during the process of brine evolution.

A geochemical characterization of the water and sediments is essential if Barber's Pan is to be effectively managed, as these components are of fundamental importance to the birds utilizing the pan and the organisms on which they feed.

Pans comprise a large part of southern African wetlands, but are as yet poorly classified (Goudie and Thomas, 1985). Geldenhuys (1982) classified highveld pans on the basis of vegetation differences and waterfowl diversity. He proposed, however, that while his classification was useful, improved predictive and, therefore, management potential of these features could only occur if detailed limnological studies, addressing both chemical and physical conditions, took place.

Day (1993) states that there is a paucity of data on the aqueous chemistry of southern African inland saline systems and Seaman *et al.* (1991) note that the only comprehensive chemical analysis for any South African saline water–body is that of Ashton and Schoeman (1983) on the Pretoria Salt Pan. Furthermore, with the exception of a few publications dealing (in part) with the soils and associated materials of pan floors and margins, very little pedogeomorphic work has been carried out on pans in southern Africa (Verster *et al.*, 1992). This study is, therefore, also important on a larger scale in that it will aid in the classification of pans in southern Africa through the provision of a geochemical fingerprint for Barber's Pan.

## **1.2 The study area**

### **1.2.1 Physiography**

Barber's Pan is situated in an area lacking marked physiographic features (Fig. 3), and was described by Von Backström (1963) as a great undulating plane, diversified only by rises and hollows which differ little in elevation from one another and from the general plain.

Von Backström (1963) recorded that Barber's pan has a catchment area of only 39 km<sup>2</sup> with a run–off of 77 610 m<sup>3</sup> per year, and estimated that over 60 times as much water reaches it

annually via the Harts River (Fig. 4). Milstein (1975) noted that as a consequence of this small catchment, local rainfall is of minor importance to the water level.

Although Barber's pan has a natural outlet along the fossil course of the Harts River into an adjacent pan (Leeupan - Fig. 5), water has only flowed out of Barber's Pan along this outlet twice this century (1943 and 1967, [Milstein, 1975]) and consequently, Barber's Pan can be considered as largely an endorheic system. No ground water connections with the pan were observed by Von Backström (1963), with no further studies on any possible ground water contributions having been carried out to date.

### **1.2.2 Geology and soils**

Von Backström (1963) describes Barber's pan as being underlain by amygdaloidal lava of the Ventersdorp System, around 2 100 million years old. He further notes that in relatively recent geological times, more than 2 000 million years after the original lava flow, surface limestone started to form, and now practically surrounds both Barber's pan and adjacent Leeupan. Von Backström (1963) divides the surface limestone into wind-blown pan limestone and lower-lying vleilimestone. Green (1995) notes that the quality of the limestone varies from pure limestone to calcrete, which is hard and massive on the surface but soft and granular beneath the crust.

Milstein (1975) records that the soil of the reserve can be classified into two main forms, the Mispah and the Katspruit forms, with the Mispah form including most of the soil on the nature reserve while the Katspruit form is limited to relatively small areas near the pan. The Mispah soils are characterized by a diagnostic orthic A horizon situated on top of calcareous hard rock. The Katspruit soils have an orthic A horizon on a G horizon.

### **1.2.3 Climate**

Barber's pan is situated within a summer rainfall region, experiencing hot summers and cool, dry winters. Green (1995) records that the pan is situated in an area classified according to the Koppen climate classification as arid, with an average temperature below 18 °C (coded as BSK).



**Figure 3:** Views of Barber's Pan showing its situation in an area lacking marked physiographic features.



**Figure 4:** The Harts River inlet.



**Figure 5:** Leeupan, an active, deflationary pan neighbouring Barber's Pan.

The mean annual rainfall over the entire catchment averages 557 mm per annum, while the annual average daily temperature ranges are from 9 °C (minimum) to 27 °C (maximum).

Milstein (1975) notes that prevailing northerly winds have played an essential role in the formation of Barber's pan, and strong winds in spring are often associated with dust storms.

#### 1.2.4 Vegetation

Acocks's (1988) original classification of the vegetation around Barber's pan in 1953 was that of Dry *Cymbopogon–Themeda* veld. The intensification of crop – farming in the area over the last 40 years has, however, resulted in the decline of this grassland type in the area as a whole, and Milstein (1975) noted evidence of Karroid encroachment (particularly on the southern shores of Leeupan and the southeastern shores of Barber's Pan). A vegetation survey carried out in 1994 revealed that approximately 60% of the reserve's vegetation consists of formerly ploughed lands in various stages of succession (Knesl, 1994).

Natural indigenous trees and shrubs are relatively rare on the reserve, with the most common being; *Acacia karoo*, *Rhus pyroides*, *Rhus ciliata*, *Rhus lancea*, and *Diospyros lycioides*. Common grasses include *Themeda triandra*, *Cymbopogon plurinoides*, *Eragrostis lehmannia*, *Aristida congesta*, *Cynodon dactylon*, and *Urochloa mosambicensis* (Milstein, 1975; Knesl, 1994; Green, 1995).

Milstein (1975) described the aquatic vegetation as being dominated by *Potamogeton pectinatus*, with small prostrate herbs occurring on the exposed shore. He also identified a marginal zone, characterized by a belt of Juncaceae (rushes) and Cyperaceae (sedges), which leads into the open grassland surrounding the pan. Green (1995) noted that the high pH of the pan water (9.2 – 10.4) hampers the growth of higher vegetation that would normally be present in the littoral zone of fresh waters. Both Milstein (1975) and Green (1995) describe thick stands of the grass *Panicum repens* growing in shallow parts of the pan when water conditions are optimal. Knesl (1994), however, comments on the marked absence of such stands. Day (1993) suggests the possible presence of charophytes ( *Chara* sp.) on the pan bottom; a detailed survey of aquatic vegetation present in the pan is, however, lacking.

## **2. GEOMORPHOLOGICAL AND GEOCHEMICAL CHARACTERISTICS OF PANS AND ATHALASSIC SALINE LAKES – WITH SPECIAL REFERENCE TO SOUTH AFRICA**

### **2.1 Introduction**

Many arid and semi–arid regions are coincident with areas of endoreic (or internal) drainage, but the prevailing climatic conditions inhibit the formation of natural perennial lakes. As a result the water bodies in these areas are frequently ephemeral, highly saline, and in some cases supersaturated with salts. A spectrum of lacustrine features of varying scales and origins can be identified in arid and semi–arid regions, ranging from perennial salt lakes at one end to ephemeral pans at the other (Shaw and Thomas, 1989). Hardie *et al.* (1978) note that the nature of the inflow to a saline lake will determine if a lake will be perennial or ephemeral. Stable perennial lake conditions are favoured by perennial inflow and a low evaporation–to–inflow ratio, while ephemeral lake conditions are brought on by intermittent inflow and a high evaporation–to–inflow ratio.

Although these saline lakes and pans vary tremendously in terms of size, depth, and salinity, all have in common an environmental setting in which annual rainfall exceeds annual inflow from other sources. As a result, their characteristics are controlled primarily by climate. The processes that operate in these lakes and pans are hydrological, chemical, biological and sedimentological, all being intimately interdependent (Hardie *et al.*, 1978).

### **2.2 Geomorphological studies on pans**

#### **2.2.1 General characteristics of pans**

Shaw and Thomas (1989) define pans as arid zone basins of widely varying size and multifarious origin which, although generally above the present ground water table, are subject to ephemeral surface water inundation. The periodicity and extent of this inundation is highly variable and the basal and marginal sediments often display evidence of evaporite accumulation, deflation and aeolian accumulation as well as lacustrine activity.

Goudie and Wells (1995) provide an extensive review of the nature, distribution and formation of pans in arid zones. Further reviews of the subject are provided by Goudie (1991) and Shaw and Thomas (1989). Goudie and Thomas (1985) and Marshall and Harmse (1992) review pan formation in southern Africa, and Harmse *et al.* (1990) have put together a global bibliography on the subject.

Although pans exhibit a great deal of variability, Shaw and Thomas (1989) identify a number of characteristics common to most pans. The most common feature is that pans tend to occupy topographic lows, although not necessarily the lowest areas, in enclosed drainage basins. Pans are essentially closed systems lacking surface outflow, with the dominance of potential evaporation over precipitation and other inputs being an important contributory factor to their closed status. Standing water on pan surfaces is usually ephemeral in nature, resulting in there being distinct differences between pans and lakes of more humid regions. Pans are also characterized by having vegetation-free surfaces, particularly at their lowest elevations (Shaw and Thomas, 1989). De Bruijn (1971a), however, classified pans in the western Orange Free State into five major categories (namely: Salt, lime, clay, soil and gypsum pans) with each of these categories being further distinguished by the presence or absence of vegetation.

### **2.2.2 Models of pan development**

A consideration of early literature reveals a diversity of views accounting for pan origins. This diversity of views is coupled with the tendency for many authors to ignore the possibility of multiple formative processes and instead focus on single process explanations for pan formation (Goudie and Wells, 1995).

Uniting the various views on the origin and formation of pans, Goudie and Thomas (1985) proposed what they termed "an integrated model of pan development". This model was subsequently refined by Goudie (1991), Marshall and Harmse (1992) and Goudie and Wells (1995). The model proposed by Goudie and Wells (1995) is reflected in Fig. 6. This model of pan development proposes that pans occur as a result of the interaction of several contributory factors, namely: the availability of susceptible surfaces, disturbance or breakdown of these surfaces by animal erosion and salt weathering, the lack of permanently flowing rivers and the power of deflational aeolian processes (Marshall and Harmse, 1992).

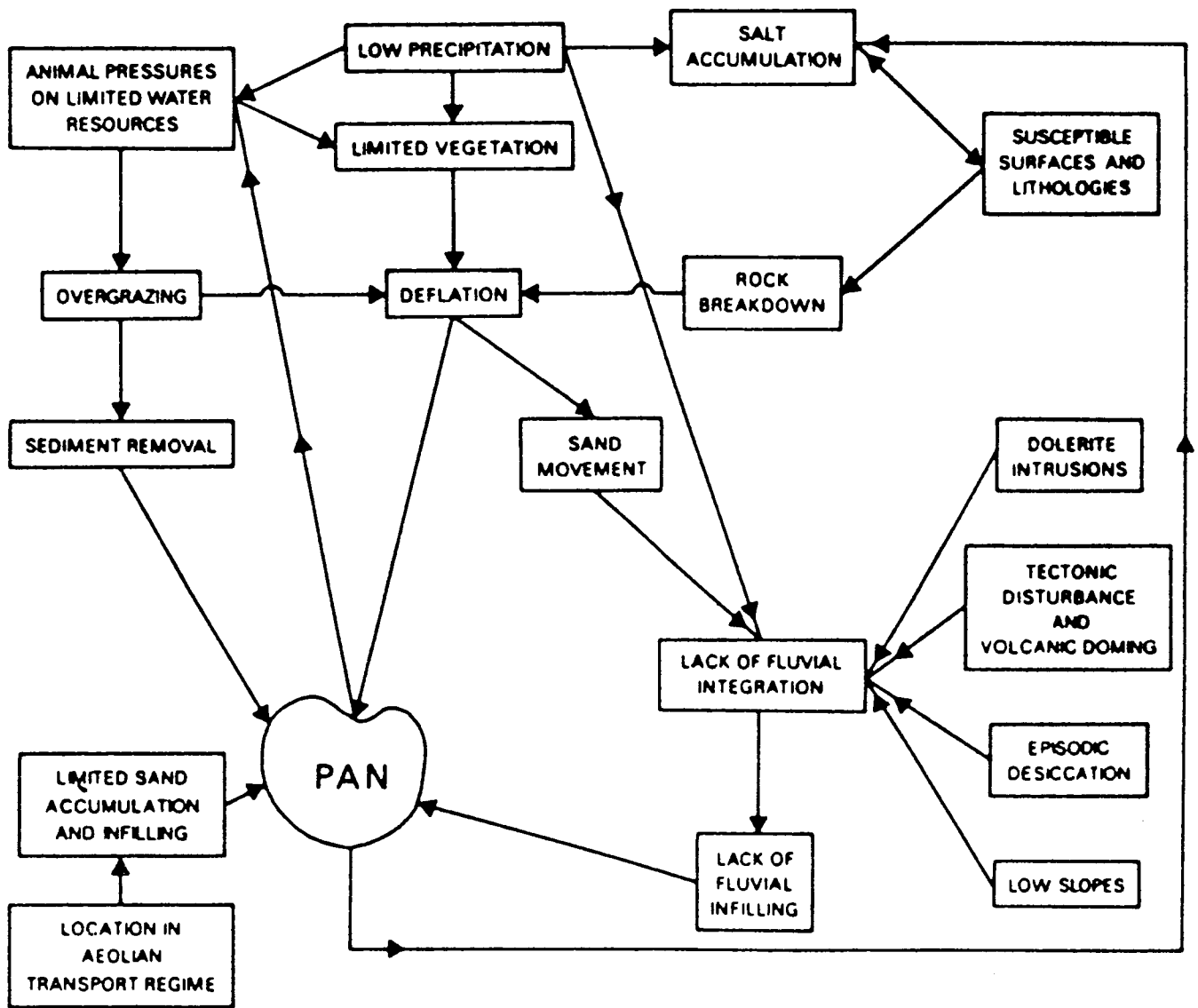


Figure 6: A model of pan development (From Goudie and Wells, 1995).

Goudie and Wells (1995) propose that the global distribution of pans indicates their preferential occurrence in arid areas, and Goudie (1991) suggests that aridity is in fact an important predisposing factor for pan development. Arid areas are associated with limited vegetation cover which favours deflation. Following the formation of a small depression and subsequent evaporation of the water in it, the salt deposit thus formed further inhibits plant growth encouraging increased deflation and promoting "halo – aeolian" (salt and wind) erosion. In low rainfall areas, animals tend to concentrate at any local source of water (and salt) such as a pan, causing trampling and overgrazing, ultimately leading to the removal of sediment from the pan surface (Goudie and Wells, 1995). All these factors acting in concert form a mechanism for pan establishment and enlargement, the soil/sediment material being rendered susceptible to deflation by salt weathering and animal trampling, with aeolian removal being

augmented by the removal of sediment by animals. The importance of wind in pan development can be seen in the characteristic elongation and alignment of pans in relation to wind direction (Goudie and Wells, 1995).

Goudie (1991) suggests that rates of sediment excavation have to exceed rates of external aeolian inputs, if pans are not to be obliterated by aeolian infilling, and Goudie and Wells (1995) propose that the location of a basin within a regime of aeolian transport may dictate its long term survival as a topographic feature.

Before pan development and expansion can occur, the initial depression must form. Some of the depressions may occur as a result of processes also active in non–arid areas including meteorite impact, tectonic activity, volcanic eruptions and karstic solution. A prolonged debate exists as to the role of solution processes, either at the surface or at depth, in pan formation (Goudie, 1991).

On the basis of their geological, geomorphological and hydrological observations of playa–lake (pan) basins on the Southern High Plains of Texas and New Mexico, Wood and Osterkamp (1987) suggest that processes other than aeolian deflation must be responsible for basin development. They propose that enlargement mechanisms include carbonate dissolution by groundwater in the unsaturated zone; piping of water and fine clastic material toward the zone of saturation; and eluviation by groundwater of dissolved and particulate matter. Goudie (1991) states that while this solution hypothesis may well be applicable to areas underlain by either surface limestones (e.g. calcretes) or deeper seated soluble rocks (e.g. salt, gypsum or limestone), many pans have developed on lithologies which are not conducive to karstic processes. Thomas *et al.* (1986) note that although deflation has often been regarded as a major pan forming process, there is increasing evidence indicating that pan development is in fact controlled by groundwater activity. The groundwater table acts as a base down to which deflation occurs, or as a control on weathering processes where pans develop in bedrock rather than on unconsolidated sediments. Bowler (1986) has suggested that depression development and morphology can be considered in terms of positive and negative surface water balances, and proposes that deflation is a consequence of basin processes rather than constituting a major formative influence.

Although the combined effects of many processes act to create and maintain pans, Goudie and Wells (1995) propose that their model (Fig. 6) identifies the two interactive processes of salt weathering and aeolian deflation as being predominantly responsible for pan formation and maintenance, with the role of the groundwater table being to control the depth to which deflation occurs and to contribute to the salt weathering process. Furthermore, they state that the area of pan formation should not be one where fluvial processes are fully integrated, nor should aeolian accumulation in the area act to fill in any irregularities in the pans surface. If these two conditions are met in dryland areas having susceptible surfaces then various circumstances may lead to the development and enlargement of hollows.

Marshall and Harmse (1992) divide the Goudie and Thomas (1985) model of pan development into processes or mechanisms that initiate pan development and those which are responsible for the propagation and evolution of a pan. They outline three integrated mechanisms that are responsible for the origin of pan fields and the localization of individual pans within these fields:

- 1) a suitable substratum has to exist, the lithology being susceptible to weathering and preferably containing salts that can aid in the chemical and mechanical weathering and erosion of the rock;
- 2) a disrupted drainage system on a flat surface where tectonic and climatic factors may combine to produce desiccation and subsequent ponding of the waters of a drainage system to form pans (in this context, deep weathering along subsurface flow paths can also contribute to pan initiation); and
- 3) geological structures such as fracture, fault or dyke intersections which aid in the weathering of certain portions of the land surface and are often responsible for the localization of individual pans in a pan field.

Once a pan or pan field has been initiated it has to be propagated through time, and often has to survive a succession of erosion cycles. Marshall and Harmse (1992) are of the opinion that many of the mechanisms proposed for the formation of pans by early authors are in fact mechanisms of pan propagation. Given that not all pans are propagated by the same mechanism, they propose four possible methods of propagation:

- 1) the biogenic model which considers the role of animal induced erosion,
- 2) the deflation model which considers wind deflation as the major agent in pan propagation,
- 3) the lithological model which considers the association between specific lithologies and the occurrence of pans (de Bruijn [1971a] showed correlations between the occurrence of dolerite dykes and sills that had intruded into karoo shales and mudstones, and the occurrence of pans), and
- 4) multiple models, or those in which the authors propose multiple mechanisms to account for the large variety of pans.

Marshall and Harmse (1992) emphasize Verhagen's (1991) so-called "ecological model" as a multiple model which explains the variation in the appearance of pans more successfully than others. In reviewing Verhagen's (1991) model, Marshall and Harmse (1992) observe that it exhibits elements of cyclicality, thereby allowing for different processes to account for the different types of pans. Verhagen (1991) emphasises the roles of animal-induced erosion and wind deflation in the formation of pans, but also considers the impact of increasing salinity of pan surface waters (which accumulate in wetter periods) due to evaporative concentration. He proposes that saline pans will ultimately be abandoned by animals as new migration patterns develop, and this absence of animals will allow the gradual recolonization of the vegetation at the pan's margins and eventually on the pan floor. This brings about the gradual reversal of deflation, allowing soil formation and humus production to commence on the pan surface. These processes culminate in the formation of a freshwater, vegetated pan which may either be "rediscovered" by animals, leading to another cycle of denudation, deflation and salination, or simply disappear.

## **2.3 Sediments and sedimentary processes in pans and saline lakes**

### **2.3.1 Saline lake deposits**

Saline lakes are surrounded by a complex of genetically interrelated depositional subenvironments that result mainly from the characteristics of the lake inflow. Hardie *et al.*

(1978) define subenvironment as "*any part of the surface of the basin that has distinctive physiography and on which a distinctive set of physical, chemical and biological processes operate*". It is, therefore, necessary to consider the closed saline lake basin as an integrated whole with the lake itself simply part of a complex system of subenvironments (Hardie *et al.*, 1978). As a result it is difficult to define a simple model of saline lake deposition, and instead Hardie *et al.* (1978) isolate individual subenvironments that are associated with modern saline lakes and describe their diagnostic features as well as the processes responsible for their formation. Using this approach they identify ten major subenvironments within modern lake basins. These are: 1) alluvial fan, 2) sandflat, 3) mudflat, 4) ephemeral saline lake, 5) perennial saline lake, 6) dune field, 7) perennial stream floodplain, 8) ephemeral stream floodplain, 9) springs and 10) shoreline features of saline lakes. Eugster and Kelts (1983) note that a particular closed basin only exhibits some of these features at any one time.

From a sedimentological perspective, Last and Schweyen (1983) identify two basic types of saline lakes: pans and perennial lakes, and propose that saline lake sediments consist of four fractions, namely:

1) very soluble evaporites (sodium – magnesium sulphates such as mirabilite, thenardite, bloedite, epsomite and halite). These occur characteristically in the sediments of shallow perennial lakes and ephemeral pans;

2) sparingly soluble precipitates such as carbonate minerals (e.g. calcite, aragonite and dolomite). In lakes where the removal of calcium by carbonate precipitation is incomplete gypsum is also formed as a sparingly soluble precipitate. Clay mineral authigenesis may occur in lakes having elevated levels of dissolved silica and alumina;

3) clastic inorganic material which is brought into the lake by surface runoff, shoreline erosion and wind; and

4) organic detritus.

Last and Schweyen (1983) outlined a number of processes influencing sedimentation in the Canadian Great Plains lakes. Hammer (1986) suggests that it is logical to assume that these processes are in fact universal. Table 1 reflects the physical processes influencing

sedimentation in saline lakes as identified by Last and Schweyen (1983) as well as biological processes influencing sedimentation in saline lakes identified by Hammer (1986).

Hammer (1986) states that while biological processes are common to both pans and perennial lakes, they play a greater role in perennial lakes. Sedimentation processes in pans tend, however, to be more complex than those in perennial saline lakes. Last and Schweyen (1983) stress that many present-day perennial lakes were probably pans during past warmer and drier periods and, likewise, many present-day pans were perennial lakes during wetter and cooler climatic periods. The sediments and related facies, as well as the biota, characteristic of Australian saline lakes have been related to three basic phases in the history/regime of each lake. One phase is typical of the wet phase of a shallow lake which can be either perennial or ephemeral. The second phase relates to a dry lake and the third to a permanent, deep lake. All three phases can alternate within one lake basin with alternations between the first two being the most frequent (De Dekker, 1988).

An interesting aspect of sedimentary processes in saline environments is that disruption of sedimentary laminations by bioturbation is usually not significant due to the low numbers (or even complete absence) of benthic animals in these environments. On the other hand, lake regression in hydrologically closed basins can lead to subaerial exposure, mud-cracking and intra-sediment growth of saline minerals which may result in the complete obliteration of any laminations (Eugster and Kelts, 1983).

#### *2.3.1.1 Depositional processes and characteristics of pan sediments*

As discussed earlier, saline pans are characteristic features of arid basins. They are flat, shallow depressions floored with layered salts and are normally dry except when storm water flooding turns the pan and its surrounding mudflats into an ephemeral lake (Lowenstein and Hardie, 1985). Saline pans therefore correspond to the ephemeral saline lake environment of Hardie *et al.* (1978), and as such need to be considered as simply one part of an integrated system of sub-environments (Fig. 7).

**Table 1:** Processes influencing sedimentation in the saline lakes (from Hammer, 1986)

---

**Processes important in all saline lakes**

<i>Physical</i>	Evaporative concentration Groundwater discharge into the basin
<i>Biological</i>	Photosynthesis Respiration Decomposition and biochemical alteration Peturbation of sediments by fauna

**Processes important in playa lakes**

<i>Physical</i>	Surface flooding, desiccation Evaporative pumping Wind transport, deflation Freezing/thawing
<i>Chemical</i>	Subaqueous precipitation of soluble salts Formation of salt crystal rafts Formation of salt spring deposits Intra-sedimentary growth of salt crystals Cyclic precipitation – dissolution Freeze-out precipitation Clay mineral authigenesis

**Processes most important in perennial lakes**

<i>Physical</i>	Stratification, destratification of the water column Shoreline processes Turbidity flow Flocculation of fine-grained material Wind/sheetflow transport
<i>Chemical</i>	Subaqueous precipitation/dissolution of sparingly soluble salts Freeze-out precipitation
<i>Biological</i>	Production Decomposition and biochemical alteration

---

In such closed systems the possibility of changing lake levels has profound consequences for sediment production and deposition. Subaqueous deposits can suddenly become mudflats which are subject to mud-cracking, scouring and salt disruption. Salt crusts, on the other hand, may become inundated and dissolve partially or completely. A consequence of this variability is that closed basin deposits are characterized by rapid and frequent facies changes, both laterally and in vertical section. These facies changes, together with indicators of

evaporative conditions, allow for distinction to be made between periods when the basin was hydrologically closed and when it was inundated with water (Eugster and Kelts, 1983).

Shaw and Thomas (1989) identify three processes involved in basin sedimentation: those resulting in deposition on the basin floor, basin subsurface and basin margin locations. They state that the dominant sediment types encountered in pans are fine sediments brought in by surface flow, together with solutes and organic materials, with the major solutes encountered being  $\text{SiO}_2$ ,  $\text{Ca}^{2+}$ ,  $\text{Mg}^{2+}$ ,  $\text{K}^+$ ,  $\text{Na}^+$ ,  $\text{Cl}^-$ ,  $\text{HCO}_3^-$ ,  $\text{CO}_3^{2-}$ , and  $\text{SO}_4^{2-}$ . These solutes are derived from both the surface and groundwater catchments and are important when salt crystallization occurs.

Pans are regarded as receptacles of sediments derived through episodic inflows or aeolian inputs. Consequently the sediments they receive are largely fine – grained. These aggradational attributes of pans contribute to their flat, horizontal surfaces and the fine – grained nature of these sediments allows for any irregularities, including those derived through uneven evaporite growth, to be smoothed out by water movement and dissolution during the episodic inflows (Shaw and Thomas, 1989).

Sediments found in saline pans consist of alternating layers of crystalline salts (having a variable thickness, but usually in the centimetre scale) and detrital siliciclastic rich mud (millimetres to centimetres thick). The mineralogy of the crystalline salt layers depends on the composition of the inflow waters with, in most cases, a single mineral dominating. As a result, the salt layers are often monomineralic. The salts most commonly found in modern saline pan deposits are halite ( $\text{NaCl}$ ), gypsum ( $\text{CaSO}_4 \cdot 2\text{H}_2\text{O}$ ), mirabilite ( $\text{Na}_2\text{SO}_4 \cdot 10\text{H}_2\text{O}$ ), thenardite ( $\text{Na}_2\text{SO}_4$ ), epsomite ( $\text{MgSO}_4 \cdot 7\text{H}_2\text{O}$ ) and trona ( $\text{NaHCO}_3 \cdot \text{Na}_2\text{CO}_3 \cdot 2\text{H}_2\text{O}$ ), with halite pans predominating (Lowenstein and Hardie, 1985).

The key to understanding saline pan deposition lies in recognizing that the pans repeatedly go through a well defined cycle of stages (Fig. 8). Last and Schweyen (1983) note that in addition to groundwater inputs, the pans receive water seasonally from direct precipitation, diffuse overland runoff and ephemeral streams. Lowenstein and Hardie (1985) record that these seasonal (or periodic) inputs convert the pans into shallow saline lakes, which are then subject to evaporative concentration until they revert by desiccation to their pan form.

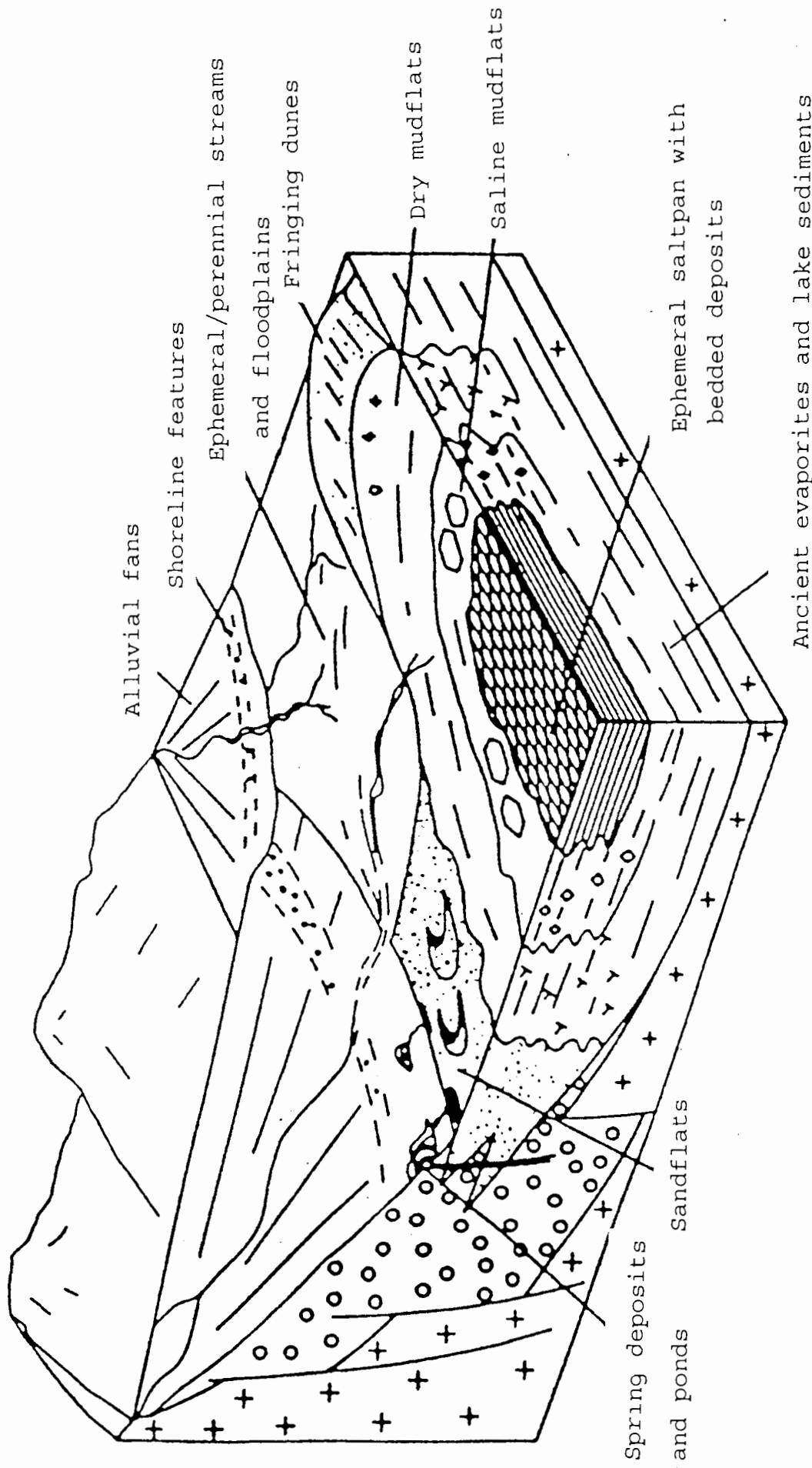


Figure 7: Idealized diagram of depositional subenvironments which can occur in arid zone playa (pan) basins (after Hardie *et al.*, 1978; from Shaw and Thomas, 1989).

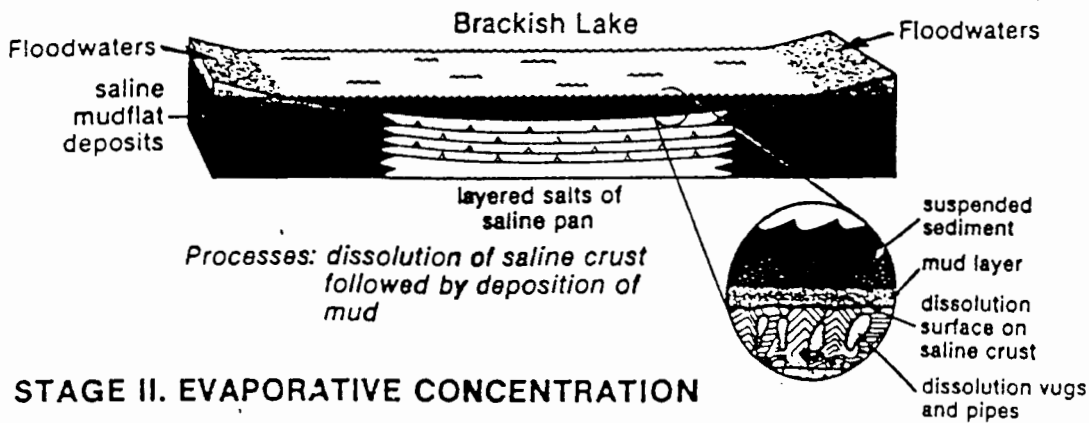
This cycle of expansion (with seasonal flooding) and gradual contraction (with evaporation) of the pans allows the ephemeral lake sub–environment to be divided into two parts based on features of the bottom sediment, namely: a salt pan, underlain by layered salts in the lowest part of the basin, and a saline mud flat underlain by muddy clastic sediment crowded with the crystals of salt minerals which surrounds the salt pan (Hardie *et al.*, 1978).

Flooding of the pan affects the sediment in several ways, the most important effect of this water inflow being that it is capable of redissolving previously precipitated soluble salts. Partial or total resolution of the previous year's precipitate or even of older salt beds can occur (Last and Schweyen, 1983). During the actual inflow of water, the freshwater runoff will preferentially dissolve the most soluble saline minerals from the efflorescent crust–covered mudflats, producing a chemically simple brine dominated by one or two major solute species, e.g. NaCl, Na<sub>2</sub>SO<sub>4</sub> or Na<sub>2</sub>SO<sub>4</sub> or Na<sub>2</sub>CO<sub>3</sub>, (Hardie *et al.*, 1978). Last and Schweyen (1983) note that the seasonal influx of water also transports clastic sediment to the basin and allows this material to be distributed and sorted within the pan. Once in the lacustrine environment, the coarse fraction may also be reworked into small beaches and bars by normal shoreline processes, while the finer components are transported basinward, eventually being deposited as thin mud laminae on the pan floor. Flocculation of clay–sized material upon exposure to the saline waters also plays an important role in the depositional process.

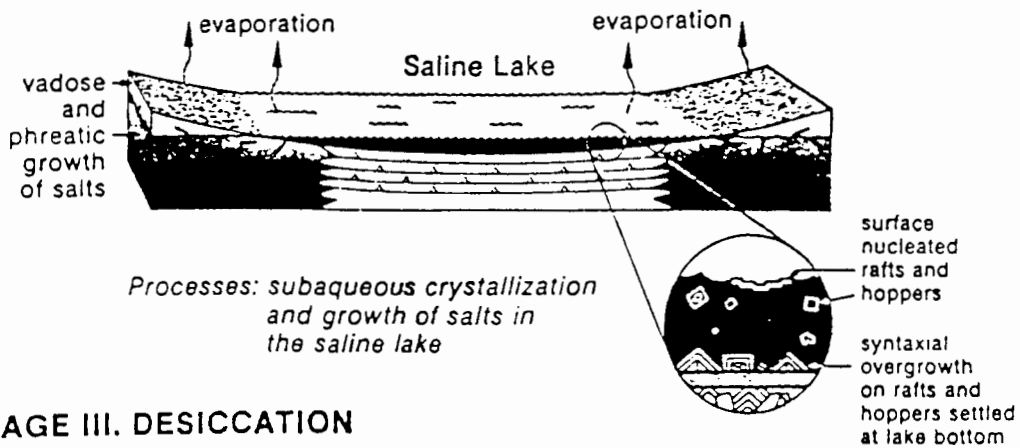
Hardie *et al.* (1978) suggest that the deposition of clastic sediment appears to take place mainly as the settling out of silt and clay sized grains from suspension. In agreement with Last and Schweyen (1983) they state that the settling out process results in a thin lamina (bed) of mud over the pan bottom, and propose that the thickness of the lamina will depend on the concentration of suspended sediment and the depth of water. It is unlikely, however, to exceed several millimetres (to tens of millimetres) in depth as mud sized grains are not major weathering products in arid zones and because the inflow waters are seldom very deep.

# THE SALINE PAN CYCLE

## STAGE I. FLOODING



## STAGE II. EVAPORATIVE CONCENTRATION



## STAGE III. DESICCATION

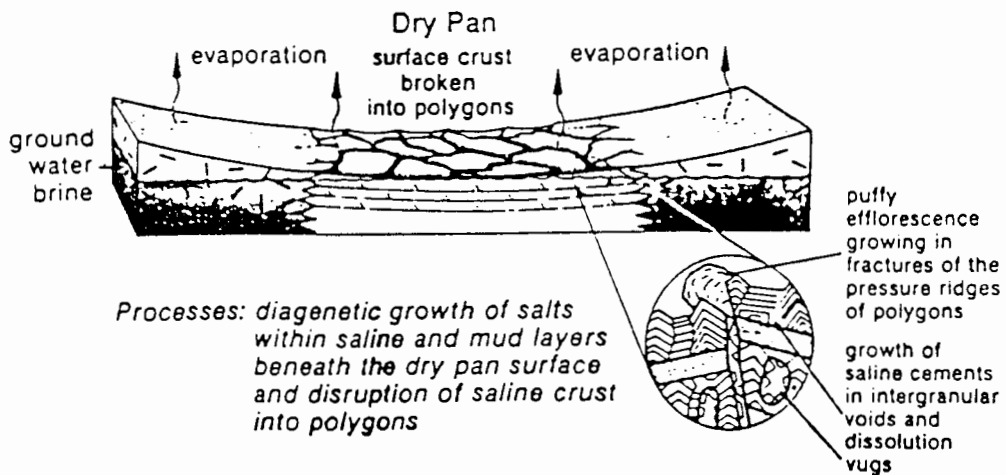


Figure 8: A model of the saline pan cycle (from Lowenstein and Hardie, 1985).

With time, the shallow ephemeral water body becomes concentrated by evaporation. In NaCl-rich systems, continued evaporation concentrates the lake brines to the point of saturation with halite at which point a period of salt deposition occurs (Lowenstein and Hardie, 1985). The precipitation of salt from the ponded surface brine may not occur until the surface covering of water has been considerably reduced, and Hardie *et al.* (1978) note the occurrence of several interesting post-depositional features as the pan dries up. These include polygonal cracking and overthrusting of the dry salt layer, growth of crystals in the underlying mudlayer and bacterial reduction of  $\text{SO}_4$  to produce  $\text{H}_2\text{S}$  and iron sulphides in the mud layer, giving it a black colour and making it anaerobic. Hammer (1986) notes that these sulphate-reducing bacteria in the mud layer help prevent gypsum from being incorporated into the sedimentary record.

As the water on the pan surface is evaporated to dryness the residual brine, saturated with halite and possibly sustained by perennial ground water flow, permeates the salt and sediment layers just below the pan's surface (Lowenstein and Hardie, 1985). With continued evaporation, Hardie *et al.* (1978) propose that the evaporative pumping mechanism described by Hsü and Siegenthaler (1969) will cause continued evolution of the subsurface brine in the upper vadose zone, leading to widespread precipitation of salts and the development of an efflorescent salt crust at the sediment surface. Lowenstein and Hardie (1985) also note that the pervasive growth of halite in the subsurface will cause the pan surface to fracture and buckle as a consequence of volume expansion, resulting in an extensively mudcracked surface.

The alkaline earth carbonates are the most abundant constituents of chemical sediments in closed basins. Although salt pans (as opposed to salt lakes) as such are not environments where substantial Ca-Mg- $\text{CO}_3$  deposition takes place, they may be surrounded by carbonate-rich mud flats. This is a consequence of the salt pan brines being poor in either Ca and Mg or in  $\text{CO}_3$ . Alkaline earth carbonates in salt pans are of clastic derivation or are formed through unusual processes such as the mixing of brines with dilute waters. Mudflats associated with salt pans can be important in the production, reworking and deposition of Ca-Mg carbonates, and the outer fringes of these flats may have waters dilute enough to precipitate substantial amounts of Ca-Mg carbonates in response to capillary evaporation (Eugster, 1980).

The deposits of saline minerals formed as a consequence of evaporative concentration are usually zoned laterally, with the most soluble minerals being in the centre. Vertical zonation may, however, also occur with the most soluble minerals at the top (Eugster and Kelts, 1983). Handford's (1982) study of the sedimentology of Bristol Dry Lake, California provides an example of this lateral zonation. He found the facies of the pan basin to conform to a bull's eye pattern with transects from the alluvial fan fringing the pan to the pan centre revealing the following pattern: Crudely-bedded alluvial fan clastics interfingering with pan-margin sandflat, wadi sand and silt, followed by progressive concentric rings of gypsum, anhydrite, chaotic mud halite and clay and finally salt pan halite beds in the centre. Hardie *et al.* (1978) showed a similar concentric pan of evaporite salts in the Saline Valley pan, California (Fig. 9).

Hardie *et al.* (1978) note that a salt pan is usually surrounded by mudflats which develop as evaporation shrinks the surface water covering the pan. They distinguish between a saline mudflat which is saturated with brine and from which a mass of salt crystals have grown so as to completely destroy the depositional sedimentary structures, and a dry mudflat, wherein the sedimentary structures are well preserved, characterized by polygonal mudcracks and thin saline crusts.

In their study on the saline lakes of the Canadian Great Plains, Last and Schweyen (1983) identified two types of mudflats: a saline mudflat and a clastic mudflat. The saline mudflat consisted of fine-grained clastic sediment together with crystals of salt minerals which evolved within the brine-saturated sediment after the evaporation of overlying water. The clastic mudflat, on the other hand, was dominated by fine-grained detrital material but lacked intrasedimentary salt crystals and tended to have a very thin efflorescent crust.

A single inflow event can, therefore, be seen to result in the deposition of a thin mud layer overlain by a thicker crystalline salt layer. With time, repeated flood events will superimpose mud layers (couplets) on top of each other and thus lead to a salt pan facies of tens or even hundreds of metres thick (Hardie *et al.*, 1978).

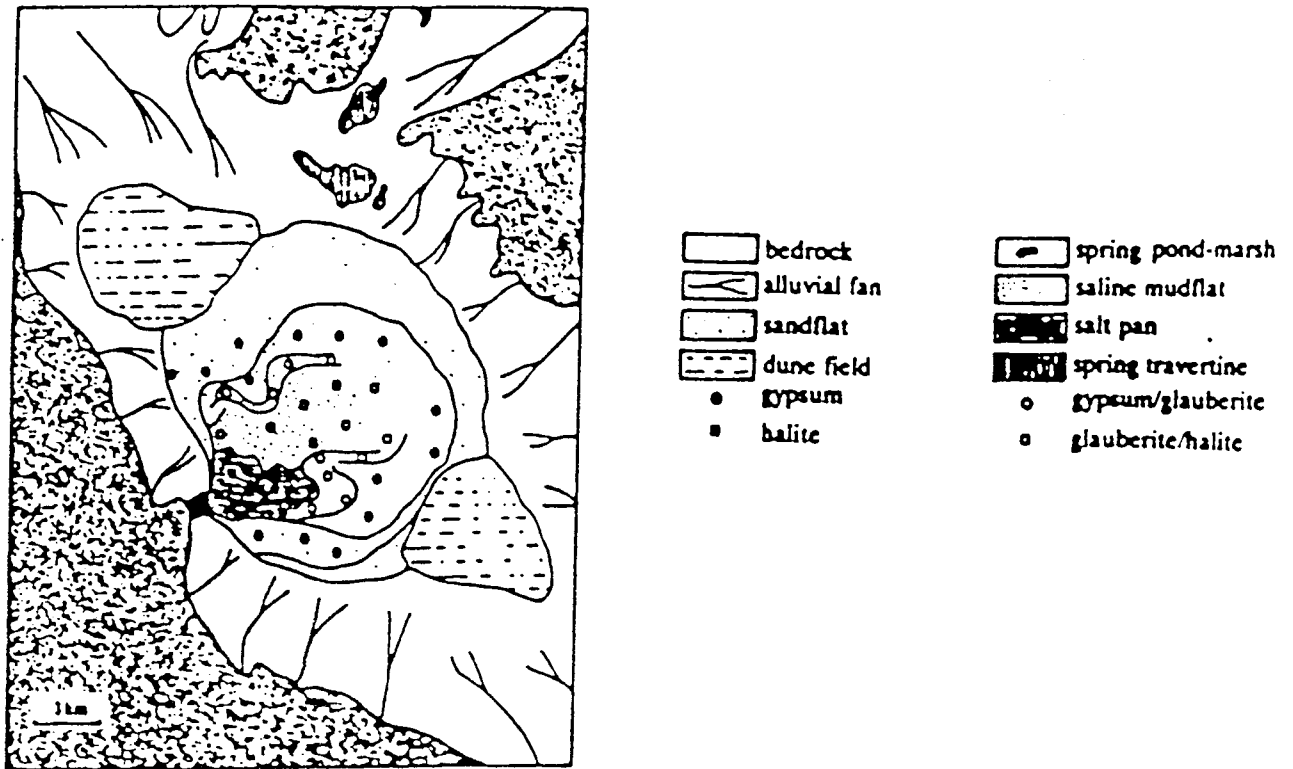


**Figure 9:** Map showing the concentric arrangement of evaporative salts in the Saline Valley Playa, California (After Hardie *et al.*, 1978).

### 2.3.1.2 South African pan sediments

Verster *et al.* (1992) review the occurrence, classification, properties and genesis of the soils, pedogenic duricrusts and unconsolidated sediments covering pan floors and margins in southern Africa. They subdivide pans into three geographical regions and eleven pan fields on the basis of climate, and go on to establish broad relationships between pan soils and environmental factors.

Geomorphologically, pans are similar to valley bottoms where fluvial, colluvial and aeolian deposits tend to accumulate. In the low-lying areas where pans are located, surpluses and

shortages of water appear to regulate soil type. Gleying is regarded as the predominant process, but decreases in intensity from the humid to the arid regions. In arid regions, clay illuviation forming diagnostic cutanic subsoils is the prevalent process. The topsoil of pans in humid areas shows high accumulations of organic matter (9.3%). Climate also regulates the leaching of ions, with the consequence that pan soils in the humid regions display slightly calcareous features. Pan soils in arid areas show an increased accumulation of salts on the surface due to efflorescence, and the pan soils sampled showed a greater accumulation of salts and extractable cations than associated valley bottom equivalents. This is attributable to the closed system conditions operating in pan environments (Verster *et al.*, 1992).

Pans of the western Orange Free State were classified on the basis of economic minerals present in their sediments. Three major classes were identified, namely: salt, gypsum and lime pans. Pans lacking economic minerals were classed as either soil or clay pans. Subclasses within these classes were identified on the basis of the presence or absence of vegetation on the pan surface, which is related to the depth of the water table (de Bruijn, 1971b).

Shaw and Thomas (1989) note Mabbutt (1977) as stating that clay-floored pans are characteristic of regimes having a low groundwater input, or where the pan surface is above the influence of capillary rise from the water table. These pans tend to have a flat clay or sandy clay surface either as the pan base or as the higher surround to a more saline lake basin. Shaw and Thomas (1989) note that the dominant sediment in these pans is clastic material deposited from suspension during inundation, although sand lenses may be deposited under more energetic conditions. The clay surface forms an impervious layer, preventing groundwater recharge at the pan centre. Increasing salinity, either from hydrological or climatic factors, will cause the evolution of clay floored pans to salt pans. This transition is characterized by the deposition of evaporites.

### 2.3.1.3 Saline lake sediments

A perennial saline lake can be defined as a surface body of brine that persists for many years without drying up. Both shallow and deep perennial saline lakes occur, and those more than several metres deep are usually stratified (Hardie *et al.*, 1978). Last and Schweyen (1983) state that stratification of the water column is one of the most important features influencing chemical sedimentation in saline lakes.

Stratification within lakes is defined in terms of the circulation of water within them, and on this basis two types of stratified lakes are distinguished. Lakes which have circulation occurring throughout the entire water column are termed holomictic lakes. Lakes that do not undergo complete circulation, so that the primary water mass does not mix with a lower portion, are termed meromictic lakes. Thermal stratification is common in lakes deeper than about 10 m. The surface waters in these lakes are heated during warmer periods of the year, largely by solar radiation, becoming less dense. The heating usually takes place faster than the heat can be distributed by mixing and consequently the lake becomes stratified into three zones: an upper epilimnion, transitional metalimnion and lower hypolimnion. In meromictic lakes the perennially isolated, lower water mass is termed the monimolimnion; this underlies the upper mixolimnion which periodically circulates. The two strata are separated by a steep salinity gradient termed the chemocline. When some external event brings freshwater into a saline lake the resulting condition is referred to as ectogenic meromixis. The usual result is to have a superficial layer of less dense, less saline water overlying a monimolimnion of saline, denser, water (Wetzel, 1983).

Wetzel (1983) records that Hudec and Sonnenfeld (1974) describe an interesting variant of ectogenic meromixis that is found in many saline lakes of arid regions or in small depressions that occasionally receive salt water intrusions. These lakes often overlies large deposits of soluble salts (e.g. magnesium sulphate) and are only a few metres in depth. Infusion of large amounts of fresh water, either naturally during wet periods or artificially as a consequence of nearby irrigation schemes, creates strong meromictic stratification that may persist for several years. Hardie *et al.* (1978) propose that such very shallow perennial lakes are usually thoroughly mixed by wind action and consequently have a sedimentary record resembling that of an ephemeral saline pan and should, therefore, be considered as such. Last and Schweyen (1983) emphasize the importance of density flow as a depositional process in saline lakes and propose that thermoclines and chemoclines can in fact act as "sediment-traps" for large amounts of suspended matter injected into the lake by interflows of medium density.

The primary process operating in perennial lakes is evaporation and in climates arid enough to permit the existence of saline lakes, evaporation is usually continuous. This leads to the concentration of the surface brine and resultant nucleation and growth of saline minerals in this brine. Both the newly concentrated brine and the saline minerals precipitated from it sink down toward the lake bottom allowing less dense and less concentrated inflow to float in

above them. The inflow is in turn concentrated by evaporation allowing the cycle to continue. This continuous repetition of inflow  $\Rightarrow$  evaporation  $\Rightarrow$  saline mineral precipitation  $\Rightarrow$  sinking of brine  $\Rightarrow$  settling of chemical sediment is an essential feature of stratified lakes where evaporation exceeds inflow (Hardie *et al.*, 1978).

Since the sediments of perennial lakes are not regularly influenced by the processes associated with subaerial exposure, their sedimentary facies are different to those of ephemeral lakes. Brine lowering is not a frequent occurrence and consequently the wide peripheral mud flats with efflorescent crusts and secondary salt crystals associated with pans do not occur. Sedimentation in perennial lakes tends rather to be dominated by conventional lacustrine processes including shoreline erosion and deposition, delta construction, density flow, pelagic fallout sedimentation and the subaqueous deposition of salts (Last and Schweyen, 1983).

The chemical sediments of perennial lakes that are deep enough to be stratified are relatively uncomplicated, consisting largely of laterally continuous saline mineral laminae and thin beds with clastic sediment (mud) partings. These mineral layer – clastic layer couplets are termed "varves" by many authors. This varve interpretation arises as a consequence of authors comparing the saline lake deposits with temperate zone non – saline lake sediments. Since evaporation normally affects saline lakes continuously, chemical precipitation is also continuous throughout the year. Layering in saline lakes is, therefore, not due to seasonal pulses of chemical precipitation but rather due to storm – flood influxes of clastic sediment that punctuate the continuously deposited chemical sediment. While some of these clastic inputs occur seasonally, most are irregularly spaced (Hardie *et al.*, 1978).

Hardie *et al.* (1978) note that the thickness of the chemical layers making up the lake sediment depends on the solubility of the particular saline mineral, nett annual evaporation and the interval between inputs of clastic sediment. They suggest that carbonate laminae are usually fractions of a millimetre thick while halite laminae form beds several centimetres thick, and propose that the most probable deposition mechanism for chemical sediments is simply precipitation. Similarly, the clastic sedimentation process is attributed to "settling – out" causing the formation of thin mud laminae with occasional massive storms producing unchannelled sheet floods as a dense underflow from which a graded clastic layer can be deposited.

Alkaline earth carbonates do accumulate in active perennial salt lakes. These carbonates can be carried into the lake as clastics or precipitate as a consequence of evaporative concentration. The primary precipitation of carbonate has been well researched and the principal sources of carbonate and the precipitation mechanisms have been found to be essentially the same in fresh and saline lakes (Eugster, 1980).

Last and Schweyen (1983) propose that clastic sedimentation is controlled by several processes. In marginal areas of the lakes wind-generated waves can influence the bottom and sedimentation occurs in equilibrium with the wave energy available. Coarse-grained clastics (sand and gravel) generally remain in the near-shore region while finer particles of silt and clay are held in suspension and transported basinward. They also suggest that the ideal sedimentation pattern is influenced by wave agitation and further modification of the distal fining pattern is caused by accelerated settling of the fines due to increased clay flocculation in the saline water.

Other sedimentary features besides the layering are diagenetic in origin. Fine-grained chemical sediments soaking in the bottom brine can recrystallize to form a more stable coarse crystalline mosaic. This process destroys the fine laminae formed by the settling out process. Where organic matter has accumulated in the bottom sediment, the interstitial brines may undergo bacterial reduction of sulphate ions. This bacterial reduction process can result in the dissolution of gypsum or other sulphate minerals should they be present (Hardie *et al.*, 1978). Hammer (1986) records that in their study of Dead Sea littoral sediments, Neev and Emery (1967) found that although gypsum was being precipitated at a rate of around 1 mm per year, the bottom sediments below the littoral zone contained only very small amounts of gypsum compared to calcite and aragonite. Neev and Emery (1967) concluded that although the gypsum was being precipitated, it was being reduced to H<sub>2</sub>S and calcium by bacteria in the anaerobic environment. Hardie *et al.* (1978) note that the sulphide-rich anaerobic conditions produced in the sediment by bacterial reduction of sulphate also allows ferric oxides and oxyhydroxides (of clastic origin) to dissolve, raising the ferrous iron concentration. This can lead to the precipitation of black iron sulphides, e.g. mackinawite and greigite, which ultimately convert to pyrite or marcasite.

Baumann *et al.* (1975) [cited in Hammer, 1986] examined the sediments of Lake Shala, a saline lake in the Ethiopian rift valley. They observed that it was thermally stratified and very

deep. The salinity below the thermocline was higher than at the hypolimnion/metalimnion boundary. As a consequence, the sediments are unlikely to be even periodically aerated. The sediments were found to be extremely fine grained compared with other lacustrine sediments and poorly sorted such that the decrease in particle size from periphery to centre was not observed. Smectite, montmorillonite and illite were the predominant clay minerals, with illite increasing in amount with increasing grain size. Carbonates in the sediment were found to consist of coarse allochthonous material with a fine autochthonous fraction.

In contrast, Marchant and Williams (1977) investigated the sediments of the hypersaline Pink and Cundare Lakes in Victoria, Australia. Their study of the sediments was part of an investigation of the energetics and population dynamics of an anostracan crustacean (*Parartemia zietziana*) and hence focused on the organic content of the sediments. They, however, made several general observations. Both the lakes are very shallow (approximately one metre deep) and hence polymictic (i.e. they have permanent aerobic environments above their sediments). The sediments were found to be composed largely of clays and no calcareous deposits or oölites were observed. The faecal pellets of *P. zietziana* were abundant in the sediment and contributed significantly to its energy content.

## **2.4 Water chemistry of athalassic saline waters**

### **2.4.1 Water composition of saline lakes**

Hammer (1986) reviews the debate pertaining to the definition and characterization of athalassic (inland) saline waters. He goes on to define athalassic saline lakes as those which have had no connection to the sea in geologically Recent times, or have been evaporated to dryness after having been flooded by marine waters and subsequently reflooded. He suggests that this definition indicates that the biota of these systems have no direct connection to the sea, precluding the application of the term "brackish" to describe these systems.

Williams's (1964) definition of saline lake water (i.e. water having a minimum of  $3\text{g}\cdot\text{dm}^{-3}$  salt content) has been widely accepted by limnologists, although it may be a little low if the physiological differences between fresh and saline water biota are considered. Three types of saline lakes can be distinguished on the basis of their salinity, namely: hyposaline ( $3 - 20\text{g}\cdot\text{dm}^{-3}$  dissolved salts), mesosaline ( $20 - 50\text{g}\cdot\text{dm}^{-3}$  dissolved salts) and hypersaline ( $\geq 50$

g.dm<sup>-3</sup> dissolved salts) lakes. Freshwater lakes can be defined as having  $\leq 0.5$  mg.dm<sup>-3</sup> dissolved salts, while lakes containing between 0.5 mg.dm<sup>-3</sup> and 3 g.dm<sup>-3</sup> dissolved salts are termed subsaline (Hammer, 1986).

Wetzel (1983) states that for all practical purposes the concentrations of the four major cations (Ca<sup>2+</sup>, Mg<sup>2+</sup>, Na<sup>+</sup> and K<sup>+</sup>) and the four major anions (HCO<sub>3</sub><sup>-</sup>, CO<sub>3</sub><sup>2-</sup>, SO<sub>4</sub><sup>2-</sup> and Cl<sup>-</sup>) usually constitute the total ionic salinity of the water. Concentrations of elements such as nitrogen, phosphorus and iron, while of immense biological importance, contribute little to total salinity.

Langbein (1961) states that the classic explanation for the salt content of saline lakes is that the salt load accumulates continuously, with the exception of soluble salts which precipitate and any salts which may be lost on the rare occasions that such lakes overflow. If this explanation were correct then many closed saline lakes would be saturated with one or more common salts. Hammer (1986), however, records that researchers have shown that the majority of closed lakes have a relatively low salinity, which suggests that salt accumulation in these basins is offset by some process of salt wastage. Hutchinson (1937) [cited in Hammer, 1986] reviewed the work of several authors and concluded that salts may be removed from desiccated basins by deflation or may be covered by periodic influxes of sediment. Langbein (1961) proposed fluctuating lake levels as a mechanism for salt loss, concluding that a long term balance exists between salt input and salt loss, with the salt content of the lake varying around this balance in the same way that lake levels fluctuate around the balance between water input and output.

The salt composition of inland saline lake waters is largely determined by the nature of the influent waters, the composition of atmospheric precipitation and the differential precipitation and solution of salts as evaporative concentration proceeds or solution occurs. Exchange systems in the sediment can then further modify the resulting solution. The principle source of salts for closed saline lakes is the weathering of surficial rock. Salts released by weathering can dissolve and be transported to the lake by surface runoff or other inflowing water (Hammer, 1986).

Three extreme types of saline lake water can be distinguished on the basis of their dominant anion. The most common saline lakes are those in which the chloride anion is dominant. Carbonate lakes have relatively low salinities (a few exceptions occur in Chad, Kenya and

Tanzania) and all have sodium associated as their major cation. Typically these carbonate dominated waters are characteristic of fresh and subsaline waters around the world, with most carbonate dominated saline waters being classified as hyposaline. The carbonate referred to includes both carbonate and bicarbonate. Sulphate dominated lakes constitute the third major category and all possible intermediate mixtures of these three extremes occur (Table 2) (Hammer, 1986).

Hammer (1986) further identifies eight subtypes of anion dominance, of which chloride–carbonate, chloride–sulphate and sulphate–chloride occur frequently in saline lakes, with chloride–sulphate lakes being the most widely distributed subtype. He also records three major types (Na, Mg and Ca) and six intermediate types (NaMg, NaCa, CaMg, MgNa, CaMgNa and NaK) of cation dominance that have been recognized in world saline waters. He notes that sodium is the most common dominant cation and the only one to exceed 25% cation equivalence in over 80% of the saline lakes that have been investigated.

**Table 2:** Previously recorded chemical subtypes (multiple anion dominance) of athalassic saline lake waters (adapted from Hammer, 1986)

CHEMICAL SUBTYPES OF SALINE LAKE WATERS	
NaCO <sub>3</sub>	NaClSO <sub>4</sub>
NaClCO <sub>3</sub>	NaMgClSO <sub>4</sub>
NaCO <sub>3</sub> SO <sub>4</sub>	NaMgSO <sub>4</sub> Cl
NaMgClCO <sub>3</sub>	NSO <sub>4</sub> Cl
NaCO <sub>3</sub> SO <sub>4</sub> Cl	MgNaSO <sub>4</sub> Cl
NaClCO <sub>3</sub> SO <sub>4</sub>	MgNaClSO <sub>4</sub>
NaSO <sub>4</sub> CO <sub>3</sub>	

The pH of saline lakes tends to be alkaline with values ranging up to eleven. Minor chemical constituents have not been well documented despite the vast amount of literature available on major ions (Hammer, 1986). This may be due to the fact that many of these constituents are present in trace quantities and analytical techniques sensitive enough to detect such low concentrations have only recently become available.

#### 2.4.2 Water chemistry of southern African inland saline lakes

Seaman *et al.* (1991) and Day (1993) record that although salt lakes are geographically widespread and numerous in southern Africa, they have received very little limnological attention with the result that the literature on these systems, particularly on details of their water chemistry, is very limited. Seaman *et al.* (1991) provide a recent synthesis of what literature there is, while Day (1993) looks at the major ion chemistry in some of these systems.

Seaman *et al.* (1991) record that the majority of southern African saline lakes are shallow and ephemeral. The waters in these saline pans are dominated by  $\text{Na}^+$  and  $\text{Cl}^-$  ions (Seaman *et al.*, 1991; Silberbauer and King, 1991). While  $\text{Na}^+$  is invariably the dominant cation, a variety of patterns have been observed for the other cations, the most common being  $\text{Ca}^{2+} > \text{Mg}^{2+} > \text{K}^+$  and  $\text{Mg}^{2+} > \text{Ca}^{2+} > \text{K}^+$ . The dominant anion was usually  $\text{Cl}^-$ , although in a few cases  $\text{SO}_4^{2-}$  was found to be dominant. The most common patterns of anion dominance recorded are  $\text{Cl}^- > \text{SO}_4^{2-} > \text{HCO}_3^- > \text{CO}_3^{2-}$  and  $\text{Cl}^- > \text{HCO}_3^- + \text{CO}_3^{2-} > \text{SO}_4^{2-}$ . The diversity of anionic patterns of dominance decreases with increasing salinity, and all highly saline waters have  $\text{Cl}^-$  as the dominant anion (Seaman *et al.*, 1991). Seaman *et al.* (1991) further suggest that the ions in South African lake waters are of connate origin. Many of the South African salt pans overlie Dwyka and Ecca shales, which have sodium, calcium and magnesium chlorides and sulphates as their major salts. As a consequence, Seaman *et al.* (1991) assume that most of the salts in the pans are of geologic origin. They also record that very little data pertaining to pH values of southern African saline lake waters is available, but most published values are greater than 7.

Ashton and Schoeman's (1983) study of the Pretoria Salt pan provides the most complete analysis of any South African salt pan (Seaman *et al.*, 1991). Their study showed the pan to be meromictic with a very steep chemocline. They also determined the concentrations of a broad range of major and minor elements; all, with the exception of lithium, showed increasing concentration with depth.

### 2.4.3 The evolution of saline lake waters

Evaporation occurs in all climates; it is only in relatively arid climates, however, that evaporative concentration exerts a major control on water composition (Drever, 1988). Evaporative concentration serves to increase solute load, leading to mineral precipitation as the waters become supersaturated with various solutes (Eugster, 1980).

Garrels and MacKenzie (1967) modeled the evolution of carbonate-rich spring waters from the Sierra Nevada mountains based on evaporation at constant temperature and pressure (Fig. 10). Their model showed that with slight evaporative concentration, calcite would start to precipitate. With continued evaporation, calcite would precipitate until the calcium in the solution was completely depleted. The second mineral to precipitate would be sepiolite ( $\text{Si}_8\text{Mg}_5\text{O}_{20}(\text{OH})_2(\text{OH}_2)_4 \cdot 4\text{H}_2\text{O}$ ). The precipitation of sepiolite removes magnesium, silicate, carbonate and bicarbonate from solution, and it continues to precipitate (together with calcite) until most of the calcium has been removed from solution. Further evaporative concentration precipitates amorphous silica, but no sodium or potassium salts. Garrels and Mackenzie (1967) also predicted that the pH of the solution would remain relatively constant during the precipitation of calcium carbonate and sepiolite. With continued evaporation the pH would then increase to around 10. The end result predicted by their model was a strongly alkaline sodium carbonate brine.

Drever (1988) notes that theoretically dolomite would precipitate before sepiolite, but because of its slow rate of precipitation compared to sepiolite, Garrels and Mackenzie (1967) opted for sepiolite as the more realistic option.

Hardie and Eugster (1970) generalized the Garrels and Mackenzie (1967) model so as to cover a wide range of starting compositions of waters which can then undergo evaporative concentration. In their model, the partial pressure of  $\text{CO}_2$  is kept constant and the water compositions are restricted to  $\text{SiO}_2$ , Ca, Mg, Na, K,  $\text{HCO}_3^-$ ,  $\text{CO}_3^{2-}$ ,  $\text{SO}_4^{2-}$ , and Cl, which have been shown to dominate the composition of saline lakes. The most important concept in the Hardie–Eugster (1970) model is that of the "chemical divide". This concept reflects the general principle that *"whenever a binary salt is precipitated during evaporation, and the effective ratio of the two ions in the salt is different from the ratio of the*

concentrations of these two ions in solution, further evaporative concentration will result in an increase in the concentration of the ion present in greater relative concentration in solution and a decrease in the concentration of the ion present in lower relative concentration" (Drever, 1988).

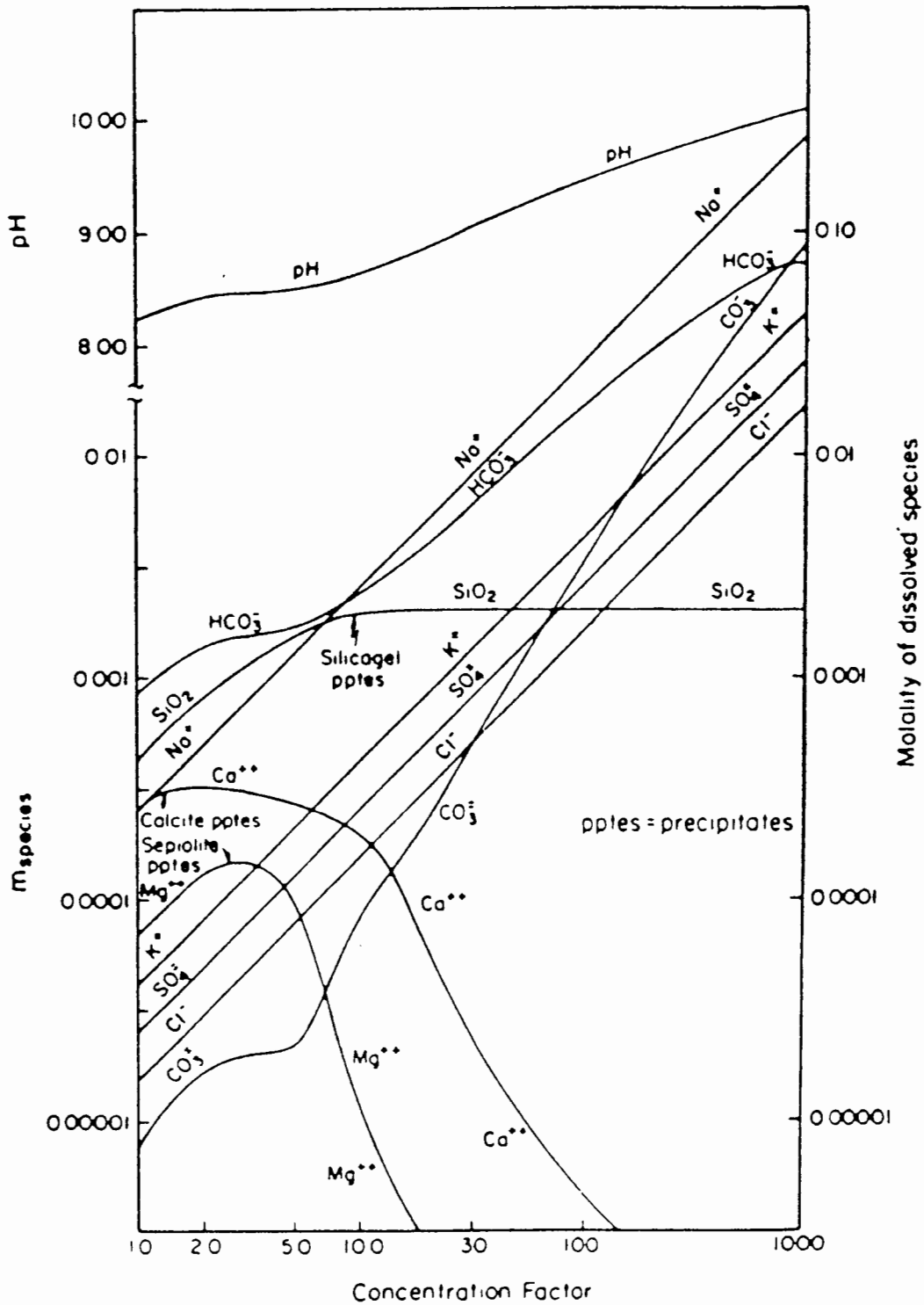


**Figure 10:** The calculated evolution of typical Sierra Nevada spring water at constant temperature in equilibrium with the atmosphere (After Garrels and Mackenzie, 1967; from Hammer, 1986).

Essentially, Hardie and Eugster (1970) recognized that the precipitation of one or more mineral phases has a profound effect on the subsequent development of the water composition, with critical "decisions" being made early on in the evaporative process. According to the model (Fig. 11), calcite is the first mineral to precipitate and serves to separate calcium-rich from calcium-poor waters. Hammer (1986) notes that sepiolite precipitation in the model represents a complication, while gypsum precipitation also represents a critical division. Four major brine types are predicted by the model; Hammer (1986) summarizes them as follows:

- 1) Na-CO<sub>3</sub>-Cl-SO<sub>4</sub> brine, which results from the precipitation of calcite and sepiolite, and occurs early on when the solution is still relatively dilute;
- 2) Na-Cl-SO<sub>4</sub> brine;
- 3) Ca-Mg-Cl-SO<sub>4</sub> brine; and
- 4) Na-Mg-Cl-SO<sub>4</sub> brine, which can only form when sepiolite precipitation is retarded through, for example, low silica concentration.

The most important conclusion that can be drawn from the Hardie-Eugster (1970) model are that brines should be chemically simple, containing relatively few ions as major species (Drever, 1988).

In their original model, Hardie and Eugster (1970) followed Garrels and Mackenzie (1967) in that magnesium was removed as sepiolite. Drever (1988) states that while sepiolite does fulfil this function occasionally, the most common magnesium containing phases to be formed in nature appear to be montmorillonite, dolomite, or high-magnesium calcite. Eugster and Hardie (1978) subsequently revised their model (Fig. 11) so as to incorporate calcite and dolomite as precipitates. Their revised model illustrates the evaporative concentration of three inflow waters differing in their (Ca+Mg)/HCO<sub>3</sub> ratios, allowing evaporative concentration of these inflow waters to follow three different paths: path I having an excess of bicarbonate over alkaline earths (soft water), path II an excess of alkaline earths over bicarbonate (hard water), and path III being intermediate (Eugster, 1980).

Both the Garrels-Mackenzie (1967) and Hardie-Eugster (1978) models consider brine evolution in terms of mineral precipitation. Mineral precipitation is, however, only one of several fractionating mechanisms that influence brine evolution. In total five fractionating mechanisms that take place between dilute water inflow and concentrated brines in

hydrologically closed basins have been identified, namely: mineral precipitation, dissolution of efflorescent crusts and sediment coatings, sorption of active surfaces, degassing and redox reactions (Eugster and Jones, 1979).

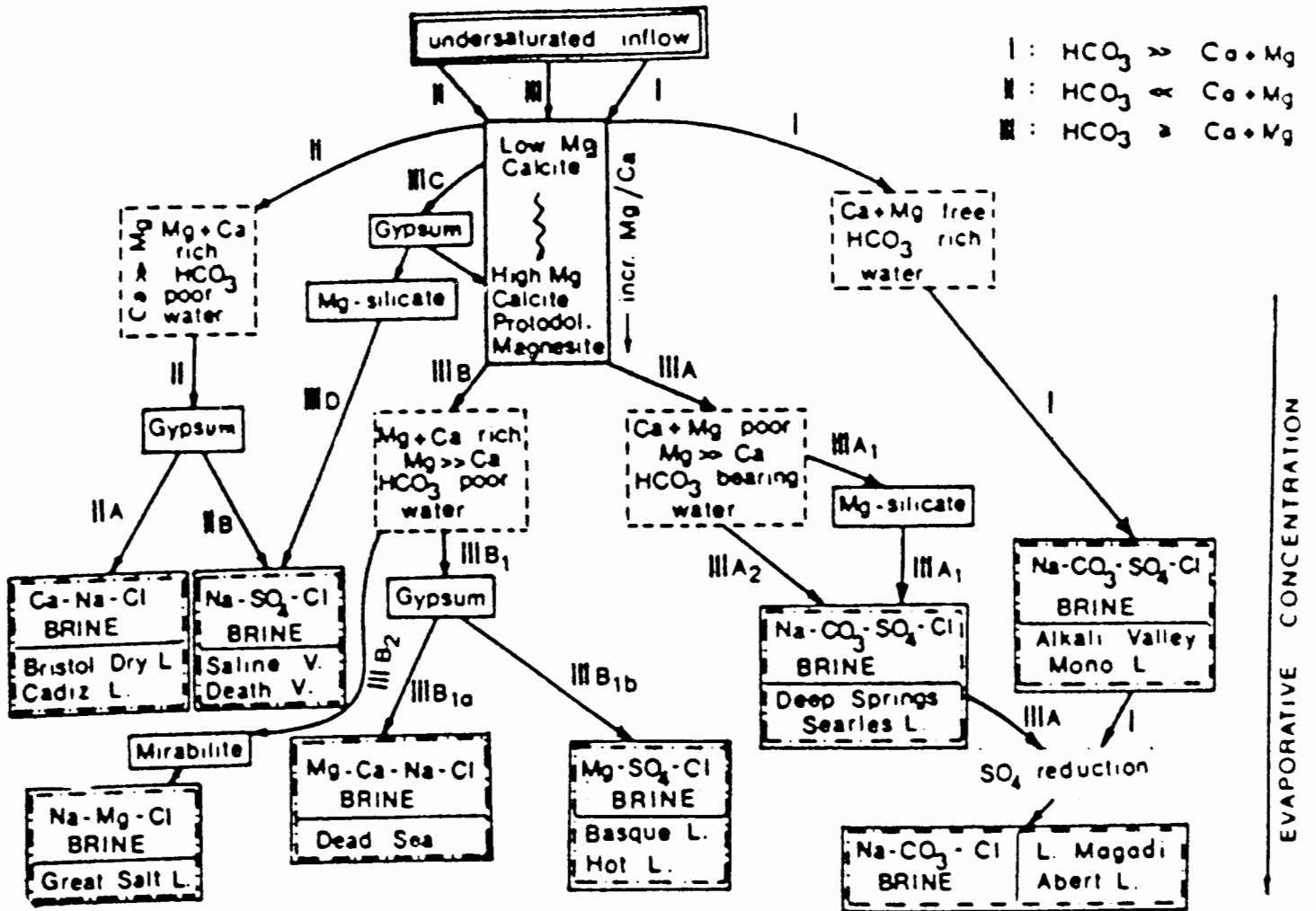


Figure 11: Flow diagram for the geochemical evolution of closed lake basin brines (After Eugster and Hardie, 1978; from Hammer, 1986).

Drever and Smith (1978) note that in arid climates occasional heavy rains cause partial re-solution of salts deposited in the soil and vadose zone. They studied the kinetics of re-solution of these salts by evaporating waters of different compositions in a sand tray and then leaching the sand with distilled water. They found that the relative rates of dissolution were  $\text{Na}^+$  and  $\text{Cl}^-$  most rapid, then  $\text{K}^+$ ,  $\text{SO}_4^{2-}$ ,  $\text{Mg}^{2+}$ ,  $\text{Ca}^{2+}$ , carbonate species and finally  $\text{SiO}_2$ . Eugster (1980) records that efflorescent crusts are common in all closed basins having sufficient inflow. In accordance with Drever and Smith's (1978) findings, when rain or dilute runoff come into contact with these crusts, the most soluble are taken back into solution. Although the partial dissolution of these efflorescent crusts does not lead to fractionation between components of the same soluble phases (e.g.  $\text{Na}^+$  and  $\text{Cl}^-$ ), the differences in solubility between halite, trona and thenardite are sufficient to produce fractionation between  $\text{Cl}^-$ ,  $\text{HCO}_3^- + \text{CO}_3^{2-}$ , and  $\text{SO}_4^{2-}$ , which is responsible for the lateral zonation of saline minerals in salt pans (Eugster, 1980).

The differential uptake and exchange of cations on active surfaces has been implicated in a number of solute losses, and degassing of  $\text{CO}_2$  in response to equilibration with the atmosphere or to temperature changes leads to a decrease in the total carbonate species, while the carbonate alkalinity remains constant. This is one of the important mechanisms by which the pH of alkaline waters rises during evaporative concentration (Eugster, 1980).

One of the more important redox reactions that can act as a fractionating mechanism is the reduction of sulphate to sulphide which removes sulphates from natural waters and may account for the unexpectedly low sulphate concentrations in some waters. Since the solubility of oxygen decreases as salinity increases, the anoxic conditions required for this reaction develop rather easily in brines (Drever, 1988).

Depending on the extent of fractionation during brine evolution and the effectiveness of the individual fractionation processes, solutes may behave in a variety of patterns. Five basic types of behaviour have been identified, these are illustrated in Fig. 12. A type I solute is one that remains in solution throughout the concentration process (i.e. perfectly conserved species like  $\text{Na}^+$  and  $\text{Cl}^-$ ). Type IIa and IIb solutes are a cation and anion that co-precipitate; with solute b being rapidly depleted at the saturation point. Solute IIa increases, but less rapidly than a conserved species. Typical examples would be  $\text{Ca}^{2+}$  and  $\text{CO}_3^{2-}$ . A type III solute is removed from solution gradually by a variety or combination of mechanisms (e.g. mineral precipitation, sorption or degassing). Carbonates behave in this way at Lake Magadi, Kenya. Removal

mechanisms that are not strongly concentration dependent, but are effective over only the middle part of the concentration range (e.g. ion exchange, surface adsorption and biogenic reduction), produce a type IV curve.  $K^+$  and  $SO_4^{2-}$  commonly show this behaviour. Uncharged solutes simply remain constant when they reach saturation with respect to a corresponding solid phase; they show type V curves (e.g.  $SiO_2$ ) (Eugster and Jones, 1979).

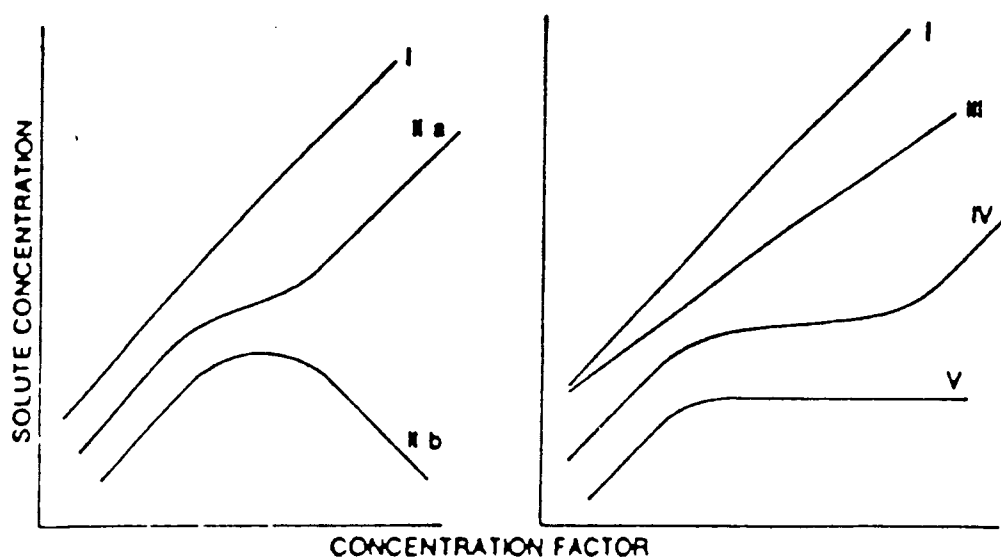


**Figure 12:** Schematic plots of individual solute content versus the degree of overall solution concentrations, illustrating the characteristic effect of specific mechanisms on changes in chemical composition (from Eugster and Jones, 1979).

Al-Droubi *et al.* (1980) applied the concept of residual alkalinity together with a parameter from the Eugster–Hardie (1970) model to predict the chemical evolution of natural waters by evaporation. They noted that during the evaporation of natural waters, the total molality of elements, pH and alkalinity can fluctuate during the concentration processes. They showed that these fluctuations could be interpreted at first approximation by using the generalized residual alkalinity concept. As a result of their calculations, however, they concluded that the complexity of natural cases requires that these calculations be carried out by a computer programme designed to calculate the distribution of aqueous species and the precipitation of minerals on the basis of equilibrium reactions. They applied the programme EVAPOR, which

calculates the chemical composition of solutions submitted to evaporation on the basis of the equilibrium reactions proposed by Garrels and Mackenzie (1967), to the Lake Chad saline system.

A study of the hydrochemistry of the Lake Magadi basin, Kenya, revealed that evaporative concentration was the overall process responsible for the chemical evolution of brines in the basin. This process of brine evolution included mineral precipitation in the unsaturated zone, re-solution and re-precipitation of efflorescent crusts with the consequent cycling of salts. A large fraction of the solutes were, in fact, derived from the dissolution of efflorescent crusts (Jones *et al.*, 1977). Kilham and Cloke (1990) studied the evolution of saline lake waters in the Basotu Lake District, Tanzania. They identified two distinct evolutionary pathways, a gradual path and a rapid one. Solute evolution along the gradual path was governed by mineral precipitation, sorption and ion exchange, CO<sub>2</sub> degassing and sulphate reduction (i.e. the five fractionating mechanisms identified by Eugster and Jones, 1977), all of which were coupled to evaporative concentration. The rapid evolutionary path on the other hand involved a mixing event with sudden release of H<sub>2</sub>S to the atmosphere. This release alters the water chemistry as the loss of sulphide produces an equivalent permanent alkalinity.

Two basic factors were identified as controlling brine chemistry during the overall evolution of saline waters in the basins of the Cariboo Plateau in British Columbia, Canada; namely bedrock composition, which controls the availability and initial ratio of most ions in the dilute runoff waters, and extensive carbonate precipitation, which acts as a major chemical divide giving rise to two brine types (Renaut, 1990).

While the concept of a "closed" system can be used to explain surface water budgets, it is not very applicable to the evolution of brines where surface water – groundwater exchange driving high salinity drying stages becomes a controlling factor affecting salt budgets. If subsurface waters are frequently diluted by surface water – groundwater exchange, evaporites will not be preserved in the record even though the surface system appears hydrologically closed. This is because the process of interstitial water evolution which controls efflorescence, deflation and salt-weathering exerts a dominating influence on basin geomorphic expression and hydrochemical fractionation (Bowler, 1986). Arakel *et al.* (1990) state that on the basis of their field observations and petrochemical characterization of playa (pan) sediments in western and central Australia, localized discharge of groundwater from shallow aquifers in calcrete

deposits plays a fundamental role in the geochemical evolution of playa–lake marginal facies. They suggest that while their data indicates that evaporative concentration and salt recycling are major controls on playa geochemistry, it does not completely explain brine evolution. They conclude that the distribution of chemical facies in playas reflects the significant impact of variation in the groundwater pattern on the geochemical evolution of the playa–lakes.

#### **2.4.4 Mineral solubility equilibria**

In considering the precipitation of minerals as a consequence of evaporative concentration, the concept of mineral stability comes to the fore. Drever (1988) proposes that mineral stability relationships can be thought of in several ways, which he summarises as the following three questions:

- 1) Is a solution A supersaturated, undersaturated, or in equilibrium with mineral B ?
- 2) Which mineral, B or C, in contact with solution A is the more stable ?
- 3) Is solution A in equilibrium with mineral B if certain assumptions are made concerning a component that has been measured ?

When minerals containing a given element are shown as a function of the activity of the element in solution and some other important variable (e.g. pH) the most soluble mineral (solid A in Fig. 13) is the least stable, while the least soluble mineral (solid C in Fig. 13) is most stable. Thermochemical data can be used to predict mineral stability sequences, since the least soluble minerals have the lowest free energy. While thermochemical considerations show which reactions are possible, kinetic considerations are necessary to predict the duration of such transformations. Elements in solid phases having rapid precipitation/dissolution kinetics will have solubility controlled equilibrium aqueous concentrations, while in the absence of the solubility–controlling solids, adsorption–desorption reactions will control the aqueous concentrations (Rai and Kittrick, 1989).

The calculation of mineral equilibria in systems where all phases have constant composition can be approached through the use of Gibbs free energies and the dependence of these functions on temperature and pressure. When one or more of the phases are in solution, however, chemical potentials are more convenient descriptors since they incorporate the variation of free energy with composition.

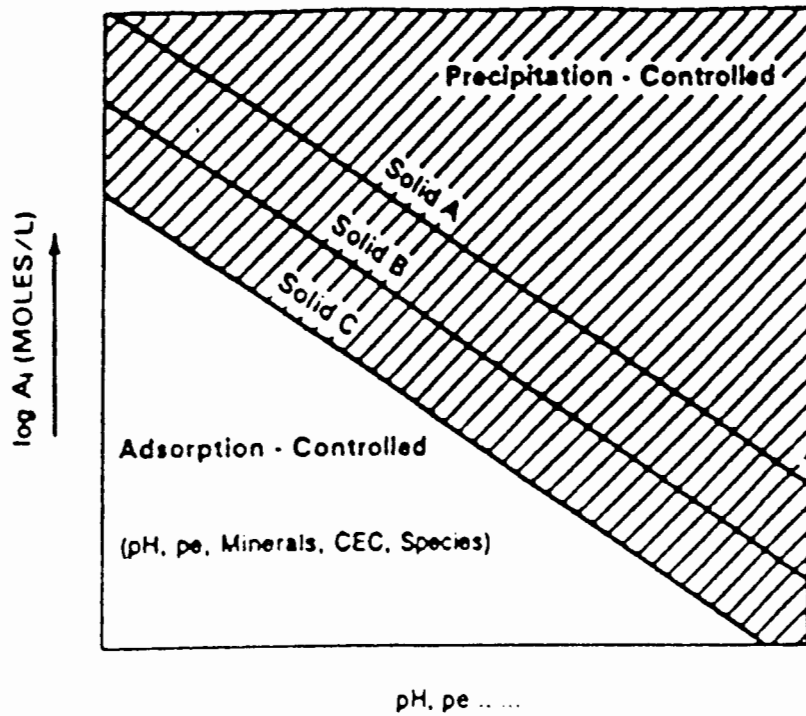
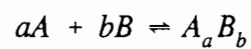


**Figure 13:** Schematic representation of mechanisms that control aqueous concentration of elements (from Rai and Kittrick, 1989).

The thermodynamic equilibrium constant ( $K^0$ ) for the general reaction



carried out under isothermal and isobaric conditions, can be defined as (Nordstrom and Munoz, 1994):

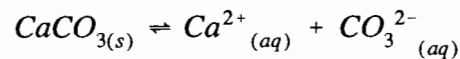
$$K^0 = \frac{A_a B_b}{A^a B^b}$$

The expression for  $K^0$  was developed from the following relationship using chemical potentials:

$$\Delta G^{\circ}r = -2.303 RT \text{Log} K$$

Where:  $\Delta G^{\circ}r$  = Gibbs free energy of the reaction  
 $R$  = gas constant per mole  
 $T$  = thermodynamic temperature  
 $K$  = equilibrium constant

The solubility of a solid phase can be represented by a constant known as the solubility product constant ( $K_{sp}$ ) which is defined by the product of ion activities in solution, where the ions are the same as those that make up the original solid phase (Lumsdon and Evans, 1995). For example, when an aqueous solution has reached saturation equilibrium with respect to calcite ( $\text{CaCO}_3$ ), then the reaction



is at reverse equilibrium and the mass-action expression

$$K_{sp} = \frac{(A_{\text{Ca}^{2+}} \cdot A_{\text{CO}_3^{2-}})}{A_{\text{CaCO}_3}}$$

applies. In this solution the ion activity product (IAP) should be the same as the solubility product constant ( $K_{sp}$ ). The logarithm of the ratio of IAP/ $K_{sp}$  is commonly called the saturation index (S.I.):

$$S.I. = \log \left( \frac{IAP}{K_{sp}} \right)$$

A positive index occurs if the solution is supersaturated and the mineral has a tendency to precipitate. A negative index indicates undersaturation in which case the mineral has a tendency to dissolve. At equilibrium S.I. = 0 (Nordstrom and Munoz, 1994; Lumsdon and Evans, 1995).

Geochemical modelling based on such thermodynamic principles can be used to interpret and/or predict mineral stability equilibria. Although a number of models have been developed for the thermodynamic description of aqueous solutions, two approaches are utilized primarily in geochemical applications, namely: ion–association models and specific interaction models (Plummer, 1992).

Ion–association models account for the non–ideality of aqueous solutions by individual ion activity coefficients and the formation of aqueous complexes from hydrated individual ions. Specific interaction models use a complex extension of the Debye–Hückel expression to define the excess free energy of aqueous solutions. This approach is capable of representing mean activity coefficients over a wide range of concentrations in both single and mixed–electrolyte solutions. Various computer programs have been built around these two approaches. These programs incorporate extensive thermodynamic databases and consider many more aqueous species than the original theoretical models, allowing for the effective modelling of species interactions and mineral solubility equilibria in aqueous systems (Plummer, 1992).

## **2.5 Nutrient status of athalassic saline lakes**

This is not intended to be a comprehensive review of the broad subject of nutrient requirements by aquatic organisms and nutrient dynamics in aqueous systems, but rather a brief evaluation of some of the more important concepts.

### **2.5.1 Essential elements**

The simplest definition of an essential element is that it is one required for the maintenance of life, its absence or inadequate supply resulting in the death of the affected organism. Severe deficiencies of an element that result in death are, however, difficult to produce, particularly if the element is required in very low concentrations. As a consequence, a broader definition

of essential elements has been adopted, namely: an essential element is one which consistently results in the impairment of a function from optimal to suboptimal when intake is deficient. This impairment can, however, be rectified through the supplementation of physiologically required levels (Mertz, 1981).

Essential elements required in plant nutrition can be divided into macronutrients, micronutrients and beneficial elements. The macronutrients are carbon, hydrogen, oxygen, nitrogen, phosphorus, sulphur, calcium, magnesium and potassium. The micronutrients are iron, manganese, molybdenum, copper, boron, zinc, chlorine and vanadium. Beneficial elements include sodium, cobalt, and silicon. Not all of these elements are required for all plants, but all have been found to be essential in some. A requirement for cobalt, for example, has only been established for biological nitrogen fixation systems, as in legume nodules (Wild and Jones, 1988).

The list of essential elements required by animals is the same as for plants, with the exception of boron which is apparently not required and the addition of selenium, fluorine, iodine, chromium, tin, arsenic and nickel (Wild and Jones, 1988).

Hammer (1986), in reviewing the chemistry of inland saline lakes, notes that very little information on the basic plant nutrients (such as phosphorus, nitrogen or silica) can be found in the saline lake literature.

Twinch and Ashton (1983) record that in wetlands (which by their definition includes pans) nitrogen and phosphorus are the rate limiting nutrients in primary productivity, and Hammer (1986) records that phosphorus is likely to be the nutrient limiting phytoplankton growth in saline lakes. Twinch and Ashton (1983) stress that distinct differences in nutrient cycling pathways occur between perennial and ephemeral wetlands and identify the main components of nutrient cycles in these two systems as being: inputs and outputs of the nutrients; sediment–water exchange; inorganic/organic cycling; active uptake by plants and epiphytes; grazing of these plants; leaching; and detritus/litter formation. The importance of each step varies with wetland type and the nutrient in question.

### 2.5.2 Nutrient dynamics

The transport and cycling of nutrients through the various pools in water, soil and sediment controls the long and short term productivity of water bodies. An understanding of the size of these pools and the fluxes between them is essential in assessing the effectiveness of management measures aimed at reducing external input, as well as in predicting the resilience of aquatic systems towards change in trophic character. Large pools of nutrients such as phosphorus in surficial sediments and nitrate in ground water have the potential to promote the prolonged stimulation of productivity (Lijklema, 1994).

Although nutrient loading from external sources contributes to the eutrophication of lakes, organic-rich sediments themselves release nutrients to overlying waters. In lacustrine sediments phosphorus and nitrogen occur in both organic and inorganic forms, with organic forms often predominating (Gales *et al.*, 1992). Gales *et al.* (1992) suggest that the transformations regulating the breakdown of organic nitrogen and phosphorus can be critical in supplying nutrients to phytoplankton and other biota.

Nutrients are, in varying amounts and forms, almost continuously transported to lake bottoms by sedimentation. A variety of biological, physical, chemical and mechanical processes act to cycle these nutrients between the lake sediments and water, with nutrient turnover being strongly influenced by hydrological conditions, lake morphology, water residence time, temperature regimes and the size and density of particles (Forsberg, 1989).

### 2.5.3 Phosphorus

Phosphorus plays a major role in metabolism, and in comparison to other macronutrients required by biota is usually the least abundant and first to limit productivity. Orthophosphate ( $\text{PO}_4^{3-}$ ) is the only directly utilizable form of soluble inorganic phosphate. Phosphate is very reactive, interacting with numerous cations, particularly under oxidizing conditions, to form relatively insoluble compounds. Its availability is also reduced by adsorption to inorganic colloids and particulate matter (Wetzel, 1983).

In summarizing the data on minor chemical constituents in inland saline lakes, Hammer (1986) records that these lakes tend to have higher phosphorus concentrations than freshwater lakes. He concludes that, with the exception of Antarctic and possibly meromictic lakes, phosphorus is unlikely to limit plant growth in saline lakes. At high salinities, however, decreases in phosphorus concentration related to sedimentation processes occur. While African saline waters generally have high phosphorus concentrations, low levels in some lakes may be attributable to tremendous macrophyte productivity. In North America, researchers have found that phosphorus concentrations are generally inversely related to phytoplankton biomass (Hammer, 1986).

The largest pool of phosphorus within a lake is usually associated with the sediments, which play a major role in the phosphorus cycle. This sediment-bound phosphorus constitutes a vast source of potential nutrients for the aquatic biota (Pettersson, 1984). Sediments can serve as both a source and sink for phosphorus (Twinn and Peters, 1984; Holdren and Armstrong, 1980). Pettersson (1984) notes that, traditionally, aerobic sediments in oligotrophic lakes have been considered a sink for phosphorus, while anaerobic sediments in very eutrophic lakes are regarded as a source.

Twinn and Peters (1984) suggest that under aerobic conditions, sediment-water phosphate exchange probably depends on mineral-water equilibria, adsorption-desorption processes, mixing patterns in the water and benthic biological activity. The overall effect is that aerobic sediments can approximate a dynamic equilibrium with dissolved phosphate,  $\text{PO}_4^{3-}$  enrichment in the overlying water causing a flux of phosphate into the sediment. Reductions in phosphate below equilibrium levels (e.g. due to algal demand) can induce sediment release of phosphate, thereby buffering changes in the phosphate concentration of the overlying water.

Viner (1975) studied the factors that may influence the concentration of phosphate in the water of the shallow, tropical Lake George, Uganda. He suggests that substantial quantities of insoluble  $\text{CaCO}_3$  and oxidized iron complexes probably occur permanently in the lake, and proposes that a significant relationship exists between these iron complexes and  $\text{PO}_4^{3-}$ . His laboratory experiments showed that the amount of calcium, iron, pH and dissolved organic matter all influenced phosphate concentrations. At high pH, calcium exerted the most influence, suggesting hydroxyapatite precipitation. Analysis of superficial mud in the lake supported this finding.

The classical mechanism by which sediment phosphorus is mobilized for subsequent transport to the overlying water has been described as the dissolution of iron III hydroxide gels, containing phosphorus, through the reduction of iron III to iron II (Jansson, 1984).

#### **2.5.4 Nitrogen**

The nitrogen cycle is a complex biochemical process in which various forms of nitrogen are altered by nitrogen fixation, assimilation, and reduction of nitrite to  $N_2$  by denitrification. The cycle is essentially microbial in nature, with bacterial oxidation and reduction of nitrogen compounds being coupled with photosynthetic assimilation and utilization by algae and aquatic plants. While the nitrogen cycle of fresh waters is understood qualitatively, the complex dynamics of quantitative transformation rates have not been clearly delineated, especially at the sediment–water interface where intensive bacterial metabolism occurs (Wetzel, 1983). Nitrogen has a variety of forms in fresh water, and aquatic plants show some diversity as to the form of nitrogen used preferentially. Ammonia and nitrite are generally regarded as decomposition products of the nitrogen cycle, while nitrate is the preferred form for plant use. The various nitrogen fractions in saline lakes have similar concentration ranges to those in non–saline lakes and these are likely to be related to productivity levels (Hammer, 1986).

#### **2.5.5 Other nutrients**

Calcium has been implicated in numerous ways in the growth and population dynamics of freshwater fauna and flora. It is required for the normal metabolism of higher plants and is essential for the maintenance of the structural and functional integrity of cell membranes. Magnesium is required universally by chlorophyllous plants for the magnesium porphyrin component of chlorophyll molecules and in enzymatic transformations. Sodium and potassium are involved primarily in ion transport and exchange, while chloride is influential in general osmotic salinity balance and ion exchange (Wetzel, 1983). Silica is essential for the growth of diatoms and some other algal groups, being an integral component in their frustules (Hammer, 1986). Talling and Talling (1965) propose that in African lake waters, dissolved silica shows an upward trend with increasing concentration. They attribute this to the increased rate of solution of silicon compounds in saline waters of high pH and alkalinity.

Iron is required in the enzymatic pathways of chlorophyll and protein synthesis and also in respiratory enzymes. Both iron and manganese are functional components of nitrate assimilation and are essential catalysts of numerous enzyme systems. Concentrations of ionic iron are exceedingly low in aerated water, with most iron occurring as ferric hydroxide and as complexes with organic, especially humic, compounds. The solubility of manganese is considerably higher than that of iron, but its reactions are analogous to those of iron. Under anaerobic conditions of both low pH and low redox potential, ferrous and manganous ions diffuse from lake sediments and accumulate in the anaerobic hypolimnetic water of productive lakes (Wetzel, 1983).

Sulphur is used in both organic and inorganic forms for protein synthesis. It is seldom limiting in fresh waters, but the dynamics of sulphate, and the hydrogen sulphide produced by the decomposition of organic matter, can alter conditions in stratified, productive lakes and so affect the cycling of other nutrients, as well as productivity and biotic distribution. Under strongly reducing conditions, sulphate is reduced to sulphide and under these conditions, highly insoluble metal sulphides can form. In hypereutrophic lakes, high concentrations of hydrogen sulphide can lead to significant decreases in dissolved iron (Wetzel, 1983). Hammer (1986) notes that  $H_2S$  is characteristic of the monimolimnia of all meromictic lakes and may coexist with oxygen in the chemoclines. Since  $H_2S$  has toxic properties, most life other than bacterial is excluded from zones rich in  $H_2S$ .

Quantitative information on the dynamics of other essential metallic micronutrients (i.e. zinc, copper, cobalt, molybdenum, vanadium, and selenium) is limited. In most natural waters, micronutrient concentrations and availability are usually adequate to meet metabolic requirements within the constraints of light, temperature, and macronutrient availability (Wetzel, 1983).

## **2.6 Conclusions**

A review of the relevant literature has shown that two distinct types of water bodies are usually associated with arid areas where evaporation exceeds inflow; namely ephemeral pans and perennial saline lakes. Pans can be seen to have multifarious origins with the key factors involved in their formation being salt weathering and aeolian deflation.

The sediments of pans and inland saline lakes are distinctly different. Pan sedimentary processes are governed by seasonal or episodic influxes of water and have characteristic, laterally zoned, mineral deposits. Perennial lake sediments are not regularly desiccated and tend to be formed through conventional lacustrine processes.

Evaporative concentration of the saline lake water leads to mineral precipitation and the deposition of chemical sediments. The process of brine evolution is dependent on the composition of the inflow waters as well as several fractionating mechanisms. Different evolutionary pathways influence both the nature of the chemical sediments formed and the final composition of the saline brine. Saline lake brines are usually chemically simple, being dominated by a few major ion species.

The transport and cycling of nutrients through the water, surrounding soil and sediments determines lake productivity. Very little information pertaining to plant basic nutrients in saline lake water has been recorded. For phosphorus, water–sediment interactions appear to be important determinants of its availability, sediments serving both as sources and sinks. Micronutrients are not normally limiting in water bodies.

### 3. THE AQUEOUS CHEMISTRY OF BARBER'S PAN

#### 3.1 Introduction

As was noted in Chapters one and two, very little literature is available on the aqueous chemistry of South African inland saline systems (Seaman *et al.*, 1991; Day, 1993). Furthermore, although pans comprise a large part of South African wetlands, they remain poorly classified (Goudie and Thomas, 1985) and Geldenhuys (1982) has suggested that improved predictive and management potential of South African pans can only be achieved through detailed limnological studies.

The biogeographical importance of Barber's Pan as a wetland of international importance, particularly from the point of view of avifauna conservation, has been confirmed by its RAMSAR status. The pan is also unique in that it is a perennial water body in an area characterized by shallow ephemeral waters. An understanding of its aqueous chemistry is essential if the pan ecosystem is to be effectively managed, because of the fundamental importance of the water to the pan biota. Day (1993) states that analyses of the pan water carried out by the Department of Water Affairs and Forestry (DWAF) provide the most complete record for the evaporative concentration of an inland pan in South Africa.

The main objectives of this chapter are to gain some insight into the aqueous chemistry of Barber's Pan. The chapter describes the methods used to collect water samples from the pan, analytical techniques used, and also discusses the results. The evolution of a saline brine in the pan is described and the behaviour of major solutes during this process is discussed. Chemical modelling was used to investigate mineral solubility equilibria and the speciation of ionic components in the water. The results of this modelling are described and then discussed with the intention of interpreting the water composition as well as evaluating the pollutant status of, and nutrient dynamics within, the pan.

## **3.2 Water sampling and analysis**

### **3.2.1 Sample collection**

A total of twenty water samples were taken from Barber's pan on the 7th and 8th of August 1995 from 5 sampling locations situated on a south–west to north–east transect across the pan (Fig. 14). The sample locations were determined by means of a geographical positioning system (GPS). The samples were collected in pre–rinsed plastic bottles. Four samples were collected at each of the five locations. Two of the four samples collected at each location were acidified to a pH of between 2 and 3 using 55% nitric acid ( $\text{HNO}_3$ ) to facilitate subsequent cation analysis. Samples were collected throughout the day and were analyzed after 2 weeks of storage at room temperature.

Supernatant water associated with nine of the Van Veen grab sediment samples was obtained by decanting water from the bottles containing the grab sediment samples. Only water above the sediment was decanted. These samples were also subjected to the various analyses carried out on the twenty samples described above. Pore water obtained through the centrifugation of the nine sediment samples was also analyzed.

### **3.2.2 Water analyses**

#### *3.2.2.1 On–site determinations*

Water depth at the point of sampling was determined using a graduated shot line. A Grant/YSI 3800 Water Quality Logging System (Fig. 15) was then used to determine the electrical conductivity (EC), pH, temperature, and salinity at depths of 0.25m, 1m, 2m, 3m and 4m, depending on the water depth at the particular sampling location. Salinity was computed by the Grant system from the temperature and uncompensated conductivity measurements. The maximum water depth measured was 4.3m.

### 3.2.2.2 Laboratory analyses

#### 3.2.2.2.1 Electrical conductivity (EC) and pH

EC was measured on unfiltered, unacidified water samples using a Crison Micro electrical conductivity meter, while pH was measured on the same unfiltered, unacidified water samples using a Crison Micro pH2001 pH meter.

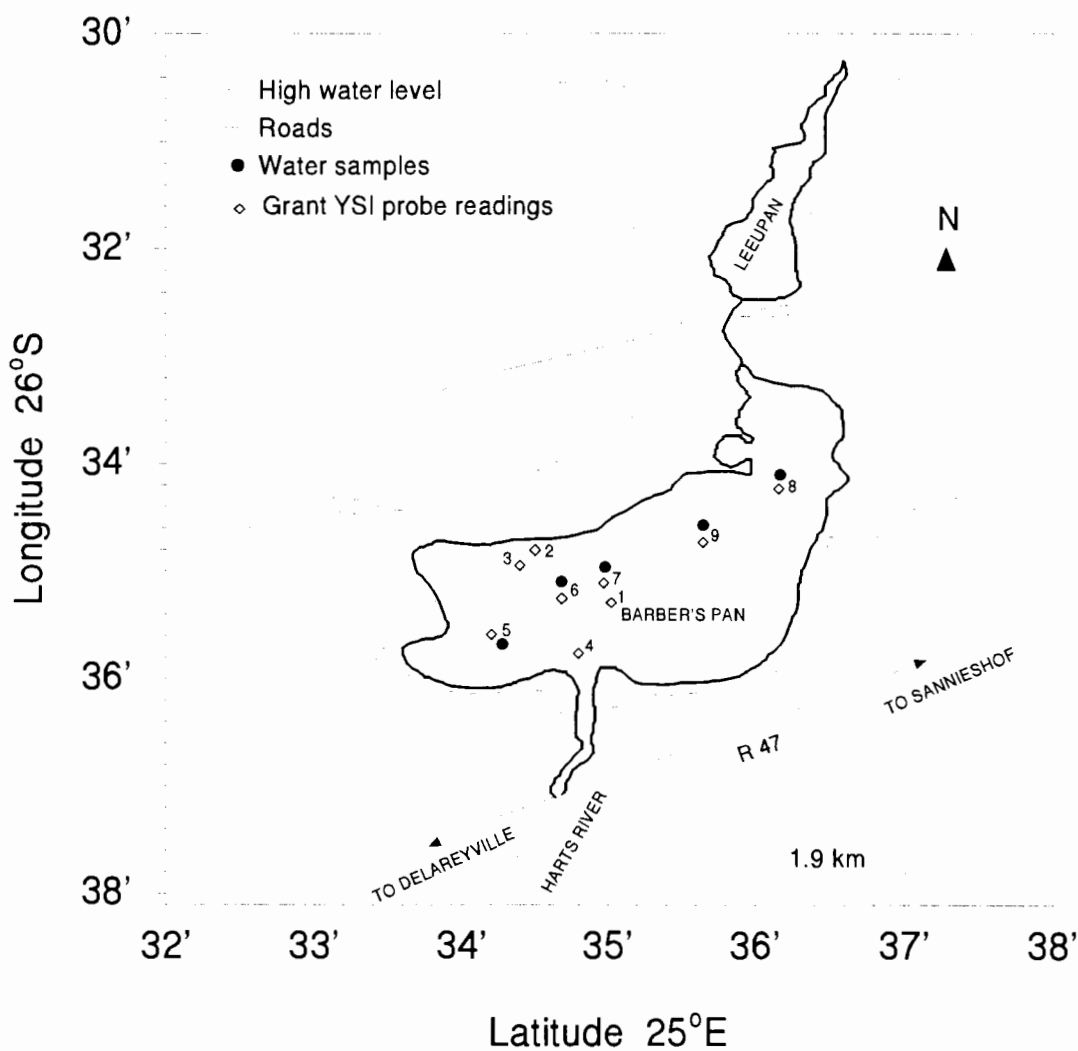


**Figure 14.** A map of the study area showing sites where bulk pan water samples and Grant/YSI 3800 probe readings were taken.

### 3.2.2.2.2 Alkalinity

The total alkalinity (end–point pH = 4.3) and carbonate (CO<sub>3</sub>) alkalinity (end–point pH = 8.3) of the unfiltered water samples was determined by means of an electrometric titration (as per American Public Health Association, 1985). This involved titrating a 30ml aliquot of sample against 0.025M HCl. A Crison Micro pH2001 pH meter was used to determine the end–points.

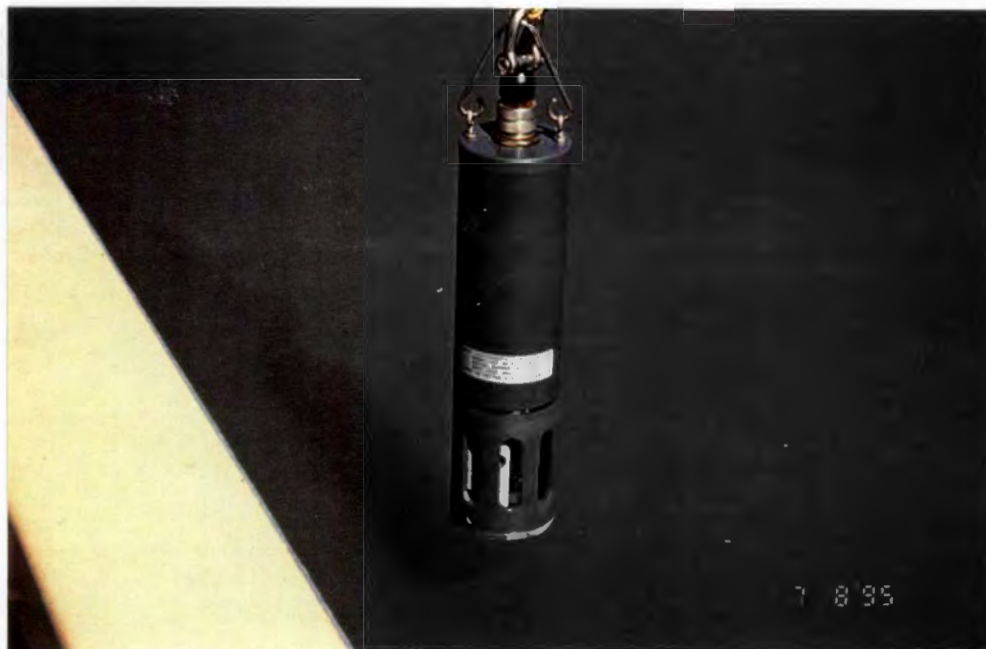


**Figure 15:** The Grant/YSI 3800 Water Quality Logging System used for on-site determinations of EC, pH, temperature, and salinity.

### 3.2.2.2.3 Anions

High performance ion chromatography (HPIC) was used to determine the Cl<sup>-</sup>, SO<sub>4</sub><sup>2-</sup>, NO<sub>2</sub><sup>-</sup>, NO<sub>3</sub><sup>-</sup>, PO<sub>4</sub><sup>3-</sup> and Br<sup>-</sup> content of the filtered, unacidified water samples. Deionised water was used to dilute the samples to an EC < 100 µS/cm prior to the analysis. Deionized water was prepared by passing tap water through a Milli-Q system (Millipore Corporation, Bedford, U.S.A). In brief, tap water is first filtered through 30 and 3µm filters. It then passes through a reverse osmosis membrane and organics-removal cartridge before being deionized. Finally the water is filtered through a 0.22µm filter.

The analysis was carried out by means of a Dionex DX300 series suppressed IC system, which was coupled to the AI-450 chromatography software package. An HPIC-AG4A column was used as a guard column, with an HPIC-AS4A-SC separator column. The eluent flow rate was 2.0 ml/min and suppression was achieved by an anion micromembrane suppressor (AMMS). A mixed sodium carbonate/sodium bicarbonate (1.80 mM Na<sub>2</sub>CO<sub>3</sub>; 1.70 mM NaHCO<sub>3</sub>) eluent was used. The run time per sample was 8 minutes. The water samples were filtered through an On-Guard P filter to remove organics and particulates prior to the analysis. The detection limits of the apparatus used for the anions determined was of the order of 1 mg.dm<sup>-3</sup> (Willis, pers comm.)<sup>2</sup>.

#### 3.2.2.2.4 Phosphate

Phosphate (PO<sub>4</sub><sup>3-</sup>) was also determined colorimetrically using the method of Murphy and Riley (1962). A Turner Corporation (California, U.S.A.) model 340 spectrophotometer was used for the determinations. The method is considered to be specific for the orthophosphate (PO<sub>4</sub><sup>3-</sup>) form of phosphorus, and entails the conversion of orthophosphate to phosphomolybdate by acidified ammonium molybdate reagent.

#### 3.2.2.2.5 Total elemental concentrations

Inductively coupled plasma atomic emission spectroscopy (ICP-AES) was used to determine the total concentrations of zinc, lead, nickel, silicon, manganese, iron, magnesium, aluminium, copper, calcium, sodium and potassium.

A Jobin/Yvon 70C combined simultaneous/sequential ICP spectrometer was used for the analysis, together with J-Yess version 4.0 software. Instrumental conditions and detection limits as per Potts (1987) and Thomas and Goldstone (1994).

#### 3.2.2.2.6 Silicon

The blue silicomolybdous acid procedure (Weaver *et al.*, 1968) was used to determine soluble Si. This procedure employs the blue silicomolybdous acid complex for the colorimetric

---

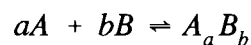
<sup>2</sup> Assoc. Prof. J.P. Willis, Department of Geological Sciences, University of Cape Town.

determination of Si. A Turner Corporation (California, U.S.A.) model 340 spectrophotometer was used for the actual determinations.

### 3.2.2.2.7 Prediction of chemical speciation and saturation indices (S.I.)

The mathematical model MINTEQA2 (Allison *et al.*, 1991), a geochemical equilibrium speciation model for dilute aqueous systems, was used to investigate the ionic speciation occurring in the Barber's Pan water, as well as to calculate saturation indices for minerals likely to occur under the prevailing conditions.

MINTEQA2 is based on the assumption of thermodynamic equilibrium between phases, with the thermodynamic equilibrium constant defined as follows:



$$K^0 = \frac{A_a B_b}{A^a B^b}$$

where A and B are chemical entities that react to form a reaction product  $A_a B_b$ , having a thermodynamic equilibrium constant  $K^0$ . MINTEQA2 uses the Davies equation to quantify the various chemical reactions modelled. The Davies equation is an extension of the Debye–Hückel equation in which the ion–size–dependent parameters are the same for each charged ion (Lumsdon and Evans, 1995).

$$\log y_i = -Az^2 \left( \frac{\sqrt{I}}{1+\sqrt{I}} - 0.24I \right)$$

**z** = valence of ion species

**y<sub>i</sub>** = Activity Coefficient

**A** =  $1.82 \times 10^6 (\epsilon T)^{-3/2}$

**I** = Ionic Strength ( $\text{mol.dm}^{-3}$ )

**ε** = Dielectric Constant (78.3 for water at 298 K)

**T** = Absolute Temperature (K)

### **3.2.3 Department of Water Affairs and Forestry (DWAF) database**

Water analyses carried out on Barber's Pan by the Department of Water Affairs and Forestry (DWAF) over the period 24th July 1982 to 1st June 1995 (a total of 290 analyses) were obtained. This data set comprises the most complete record of evaporative concentration for a South African pan (Day, 1993) and allows for a comprehensive discussion of brine evolution in the pan. The full data set is given in Appendix 3.

A comprehensive description of the analytical methods used by the DWAF can be found in van Vliet *et al.* (1988). In summary, metals are determined by atomic absorption spectrophotometry, chloride and alkalinity titrimetrically and TDS and sulphate gravimetrically. The samples were not preserved prior to analysis (Day, 1993).

## **3.3 Results and discussion of water analyses**

### **3.3.1 On-site determinations**

On-site determinations with the Grant/YSI 3800 Water Quality Logging System were taken at sample sites 1–9 (Fig. 14) (data in Appendix 1). These indicated that the bulk pan water composition, in terms of pH, EC, temperature and salinity, was very uniform throughout the pan, with no evidence of stratification. The pH values recorded on site ranged between 9.0 and 9.8, with a mean value of 9.5, while EC values ranged from 1.83 to 2.14 mS/cm, having a mean of 1.96 mS/cm. Salinity showed a range of 1.2–1.4‰, while temperature decreased with depth, from between 12–15°C in the upper 0.25m to around 11°C at depths of 3–4m. The deepest point recorded with the graduated shot–line was 4.3m. This depth is substantially lower than the 7–8m levels recorded during 1994 by the Department of Water Affairs and Forestry (DWAF); the reduction being attributable to evaporation and drought conditions which have prevailed over the last year.

### 3.3.2 Laboratory analyses

#### 3.3.2.1 Electrical conductivity (EC)

Results of the various water analyses carried out on the bulk, supernatant and interstitial water samples are given in Tables 3, 4 and 5.

EC's recorded for the bulk pan water were very consistent, all in the range 1.90–1.94 mS/cm. These results compared well with the on-site determinations made using the Grant/YSI 3800 Water Quality Logging System as well as with DWAF data collected over the past 14 years.

Sediment supernatant waters obtained from various sediment samples were found to have EC values which were slightly higher than those of the bulk pan water samples, being in the range 1.96–2.36 mS/cm. Sediment interstitial waters had EC values ranging from 2.10 to 2.43 mS/cm, which are greater than those recorded for the bulk pan water, and in some instances for the supernatant water.

Hammer (1986) states that the salinity of an inland water may be regarded as representing the concentration of all ionic constituents present. Total dissolved solids (TDS) is a measure of the total amount of material dissolved in a water sample. It is usually measured by weighing the residue from a known volume of filtered water (pore size 0.2–0.5 µm) evaporated to dryness at a temperature (< 70°C) low enough to prevent the volatilization of labile dissolved organic carbon (Dallas and Day, 1993).

The EC of a water sample is often determined in place of TDS. Since it is a function of the number of charged particles (ions) in solution and the majority of dissolved material in most waters are ionic, TDS and EC usually correlate closely for a particular type of water (Dallas and Day, 1993). Hammer (1986) states that a number of studies investigating the relationship between EC and TDS in saline lakes in Saskatchewan as well as in Australia showed highly significant correlations between the two parameters. The determination of EC is also far quicker and more convenient than the determination of TDS.

**Table 3:** Analysis of Barber's Pan bulk pan water (duplicate water samples from the same sampling location are denoted x and y).

Sample No.	5x	5y	6x	6y	7x	7y	8x	8y	9x	9y
<b>Alkalinity (as mg.dm<sup>-3</sup> CaCO<sub>3</sub>)</b>										
CO <sub>3</sub> <sup>2-</sup>	62.5	64.2	60	58.3	58.8	59.2	73.3	58.3	58.3	60
HCO <sub>3</sub> <sup>-</sup>	579	530	554	559	530	530	530	546	529	532
Total	642	595	614	611	589	589	600	605	587	592
<b>EC (mS/cm)</b>	1.93	1.94	1.92	1.93	1.92	1.93	1.92	1.90	1.91	1.91
<b>pH</b>	9.2	9.2	9.2	9.2	9.3	9.3	9.2	9.2	9.2	9.2
<b>Anions (mg.dm<sup>-3</sup>)</b>										
Cl <sup>-</sup>	373	368	362	369	347	364	375	374	370	367
SO <sub>4</sub> <sup>2-</sup>	36.8	36.2	36.2	36.4	34.2	37.1	35.5	36.3	35.9	35.8
PO <sub>4</sub> <sup>3-</sup>	0.06	0.02	0.01	0.02	0.02	0.03	0.02	0.02	BDL	BDL
<b>Total Elemental Concentrations (mg.dm<sup>-3</sup>)</b>										
Si <sup>1</sup>		0.31		0.34	0.37	0.43	0.54	0.36	0.32	0.34
Si <sup>2</sup>		1.40		1.20	1.38		1.75		1.23	
Zn		0.07		0.08	0.16		0.07		0.12	
Pb		0.39		0.44	0.50		0.37		0.49	
Ni		0.08		0.21	0.17		0.01		0.11	
Mn		BDL		BDL	0.04		BDL		0.04	
Fe		0.41		0.39	0.36		0.40		0.31	
Mg		72.3		71.2	73.1		72.5		73.2	
Al		1.21		0.89	0.88		1.85		0.62	
Cu		0.001		0.01	0.01		0.003		0.01	
Ca		16.5		16.2	16.8		17.5		16.6	
Na		366		363	360		364		362	
K		71.9		71.4	70.6		71.5		71.3	

Explanatory Notes for Table 3: <sup>1</sup> – dissolved Si determined by Silicomolybdous blue method  
<sup>2</sup> – total Si determined by ICP–AES  
BDL – below detection limits

For South Africa as a whole, Dallas and Day (1993) record the following relationship between TDS and EC:

$$\text{TDS (mg.dm}^{-3}\text{)} = \text{EC (mS.m}^{-1}\text{)} \times 6.6$$

They note, however, that this relationship does not hold particularly well for waters very rich in dissolved organic carbon, and that variations occur in the relationship depending on the proportions of major ions in solution.

The average EC for the bulk pan water was recorded as 1.92mS.cm<sup>-1</sup>. Using the above mentioned formula, this translates to a TDS value of 1.3 g.dm<sup>-3</sup>. Hammer (1986) defines athalassic saline lake waters as those having salinities greater than or equal to 3 g.dm<sup>-3</sup>. Waters having salinities between 0.5 and 3 g.dm<sup>-3</sup> are classified as subsaline, while freshwaters have < 0.5 g.dm<sup>-3</sup> salinity. With its present solute load, Barber's Pan can, therefore, be classified as subsaline. The maximum EC value (1080 mS/m) recorded for the most concentrated water sample in the DWAF database, produced an equivalent value of 7.1 g.dm<sup>-3</sup> TDS.

This indicates that, at its most concentrated, the pan would definitely be classified as saline. This large difference in TDS values can be attributed to cycles of evaporative concentration of the pan followed by periodic inundations of water from the Harts River, suggesting that these are the major mechanisms controlling the salinity of the pan water.

Dallas and Day (1993) note that the term *salinity* is often used to describe the saltiness of water and state that it is usually defined as the mass (g) of dissolved inorganic solids in 1kg of sea water. In sea water, the quantity of dissolved organic matter (DOM) is very small relative to the amount of inorganic matter, with the consequence that salinity and TDS are virtually the same in sea water. In fresh water, however, the proportion of DOM may form a significant fraction of the whole, causing salinity and TDS to differ quite significantly. In Barber's Pan, on site determinations with the Grant/YSI 3800 Water Quality Logging System (discussed in 3.3.1) gave salinity values ranging between 1.2 – 1.4‰, which are very similar to the calculated TDS average of 1.3 g.dm<sup>-3</sup>. This suggests that the quantity of DOM in the bulk Pan water is very small relative to the amount of dissolved inorganic matter.

**Table 4:** Analysis of Barber's Pan sediment supernatant.

Sample No.	4	5	10	17
<b>Alkalinity (as mg.dm<sup>-3</sup> CaCO<sub>3</sub>)</b>				
CO <sub>3</sub> <sup>2-</sup>		4.6		
HCO <sub>3</sub> <sup>-</sup>		663	678	641
Total	*	668	*	*
<b>EC (mS/cm)</b>	2.12	1.97	2.01	2.01
<b>pH</b>	8.5	8.2	8.1	8.2
<b>Anions (mg.dm<sup>-3</sup>)</b>				
Cl <sup>-</sup>	336	363	357	359
SO <sub>4</sub> <sup>2-</sup>	19.2	11.7	9.8	18.8
PO <sub>4</sub> <sup>3-</sup>	BDL	BDL	0.16	0.01
<b>Total Elemental Concentrations (mg.dm<sup>-3</sup>)</b>				
Si <sup>1</sup>		5.99	4.72	3.00
Si <sup>2</sup>	7.40	9.15	7.01	5.78
Zn	0.06	0.16	0.08	0.07
Pb	0.41	0.92	0.45	0.46
Ni	0.28	0.11	0.12	0.05
Mn	BDL	0.04	0.05	0.04
Fe	0.13	0.27	0.15	0.13
Mg	97.8	76	87.6	83.6
Al	0.16	0.24	0.20	0.13
Cu	0.01	0.06	0.01	BDL
Ca	25.9	17.5	19.7	20.0
Na		370	365	360
K		63.5	74.1	65.3

Explanatory Notes for Table 4:

<sup>1</sup> – Si determined by Silicomolybdous blue method<sup>2</sup> – Si determined by ICP–AES

BDL – below detection limit

\* - Alkalinity was not determined for certain samples due to insufficient sample volume

**Table 5:** Analysis of Barber's Pan sediment interstitial water.

<b>Sample No.</b>	<b>4</b>	<b>5</b>	<b>8</b>	<b>16</b>	<b>17</b>
<b>EC (mS/cm)</b>	2.10	2.10	2.27	2.20	2.26
<b>pH</b>	8.5	8.5	8.2	8.0	8.7
<b>Anions (mg.dm<sup>-3</sup>)</b>					
Cl <sup>-</sup>	365	368	370	399	360
SO <sub>4</sub> <sup>2-</sup>	12.6	18.7	10.4	20.2	8.2
PO <sub>4</sub> <sup>3-</sup>	0.26	0.10	0.55	2.1	0.44
<b>Total Elemental Concentrations (mg.dm<sup>-3</sup>)</b>					
Si <sup>1</sup>	6.5	4.2	9.1	10	6.2
Si <sup>2</sup>	9.03	8.6	18.5	16.9	10.7
Zn	0.15	0.16	0.07	0.07	0.30
Pb	0.94	1.02	0.50	0.51	2.02
Ni	0.34	0.18	BDL	0.25	0.24
Mn	BDL	BDL	0.04	0.09	BDL
Fe	0.23	0.24	0.22	0.19	0.46
Mg	79.8	81.3	104	90	102
Al	0.13	0.16	0.28	0.22	0.29
Cu	0.05	0.02	0.01	BDL	0.03
Ca	22.3	18.8	29.4	29	26.4
Na	328	360	371	369	396
K	55.8	77.3	77.5	74.4	66

Explanatory Notes for Table 5:

<sup>1</sup> – Si determined by Silicomolybdous blue method<sup>2</sup> – Si determined by ICP–AES

BDL – below detection limit

Alkalinity was not determined due to insufficient sample volume

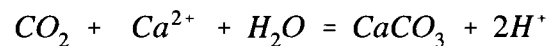
Unavailability of suitable instrumentation at the time the analyses were carried out prevented DOM from being determined in the pan water.

### 3.3.2.2 pH

The pan water was found to be very alkaline, all samples having pH values of about 9.2. This is in agreement with Water Affairs data collected over the past 14 years and also compares closely with the on-site determinations made with the Grant/YSI 3800 Water Quality Logging System.

The pH values determined for the supernatant waters were found to range from 7.9 to 8.5, while those of the interstitial water samples varied between 8.0 and 8.7. Both are approximately 1 order of magnitude lower than the pan water samples.

The lower pH of the supernatant and pore water samples may be attributable to microbial-reduction in the largely anaerobic sediments leading to the production of H<sub>2</sub>S. This is discussed further in section 3.3.3. Hammer (1986) records that Timms and Brand (1973) found that H<sub>2</sub>S accumulation probably lowers pH. Alternately, the production of CO<sub>2</sub> through the microbial decomposition of organic matter could possibly lead to the precipitation of Ca as CaCO<sub>3</sub> by the following reaction:



The production of H<sup>+</sup> ions by this reaction would be promoted at high pH, consuming alkalinity and lowering the pH.

The rates of bacterial sulphur metabolism *in situ* have only been studied in a few aquatic systems, but in several of those that have been studied the most intensive rates of bacterial reduction of sulphates occurred close to sediments and in the water layers on the littoral slopes at the upper boundary of the anaerobic H<sub>2</sub>S zone. Actual rates of sulphate reduction within sediments have been shown to vary between lakes, but have generally been lower in the sediment than in the overlying water (Wetzel, 1983). This may explain why the pH values recorded for the sediment supernatant water samples were, in most cases, lower than those recorded for the interstitial water samples.

The pH of natural waters has an important influence on chemical reactions accompanying sedimentary processes, being particularly significant in controlling the precipitation of various

mineral solids. pH also plays an important role in the transport of alumina and silica in solution. Aluminium hydroxide ( $\text{Al}[\text{OH}]_3$ ) is readily soluble at pH values  $< 4$  and  $> 9$ , but is virtually insoluble between pH 5 and 9 (Fig. 16). Silica solubility increases with increasing pH (Fig. 16). In Barber's Pan, the total Al concentration recorded in the bulk pan water is on average 5x greater than that recorded in the interstitial water. This is likely to be a consequence of the difference in pH between the bulk and interstitial waters, with the Al being largely insoluble at the lower pH values recorded in the interstitial water. Si does not follow this trend, having far lower concentrations in the bulk pan water than in the interstitial water. This may be attributable to a number of factors including biological uptake (by diatoms), and the presence of colloidal Si from the hydrolysis of clay minerals. This is discussed further in section 3.3.2.5.10.

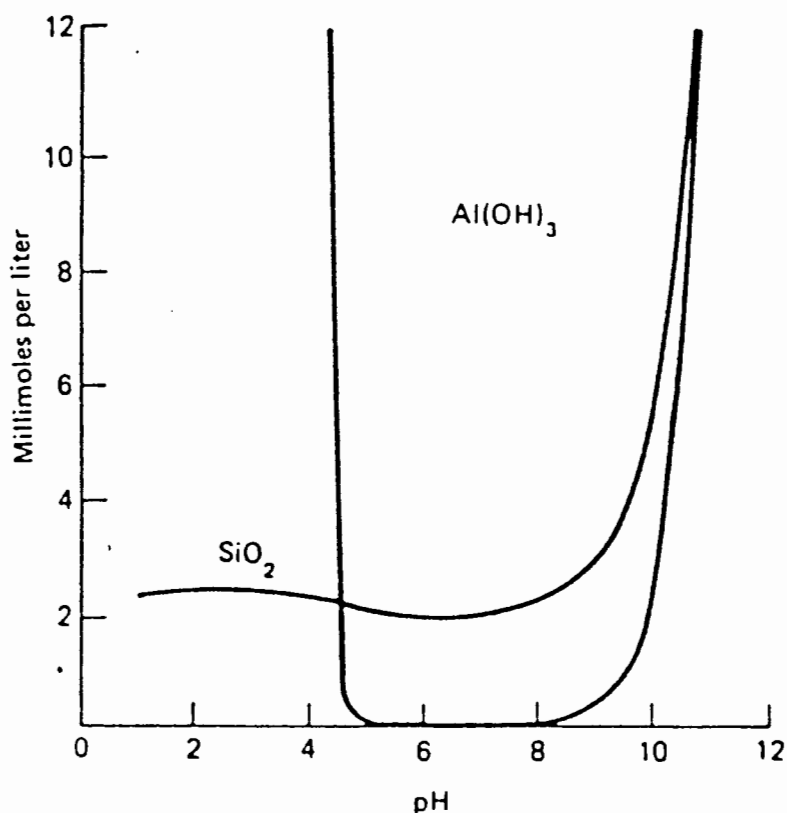


**Figure 16:** The solubility of amorphous silica and aluminium hydroxide as a function of pH at 25 °C (from Mason and Moore, 1982).

### 3.3.2.3 Alkalinity

Stumm and Morgan (1970) define alkalinity as follows: "for solutions that contain no protolysis system other than that of aqueous carbonate, alkalinity is a measure of the quantity of acid per litre required to attain a pH equal to that of a  $C_T$ -molar solution of  $\text{H}_2\text{CO}_3$ ". Dallas and Day (1993) record that the most important buffering system in natural waters is

the carbonate–bicarbonate one and propose that alkalinity can, therefore, be viewed as a measure of buffering capacity.

Very high alkalinities were recorded in the bulk pan water and sediment supernatant water, with the three alkalinities determined from the sediment supernatant water being approximately 10 % higher than those of the bulk pan water.

Alkalinity was not determined for the sediment interstitial waters as there was insufficient volume of sample in all cases.

Barber's Pan is, therefore, likely to be very well buffered. Evidence for this extensive buffering can be seen in the relatively high pH of the sediment supernatant and interstitial waters, despite the reducing environment of the sediments and likely formation of iron sulphides. The formation of iron sulphides is discussed further in section 3.3.3.

#### 3.3.2.4 Ion dominance in Barber's Pan

As discussed in section 2.4.1 for all practical purposes, the concentrations of the four major cations ( $\text{Ca}^{2+}$ ,  $\text{Mg}^{2+}$ ,  $\text{Na}^+$  and  $\text{K}^+$ ) and the four major anions ( $\text{HCO}_3^-$ ,  $\text{CO}_3^{2-}$ ,  $\text{SO}_4^{2-}$  and  $\text{Cl}^-$ ) usually constitute the total ionic salinity of water. The average concentration of these constituents for the bulk pan water are reflected in Table 6.

From Table 6, the dominant anion determined in the bulk pan water can be seen to be  $\text{Cl}^-$ . The only other anions present in significant quantities were  $\text{HCO}_3^-$ ,  $\text{CO}_3^{2-}$  and  $\text{SO}_4^{2-}$ .

$\text{NO}_2^-$  and  $\text{NO}_3^-$  levels were found to be below the detection limits of the HPIC.  $\text{F}^-$  levels of between  $0.2\text{--}0.3 \text{ mmol}\cdot\text{dm}^{-3}$  ( $3\text{--}5 \text{ mg}\cdot\text{dm}^{-3}$ ) were also recorded by the ion chromatograph. These levels cannot, however, be considered to be accurate since the Dionex suppressed ion chromatography system used fails to distinguish the  $\text{F}^-$  peak from a pronounced water dip when using  $\text{NaCO}_3/\text{NaHCO}_3$  eluent, making accurate quantitative determinations difficult (Willis, pers comm.)<sup>3</sup>.  $\text{Br}^-$  levels ranging between  $0.04\text{--}0.06 \text{ mmol}\cdot\text{dm}^{-3}$  ( $3.7\text{--}4.8 \text{ mg}\cdot\text{dm}^{-3}$ ) were also determined in five of the bulk pan water samples

---

<sup>3</sup> Assoc. Prof. J.P. Willis, Department of Geological Sciences, University of Cape Town.

that were only subject to a ten times dilution prior to being analyzed by the ion chromatograph.

**Table 6:** The average concentration of the major ionic constituents of bulk pan water from Barber's Pan.

Ionic Constituent	Concentration (mmol $\cdot$ dm $^{-3}$ )
Anions	
Cl $^{-}$	10.2
HCO $_3^{-}$	12.0
CO $_3^{2-}$	1.2
SO $_4^{2-}$	0.7
Cations*	
Na $^{+}$	15.8
Mg $^{2+}$	6.0
K $^{+}$	1.8
Ca $^{2+}$	0.84

\* Assuming elements determined by ICP–AES are present in ionic form.

Cation determinations could not be made using the Dionex DX300 series suppressed IC system as a consequence of instrumental problems; instead total elemental concentrations of Zn, Pb, Ni, Si, Mn, Fe, Mg, Al, Cu, Ca, Na and K were determined using ICP–AES. By far the most dominant element determined by ICP–AES was Na, which would, therefore, most likely be the dominant cation. In addition to Na, the other dominant elements present in the bulk pan water were found to be Mg, K and Ca. All other elements analyzed for were found to be present in trace amounts.

The ion relationship of the bulk pan water was Na>Mg>K>Ca which differs from the common cationic proportions of Ca>Na>Mg>K attributed by Wetzel (1983) to water draining from igneous rock. Combrinck (1966) stated that Barber's Pan cannot be considered a typical hard–water lake since the carbonates, sulphates and chlorides occur in the proportions Cl>CO $_3$ >SO $_4$ , and not the typical CO $_3$ >Cl>SO $_4$ . This is indeed the case, with the ionic proportions of the bulk pan water reflecting the relationship described by Combrinck (1966).

Combrinck (1966) recorded relatively low values of total hardness for the pan water, ascribing this to low concentrations of Mg in the water of the Little Harts River (Smuts' diversion), and to the fact that the  $\text{CaCO}_3$  has a tendency to precipitate (low solubility product) at pH values greater than 8.4, particularly in the presence of high concentrations of other more soluble salts, as is the case in Barber's Pan.

The bulk pan water is, therefore, dominated by  $\text{Na}^+$  and  $\text{Cl}^-$ . Waters in the majority of South African saline pans are dominated by  $\text{Na}^+$  and  $\text{Cl}^-$  ions (Seaman *et al.*, 1991 ; Silberbauer and King, 1991) as are most salt lakes world wide (Hammer, 1986). A Piper plot of the average bulk water composition is given in Figure 18. The data in Table 6 was used to determine the average bulk water composition. Comparing Figure 18 with the hydrochemical facies given in Figure 17 confirms the classification of the bulk pan water as a NaCl-dominated water.

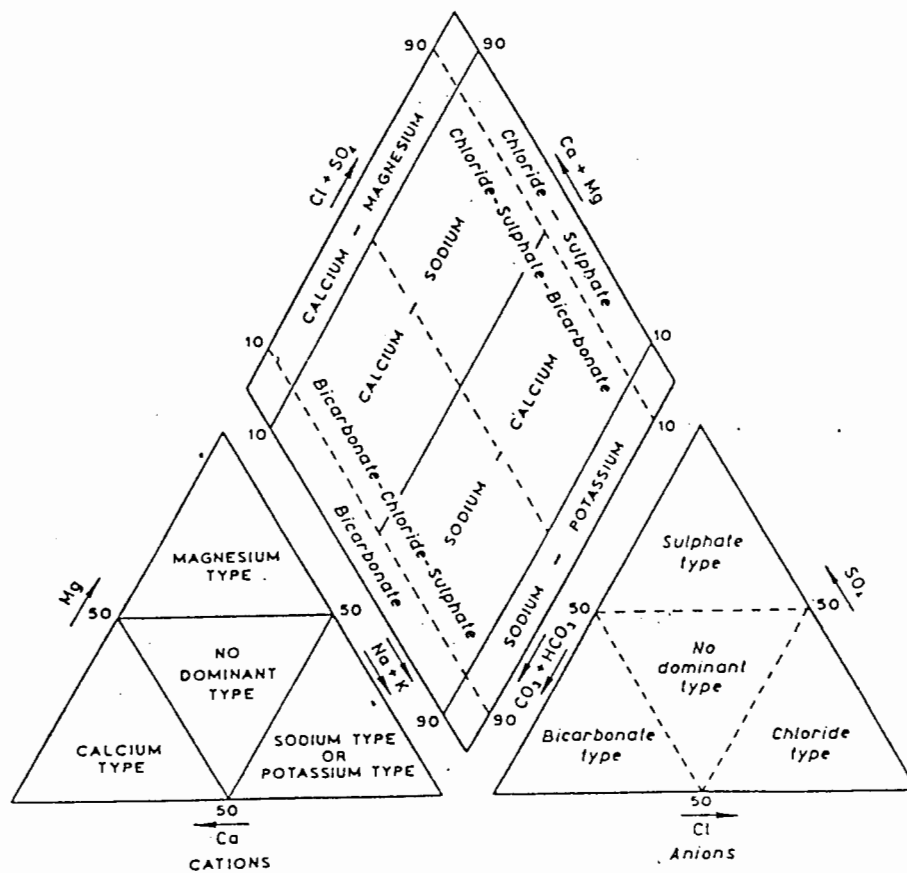


**Figure 17:** Piper trilinear diagram showing hydrochemical facies (from Ward, 1975).

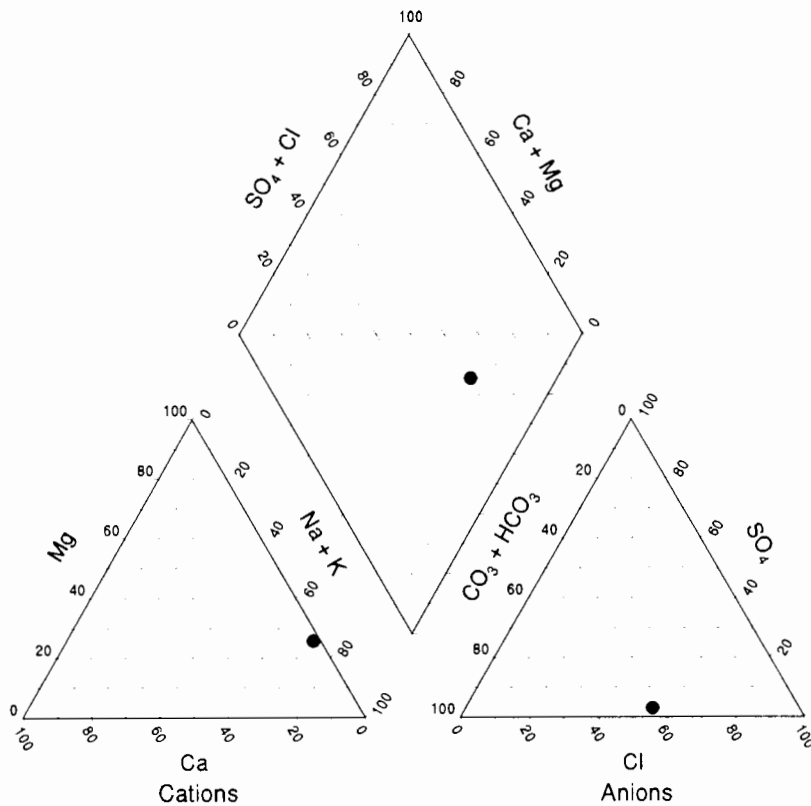


**Figure 18:** A Piper diagram representation the average bulk water composition of Barber's Pan.

### 3.3.2.5 Chemical speciation modelling

There is a growing realization that the distribution, mobility and biological availability of chemical elements depends not simply on their concentrations but, critically, on the chemical and physical associations which they undergo in natural systems. Changes in environmental conditions, whether natural or anthropogenic, can strongly influence the behaviour of both essential and toxic elements by altering the forms in which they occur. Among the most important controlling variables are pH, redox potential and the availability of "reactive" species such as complexing ligands, both organic and inorganic, colloidal matter and particle surfaces for adsorption (Ure and Davidson, 1994).

The geochemical equilibrium speciation modelling programme MINTQA2 was used to model the speciation occurring in the pan water. As the composition of the bulk pan water has been shown to be extremely homogeneous, a single run through the model (using bulk pan water sample 5) was sufficient to provide a typical speciation for the bulk pan water (see

Table 7). The speciation for interstitial water sample 5 is given in Table 8. An example of the complete output from a MINTEQA2 run is given in Appendix 4.

#### 3.3.2.5.1 Charge balance

Charge balances calculated by MINTEQA2 for the various samples prior to speciation were in the range 1 – 5%, suggesting that the concentrations of most of the major ions had been accounted for. As no alkalinity values were determined for the interstitial water samples, alkalinity values for these samples were estimated by comparison with the equivalent supernatant water sample and then correlated with charge balance. In all cases the charge balance before speciation remained < 5%, confirming the validity of the assumed concentrations.

#### 3.3.2.5.2 Calcium

MINTEQA2 predicted that Ca in the bulk pan water was largely in the form of the free ion  $\text{Ca}^{2+}$ , with  $\text{CaHCO}_3^+$ ,  $\text{CaCO}_3^0$  and  $\text{CaSO}_4^0$  occurring as minor species. In the interstitial waters,  $\text{Ca}^{2+}$  was also predicted as the dominant species with  $\text{CaHCO}_3^+$  and  $\text{CaCO}_3^0$  occurring as minor species. Negligible  $\text{CaSO}_4^0$  was predicted to occur in the interstitial waters. This may be a consequence of several factors, namely: the the lower concentration of  $\text{SO}_4^{2-}$  in this more reduced environment and the the higher concentrations of  $\text{HCO}_3^-/\text{CO}_3^{2-}$  (refer to 3.3.3 for discussion).

Day (1993) notes that Barber's Pan is an unusual system in that Mg dominates over Ca even at low salinities. MINTEQA2 predicted that the pan waters are supersaturated with respect to calcite and aragonite which would account for the removal of much of the Ca from the water to the sediments. This is discussed further in section 3.3.2.6. Another possible explanation for the relatively low calcium is a high rate of biological uptake. Day (1993) states that charophytes (*Chara* sp.) on the pan bottom could possibly sequester sufficient calcium to reduce the concentration of  $\text{Ca}^{2+}$  in the pan water. The most likely cause for the low calcium, however, is the precipitation of carbonate minerals in view of the fact that the water is supersaturated with respect to them, implying that there is potential for still further calcium carbonate precipitation.

**Table 7:** Chemical species predicted by MINTEQA2 as likely to be present in bulk pan water sample no. 5.

Constituent	Percentage Speciation Predicted
Na	Na <sup>+</sup> (99.5%)
Mg	Mg <sup>2+</sup> (86%), MgCO <sub>3</sub> <sup>0</sup> (10%), MgHCO <sub>3</sub> <sup>+</sup> (3%), MgSO <sub>4</sub> <sup>0</sup> (1%)
K	K <sup>+</sup> (99.9%)
Ca	Ca <sup>2+</sup> (83%), CaCO <sub>3</sub> <sup>0</sup> (14%), CaHCO <sub>3</sub> <sup>+</sup> (2%), CaSO <sub>4</sub> <sup>0</sup> (1%)
Cl	Cl <sup>-</sup> (100%)
CO <sub>3</sub>	HCO <sub>3</sub> <sup>-</sup> (85%), CO <sub>3</sub> <sup>2-</sup> (8%), MgCO <sub>3</sub> <sup>0</sup> (5%), MgHCO <sub>3</sub> <sup>+</sup> (1%)
SO <sub>4</sub>	SO <sub>4</sub> <sup>2-</sup> (84%), MgSO <sub>4</sub> <sup>0</sup> (10%), NaSO <sub>4</sub> <sup>-</sup> (3%) CaSO <sub>4</sub> <sup>0</sup> (2%)
PO <sub>4</sub>	MgPO <sub>4</sub> <sup>-</sup> (48%), HPO <sub>4</sub> <sup>2-</sup> (31%), MgHPO <sub>4</sub> <sup>0</sup> (14%), CaPO <sub>4</sub> <sup>-</sup> (5%), CaHPO <sub>4</sub> <sup>0</sup> (1%)
Si	H <sub>4</sub> SiO <sub>4</sub> (90%), H <sub>3</sub> SiO <sub>4</sub> <sup>-</sup> (10%)
Pb	Pb(CO <sub>3</sub> ) <sub>2</sub> <sup>2-</sup> (55%), PbCO <sub>3</sub> <sup>0</sup> (45%)
Zn	Zn(CO <sub>3</sub> ) <sub>2</sub> <sup>2-</sup> (86%), ZnCO <sub>3</sub> <sup>0</sup> (8%), Zn(OH) <sub>2</sub> <sup>0</sup> (6%)
Cu	Cu(OH) <sub>2</sub> <sup>0</sup> (96%), CuCO <sub>3</sub> <sup>0</sup> (2%), Cu(CO <sub>3</sub> ) <sub>2</sub> <sup>2-</sup> (1%)
Ni	NiCO <sub>3</sub> <sup>0</sup> (54%), Ni(CO <sub>3</sub> ) <sub>2</sub> <sup>2-</sup> (46%)
Al	Al(OH <sub>4</sub> ) <sup>-</sup> (85%), Al(OH) <sub>3</sub> <sup>0</sup> (16%)
Fe	Fe <sup>2+</sup> (88%), FeOH <sup>+</sup> (10%), FeSO <sub>4</sub> <sup>0</sup> (1%)
H <sub>2</sub> O	Al(OH <sub>4</sub> ) <sup>-</sup> (84%), Al(OH) <sub>3</sub> <sup>0</sup> (12%), OH <sup>-</sup> (4%)
H	HCO <sub>3</sub> <sup>-</sup> (101%), MgHCO <sub>3</sub> <sup>+</sup> (2%)
F	F <sup>-</sup> (94%), MgF <sup>+</sup> (6%)

**Table 8:** Chemical species predicted by MINTEQA2 as likely to be present in interstitial pan water sample no. 5.

Constituent	Percentage Speciation Predicted
Na	Na <sup>+</sup> (99.7%)
Mg	Mg <sup>2+</sup> (93%); MgCO <sub>3</sub> <sup>0</sup> (3%); MgHCO <sub>3</sub> <sup>+</sup> (4%)
K	K <sup>+</sup> (100%)
Ca	Ca <sup>2+</sup> (93%), CaCO <sub>3</sub> <sup>0</sup> (4%), CaHCO <sub>3</sub> <sup>+</sup> (2%)
Cl	Cl <sup>-</sup> (100%)
CO <sub>3</sub>	HCO <sub>3</sub> <sup>-</sup> (94%), CO <sub>3</sub> <sup>2-</sup> (2%), MgCO <sub>3</sub> <sup>0</sup> (1%), MgHCO <sub>3</sub> <sup>+</sup> (2%)
SO <sub>4</sub>	SO <sub>4</sub> <sup>2-</sup> (82%), MgSO <sub>4</sub> <sup>0</sup> (12%), NaSO <sub>4</sub> <sup>-</sup> (3%) CaSO <sub>4</sub> <sup>0</sup> (2%)
PO <sub>4</sub>	MgPO <sub>4</sub> <sup>-</sup> (19%), HPO <sub>4</sub> <sup>2-</sup> (48%), MgHPO <sub>4</sub> <sup>0</sup> (26%), CaPO <sub>4</sub> <sup>-</sup> (2%), CaHPO <sub>4</sub> <sup>0</sup> (3%), H <sub>2</sub> PO <sub>4</sub> <sup>-</sup>
Si	H <sub>4</sub> SiO <sub>4</sub> (98%), H <sub>3</sub> SiO <sub>4</sub> <sup>-</sup> (2%)
Pb	Pb(CO <sub>3</sub> ) <sub>2</sub> <sup>2-</sup> (22%), PbCO <sub>3</sub> <sup>0</sup> (77%)
Zn	Zn(CO <sub>3</sub> ) <sub>2</sub> <sup>2-</sup> (65%), ZnCO <sub>3</sub> <sup>0</sup> (26%), Zn(OH) <sub>2</sub> <sup>0</sup> (3%), Zn <sup>2+</sup> (4%), ZnHCO <sub>3</sub> <sup>+</sup> (1%)
Cu	Cu(OH) <sub>2</sub> <sup>0</sup> (86%), CuCO <sub>3</sub> <sup>0</sup> (12%), Cu(CO <sub>3</sub> ) <sub>2</sub> <sup>2-</sup> (2%)
Ni	NiCO <sub>3</sub> <sup>0</sup> (83%), Ni(CO <sub>3</sub> ) <sub>2</sub> <sup>2-</sup> (17%)
Al	Al(OH <sub>4</sub> ) <sup>-</sup> (52%), Al(OH) <sub>3</sub> <sup>0</sup> (48%)
Fe	Fe <sup>2+</sup> (97%), FeOH <sup>+</sup> (2%)
H <sub>2</sub> O	Al(OH <sub>4</sub> ) <sup>-</sup> (53%), Al(OH) <sub>3</sub> <sup>0</sup> (36%), OH <sup>-</sup> (6%), Cu(OH) <sub>2</sub> <sup>0</sup> (2%), Mg(OH) <sup>+</sup> (1%)
H	HCO <sub>3</sub> <sup>-</sup> (97%), MgHCO <sub>3</sub> <sup>+</sup> (2%)

### 3.3.2.5.3 Magnesium

Mg, like Ca, was predicted as occurring predominantly as the free ion  $\text{Mg}^{2+}$  with  $\text{MgHCO}_3^+$ ,  $\text{MgCO}_3^0$  and  $\text{MgSO}_4^0$  being other minor species present. As with Ca, the interstitial water was predicted as having no  $\text{MgSO}_4^0$  and a greater proportion of  $\text{Mg}^{2+}$ , while  $\text{MgHCO}_3^+$  and  $\text{MgCO}_3^0$  remained the other minor species present.

Wetzel (1983) records that Mg compounds are much more soluble than their Ca counterparts with the consequence that significant amounts of Mg rarely precipitate. He also states that the monocarbonates of hardwater lakes are usually more than 95 %  $\text{CaCO}_3$  under ordinary  $\text{CO}_2$  pressures, with  $\text{MgCO}_3$  and  $\text{Mg}(\text{OH})_2$  only precipitating at very high pH values ( $>10$ ) under most natural conditions. In the case of Barber's Pan, MINTEQA2 predicted that the water was supersaturated with respect to both  $\text{MgCO}_3$  (magnesite) and  $(\text{Ca,Mg})\text{CO}_3$  (dolomite). As calcite is usually the first mineral to precipitate in almost all natural waters (Drever, 1988), a greater amount of  $\text{CaCO}_3$  may be removed than  $\text{MgCO}_3$ , increasing the Mg/Ca ratio in the pan (refer to 3.3.2.6). The saturation index calculated by MINTEQA2 for dolomite was shown to exceed that calculated for calcite in both the bulk and interstitial water samples (Table 10). As will become clear in section 3.3.2.6, other Mg-containing solid phases, especially Mg-silicates such as sepiolite and palygorskite, are likely to have an important influence on equilibrium Mg concentrations in the pan water.

### 3.3.2.5.4 Sodium, potassium and chloride

The proportions of Na and K occurring as highly soluble cations of numerous salts are so large that alteration of their concentrations in natural waters is not common, and they behave largely as conservative species. Moderate reductions in the epilimnetic concentrations of K attributed to algal utilization have been recorded in some lakes (Wetzel, 1983). In both the bulk and interstitial pan waters MINTEQA2 predicted that virtually 100 % of the K and Na would be present as free  $\text{Na}^+$  and  $\text{K}^+$  ions. Cl also behaves as a conservative species (Eugster, 1980) and MINTEQA2 predicted that it too would be present entirely as free  $\text{Cl}^-$ .

### 3.3.2.5.5 Iron

Iron exists in solution either as  $\text{Fe}^{2+}$  or  $\text{Fe}^{3+}$ . The amounts of iron in solution in natural waters and the rate of oxidation of  $\text{Fe}^{2+}$  to  $\text{Fe}^{3+}$  is dependent primarily on pH, Eh and temperature (Wetzel, 1983). For the purposes of the MINTEQA2 speciation, all iron was assumed to be in the reduced  $\text{Fe}^{2+}$  state, since ferrous iron constituents tend to be more soluble than ferric iron ones (Wetzel, 1983). MINTEQA2 predicted that the majority of the iron would be present as the free  $\text{Fe}^{2+}$  ion species with small amounts of  $\text{FeOH}^+$  and  $\text{FeSO}_4^0$ . Wetzel (1983) states that soluble ferrous iron occurs mainly as hydrated  $\text{Fe}^{2+}$  and hydrated hydroxo ions.

Dallas and Day (1993) state that iron compounds in water are very easily oxidised. It is, therefore, very likely that a certain proportion of the iron present in the pan water is in the ferric state. Wetzel (1983) records that the most common species of ferric iron in natural waters is hydrated ferric hydroxide ( $\text{Fe}[\text{OH}]_3$ ) which has a very low solubility. He further states that much of the iron in normal lake water is present as suspensions of flocculated  $\text{Fe}[\text{OH}]_3$  which is removable by filtration with membranes of pore size  $0.5 \mu\text{m}$ . As all the water samples were filtered through  $0.2 \mu\text{m}$  filters prior to ICP–AES analysis, most flocculated iron present is likely to have been removed.

Ferrous iron usually occurs at very low concentrations in solution and is usually in particulate and colloidal form, presumably associated with soil and sediment particles (Wetzel, 1983). The decrease in iron concentration observed from bulk pan water to interstitial water may well be attributable to the precipitation of ferrous iron compounds like  $\text{FeCO}_3$ ,  $\text{Fe}(\text{OH})_2$  and  $\text{FeS}$ . Wetzel (1983) states that the solubility of  $\text{Fe}^{2+}$  is generally controlled by  $\text{FeCO}_3$  and that, even at low pH, carbonate concentrations are usually sufficient to limit solubilization. The presence of iron sulphides in the sediments is discussed in section 3.3.3.

The quantity of total iron found in most typical, neutral or alkaline, freshwater lakes is between  $50\text{--}200 \mu\text{g}\cdot\text{dm}^{-3}$ , although higher levels have been recorded in certain alkaline lakes rich in organic matter (Wetzel, 1983). In the bulk pan water the average concentration was  $372 \mu\text{g}\cdot\text{dm}^{-3}$ . Hammer (1986) records that iron is present at  $< 1 \text{mg}\cdot\text{dm}^{-3}$  in most saline lakes where this parameter was measured. Talling and Talling (1965) contend that high concentrations of both iron and manganese in shallow lakes may be attributable to upward transport by turbulence. Hammer (1986) supports their contention, noting that the mud–water

interface is a zone of decomposition where the redox potential may be low enough to produce a reducing environment, as is the case in Barber's Pan. Ferrous and manganous ions can then be released to the water, being recirculated until they precipitate.

#### 3.3.2.5.6 Manganese

Although Mn occurs in several valence states,  $Mn^{3+}$  is thermodynamically unstable in aqueous solutions under normal conditions and  $Mn^{4+}$  compounds are insoluble at most pH values prevailing in natural environments. Above pH 8.5  $Mn^{2+}$  forms an intermediate complex, being adsorbed onto manganese oxides. The  $Mn^{2+}$  of these oxide complexes can react relatively rapidly with other anions, precipitating as  $MnCO_3$ ,  $MnS$  and  $Mn(OH)_2$ . Mn can also be adsorbed to iron oxides, coprecipitating with  $Fe(OH)_2$  when the pH exceeds 7 (Wetzel, 1983). The  $Mn^{2+}$  concentrations in both the bulk and interstitial pan water were, in most cases, below the detection limits of the ICP – AES instrument. Considering the high pH of the pan water and the supersaturation with carbonate minerals predicted by MINTEQA2, it is likely that most of the  $Mn^{2+}$  present had precipitated as  $MnCO_3$  and  $Mn(OH)_2$ . Some may have coprecipitated with  $CaCO_3$ . The lowering of the  $SO_4^{2-}$  concentration from the bulk pan water to the sediments suggests the formation of sulphide minerals (discussed in 3.3.3). Some of the  $Mn^{2+}$  may, therefore, be bound in  $MnS$ .

Mn present in trace amounts in bulk pan water sample 9 was predicted as occurring predominantly in the form of the free  $Mn^{2+}$  ion. Other minor species that were predicted by MINTEQA2 as also likely to be present, albeit making up a very small proportion of the total dissolved Mn, were  $MnCl^+$ ,  $MnSO_4^0$  and  $MnHCO_3$ .

#### 3.3.2.5.7 Carbonate/bicarbonate

MINTEQA2 predicted that the dominant form of carbonate in the pan water would be  $HCO_3^-$ . The relationship between pH and the percentage of free  $CO_2$ ,  $HCO_3^-$  and  $CO_3^{2-}$  ions in natural waters has been well documented. Practically, most  $CO_2$  in natural waters is in the form of  $HCO_3^-$ , with  $CO_3^{2-}$  only being present in significant quantities at pH values  $> 10$ . Free  $CO_2$  only dominates at pH  $< 4$  (Drever, 1988; Dallas and Day, 1993).

#### 3.3.2.5.8 Sulphate

Wetzel (1983) states that the predominant form of dissolved sulphur in natural waters is  $\text{SO}_4^{2-}$ . During the decomposition of organic matter, sulphur is released in the form of  $\text{H}_2\text{S}$  which, under oxic conditions, is very rapidly oxidized. Strongly alkaline waters may contain some  $\text{HS}^-$  and very low concentrations of  $\text{S}^{2-}$  since  $\text{H}_2\text{S}$  is very soluble and can dissociate. MINTEQA2 predicted that  $\text{SO}_4^{2-}$  was the dominant form of sulphur present in the pan water, with lesser quantities of  $\text{MgSO}_4^0$ ,  $\text{CaSO}_4^0$  and  $\text{NaSO}_4^-$  also present.  $\text{H}_2\text{S}$  and  $\text{FeS}$  were associated with the pan sediments (section 3.3.3). Metal sulphides are exceedingly insoluble at neutral or alkaline pH values and any  $\text{Fe}^{2+}$  released from the sediments is likely to react with  $\text{H}_2\text{S}$  to form  $\text{FeS}$  which then precipitates. As a consequence,  $\text{H}_2\text{S}$  only accumulates in alkaline waters after most of the  $\text{Fe}^{2+}$  has been precipitated as  $\text{FeS}$  (Wetzel, 1983). The presence of  $\text{H}_2\text{S}$  and  $\text{FeS}$  in the pan sediment samples therefore suggests that most of any  $\text{Fe}^{2+}$  that may be present in the water has already been precipitated as  $\text{FeS}$ . Wetzel (1983) also records that the removal of sulphide through precipitation (with  $\text{Fe}^{2+}$ ) permits the migration of other metals such as Cu, Zn and Pb to the sediments. These form even more insoluble sulphides than  $\text{FeS}$ . Precipitation of these sulphides may contribute to the removal of other metal ions from the pan water.

The concentration of  $\text{SO}_4^{2-}$  in the bulk pan water (average =  $34 \text{ mg.dm}^{-3}$ ) is above the 5–30  $\text{mg.dm}^{-3}$  range recorded by Wetzel (1983) for oxic waters world-wide. He does, however, note that far higher concentrations are frequently found in sulphate-dominated saline lakes. The average concentration of  $\text{SO}_4^{2-}$  in the interstitial waters was found to be  $13 \text{ mg.dm}^{-3}$ , 2.6x lower than that recorded for the bulk water. In the light of the above discussion and that in section 3.3.3, it is likely that this decrease in  $\text{SO}_4^{2-}$  is attributable to the precipitation of sulphides in the more reducing environment associated with the sediments. A certain amount of sulphur may also be lost in the form of  $\text{H}_2\text{S}$  (Kilham, 1984).

#### 3.3.2.5.9 Phosphorus

The greatest proportion of phosphorus in freshwaters occurs as organic phosphates and cellular constituents in the biota, adsorbed to inorganic and dead particulate organic materials. Inorganic P occurs predominantly as orthophosphate ( $\text{PO}_4^{3-}$ ). Dissolved P is composed of  $\text{PO}_4^{3-}$ , polyphosphates, organic colloids or phosphorus combined with adsorptive colloids and low molecular weight phosphate esters. Pyrophosphate, triphosphate and higher polyphosphate anions additionally form complexes, chelates and insoluble salts with a number of metal ions.

The extent of complexing and chelation between various phosphates and metal ions in natural waters depends upon the relative concentrations of the phosphate and metal ions, the pH and the presence of other ligands such as  $\text{SO}_4^{2-}$ ,  $\text{CO}_3^{2-}$ ,  $\text{F}^-$  and organic species (Wetzel, 1983).

In both the bulk and interstitial pan waters MINTEQA2 predicted that phosphate could occur as several different species. In the bulk pan water the two predominant species predicted were  $\text{MgPO}_4^-$  and  $\text{HPO}_4^{2-}$ , with lesser quantities of  $\text{MgHPO}_4^0$ ,  $\text{CaHPO}_4^0$  and  $\text{CaPO}_4^-$  occurring, while in the interstitial waters the same five species were predicted as occurring, but with  $\text{HPO}_4^{2-}$  and  $\text{MgHPO}_4^0$  as the two predominant species.

Stumm and Morgan (1970) state that, since phosphate concentrations are usually low, complex formation between the major cations and the various phosphate anions has a small effect on the metal ion distribution, but can significantly affect the phosphate distribution. For metal ions such as  $\text{Fe}^{3+}$ ,  $\text{Mn}^{2+}$ ,  $\text{Zn}^{2+}$  and  $\text{Cu}^{2+}$ , which are present in concentrations comparable to or lower than that of phosphate, complexation with phosphate anions can significantly affect their distribution. The major cations complexing with phosphate in the pan water were predicted to be  $\text{Ca}^{2+}$  and  $\text{Mg}^{2+}$ , with Mg phosphate complexes predominating. This is attributable to the predominance of Mg over Ca in the pan water discussed in sections 3.3.2.5.3 and 3.3.2.6. MINTEQA2 also predicted that the water was likely to be supersaturated with respect to hydroxyapatite. MINTEQA2 predictions on samples from the DWAF database, which included  $\text{F}^-$ , suggested that even in its most dilute form the pan water would be supersaturated with respect to fluorapatite. Phosphate mineral solubility is discussed in section 3.2.2.6. Exchange of phosphorus between sediments and the overlying water is a major component of the phosphorus cycle in natural waters and is discussed in section 4.4.6, as is the difference in phosphate concentration between the bulk and interstitial pan water.

#### 3.3.2.5.10 Silicon

Two major forms of Si occur in freshwaters, namely dissolved silicic acid ( $\text{H}_4\text{SiO}_4$ ) and particulate silica ( $\text{SiO}_2$ ). Surface adsorption of silicic acid leads to a situation whereby nearly all natural waters are greatly undersaturated with respect to silica. Si complexes with iron and aluminium hydroxides which decrease the solubility of silicates in sediments, particularly in interstitial waters at pH values greater than 7 (Wetzel, 1983).

MINTEQA2 predicted that the majority of the Si in the bulk pan water was likely to be in the form of dissolved silicic acid ( $\text{H}_4\text{SiO}_4$ ), with the remainder occurring as  $\text{H}_3\text{SiO}_4^-$ . In the interstitial waters, MINTEQA2 predicted the same two species as the most likely forms of Si, but with an even greater proportion occurring as  $\text{H}_4\text{SiO}_4$ . The concentration of monomeric silica in the interstitial waters was found to be much greater than that in the bulk pan water. Wetzel (1983) states that the interstitial water of lake sediments is usually enriched in dissolved silica at concentrations far in excess of those of water entering the lake. He further notes that the dissolved silica of interstitial waters is not in equilibrium with amorphous silica but rather with chemically bound or adsorbed silica and that the actual Si concentration of the interstitial waters is controlled by the dissolution of ferroaluminium silicate, a complex formed in the sediments by the reaction of silica from diatoms with aluminium and ferric hydroxides, or through the hydrolysis of clay minerals. This may be the case in Barber's Pan since the ICP–AES determination of Si gave consistently higher values than the colorimetric determination (section 3.3.2.6), suggesting the presence of colloidal aluminosilicate material in the water samples.

Combrinck (1966) suggests that the Si concentrations in Barber's Pan are markedly influenced by the activities of the diatoms, plankton and benthic organism populations, and Wetzel (1983) notes that diatoms can assimilate large quantities of silica and markedly modify the flux rates of silica in lakes and streams. As was the case with Ca, however, it will be seen from later considerations of mineral solubility equilibria that the water is supersaturated with respect to a number of phyllosilicate clay minerals, which would provide an adequate non-biological explanation for low Si concentrations in solution.

#### 3.3.2.5.11 Lead

The Pb in both the bulk and interstitial pan water was predicted as occurring largely in two forms;  $\text{Pb}(\text{CO}_3)_2^{2-}$  and  $\text{PbCO}_3^0$ . In the bulk pan water the two species occurred in similar proportions,  $\text{Pb}(\text{CO}_3)_2^{2-}$  being slightly more dominant. In the interstitial waters  $\text{PbCO}_3^0$  was predicted to be by far the dominant species. This difference is likely to be a function of pH and Eh since the interstitial waters had lower pH values and, being associated with the more reducing sedimentary environment, are also likely to have lower Eh values. The mineral controlling Pb solubility in the pan water was predicted to be cerrusite ( $\text{PbCO}_3$ ). Pb solubility interactions are discussed in section 3.3.2.6. Fergusson (1990) describes lead carbonate species

as being almost insoluble. Pb concentrations in the bulk pan water were found to be lower than those of the interstitial water. This may be a consequence of the precipitation of  $\text{PbCO}_3$  and also of the coprecipitation of Pb with calcium and magnesium carbonates. The more reducing conditions and lower pH of the interstitial water are likely to increase Pb solubility and hence increase its concentration in solution.

#### 3.3.2.5.12 Zinc, copper and nickel

MINTEQA2 predicted that the dominant Zn species in the pan water was likely to be  $\text{Zn}[\text{CO}_3]_2^{2-}$ , with small amounts of  $\text{ZnCO}_3^0$  and  $\text{Zn}(\text{OH})_2^0$  also present. Zn carbonates form sparingly soluble solids under pH and Eh conditions prevalent in most natural waters. Those waters in equilibrium with atmospheric  $\text{CO}_2$  are likely to precipitate any  $\text{ZnCO}_3$  present (Stumm and Morgan, 1970). The pan waters were found to have a high pH and MINTEQA2 predicted that the water was supersaturated with  $\text{CO}_3$  compounds. Under these conditions the precipitation of  $\text{ZnCO}_3$  is likely. However, MINTEQA2 calculated that the water was undersaturated with respect to Zn hydroxide and carbonate minerals, with only  $\text{ZnSiO}_3$  apparently slightly supersaturated (S.I. = 0.538 for bulk pan water sample no. 5).

Ni ions tend to be soluble at pH values < 6.5, while at values greater than 6.7 they occur largely as insoluble hydroxides. In freshwaters, about half the total Ni present is in the ionic form, with the remaining 50% forming stable organic complexes, many of which readily adsorb onto clay particles (Dallas and Day, 1993). According to the MINTEQA2 speciation, the Ni in the pan water is likely to occur in essentially two forms;  $\text{Ni}[\text{CO}_3]_2^{2-}$  and  $\text{NiCO}_3^0$ , with the proportion of  $\text{NiCO}_3^0$  relative to  $\text{Ni}[\text{CO}_3]_2^{2-}$  increasing in the interstitial waters. Both waters were predicted to be slightly undersaturated but in virtual equilibrium with  $\text{Ni}(\text{OH})_2$  (SI = -0.688 [bulk water] and -0.902 [interstitial water] for sample no. 5).

Cu compounds tend to precipitate under alkaline conditions (Dallas and Day, 1993). The Cu concentrations in all three categories of pan water were exceptionally low, being close to the lower limits of detection of the ICP–AES instrument used. This is probably attributable to the high pH and very alkaline conditions characterizing the pan waters and making the Cu species present insoluble. MINTEQA2 predicted that  $\text{Cu}(\text{OH})_2$  would be the dominant Cu species in the water, with a small proportion of the Cu also occurring as  $\text{CuCO}_3^0$  and  $\text{Cu}[\text{CO}_3]_2^{2-}$ .

### 3.3.2.5.13 Aluminium

As discussed in section 3.3.2.2, Al solubility is strongly pH dependent. In the bulk pan water, which was found to have an average pH of 9.2, MINTEQA2 predicted that soluble Al would be present largely as  $\text{Al(OH)}_4^-$  with lesser amounts in the form of  $\text{Al(OH)}_3^0$ . In the interstitial waters, which had an average pH of 8.4, the Al was predicted as being approximately equally distributed between the two species. The concentration of Al in the water and the mineral equilibria likely to influence it are discussed in section 3.3.2.6.

### 3.3.2.5.14 Fluorine

Although F concentrations were not accurately determined, HPIC analyses confirmed the presence of  $\text{F}^-$  in the samples as did the numerous analyses from the DWAF database. The concentration of  $\text{F}^-$  in the pan water appears to be in the range  $3-5 \text{ mg.dm}^{-3}$  (as discussed in section 3.3.2.4). In order to determine what possible species of F could exist in the pan water,  $5 \text{ mg.dm}^{-3} \text{ F}^-$  was included with the other ion data for bulk pan water 5 and subjected to a MINTEQA2 run. MINTEQA2 predicted that the dominant species of fluorine in the bulk pan water would be  $\text{F}^-$  with trace amounts of  $\text{MgF}^-$ . Possible solid phase control of F solubility is discussed in section 3.3.2.6.

### 3.3.2.6 Mineral solubility equilibria

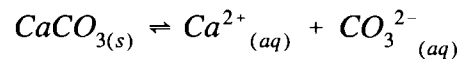
In investigating the solubility of minerals, one must determine whether a solid phase is likely to be controlling the concentration of a particular element in solution, and if so, which solid phase (Sposito, 1989). This can be achieved by using thermochemical data to predict mineral stability sequences since the least soluble minerals are the ones with the lowest free energy (Rai and Kittrick, 1989). MINTEQA2 was used to predict not only the chemical speciation of the pan water, but also to calculate saturation indices of minerals likely to occur in the pan system.

In a closed system, all surface or near-surface waters are subject to evaporative concentration. This increases the solute load of the waters, eventually leading to the precipitation of mineral phases. The precipitation reactions can be seen to act as a

fractionating mechanism, with the precipitation of each mineral having a profound effect on the subsequent development of the water composition (Eugster, 1980).

Drever (1988) records that with almost all natural waters, the first mineral to precipitate is calcite ( $\text{CaCO}_3$ ). MINTEQA2 predicted that Barber's Pan was supersaturated with respect to calcite, aragonite ( $\text{CaCO}_3$ ), huntite ( $\text{Mg}_3\text{Ca}[\text{CO}_3]_4$ ), dolomite ( $\text{CaMg}[\text{CO}_3]_2$ ) and magnesite ( $\text{MgCO}_3$ ).

Eugster (1980) states that the precipitation of calcite is governed by the reaction:



The solubility product for calcite is given by the relation

$$K_{sp} = \frac{(A_{\text{Ca}^{2+}} \cdot A_{\text{CO}_3^{2-}})}{A_{\text{CaCO}_3}}$$

in which **A** stands for the activity of the species designated in the subscript.

As long as the solution is in equilibrium with calcite, the activities of  $\text{Ca}^{2+}$  and  $\text{CO}_3^{2-}$  must vary inversely. The mass balance condition, however, requires that 1 mole of calcite forms by removing 1 mole of  $\text{CO}_3^{2-}$  from solution. This implies that the  $\text{Ca}/\text{CO}_3^{2-}$  ratio must change, unless it was precisely one at the outset.

Evaporative concentration combined with calcite precipitation will enrich the residual solution in the more abundant species and deplete it in the other. In this way, calcite precipitation acts as a chemical divide since waters that are initially carbonate-rich will experience a further relative enrichment of carbonate and depletion of calcium and vice versa. As calcite precipitates the Mg/Ca ratio in the solution will increase leading to the precipitation of a low-Mg calcite and eventually high-Mg calcite and protodolomite (Eugster, 1980). Eugster and Kelts (1983) state that the actual sequence of precipitation as the Mg/Ca ratio increases would be:

pure calcite  $\Rightarrow$  low-Mg calcite  $\Rightarrow$  aragonite  $\Rightarrow$  high-Mg calcite  $\Rightarrow$  dolomite

Using three samples from the DWAF database which represent the pan water in its most dilute, median and most concentrated forms over the last 14 years the Mg/Ca ratio can be seen to increase with increasing concentration (Table 9), conforming to this pattern.

The Mg/Ca ratio of the water sampled during this study was found to be intermediate between the most dilute and the median situation recorded over the last 14 years. Considering the saturation indices (S.I.) predicted by the MINTEQA2 model (Table 10) and the increasing Mg/Ca ratio it is feasible that Mg and Ca carbonate minerals could be precipitating in the pan at present concentration levels.

**Table 9:** Mg/Ca ratios for several water samples from Barber’s Pan. The Water Affairs data represents the pan water in its most dilute, median and most concentrated forms over the last 14 years. The Mg/Ca ratio increases with increasing concentration suggesting the precipitation of calcite.

Sample No.	Mg/Ca Ratio
Water Affairs Data	
Most Dilute	1.3
Median Concentration	5.6
Most Concentrated	11.9
Sample No. 5	
Bulk Pan Water	4.4
Sediment Interstitial Water	4.3

At present, the Mg/Ca ratio in Barber’s Pan can be seen to favour the precipitation of MgCO<sub>3</sub> minerals. In addition to predicting that the water was supersaturated with respect to calcite and aragonite, MINTEQA2 calculated a very strongly positive S.I. for dolomite relative to calcite and aragonite, and also predicted the supersaturation of the water with respect to other MgCO<sub>3</sub> minerals such as magnesite (Table 10).

The fibrous Mg–silicate clays, sepiolite ( $\text{Si}_{12}\text{Mg}_8\text{O}_{30}(\text{OH})_4(\text{OH}_2)_4 \cdot 8\text{H}_2\text{O}$ ) and palygorskite ( $\text{Si}_8\text{Mg}_5\text{O}_{20}(\text{OH})_2(\text{OH}_2)_4 \cdot 4\text{H}_2\text{O}$ ), are known to occur in lacustrine environments of semi–arid to arid regions, and their occurrence has been associated with aquatic conditions characterized by alkaline solutions with high Si and Mg activities which commonly occur in pan/playa type environments. In these closed catchments, high Mg and Si activities can be attributed either to concentration of ground water solutions by evaporation close to the surface, or to inflow–evaporation cycles characteristic of such environments. A further consequence of this environmental setting is that sepiolite and palygorskite are always associated with a large variety of evaporites such as carbonates (primarily dolomite), sulphates (mainly gypsum [ $\text{CaSO}_4$ ]), halite [ $\text{NaCl}$ ], thernardite [ $\text{Na}_2\text{SO}_4$ ] and chert (Singer, 1989). Weaver (1989) records that studies on Pleistocene playas in the vicinity of Mound Lake in the southern High Plains, Texas, found that palygorskite and sepiolite were associated with carbonate layers (palygorskite with calcite, and sepiolite with dolomite) interbedded with detrital material. The silicate minerals apparently formed during times of periodic desiccation, and the two associations (calcite and dolomite) suggest that the availability of Mg fluctuated. Supersaturation with respect to and hence the possible precipitation of crystalline sepiolite was predicted by the MINTEQA2 model as occurring in the three samples taken from the DWAF database, as well in the interstitial water samples extracted and analyzed.

Palygorskite was not considered by MINTEQA2, as it is not included in the MINTEQA2 data base of minerals. Plotting the Mg and Si activities onto a stability diagram for the palygorskite–smectite system constructed by Elprince *et al.* (1979) (Fig. 19) indicates that at different stages of evaporative concentration smectite, but more probably palygorskite, could precipitate in Barber’s Pan. This interpretation must necessarily be a tentative one, however, since the smectite stability field in Fig. 19 is based on an assumed fixed value for Al activity in solution – one which, because of difficulties (described later) associated with Al analysis, could not be replaced by one derived from Al analysis of the pan water. The X–ray diffractograms of the Barber’s Pan clay fraction (section 4.4.2) confirm the presence of smectitic material, but not of palygorskite or sepiolite. From the DWAF data base it can be seen that it almost dried out completely in 1988. Prior to that date the last recorded occasion on which it dried up was in 1913 (before Smuts’ diversion) (Milstein, 1975).

With respect to phosphate, MINTEQA2 calculations favour the proposition that the minerals governing its solubility in the pan are hydroxyapatite and fluorapatite. No accurate  $\text{F}^-$

analyses were conducted on the water samples collected, but the HPIC analyses indicated the presence of  $F^-$  at concentrations in the  $3-5 \text{ mg.dm}^{-3}$  range as did water analyses from the DWAF database. As a consequence, only the DWAF analyses had  $F^-$  included in their inputs into MINTEQA2. MINTEQA2 predicted supersaturation with respect to both fluorapatite and fluorite when a concentration of  $5 \text{ mg.dm}^{-3} F^-$  was included with the other analytical data from bulk pan water sample no. 5.

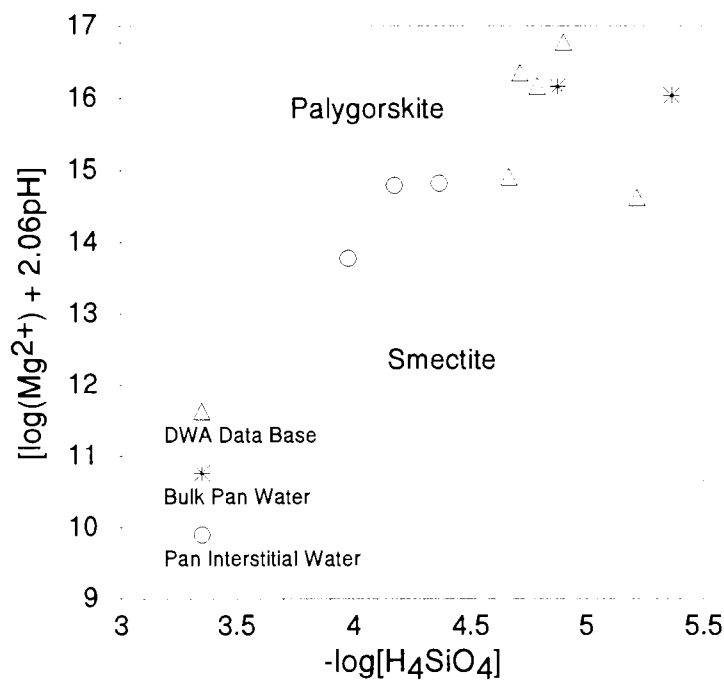


**Figure 19:** Stability–diagram for palygorskite–smectite system in Barber’s Pan, using the stability boundaries of Elprince *et al.*, 1979.

Lindsay (1979) constructed a unified solubility diagram of the various Ca, Al, and Fe phosphates that are present in soils, where phosphate solubility is expressed in terms of the predominant ionic species relative to pH. At pH values above 7.2 (as is the case in Barber’s Pan) the dominant species of  $PO_4^{3-}$  predicted by Lindsay (1979) was  $HPO_4^{2-}$ .

Plotting the log activities of  $HPO_4^{2-}$  predicted by MINTEQA2 onto this diagram (Fig. 20), reinforces the suggestion based on saturation indices calculated using MINTEQA2 that hydroxyapatite ( $Ca_5(PO_4)_3OH$ ) and/or fluorapatite ( $Ca_5(PO_4)_3F$ ) are likely phosphorus solubility controlling solid phases.

**Table 10:** MINTEQA2 calculated saturation indices for selected minerals possibly occurring in Barber’s Pan. Positive values indicate supersaturation; negative values indicate undersaturation.

Sample No.	Calcite	Dolomite	Sepiolite	Quartz	Magnesite	Hydroxyapatite	Fluorapatite
Bulk Pan Water							
5	1.09	2.93	-0.66	-0.78	1.36	2.43	Not Calculated
Sediment interstitial Water							
5	0.59	1.93	0.23	0.39	0.85	3.24	Not Calculated
Water Affairs Data							
Most Dilute	0.85	2.08	0.11	-0.05	0.73	5.10	15.06
Median	1.49	3.98	0.24	-0.11	1.99	5.47	16.99
Most Conc.	1.52	4.39	3.04	-0.29	2.37	3.04	12.26

Lindsay *et al.* (1979) record that when soils become reduced, the stabilities of Fe and Mn phosphate minerals are affected. They note that where acid soils are flooded and reduction occurs, the  $\text{Fe}^{2+}$  concentration increases and lowers the solubility of vivianite ( $\text{Fe}_3(\text{PO}_4)_2 \cdot 8\text{H}_2\text{O}$ ), making it the most stable phosphate mineral. Despite assuming that all the Fe in Barber's Pan was  $\text{Fe}^{2+}$  for the purposes of the MINTEQA2 speciation, the model predicted that the pan water was undersaturated with respect to vivianite. This may well be attributable to the very alkaline nature of the water, with extensive buffering from the carbonate species preventing any significant reduction in the pH (acidification) of the reduced sediments. Comparing the pH of the bulk water with that of the sediment interstitial water, a decline in pH was observed, although the interstitial water was still significantly alkaline ( $\text{pH } 8 < \text{pH} < 9$ ).

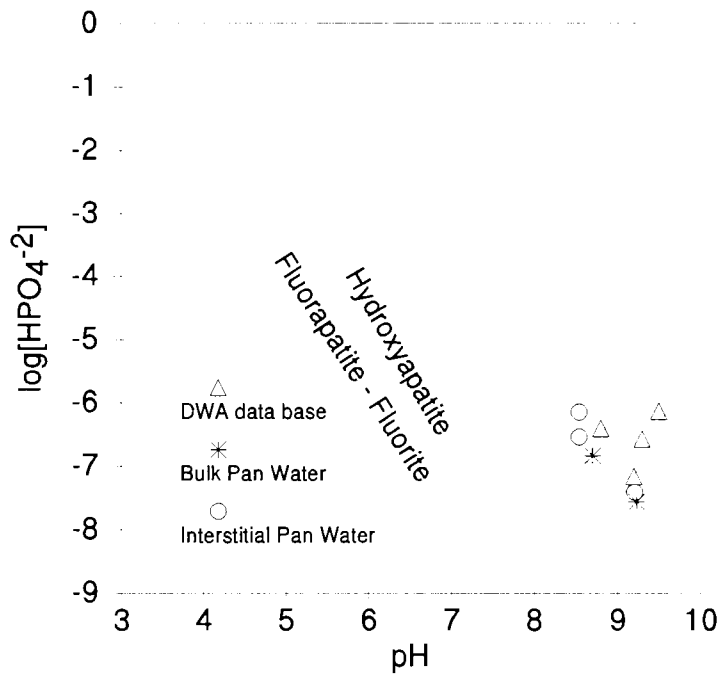


**Figure 20:** A solubility diagram for hydroxyapatite and fluorapatite–fluorite (after Lindsay, 1979).

Cerussite ( $\text{PbCO}_3$ ) was predicted as the mineral with the potential for controlling Pb solubility. This corresponds with work carried out to date which indicates that the dominant inorganic Pb species in both fresh and sea water are the lead carbonates (Fergusson, 1990). Fergusson (1990) also states that lead carbonate compounds are virtually insoluble in water. This was confirmed by the water analyses, with only a slight increase in Pb concentrations and slight decrease in pH, from the bulk pan water to the interstitial water, showing the system to move from being in virtual equilibrium with cerussite to being supersaturated.

The water samples were shown to be in virtual equilibrium with quartz ( $\text{SiO}_2$ ), allowing for more confident interpretations of the other mineral solubility equilibria, since quartz, being a fairly resistant mineral, might be expected to be in equilibrium within the system. The bulk pan water was predicted as being undersaturated with respect to  $\text{SiO}_2$ . Fluctuations in the silica concentration of the pan water were noted by Combrinck (1966), who attributed these fluctuations to the activities of diatoms, benthos and plankton.

MINTEQA2 calculated that the water samples would be supersaturated with respect to several of the Al containing minerals, namely:

- 1) the aluminium hydroxides boehmite ( $\text{a-AlOOH}$ ), gibbsite ( $\text{g-Al}[\text{OH}]_3$ ) and diaspore ( $\text{a-AlOOH}$ ),
- 2) the aluminosilicates kaolinite ( $\text{Al}[\text{OH}]_8[\text{Si}_4\text{O}_{10}]$ ), halloysite ( $\text{Al}[\text{OH}]_8[\text{Si}_4\text{O}_{10}][\text{H}_2\text{O}]_4$ ) and muscovite ( $\text{KAl}_2[\text{AlSi}_3]\text{O}_{10}[\text{OH}]_2$ ),
- 3) others like pyrophyllite ( $\text{Al}_2\text{Si}_4\text{O}_{10}[\text{OH}]_2$ ) and laumontite ( $\text{Ca}[\text{Al}_2\text{Si}_4\text{O}_{12}] \cdot 4\text{H}_2\text{O}$ ).

Many of these minerals are likely to occur in sedimentary environments, but the magnitude of the saturation indices calculated by MINTEQA2 suggests that the amount of Al in solution, as determined by ICP–AES, may in fact have been overestimated. ICP–AES determines total Al in solution, rather than dissolved Al. As a consequence, any Al present as colloidal particles ( $< 0.2 \mu\text{m}$ ) in the solution being subject to ICP–AES would be included in the total Al concentration determined.

Si was determined by both the colorimetric blue silicomolybdous acid procedure of Weaver *et al.* (1968) and by ICP–AES. The blue silicomolybdous acid procedure gave consistently lower values for Si (Table 11), than those determined by means of ICP–AES implying that the water samples did contain significant quantities of Si present in forms other than monomeric Si. The values for Si obtained by the colorimetric procedure were used in the MINTEQA2 modelling. This "overestimation" of Si by ICP–AES implies that Al, which would be associated with Si in any colloidal aluminosilicate material present in the solutions analyzed by ICP–AES, would also be overestimated. This in turn implies that no serious attempt at interpreting pan water composition in terms of aluminosilicate solubility equilibria can be made.

In waters saturated with  $\text{CaCO}_3$ ,  $\text{FeCO}_3$  is about 200x less soluble than  $\text{CaCO}_3$  unless very high ( $> 10$ ) pH values occur (Wetzel, 1983). Siderite ( $\text{FeCO}_3$ ) was indicated as a mineral that would precipitate in Barber's Pan. Berner (1971), however, states that conditions under which siderite is thermodynamically stable are severely restricted, in that Eh and the activity of  $\text{S}^-$  must be low. These conditions are met in some fresh waters that have low concentrations of dissolved  $\text{SO}_4^{2-}$  such that the anaerobic bacterial decay of organic matter enables the attainment of a low Eh and high  $P_{\text{CO}_2}$  without the formation of significant amounts of  $\text{H}_2\text{S}$ .

The lack of any Eh values prohibited the accurate determination of the oxidation state of several of the elements. For the purposes of modelling the speciation and mineral solubility equilibria using MINTEQA2, it was assumed that all Fe was in the reduced  $\text{Fe}^{2+}$  state. As a consequence, one cannot attach very much significance to the model's prediction of siderite supersaturation, without first confirming whether the iron is in fact present in a reduced state.

### **3.3.3 The evaporative concentration of Barber's Pan**

As discussed in Chapter 2, section 2.4.3, a number of models have been proposed to explain the evolution of saline lake waters. The modified Hardie–Eugster model interprets the chemistry of waters undergoing evaporation in terms of a succession of chemical divides (Fig. 11). The DWAF database provides data on the evaporative concentration of Barber's Pan over the last fifteen years. Included in this time period is the complete evaporative sequence exhibited by the pan during the drought period from 1982–1988 which would have culminated in the pan drying out during February of 1988 had it not been for sudden substantial late summer rains. The rains resulted in a significant influx of water via the Harts, extensively raising the pan level and diluting the saline brine that had evolved. Examination of the DWAF data over this period, together with modelled outputs of mineral solubility equilibria calculated by MINTEQA2, suggests that brine evolution in Barber's Pan followed the fate of the path III inflow water in Eugster and Hardies' (1978) modified brine evolution flow diagram (Fig. 11).

**Table 11:** Comparison of the Si concentrations ( $\text{mg}\cdot\text{dm}^{-3}$ ) determined by the colorimetric blue silicomolybdous acid procedure of Weaver *et al.* (1968) with those determined by ICP–AES.

Sample No.	Si determined by blue silicomolybdous acid procedure (monomeric Si)	Si determined by ICP–AES (total Si)
<b>Bulk Pan Water</b>		
5	0.31	1.40
6	0.34	1.20
7	0.37	1.48
8	0.54	1.75
9	0.32	1.23
<b>Sediment Supernatant</b>		
5	5.99	9.15
10	4.72	7.01
17	3.00	5.78
<b>Sediment Interstitial Water</b>		
4	6.49	9.03
5	4.18	8.55
8	9.05	18.5
16	9.98	16.9
17	6.21	10.7

This path models the evaporative concentration of an inflow water in which the concentration of  $\text{HCO}_3^- \geq \text{Ca}^{2+}$  and  $\text{Mg}^{2+}$ . The flow diagram predicts that the evaporative concentration of such waters would result in the precipitation of large amounts of  $\text{CaCO}_3$ . In the process, Mg becomes strongly enriched over Ca and high Mg–calcite and/or dolomite become abundant. This is indeed the case for Barber’s Pan, the data in Table 9 illustrating the enrichment of Mg over Ca. In terms of mineral solubility equilibria, the MINTEQA2 model predicts that with increasing solute concentrations in the pan, the saturation indices of the carbonate minerals (such as calcite, aragonite and dolomite) would increase.

The Eugster–Hardie flow diagram depicts a chemical divide occurring following the precipitation of the carbonate minerals (i.e. calcite, high Mg–calcite, protodolomite, magnesite, etc.). This chemical divide separates waters that are Ca and Mg rich, but  $\text{HCO}_3^-$  poor, with  $\text{Mg} \gg \text{Ca}$  (type IIIB), from those that are Ca and Mg poor, but  $\text{HCO}_3^-$  rich, with  $\text{Mg} \gg \text{Ca}$  (type IIIA). Eugster and Hardie (1978) propose that with further evaporative concentration type IIIB waters will become supersaturated with respect to gypsum, while type IIIA waters will precipitate Mg–silicate minerals and then form a concentrated  $\text{Na–CO}_3\text{–SO}_4\text{–Cl}$  brine (path IIIA<sub>1</sub>), or simply evaporate until this brine is formed without the precipitation of Mg–silicates (path IIIA<sub>2</sub>). In Barber’s Pan, MINTEQA2 predicted that with significant evaporative concentration, the Mg–silicates sepiolite and talc ( $\text{Mg}_3\text{Si}_4\text{O}_{10}[\text{OH}]_2$ ) could be induced to precipitate, but that the water would remain undersaturated with respect to gypsum, suggesting that the evaporative concentration was following path IIIA. As a final step, Eugster and Hardie (1978) proposed that  $\text{SO}_4^{2-}$  reduction could occur, with the final brine being dominated by  $\text{Na–CO}_3\text{–Cl}$ .

Eugster (1980) proposed that in order to document solute behaviour during evaporative concentration, it is necessary to identify an indicator of the degree of evaporative concentration. He states that this indicator should be a solute that does not participate in any of the fractionation mechanisms involved in brine evolution, and hence is conserved in solution. Among the major constituents, he found  $\text{Cl}^-$  to be the most useful indicator species, except in concentrated brines saturated with respect to chloride minerals. This exception is clearly not applicable in Barber’s Pan. Calculation of a  $\text{Cl}^-$  concentration factor for Barber’s Pan using values from the DWAFF database (Appendix 3) showed that during the period when Barber’s Pan almost dried up, the  $\text{Cl}^-$  concentration had increased by a factor of 13. The integrity of  $\text{Cl}^-$  as a suitable indicator of the extent of evaporative concentration in the pan was confirmed by calculating a concentration factor for  $\text{Na}^+$  using the same data.  $\text{Na}^+$  was found to have become 12.7x more concentrated during the same period, in excellent agreement with the  $\text{Cl}^-$  concentration factor.

Eugster (1980) notes that during evaporative concentration  $\text{SO}_4^{2-}$  can behave in a complex fashion, since it is subject to mineral precipitation (e.g. as gypsum), adsorption and to redox reactions. In Barber’s Pan, the  $\text{SO}_4^{2-}$  concentration increases by only a factor of 5, rather than of 13, as would be the case if it were behaving as a conservative species such as  $\text{Na}^+$  and  $\text{Cl}^-$ . This suggests that  $\text{SO}_4^{2-}$  is being removed from solution in one or other form.

Day (1993), in discussing  $\text{SO}_4^{2-}/\text{Cl}^-$  for various southern African saline systems (including Barber's Pan) noted the loss of sulphates from surface waters with increasing solute concentration due to evaporative concentration. She suggested that this loss could be to the sediments in the form of salts such as gypsum ( $\text{CaSO}_4$ ) or to the atmosphere in the form of S-containing gases (mainly  $\text{H}_2\text{S}$  formed by sulphate reduction), as a result of the physical turnover of the water column or of biotic activities. In the case of Barber's Pan, however, a plot of  $\text{Cl}^-/(\text{Cl}^- + \text{SO}_4^{2-})$  against total dissolved solids (TDS) (Fig. 21) produced a very steep curve which Day (1993) proposed may indicate biological regeneration or physical dissolution of  $\text{SO}_4^{2-}$  as total concentration increases. Alternatively, this steep curve may be the result of continuously oxidizing conditions (with less  $\text{H}_2\text{S}$  being lost) in what is a biologically very productive system.

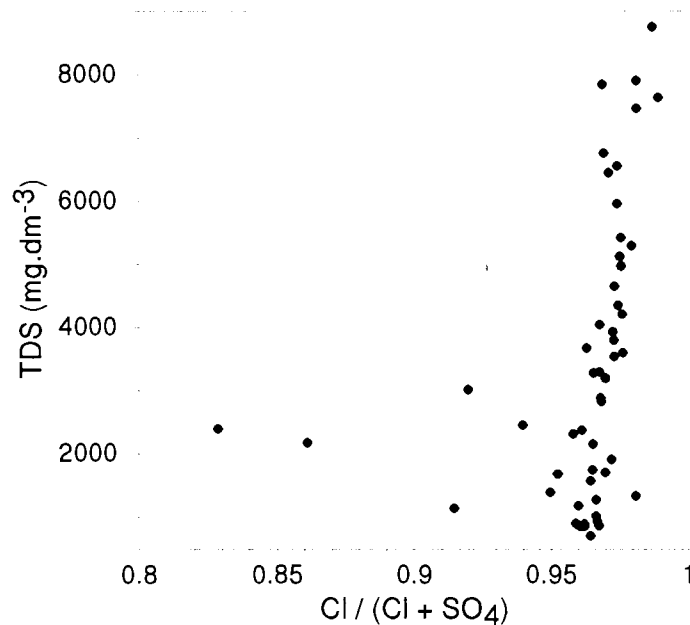


**Figure 21:** The Ratio of  $\text{Cl}^-/(\text{Cl}^- + \text{SO}_4^{2-})$  against TDS for Barber's Pan using DWAF data (1982 to 1988).

MINTEQA2 predicted that Barber's Pan would remain very undersaturated with respect to anhydrite ( $\text{CaSO}_4$ ) gypsum, mirabilite ( $\text{Na}_2\text{SO}_4\cdot 10\text{H}_2\text{O}$ ) and thenardite ( $\text{Na}_2\text{SO}_4$ ) even when evaporatively concentrated 13x. The undersaturation with respect to thenardite and gypsum implies that probably it would also be undersaturated with respect to other sulphate evaporites such as glauberite ( $\text{CaSO}_4\cdot\text{Na}_2\text{SO}_4$ ) and burkeite ( $\text{Na}_2\text{CO}_3\cdot 2\text{Na}_2\text{SO}_4$ ). The loss of  $\text{SO}_4^{2-}$  from the pan water must therefore be attributable to a combination of reduction with the consequent precipitation of iron sulphides to the sediments and the evolution and subsequent loss to the atmosphere of  $\text{H}_2\text{S}$ .

Doner and Lynn (1989) state that the first iron sulphide precipitate to form in reduced sediments and soils is amorphous FeS, which imparts a characteristic black colour to the soil, often accompanied by an odour of H<sub>2</sub>S. They also note that adding HCl to the reduced sediment will result in the greying of the soil and the release of H<sub>2</sub>S if FeS is present. The Barber's Pan sediments, particularly the deeper central sediments, were characterized by black mottles, which increased in size with time in sediment samples that were stored, undisturbed, in sealed plastic bottles. The evolution of pockets of gas over time was also observed in these sediment samples. This gas was found to have a rotten egg smell characteristic of H<sub>2</sub>S. Addition of HCl to a sample extracted from these sediments caused the evolution of H<sub>2</sub>S (rotten egg smell) and tended to lighten/bleach the colour of the sediment, suggesting the presence of amorphous FeS in the samples. Doner and Lynn (1989) also record that the presence of iron sulphides in soils is indicated by a pH of 3.0 to 3.5. In Barber's Pan, the pH of the bulk pan water was > 9.2 in all cases, while that of the sediment supernatant and interstitial waters, was in the range 8.0–8.7. The pH of all the water in the pan is likely to be strongly buffered by the high alkalinity as discussed in section 3.3.2.3; this may explain why the pH of the sediment-associated waters was not lower, as would be expected in a reduced environment.

The processes whereby sulphur is lost from freshwater lakes in east Africa appear to involve the loss of sulphate as organic-S compounds, which either remain intact or undergo diagenesis, eventually forming pyrite. Accumulation of organic-S compounds in the sediments of productive lakes occurs since these compounds are not readily metabolized by sulphate reducing bacteria. Furthermore, few of these lakes have H<sub>2</sub>S-rich hypolimnia. When H<sub>2</sub>S does occur it is primarily the result of dissimilatory sulphate reduction together with putrefaction. In these lakes sulphide can be lost by the precipitation of metal sulphides and/or the loss of H<sub>2</sub>S to the atmosphere. The formation of H<sub>2</sub>S, however, does not necessarily remove sulphur from lake waters and much of the H<sub>2</sub>S produced may eventually be oxidized back to sulphate before it is lost (Kilham, 1984).

Kilham (1984) notes that in addition to being more concentrated than freshwater lakes, east African saline lakes differ from their freshwater counterparts in three ways. Firstly, their sediments usually contain much less organic carbon (< 10 % by weight) which he suggests may indicate that decompositional processes are more effective in these waters and that organic-S is not a major component of the sediments. Secondly, sulphate reduction is so

pervasive in saline lakes that both waters and sediments often smell, at least faintly, of H<sub>2</sub>S. Thirdly, some of the most concentrated saline lakes lose sulphate as sulphate-containing minerals.

In Eugster and Hardie's flow diagram, the reduction of SO<sub>4</sub><sup>2-</sup> leads to the evolution of a Na–CO<sub>3</sub>–Cl brine. This was indeed the case with Barber's Pan after the pan water had been concentrated 13x.

### **3.3.4 Solute behaviour during the evaporative concentration of Barber's Pan**

Eugster and Jones (1979) reviewed the behaviour of major solutes during closed basin brine evolution and proposed that individual solutes behave in a variety of ways during the course of evaporative concentration. Their review is discussed in section 2.4.3.

The use of chloride as an indicator of evaporative concentration has been discussed in section 3.3.3. Its usefulness is attributable to the fact that it does not participate in any of the fractionating mechanisms identified by Eugster and Jones (1979) as controlling solute behaviour during brine evolution. It is completely conserved in solution except in the most concentrated brines which may be saturated with respect to chloride minerals (Eugster, 1980; Eugster and Jones, 1979).

A number of studies have demonstrated the usefulness of plotting other solutes against chloride to determine their behaviour during evaporative concentration (Jones *et al.*, 1977; Kilham and Cloke, 1990). Drever (1988) states that plotting the concentration of any other ion against chloride concentration reveals the extent to which that ion is controlled by evaporation. On a log–log plot, progressive evaporation should cause points to lie on a 45° line (slope = 1) regardless of the initial ratio of the concentrations of the species being plotted. For Barber's Pan, an evaporative sequence spanning the period 1982–1988 is provided by the DWAF data. This period corresponds to a severe drought in the region during which the pan almost dried out completely.

A log–log plot of Na against Cl for the pan data (Fig. 22) shows that the majority of the points fall close to the 45° line over a concentration range of 2–3 orders of magnitude. Eugster and Jones (1979) suggest that a more sensitive test of the relative behaviour of Na

and Cl is a plot of molar Na/Cl against Cl concentration. Figure 23 shows that, despite a certain amount of scatter, the Na/Cl ratio remains fairly constant.

During the evaporative concentration of the pan Na, therefore, behaved as a conservative species as did Cl (a Type I solute ([Fig. 12] according to Eugster and Jones, 1979). A comparison of the concentration factors of the two ions over this period (section 3.3.3 and Appendix 2) provides further confirmation.

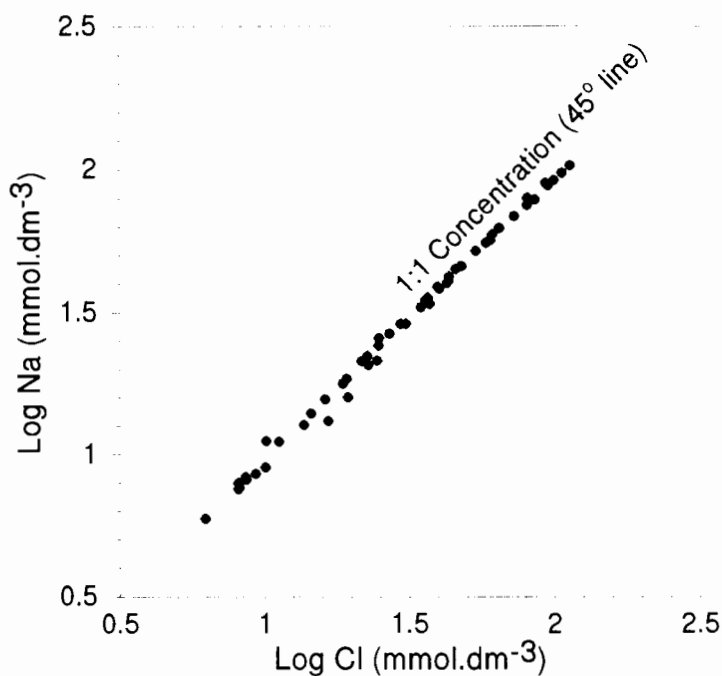


**Figure 22:** A plot of the concentration of Na against Cl for Barber’s Pan water over the period 1982 – 1988.

The alkalinity values from the DWAF data base are expressed in terms of mg/l of  $\text{CaCO}_3$ . This expression assumes that alkalinity results only from  $\text{CaCO}_3$  and  $\text{HCO}_3^-$ , which in certain lakes (e.g. closed alkaline lakes such as Barber’s Pan) implies a greater amount of Ca than is actually present. In moderately hardwater lakes nearly all of the base is present as  $\text{HCO}_3^-$ , allowing the term bicarbonate alkalinity (i.e. as  $\text{mg.dm}^{-3} \text{HCO}_3^-$ ) to be used (Wetzel, 1983). All the alkalinity values from the DWAF data base were recalculated to express the pans alkalinity in terms of  $\text{HCO}_3^-$ . Plotting bicarbonate alkalinity against Cl for Barber’s Pan (Fig. 24) shows that the  $\text{HCO}_3^-$  behaved like a type III solute (Fig. 12), being gradually removed from solution with increasing solute load.  $\text{CO}_3^{2-}$  and  $\text{HCO}_3^-$  exhibited the same behaviour during evaporative concentration in Lake Magadi, Kenya and in several lakes of the Basotu Lake District, Tanzania (Kilham and Cloke, 1990).

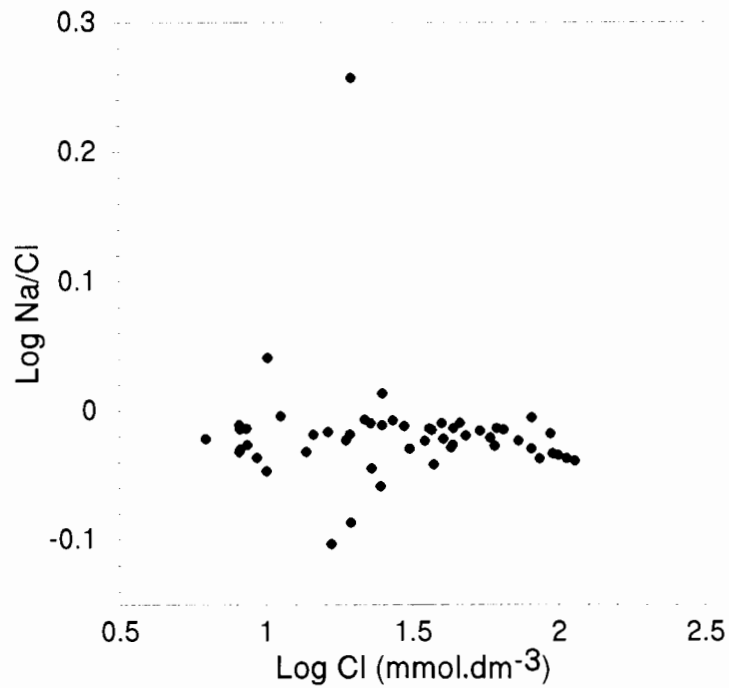


**Figure 23:** A plot of the Na/Cl ratio against Cl concentration for Barber's Pan water over the period 1982 – 1988.

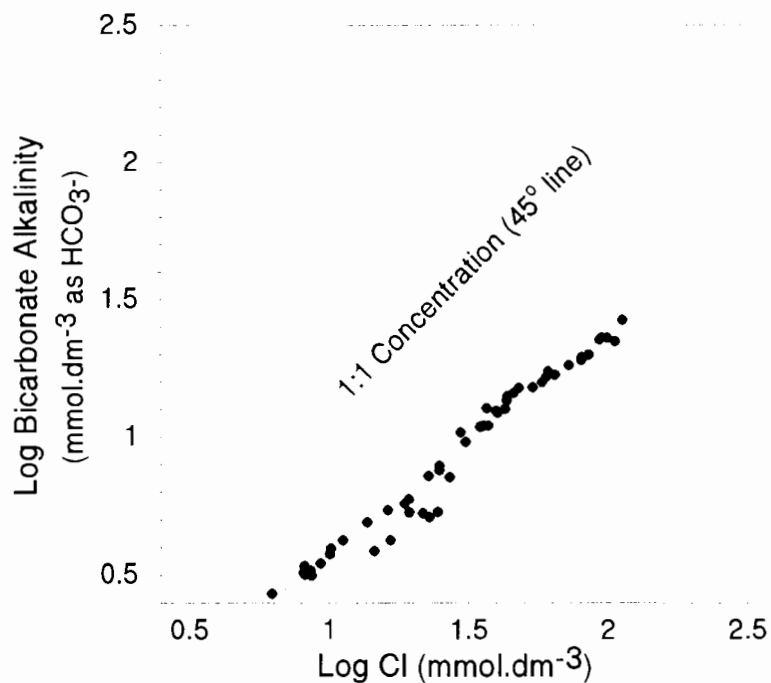


**Figure 24:** A plot of bicarbonate alkalinity against Cl concentration for Barber's Pan water over the period 1982 – 1988.

The Ca concentration in the pan declined gradually during progressive evaporative concentration, although the data shows a considerable degree of scatter (Fig. 25). The

correlation coefficient ( $r$ ) for the plot was found to be  $-0.27$  ( $P_{|r|=0} = 0.047$ ;  $n = 53$ ), indicating no significant correlation. In Lake Magadi Ca is removed rapidly from solution by precipitation as carbonate cements, following a type IIb behaviour curve (Fig. 12) (Jones *et al.*, 1977). Ca also behaves as a type IIb solute in a number of saline lakes of the Basotu Lake District (Kilham and Cloke, 1990).

In the Great Salt Lake system, U.S.A., it is, however, gradually lost from solution over the entire concentration range, following the Type III curve (Eugster and Jones, 1979). In Barber's Pan the loss is also more gradual, similarly following a Type III curve.

MINTEQA2 predicted that the pan water would be supersaturated with respect to carbonate minerals during all stages of evaporative concentration (section 3.3.2.6). Precipitation of calcite (and possibly aragonite) is therefore, likely to be the main removal mechanism of Ca from the water, although biogeochemical cycling by *Chara sp.* (section 3.3.2.5.2) may also play a role.

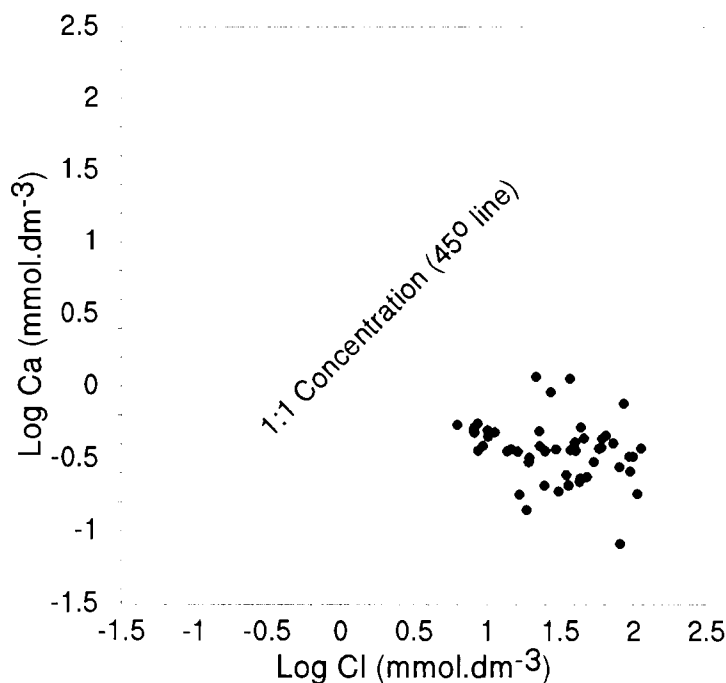


**Figure 25:** A plot of Ca against Cl concentration for Barber's Pan water over the period 1982 – 1988.

Mg followed a typical type III curve, being lost from solution gradually over the entire concentration range (Fig. 26). MINTEQA2 predicted the precipitation of Mg–carbonates such as dolomite and magnesite over the entire concentration range of the pan water (section 3.3.2.6). The precipitation of carbonates could, therefore, account for the gradual removal of Mg during evaporative concentration. In Lake Magadi and several lakes in the Basotu Lake District, Mg was initially removed from solution during evaporative concentration, but with continued evaporation began to behave like a conservative solute (Eugster and Jones, 1979; Kilham and Cloke, 1990). Barber’s Pan is unusual in that Mg is enriched over Ca even at low concentrations (e.g. when the pan water is relatively dilute following an episodic influx of water from the Harts River). More Mg than Ca is, therefore, likely to be incorporated into precipitating carbonates, which may explain its continued removal from solution even after considerable evaporative concentration.

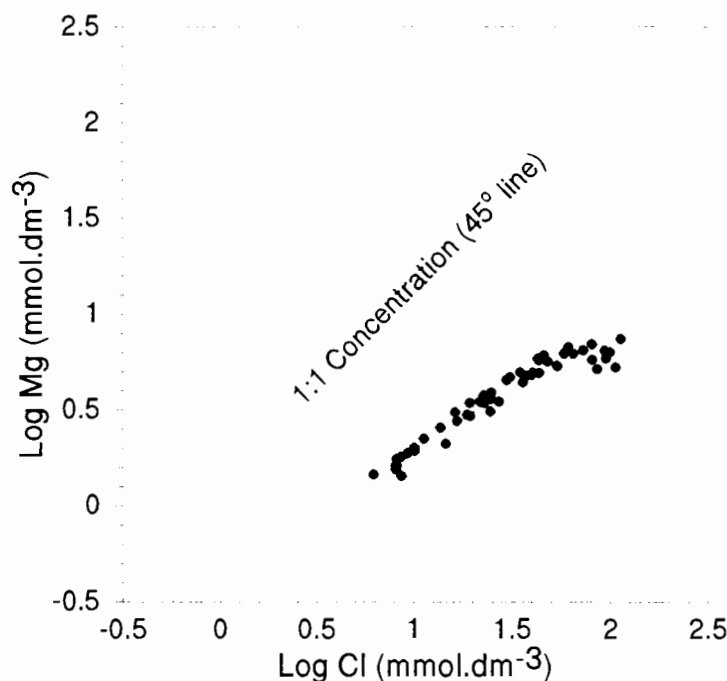


**Figure 26:** A plot of Mg against Cl concentration for Barber’s Pan water over the period 1982 – 1988.

In the data used, evaporative concentration had only progressed over one order of magnitude. In Lake Magadi, Mg only began to behave like a conservative solute after evaporative concentration had proceeded over 2 – 3 orders of magnitude. With more evaporative concentration of the pan water Mg may, therefore, begin to display the conservative solute tendencies observed at Lake Magadi and in the Basotu lake district.

In the Magadi Basin K followed a Type IV (Fig. 12) behavioral trend, initially behaving conservatively, then undergoing differential loss and finally becoming conservative again (Eugster and Jones, 1979). In the Basotu Lake District, Kilham and Cloke (1990) record that K was concentrated according to a type III trend, gradually being lost from solution. In Barber's Pan, it also appears to be very gradually lost from solution (Fig. 27), similarly following a type III curve.

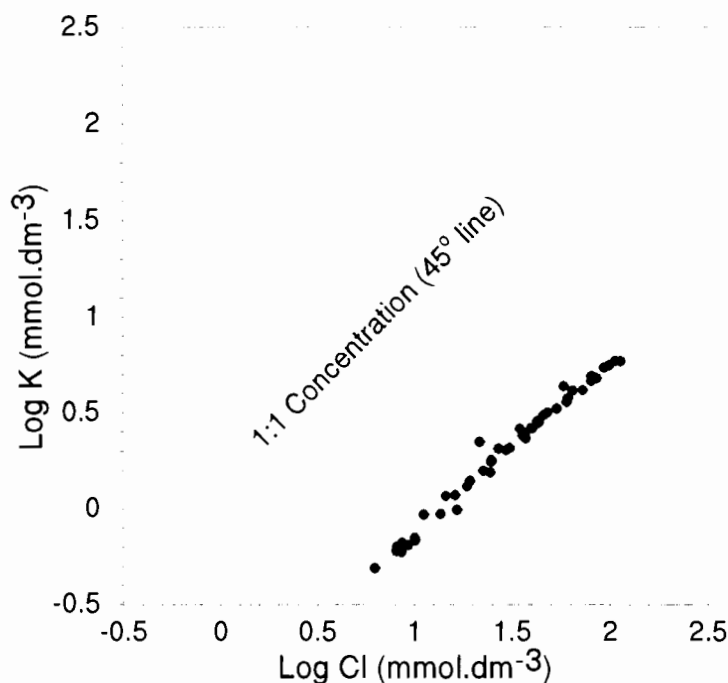


**Figure 27:** A plot of K against Cl concentration for Barber's Pan water over the period 1982 – 1988.

Figure 28 suggests that sulphate is also gradually lost from solution during evaporative concentration (type III). Calculation of a concentration factor (Appendix 2 and section 3.3.3), however, showed that the sulphate concentration in the pan water did not increase to the same extent as the concentration of Cl during evaporative concentration, indicating that approximately 60 % was removed from solution. The wide scatter in the data may be attributable to analytical error with some obviously aberrant points

being apparent on Figure 28. In many closed basins  $\text{SO}_4^{2-}$  is removed from solution by mineral precipitation (principally gypsum and mirabilite). In basins where gypsum saturation is not reached due to the loss of Ca through carbonate precipitation, sulphate may be involved in other fractionating mechanisms. Of these, sulphate reduction is well documented with products of this reduction being in the form of  $\text{H}_2\text{S}$  and/or iron sulphides. The loss of sulphate through sorption onto the surfaces of solid particles is well documented in the soil literature

(Eugster and Jones, 1979). In Barber's Pan, MINTEQA2 predicted that gypsum precipitation was unlikely. Other factors (discussed in section 3.3.3) point to the precipitation of iron sulphides in the pan, which would account for the removal of  $\text{SO}_4^{2-}$ . In the Devils Lake Chain (North Dakota, U.S.A) very little sulphate removal takes place. In these lakes, sulphate reduction may not be as important as in other saline systems because of the shallow depths and effective wind mixing that takes place (Eugster and Jones, 1979). The importance of wind in the formation of Barber's Pan has been discussed (section 1.1.3) and the pan itself is a fairly shallow body of water (usually between 4–9 m in depth). As with the Devils Lake Chain, these factors may act to reduce the extent of sulphate reduction in the pan, explaining the relatively conservative behaviour of  $\text{SO}_4^{2-}$  during evaporative concentration of the pan.

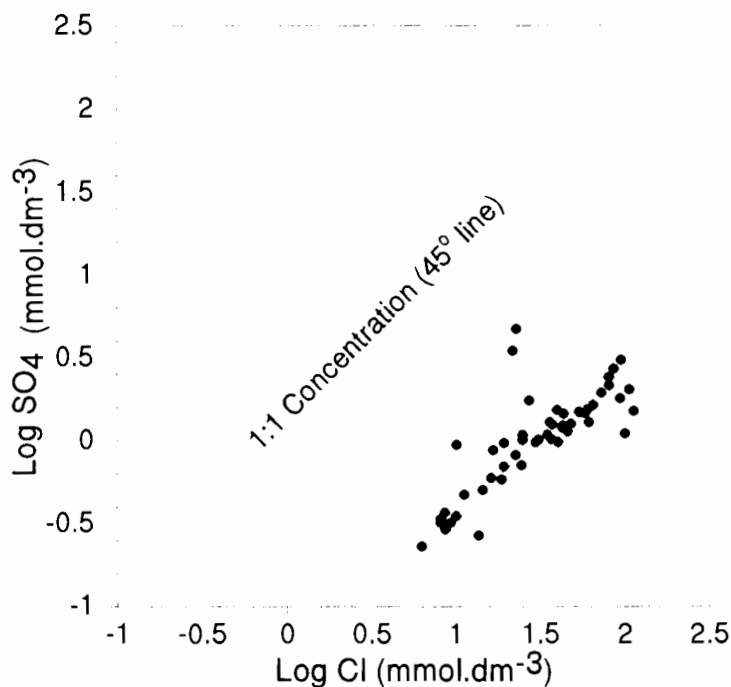


**Figure 28:** A plot of  $\text{SO}_4$  against  $\text{Cl}$  concentration for Barber's Pan water over the period 1982 – 1988.

F behaved like a type II solute, increasing until a point of saturation which was followed by the precipitation of a mineral phase, resulting in its rapid depletion (Fig. 29). MINTEQA2 predicted that the pan water would be supersaturated with respect to fluorapatite throughout the evaporative concentration sequence, the S.I. simply increasing with increased solute load.

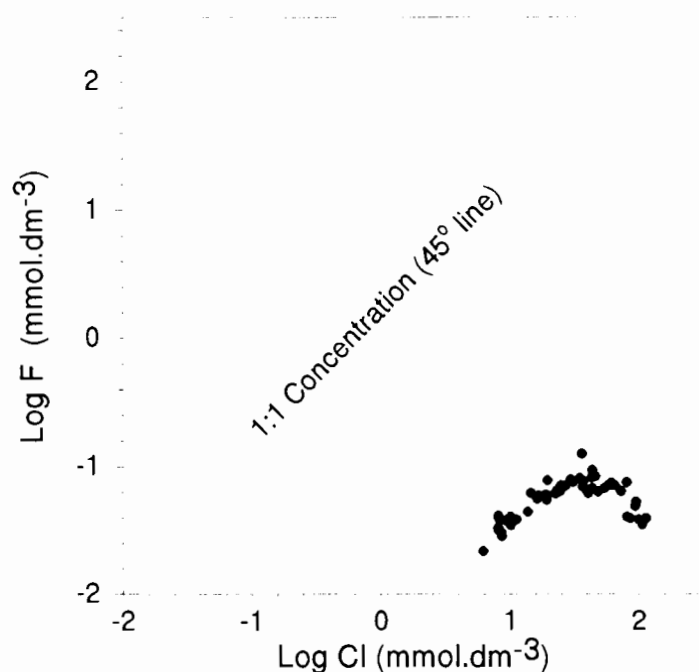


**Figure 29:** A plot of F against Cl concentration for Barber's Pan water over the period 1982 – 1988.

In the Basotu Lakes District, F appeared to follow a type III relationship, although the data showed considerable scatter. The variability in the data was attributed to the precipitation of fluorite and fluorapatite (Kilham and Cloke, 1990). In Lake Magadi, F showed very complex behaviour, with calculated saturation indices showing the water to be undersaturated with respect to fluorite although fluorite was present in the sediments (Jones *et al.*, 1977). Jones *et al.* (1977) propose that the fluorite in the sediments may have been a later authigenic product of the interaction between the fluoride rich brines and minerals such as calcite and gaylussite which are contained in the older lake beds.

The plot of Si against Cl (Fig. 30) shows a large amount of scatter. Combrinck (1966) attributed the fluctuations in silica concentrations in the pan water to the activities (uptake) of silica by diatoms, plankton and benthic organisms.

Si can be removed from natural waters by a number of different processes and consequently its behaviour differs from one closed-basin to another. At Lake Magadi, the hot springs were found to have a pH of between 9 and 10. Under such alkaline conditions species of silica other than  $\text{H}_4\text{SiO}_4$  become important (e.g.  $\text{H}_3\text{SiO}_4^-$  and  $\text{H}_2\text{SiO}_4^{2-}$ ) and the solubility of amorphous silica increases rapidly with the result that silica acts essentially as a conservative

species, its concentration increasing as pH and Cl increase, over the concentration range from hot springs to lake brines (Eugster and Jones, 1979). In the Basotu Lake District, on the other hand, Si concentrations appear to remain relatively constant as Cl concentrations increase over two orders of magnitude (type V behaviour). This is partly attributable to the removal of Si from solution by diatoms (Kilham and Cloke, 1990). In Barber's Pan, MINTEQA2 predicted that the bulk pan water was undersaturated with respect to a number of Si containing minerals, including quartz and amorphous silica, even at the highest solute load recorded, but supersaturated with respect to others. The interstitial water was predicted as being slightly supersaturated with quartz (Table 10). This suggests that some of the dissolved Si is being removed from the bulk pan water. This removal may be attributable to the activities of diatoms, plankton and benthic organism as proposed by Combrinck (1966) or possibly to the incorporation/coprecipitation of Si with aluminosilicate minerals like smectite and sepiolite. Alternately, both processes may be contributing to the removal of Si.

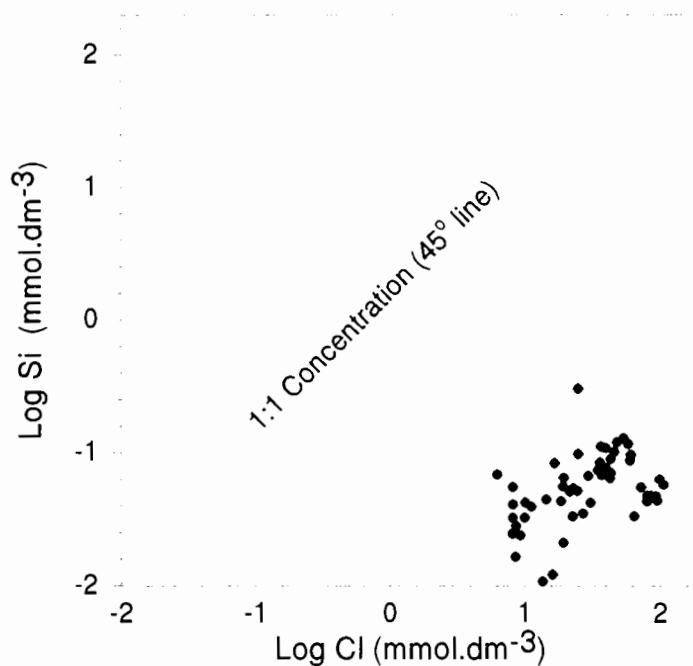


**Figure 30:** A plot of Si against Cl concentration for Barber's Pan water over the period 1982 – 1988.

### 3.3.5 The nutrient and pollutant status of Barber's Pan

Pan ecosystems have three distinctive limnological characteristics which determine the way in which they respond to changes in the input of resources (water, light and nutrients) and pollutants (Rogers *et al.*, 1989):

1. Their relatively large surface area to volume ratio gives them a limited capacity to buffer the effects of environmental factors. As a consequence, pan ecosystems experience marked fluctuations in light and temperature. Evaporative water loss from these systems is high and wind is an important factor, frequently resuspending sediments and bringing about associated changes in pH, redox status and nutrient concentrations.
2. Pans have a high littoral to pelagic zone ratio and benthic algal and aquatic plant communities generally dominate. As a consequence, organic matter production is high and a diversity of habitats exists for aquatic, amphibian and avian fauna.
3. Pans are endorheic; allochthonous inputs to the water body therefore accumulate making pans very sensitive to pollutants in general and eutrophication in particular.

#### 3.3.5.1 Nutrients in Barber's Pan

As discussed in section 2.5, the ionic composition of freshwaters is dominated by  $\text{Ca}^{2+}$ ,  $\text{Mg}^{2+}$ ,  $\text{Na}^+$ ,  $\text{K}^+$ ,  $\text{Cl}^-$ ,  $\text{HCO}_3^-$ ,  $\text{CO}_3^{2-}$  and  $\text{SO}_4^{2-}$ . Nitrogen, phosphorus, iron and the numerous minor elements, while biologically very important, do not contribute significantly to total salinity. Under a large majority of lake conditions, the most important limiting nutrients are phosphorus and nitrogen, although variations in solubility can, at times, make elements such as Fe and Si largely unavailable. Phosphorus is more frequently limiting than nitrogen (Wetzel, 1983).

##### 3.3.5.1.1 Cations

Of the major cations in freshwater, magnesium, sodium and potassium show relatively conservative behaviour under typical freshwater conditions and biotic demand for these elements is small. Calcium is more reactive, exhibiting marked seasonal and spatial dynamics.

It is a required nutrient in the normal metabolism of higher plants and is considered an essential element in algae (Wetzel, 1983). Barber's Pan is unusual in that the concentrations of magnesium dominate over calcium even at low salinities (section 3.3.2.5.2). In soft water lakes having calcium levels well below saturation levels, depletion of calcium levels by biota cannot usually be detected relative to the existing levels in the water (Wetzel, 1983). The bulk pan water contains low but significant amounts of calcium and it is, therefore, unlikely that Ca concentrations in the pan water are limiting to the pan biota.

Sodium and potassium are involved primarily in ion transport and exchange. Certain species of blue-green algae have been found to have sodium requirements of between 4 – 40 mg.dm<sup>-3</sup>. Metabolic requirements for magnesium by organisms tend also to be minor relative to concentrations commonly found in freshwaters (Wetzel, 1983). Sodium, potassium and magnesium all occur in abundance in the pan water when compared with levels recorded by Talling and Talling (1965) for a number of African lakes and are, therefore, unlikely to be limiting to primary or secondary productivity in the pan.

A number of studies have shown that the ratio of monovalent to divalent cations (M:D) can influence the distribution and dynamics of algae and aquatic plants that commonly occur in freshwaters. M:D ratios below 1.5 are considered favourable to diatoms while much higher ratios appear to favour desmid algae (Wetzel, 1983). In Barber's Pan, the M:D ratio calculated from the average value of the cations in the bulk pan water (Table 6) is 5:1. This suggests that current conditions in the pan water favour desmid algae rather than diatoms, implying that diatom populations may not play as significant a role in Si dynamics in the pan water as thought previously by Combrinck (1966). In order to draw any firm conclusion as to the role of diatoms in Si dynamics in the pan water, however, a more detailed investigation of the diatom population in the pan will have to be carried out.

#### 3.3.5.1.2 Anions

Carbonate and bicarbonate seldom limit photosynthesis in aquatic ecosystems. The assimilation of HCO<sub>3</sub><sup>-</sup> by plants having an affinity for both CO<sub>2</sub> and HCO<sub>3</sub><sup>-</sup> has been recorded and can be induced under conditions of low free CO<sub>2</sub> and high HCO<sub>3</sub><sup>-</sup> concentrations. In waters having a high pH, HCO<sub>3</sub><sup>-</sup> assimilation by large aquatic macrophytes (having morphologically

long diffusion paths) can be significant. Active transport of  $\text{HCO}_3^-$  originating from the dissociation of  $\text{CaCO}_3$  and the secretion of  $\text{OH}^-$  can result in the precipitation of  $\text{CaCO}_3$  (Wetzel, 1983). The possible presence of charophytes (*Chara sp.*) on the bottom of Barber's Pan has been discussed (section 3.3.2.5.2). Prescott (1969) records that most species of the genus *Chara* are encrusted with  $\text{CaCO}_3$  which is presumably associated with their photosynthetic activities. The plants extract  $\text{CO}_2$  from  $\text{HCO}_3^-$  thereby causing the precipitation of  $\text{CaCO}_3$ . Utilization of  $\text{HCO}_3^-$  by *Chara sp.* in the pan could, therefore, conceivably contribute to the reduction of  $\text{Ca}^{2+}$  in the pan, acting in concert with the expected precipitation of carbonate minerals like calcite and aragonite (predicted by MINTEQA2) to maintain lower than expected levels of  $\text{Ca}^{2+}$ . The presence of *Chara sp.* has, however, not been confirmed.

Both organic and inorganic forms of sulphur are utilized by living organisms. In addition to being an important nutrient, sulphur can also affect the cycling of other nutrients as well as ecosystem productivity when it undergoes oxidation and reduction. This is because metal sulphides are very insoluble at neutral or alkaline pH values. Precipitation of metal sulphides can remove metals such as Fe, Cu, Zn and Pb from the water column. Alternately, oxidation of these sulphides in aerobic sediments can release such scavenged metals back into circulation (Wetzel, 1983). The oxidation and reduction of sulphur is taking place in the pan sediments (section 3.3.3). Through these reactions the S is likely to exert some influence on the status of certain micronutrients e.g. trace metals. Concentrations of  $\text{SO}_4^{2-}$  in the pan are sufficiently high to suggest that sulphur itself is not a limiting nutrient.

Chloride is important in the general osmotic salinity balance and ion exchange of organisms. Metabolic utilization does not, however, cause significant variations in its spatial and seasonal distribution within most lakes (Wetzel, 1983). The  $\text{Cl}^-$  concentration in Barber's Pan is high and the ion behaves as a conservative solute (section 3.2.4).

#### 3.3.5.1.3 Nitrogen

Wetzel (1983) records that the levels of  $\text{NH}_4$  can range from 0–5  $\text{mg.dm}^{-3}$  in unpolluted surface waters, although concentrations are usually low, particularly in well oxygenated surface waters. Values of up to 10  $\text{mg.dm}^{-3}$  have, however, been recorded in the anaerobic hypolimnetic waters of eutrophic lakes.  $\text{NO}_2^-$  levels of natural lake waters are also generally very low, being in the range 0–0.01  $\text{mg.dm}^{-3}$ . Higher levels (up to 1  $\text{mg.dm}^{-3}$ ) have been

recorded in anaerobic interstitial waters of deep (> 90 cm) sediments and in waters receiving organic pollutants.  $\text{NO}_3^-$  levels are highly variable ranging from undetectable levels to nearly  $10 \text{ mg.dm}^{-3}$  in unpolluted freshwaters.  $\text{NO}_3^-$  also varies seasonally and spatially (Wetzel, 1983).

Levels of  $\text{NO}_2^-$  and  $\text{NO}_3^-$  in the bulk pan water were below the detection limits of the HPIC, and  $\text{NH}_4^+$  was not determined due to instrumental problems. Data from the DWAF database (expressed as  $[\text{NO}_2^-$  and  $\text{NO}_3^-]$  as N and  $\text{NH}_4^+$  as N), indicate that low concentrations of N occur in the pan water, frequently below the detection limits of the analytical technique used for the determinations. The reported values also vary widely (refer to Appendix 3).

Many components of the nitrogen cycle vary seasonally and spatially. Inputs of nitrogen from the guano of migratory waterfowl that briefly reside on a body of water in very high densities can constitute a major source of nitrogen (and phosphorus) (Wetzel, 1983). Linnman (1983) suggested that "seasonal ornithological eutrophication" could be occurring in a number of closed lake basins in Scandinavia. The impact of migrating waterfowl on the nutrient dynamics of Barber's Pan has not been investigated, but considering the large numbers frequently reported as stopping over for varying time periods, the impact may be considerable. This aspect of the nutrient dynamics in the pan should be researched in the near future.

#### 3.3.5.1.4 Phosphorus

Total phosphate concentrations in non-polluted natural waters vary widely from less than  $1 \text{ }\mu\text{g.dm}^{-3}$  to more than  $200 \text{ mg.dm}^{-3}$  in some closed saline lakes. In most uncontaminated surface waters the concentrations of total phosphorus tend to be between  $10-50 \text{ }\mu\text{g.dm}^{-3}$ . The majority of the total P in lakes is in an organic phase of which around 70% or more is within particulate organic material, the remainder being present as dissolved or colloidal organic phosphorus. Inorganic soluble phosphorus is consistently very low, constituting only a few percent of the total phosphorus present. The ratio of inorganic soluble phosphorus to other forms of phosphorus has been found to be approximately 1:20 ( or < 5% present as inorganic phosphorus) in a large number of lakes within the temperate zone, and the percentage of total phosphorus occurring as ionic phosphorus is thought to be considerably less than 5% in most natural waters (Wetzel, 1983). Ionic phosphorus ( $\text{PO}_4^{3-}$ ) is the only form in which phosphorus

is freely available for uptake by primary producers in inland waters. Milstein (1975) proposed that phosphate may be a limiting nutrient in Barber's Pan.

The exchange of phosphorus between the sediments and overlying water is a major component of the phosphorus cycle in natural waters (Wetzel, 1983), and Rogers *et al.* (1989) note that the action of wind on the large surface of a shallow lake causes significant resuspension of the sediment increasing the complexity of the sediment/water/nutrient interactions and deepening the aerobic sediment–surface microzone wherein the solubility of phosphorus is low. They further note that this would tend to remove phosphorus from the water column to the sediment, where it is not available to the phytoplankton. This appears to be an important factor in Barber's Pan and is discussed in detail in section 4.4.6.

Bacteria are of major importance in the dynamics of phosphorus cycling in water, their role in expediting phosphorus exchange across the sediment interface, however, is relatively minor in comparison to chemical equilibria processes. Sediment microflora plays an important role in increasing the concentrations of phosphorus dissolved in the interstitial water of sediments. Bacterial decomposition is proportional to bacterial densities at the interface and directly related to the general productivity of the lake (Wetzel, 1983).

A number of studies have shown the importance of submersed, floating–leaved and emergent angiosperms to the dynamics of the phosphorus cycle and the importance of littoral zone vegetation has been repeatedly emphasized (Wetzel, 1983). The aquatic vegetation of Barber's Pan is apparently dominated by *Potamogeton pectinatus* with other species that have been recorded including *Ceratophyllum demersum*, *Lagarosiphon sp.* and *Ludwigia sp.* (Milstein, 1975; Green, 1995). Recent studies on the cycling and transport of phosphorus in the *Potamogeton pectinatus*–rich littoral zone of Swartvlei, a lake in the Wilderness area of the Cape coast, showed that it was essentially a closed cycle, with any phosphorus released from decaying macrophytes being rapidly reabsorbed by epiphytic algae. This implies that very little phosphorus would be transported from this zone to the circulation of the open lake, while studies on the removal of nitrogen and phosphorus compounds from the lake water have proved unequivocally that *Potamogeton pectinatus* and its epiphytes rapidly take up and store these plant nutrients (Allanson *et al.*, 1990).

Aquatic plants in the littoral zone may act in two ways to reduce phytoplankton growth. They can sequester luxury amounts of nutrients decreasing the rate of nutrient increase in the water column (as discussed above) and they are known to produce chemicals which inhibit algal growth (Rogers *et al.*, 1989). Twinch and Breen (1980) suggest that in the majority of South African impoundments the establishment of extensive macrophyte beds is prevented by marked seasonal and shorter term fluctuation in water levels and by high water turbidity. Consequently, they suggest that the littoral zone may only be of minor importance in the cycling of phosphorus in these water bodies. In Barber's Pan, the high pH of the water is thought to hamper the growth of higher vegetation usually present in the littoral zone of freshwaters, with the consequence that the vegetation of this zone is dominated by sedges (*Juncus*, *Eleocharis* and *Cyperus spp.*) (Milstein, 1975; Green, 1995). The impact of littoral zone vegetation on nutrient cycling within the pan may thus be limited. It is important, however, to quantify the nature and extent of their influence.

The effect of benthic invertebrates on the dynamics of phosphorus cycling between the sediments and water is not completely understood, but it is apparent that the burrowing activities of largely benthic invertebrates can significantly alter the surficial oxidized zone by physical penetration (Wetzel, 1983). In Barber's Pan, the benthic population of the bottom sediments was found to be rather poor, possibly as a consequence of the limestone substrate (Milstein, 1975). The benthos are, therefore, unlikely to exert a major influence on phosphorus cycling in the pan, particularly when the resuspension of the sediment by wind is considered.

The most important form of phosphorus for plant nutrition is ionic inorganic  $\text{PO}_4^{3-}$ . Extensive investigations into the algal requirements for phosphorus allowed freshwater algae to be grouped in categories according to whether their tolerance ranges fell below, around or above  $20 \mu\text{g}\cdot\text{dm}^{-3}$ . *Uroglena sp.* and certain species of *Chara* exhibit optimal growth and have an upper tolerance limit of  $\text{PO}_4^{3-}$  concentrations below  $20 \mu\text{g}\cdot\text{dm}^{-3}$ . *Asterionella sp.* and other diatoms showed optimal growth in waters with less than  $20 \mu\text{g}\cdot\text{dm}^{-3}$ , but had tolerance limits well above this level. Green algae species showed optimal growth at concentrations above  $20 \mu\text{g}\cdot\text{dm}^{-3}$ , with tolerance limits also well above this level (Wetzel, 1983). The average concentration of  $\text{PO}_4^{3-}$  determined in the bulk pan water was  $24 \mu\text{g}\cdot\text{dm}^{-3}$ . This level was, however, very close to the detection limits of the colorimetric procedure used for the determination and thus this value may be inaccurate. Interstitial water concentrations were, however, significantly higher, an average concentration of  $855 \mu\text{g}\cdot\text{dm}^{-3}$  being recorded. The

bulk pan water therefore appears to suit most algal species, concentrations possibly being excessive for certain species of *Chara* and deficient for certain species of green algae. The possible presence of *Chara sp.* on the bottom of the pan has been noted (section 3.3.2.5.2).

On the basis of  $\text{PO}_4^{3-}$  concentrations in the bulk pan water, Barber's Pan would be classified in the meso- to eutrophic category of productivity. This categorization is based on total phosphorus in the water of a lake of which  $\text{PO}_4^{3-}$  forms only a small concentration. The actual productivity of the pan is, therefore, likely to be even higher. The very high levels of  $\text{PO}_4^{3-}$  in the interstitial water are likely to be excluded from the water column as a consequence of an oxidized microzone occurring at the sediment-water interface (described in section 4.4.6) and hence are likely to be unavailable to the pan biota (with the possible exception of rooted vegetation). Concentrations of  $\text{PO}_4^{3-}$  appear to be sufficient, however, to suggest that Barber's Pan is in fact a highly productive system, with phosphorus not being particularly limiting.

#### 3.3.5.1.5 Iron and manganese

Both Fe and Mn are essential micronutrients, but the metabolic demands for these metals are usually sufficiently low so that biota do not materially deplete their concentrations in the environment. Despite this low demand, the reactivity, very low concentrations and restricted availability (particularly of Fe) in the trophogenic zones of lakes suggest that under certain conditions the availability of Fe and Mn may well limit photosynthetic productivity (Wetzel, 1983). As mentioned in Chapter 1, Milstein (1975) suggests that Fe may be limiting to plant growth through interactions with the pan limestone.

Manganese concentrations of less than  $50 \mu\text{g}\cdot\text{dm}^{-3}$  have been found to inhibit the development of green and blue-green algae in streams and to strongly favour diatom growth (Patrick, 1978). Wetzel (1983) proposes that these responses may be ubiquitous, suggesting that the moderate levels of Mn and high levels of Ca in hard-water lakes may both contribute to the general dominance of diatoms in such lakes.

In Barber's Pan the concentrations of Mn were found to be very low (mostly below the detection limits of ICP-AES) with a concentration of  $4 \mu\text{g}\cdot\text{dm}^{-3}$  being the highest level recorded. This implies that diatom growth would be favoured over that of green and

blue–green algae. The high pH and abundance of  $\text{HCO}_3^-$  are likely to limit the solubility of both Fe and Mn in the bulk pan water (section 3.3.2.5.5 and 3.3.2.5.6) reducing their bioavailability. Reducing conditions in the sediment together with wind perturbation of the sediment (which is likely to be significant due to its shallow nature) may promote cycling of these elements. The very low levels of Mn do, however, imply a deficiency. Wetzel (1983) states that the mechanisms of assimilation of iron by organisms from the forms available in oxygenated waters are unclear, but studies have suggested that the peptizing and chelating properties of organic acids for iron appear to be the primary source of iron, demonstrating the importance of organic compounds in maintaining assimilable iron. Thus, while iron levels in the pan water are well above the normal range, concentrations of bioavailable iron may be limiting.

#### 3.3.5.1.6 Other micronutrients

Much of the discussion on Fe and Mn is applicable to other micronutrients (section 3.3.2.5.12). Generally, the concentrations and availability of micronutrients in most natural waters are adequate to sustain active populations of algae within the constraints of light, temperature and macronutrient availability. Clear cases have been recorded, however, where the concentrations/availability of micronutrients can have a limiting effect on photosynthesis. In hard–water calcareous lakes, micronutrients may be present in forms unavailable for assimilation by aquatic organisms. Dissolved organic matter also exerts a regulatory role on micronutrient availability when the ratio of organic matter to micronutrient concentration is high (Wetzel, 1983).

In Barber's Pan the precipitation of carbonate minerals may act to decrease the availability of certain micronutrients by causing their coprecipitation. As discussed in section 3.3.2.5.12, the high pH and alkalinity of the pan water is likely to decrease the solubility of Zn, Cu and Ni. The concentrations of micronutrients such as boron (B), molybdenum (Mo) and vanadium (V) in the pan water were not determined.

#### 3.3.5.1.7 Sulphur

Sulphur is nearly always present in quantities adequate to meet the high requirements by organisms for protein and sulphate ester synthesis (Wetzel, 1983). The presence of sulphur

reducing bacteria in the pan sediments and the formation of metallic sulphides was discussed in section 3.3.3, as was the formation of H<sub>2</sub>S. Sulphate levels in the bulk pan water are high and not likely to be limiting. Its redox behaviour may, however, contribute to the removal of certain micronutrients from the water to the sediments in the form of metallic sulphides.

#### 3.3.5.1.8 Silicon

Si is of immense importance to diatoms whose tests are comprised of silica. The accumulation of large quantities of Si by diatoms can markedly modify the flux rates of Si in lakes. Si requirements of other aquatic biota are, however, limited. Utilization of Si in the trophogenic zone of lakes by diatoms often reduces epilimnetic concentrations (Wetzel, 1983). Si concentrations in the bulk pan water are markedly lower than those recorded in the interstitial water (section 3.3.2.5.10). Combrinck (1966) attributed fluctuating levels of Si in the pan to the activities of diatoms, plankton and benthic organisms. As discussed in section 3.3.2.5.10, however, the supersaturation of the water with respect to several phyllosilicate clays provides an adequate non-biological explanation for low Si levels encountered in the bulk pan water.

#### 3.3.5.2 *Pollutants in Barber's Pan*

In order to effectively manage any natural ecosystem, a sound understanding of its functioning is essential. The effects of human interference on a natural ecosystem can only be determined when information pertaining to the natural characteristics and responses to change of the system and its biota have been collected (Dallas and Day, 1993). As was noted in section 3.1 literature on the physical, chemical and biological limnology of South African saline lakes is very limited.

The idea of water "quality" is a human construct and tends to evaluate water from the point of view of a human user. Good quality water is usually viewed as being pure and unpolluted if it is fit for human consumption and livestock watering. While such water might also be suitable for the majority of freshwater aquatic biota, it could well be a very hostile environment to organisms living in the sea, estuaries and inland saline lakes. It is, therefore, critical to consider the water quality of a natural ecosystem from the point of view of its natural inhabitants (Dallas and Day, 1993).

Table 12 compares a number of water quality variables determined for the bulk pan water with water quality standards stipulated for four categories of water use that may be applicable in the management and utilization of the pan. A host of other water quality variables crucial to gauging the quality of the pan water were not determined, however. In particular, pesticides and a variety of metals and other elements. It is imperative that the levels of these other possible pollutants be determined in the near future.

The following discussion focuses on those water quality criteria that were found to exceed recommended quality standards for particular uses (as specified in Table 12). The pan water is currently being used as drinking water, for the protection of aquatic life and for livestock and game watering. Furthermore, it has at times been used to irrigate crops. Consequently, an evaluation of the pan water "quality" from a human point of view (comparison with accepted standards) provides an important yardstick against which current and future uses and be evaluated.

#### 3.3.5.2.1 TDS, EC and pH

The TDS and pH of the bulk pan water exceed the WHO (1984) standards for drinking water. The EC marginally exceeds the standard proposed for livestock watering, and the pH also exceeds the standards proposed for the protection of aquatic life and for irrigation water.

Very little information is available on the salinity tolerances of riverine organisms and even less is available on the effects of salinity on whole ecosystems. Natural conductivities and TDS concentrations vary widely making it difficult, if not impossible, to recommend an absolute value (Dallas and Day, 1993).

Data from the DWAF database indicate that the TDS (and hence EC and salinity) of the pan water have shown marked variations over the last 13 years, with values ranging from 0.9–8.8 g.dm<sup>-3</sup>. The average value for TDS recorded over this period is 1.4 g.dm<sup>-3</sup>. Tolerance to TDS is very species specific, but Dallas and Day (1993) note that the rate of change of TDS is often more critical than the final salinity of a water body, since most organisms are able to adapt to slow change by physiological acclimation. In general, a salinity of between 5–8 g.dm<sup>-3</sup> seems to mark the upper limit of survival of most salinity-tolerant freshwater animals (Dallas and Day, 1993). The solute concentration in the pan is largely determined by

**Table 12:** A comparison of water quality variables determined for the bulk pan water in Barber's Pan with recommended maximum levels for a number of possible water uses.

Water Quality Variable	Standards for				
	Drinking Water <sup>1</sup>	Protection of Aquatic Life <sup>2</sup>	Livestock Watering <sup>2</sup>	Irrigation <sup>2</sup>	Barber's Pan Bulk Pan Water
pH	6.5 – 8.5	9		9	9.2
TDS (g.dm <sup>-3</sup> )	1				1.3
Alkalinity (as mg.dm <sup>-3</sup> CaCO <sub>3</sub> )		> 20			602
EC (mS/m)		Variable	1980		1921
Na (mg.dm <sup>-3</sup> )	200	500			363
Ca (mg.dm <sup>-3</sup> )		1000	1000		16.7
Mg (mg.dm <sup>-3</sup> )		1500		300	72.3
K (mg.dm <sup>-3</sup> )		50			71.3
Cl (mg.dm <sup>-3</sup> )	250	400	1500	150	367
SO <sub>4</sub> (mg.dm <sup>-3</sup> )	400	1400	1000	200	36
NO <sub>3</sub> (mg.dm <sup>-3</sup> )	10		N < 100		BDL <sup>3</sup>
NO <sub>2</sub> (mg.dm <sup>-3</sup> )			N < 100		BDL <sup>3</sup>
PO <sub>4</sub> <sup>3-</sup> (mg.dm <sup>-3</sup> )	0.3	0.3			0.03
Al (mg.dm <sup>-3</sup> )	0.2	0.1 – 1.5	5	5	1.1
F (mg.dm <sup>-3</sup> )	1.5	1.5	2	15	
Pb (mg.dm <sup>-3</sup> )	0.05	0.1	0.5	5	0.44
Ni (mg.dm <sup>-3</sup> )		0.05			0.12
Cu (mg.dm <sup>-3</sup> )	1	0.2	2	0.2	0.007
Fe (mg.dm <sup>-3</sup> )	0.3	1	10	5	0.37
Mn (mg.dm <sup>-3</sup> )	0.1	1	10	2	0.04
Zn (mg.dm <sup>-3</sup> )	5	0.1	25	5	0.1
Si (mg.dm <sup>-3</sup> )		50			0.38

Explanatory notes for Table 12:

- <sup>1</sup> – Maximum values for drinking water proposed by the World Health Organisation (WHO) (1984)  
<sup>2</sup> – Maximum values recorded by Kempster *et al.* (1980)  
<sup>3</sup> – BDL = Below detection limits

evaporative concentration and periodic inputs of water from the Harts River. Evaporative concentration in the pan is a fairly slow process (Section 3.3.3), a 13x increase in the concentration of  $\text{Cl}^-$  (which behaved as a conservative species) occurring over a 7 year period (1982 – 1988). This slow concentration process would have allowed biota to adapt to the increased solute loads. Periodic inundations of water (having a lower solute concentration) from the Harts River may, however, rapidly dilute the evolved brine causing a certain degree of osmotic stress to the salt tolerant organisms. A very rapid dilution took place during 1988 when the TDS of the pan water was reduced from  $8.8 \text{ g.dm}^{-3}$  to  $3.4 \text{ g.dm}^{-3}$  in a two week period (Fig 31). When solute concentrations in the pan water reached  $7-8 \text{ g.dm}^{-3}$  levels, large scale fish deaths were recorded.

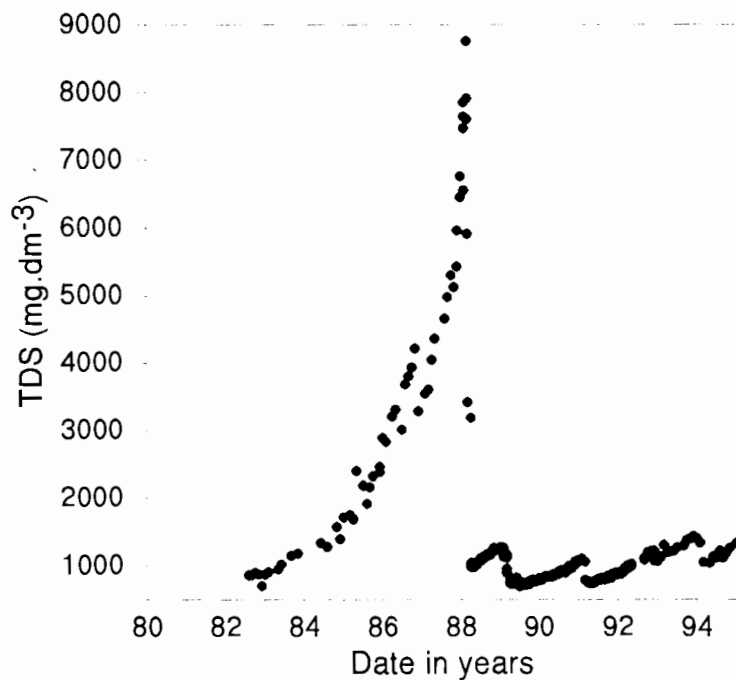


**Figure 31:** Change in TDS over time in Barber’s Pan (DWAf data - refer to Appendix 3).

Salinity can act as an antagonist or synergist in relation to a variety of toxic pollutants, with studies showing that some organisms were sensitised to, while others were protected from, the effects of various pollutants. Generally, salinity is thought to provide some protection against heavy metals, probably through the modification of their chemical speciation (Dallas and Day, 1993). The fact that the pan water is subsaline may, therefore, provide a certain amount of protection from pollution to the pan biota.

Taylor (1993) states that salinity is the most important physical determinant affecting biota in Lake St. Lucia, Natal, where different salinities appear to bring about different ecosystem states. In order to maximise biodiversity in the lake, Taylor (1993) proposed that the system should be allowed to fluctuate through its full salinity range. To allow this to happen, management should be focussed at minimizing the impact of catchment modifications on salinity levels and the rates of change of these levels. In Barber's Pan, salinization of the Harts River and excessive withdrawal of irrigation water are potential problems that need to be investigated.

The high pH of the pan water is a natural phenomenon and DWAF data shows that it has remained fairly constant over time. This suggests that the pan biota would be physiologically adapted to these pH levels. The pH of a water body influences the chemical speciation of its constituent ions and in so doing alters the bioavailability and toxicity of certain elements (Dallas and Day, 1993). The very high pH values recorded in the bulk pan water can act to reduce the solubility of trace metals present in the pan water, reducing their environmental impacts. Speciation modelling of the pan water predicted the predominance of carbonate and hydroxyl associated species (section 3.3.2.5).

#### 3.3.5.2.2 Lead

Pb values in the water exceed WHO (1984) standards for drinking water as well as those for the protection of aquatic life given by Kempster *et al.* (1980). Pb levels also approach maximum levels stipulated for water used by livestock (Kempster *et al.*, 1980). Pb is a highly toxic and cumulative pollutant (Kempster *et al.*, 1980) and these high levels in the pan water are a cause for concern. MINTEQA2 speciation predicted that most of the Pb in the water would be present as  $\text{PbCO}_3$ , which is virtually insoluble and consequently not very bioavailable. Pb levels in the surficial sediments appear low when compared to levels commonly observed in igneous rocks. Adriano (1986) records levels of  $15 \text{ mg.kg}^{-1}$  (with a range from  $2-30 \text{ mg.kg}^{-1}$ ) as the average for igneous rocks world wide. The average value for limestones is given as  $9 \text{ mg.kg}^{-1}$  (with no range stipulated). The average Pb levels in the pan sediment,  $7.1 \text{ mg.kg}^{-1}$  (range  $3.3-12.0 \text{ mg.kg}^{-1}$ ), were found to be on average half that recorded for the Harts River sediment ( $14 \text{ mg.kg}^{-1}$ ). Substantially elevated levels relative to the Harts River and Barber's Pan and Leeupan surficial sediments were, however, recorded in the single core sample analyzed. The Pb concentrations in the core increased with depth

(section 4.4.4). The shallow nature of the pan coupled with the strong winds frequently reported in the area is likely to cause a significant degree of perturbation of the bottom sediments, making it difficult to determine whether any enrichment of the superficial sediments has occurred. Such enrichment would be indicative of Pb deposition associated with anthropogenic activities (Förstner and Wittmann, 1979). Longer cores, penetrating through to the pan parent material, will have to be taken in order to determine original background levels of Pb in the pan. On this basis, conclusions could be drawn as to the actual extent of Pb contamination in the pan. As Barber's Pan is situated in a largely rural area, away from significant industrial activities, the Pb levels in the water are likely to be associated with atmospheric inputs and boating activities rather than significant point source inputs via the Harts River. Mackay (1993) records that boating activities are often the source of heavy metals via anti-fouling paints. The use of leaded fuel is also likely to contribute Pb to the pan water. Barber's Pan, being a popular angling destination, supports significant boating activities, the exact extent of which needs to be quantified.

Two further sources of Pb in the pan water could be lead sinkers (lead weights) used by anglers and lead shot from wing shooting activities. Wing shooting may have taken place prior to the pan being designated as a protected nature reserve. The extensive angling which takes place on the pan suggests that lead sinkers are likely to make a significant contribution to the overall Pb content of the sediments.

#### 3.3.5.2.3 Nickel

Nickel concentrations in the pan water exceed the standards for the protection of aquatic life recorded by Kempster *et al.* (1980). Ni ions tend to be soluble at pH values < 6.5. Above pH 6.5 Ni tends to form insoluble nickel hydroxides (Dallas and Day, 1993). MINTEQA2 predicted that Ni in the pan water would be approximately equally distributed between the two species  $\text{NiCO}_3$  and  $\text{Ni}(\text{CO}_3)_2^{2-}$ . The high pH of the pan water together with the association of Ni with carbonate is likely to substantially decrease the availability of Ni to biota in the pan. MINTEQA2 also predicted that the pan water was supersaturated with respect to carbonate minerals such as calcite. Coprecipitation of Ni with carbonate minerals could also, therefore, contribute to its removal to the sediments. Much of the discussion pertaining to Pb is applicable to Ni. As for Pb, boating activities are the likely source of Ni in the pan and

longer sediment cores will need to be taken in order to determine natural background levels in the sediment.

#### 3.3.5.2.4 Aluminium

Aluminium levels in the pan water are high, exceeding WHO (1984) standards for drinking water. The Al levels are, however, lower than the standards stipulated in Table 12 for other water uses. The elevated pH levels can be attributed to two factors, namely, the high pH and the inclusion of colloidal aluminosilicate material into the total Al concentration determined. The effect of the elevated pH on Al solubility is discussed in section 3.3.2.2, while the overestimation of Al concentration in the water through the inclusion of colloidal aluminosilicate material is discussed in section 3.3.2.6. Speciation modelling of the pan water using MINTEQA2, predicted the predominant form of Al in the water to be  $\text{Al}(\text{OH}_4)^-$  (section 3.3.2.5.13).

#### 3.3.5.2.5 Iron

Fe concentrations slightly exceed WHO (1984) standards for drinking water. As Fe concentrations in drinking water are important in terms of the aesthetic quality of drinking water (i.e. taste) rather than toxic effects, this slightly increased level is unlikely to present a problem. The Fe could, in fact, be largely colloidal, being resuspended in the water column through wind action (discussed in section 3.3.2.5.5).

#### 3.3.5.2.6 Chloride

The chloride levels in the pan exceed the maximum level recommended by Kempster *et al.* (1980) for water to be used in irrigation confirming its unsuitability for agricultural use. The Cl levels in the pan also exceed recommended standards for drinking water, but are well below the recommended standard for livestock (and hence wildlife) watering. The Cl levels are also just below the maximum level recommended for aquatic life. Considering the fluctuating salinity and present subsaline status of the pan water, the pan aquatic organisms are, however, likely to have adaptations for coping with elevated levels (as discussed in sections 3.3.5.2.1 and 3.3.5.2.6).

#### 3.3.5.2.7 Potassium

K levels exceed the standards stipulated by Kempster *et al.* (1980) for the protection of aquatic life. As discussed in several sections above, Barber's Pan is a subsaline environment, periodically becoming saline. The biota within the pan are, therefore, likely to be physiologically adapted to high solute levels. K is non-toxic being involved primarily in ion transport and exchange. The levels recorded in the pan are, therefore, most likely to be within the tolerance limits of the pan biota.

#### 3.3.5.2.8 Phosphorus

$\text{PO}_4^{3-}$  levels in the bulk pan water are low. Interstitial waters were, however, found to be enriched in  $\text{PO}_4^{3-}$  and the deeper pan sediments contained substantial amounts of extractable phosphorus (section 4.4.6). Eutrophication in the pan is not likely to be a problem at present as significant quantities of phosphorus appear to be trapped under an assumed oxidized microzone at the sediment water interface. The rural situation of Barber's Pan suggests that significant anthropogenic inputs via infrequent inflows are not significant. The small catchment and flat topography of the pan and its environs (section 1.2.1) preclude significant contributions of phosphorus from surrounding agricultural lands by surface runoff. The possible occurrence of seasonal eutrophication by migrating avifauna still needs to be investigated.

#### 3.3.5.2.9 General discussion with regard to the status of pollutants in the pan

With the exception of Pb and Ni, the pan appears to be unpolluted with respect to the water quality variables evaluated. A potential source of pollution which has not been investigated is that of biocides from surrounding agricultural land. Considering the potentially severe impact such pollutants could have on the biota (in particular on bird and fish populations) it is strongly recommended that the extent of contamination of the pan (if any) by biocides be quantitatively determined in the near future.

This study established the levels of several potential pollutants in the pan water. Not having previous values to compare these values against makes it difficult to assess the present water quality, particularly from the viewpoint of biota utilizing the pan. As a consequence, some of

the interpretations made may be construed as being subjective. It must be borne in mind, however, that the data are mainly intended for use as benchmark values against which the results of future water monitoring actions can be compared.

### 3.4 Conclusions

The bulk pan water is well mixed, having a very uniform composition throughout. The water can be described as being very alkaline, subsaline and with  $\text{Na}^+$  and  $\text{Cl}^-$  as the dominant ions.  $\text{HCO}_3^-$  is also abundant. The pan water is unusual in that Mg concentrations dominate over those of Ca. The interstitial waters are also very homogeneous, but contain higher concentrations of most solutes determined than the bulk pan water. Exceptions to this are Al and  $\text{SO}_4^{2-}$ , with both their concentrations decreasing in the interstitial water. The decrease in Al is attributed to the decreased pH of the interstitial waters (on average 1 pH unit lower than that of the bulk pan water) lowering its solubility.  $\text{SO}_4^{2-}$  concentrations are thought to be lower in the interstitial waters as a consequence of the reduction of  $\text{SO}_4^{2-}$  by bacteria in the sediments.  $\text{H}_2\text{S}$  and metal sulphides were present in the surficial sediments of the pan. The lower pH of the interstitial water may be attributable to the production of  $\text{CO}_2$  from the decomposition of organic matter leading to the precipitation of  $\text{CaCO}_3$ . The production of  $\text{H}^+$  ions by this reaction could consume alkalinity and therefore lower the pH.  $\text{PO}_4^{3-}$  and Si concentrations were particularly enriched in the interstitial waters relative to the bulk pan water. Depletion of Si in the bulk pan water was attributed to the precipitation of silicate minerals as well as to the activities of diatoms. The enrichment of the  $\text{PO}_4^{3-}$  in the interstitial waters relative to the surface waters was attributed to an oxidized microzone preventing its release into the bulk water column. The pan sediments can, therefore, be seen to be acting largely as a sink for phosphorus. This is discussed further in Chapter four.

Chemical speciation modelling using the thermodynamic equilibrium model MINTEQA2 predicted the predominance of carbonate and hydroxide species. This is likely to be a function of the high pH and  $\text{HCO}_3^-$  concentration. Carbonate and hydroxide species were dominant in the speciation interactions despite the overall dominance of  $\text{Na}^+$  and  $\text{Cl}^-$ , which were predicted as occurring as free ions.

MINTEQA2 predicted that the waters were supersaturated with respect to a number of carbonate minerals that could occur under the given conditions. These included calcite, dolomite, hydroxyapatite and fluorapatite. Precipitation of these minerals could scavenge other ions, trace metals (e.g. Pb) in particular, from solution. Phosphate solubility appeared to be governed by the minerals fluorapatite and hydroxyapatite. The precipitation of these minerals would contribute significantly to the removal of  $\text{PO}_4^{3-}$  from the bulk pan water to the sediments.

Examination of the DWAF data together with modelled outputs of mineral solubility equilibria suggested that brine evolution in Barber's Pan as a result of evaporation followed the fate of the path III inflow water described in Eugster and Hardie's (1978) model of brine evolution. The ratio of Mg/Ca in the bulk pan water increased with evaporative concentration. Three major chemical divides are likely to play an important role in brine evolution in the pan. The first major divide predicted by MINTEQA2 was the precipitation of carbonate minerals (e.g. calcite and dolomite) which would result in the evolution of  $\text{HCO}_3^-$  rich water having Mg strongly enriched relative to Ca. The second chemical divide predicted was the precipitation of Mg-silicate minerals (e.g. sepiolite and talc) leading to the formation of a Na-CO<sub>3</sub>-SO<sub>4</sub>-Cl water. The final divide predicted was the removal of  $\text{SO}_4^{2-}$  through the reduction and precipitation of iron sulphides and evolution of  $\text{H}_2\text{S}$ . The final water composition would thus be dominated by Na, CO<sub>3</sub> and Cl. The sequence of evaporative data from the DWAF confirmed this hypothesis.

During evaporative concentration Na and Cl behaved as conservative solutes.  $\text{HCO}_3^-$  was seen to be gradually removed from solution with increasing evaporation. This corresponded with MINTEQA2 predictions that the water would be increasingly supersaturated with respect to carbonate minerals. Ca levels remained approximately constant during evaporative concentration, suggesting a constant rate of removal. Mg and K showed a gradual decline in concentration with evaporation. The removal of Ca was thought to be through the precipitation of calcite, while Mg removal could have taken place through the precipitation of dolomite, magnesite, sepiolite and talc. A plot of  $\text{SO}_4$  concentration against Cl indicated that  $\text{SO}_4$  was being gradually removed from solution with evaporation. The calculation of a concentration factor for  $\text{SO}_4^{2-}$  relative to  $\text{Cl}^-$  in the bulk pan water indicated that it had only increased 5x as compared to the 13x increase of  $\text{Cl}^-$ . The presence of amorphous iron sulphides in the sediments was also noted as was the evolution of  $\text{H}_2\text{S}$ , showing that sulphur was, in fact,

being removed from solution. F initially behaved in a conservative fashion increasing until a point of saturation after which it was rapidly depleted, most likely in the form of fluorapatite. The Si data showed a large degree of scatter, possibly attributable to diatom activity and the coprecipitation of Si with other minerals. MINTEQA2 predicted that the water would remain undersaturated (or in virtual equilibrium) with Si minerals such as quartz and amorphous silica even at the highest solute levels recorded, while becoming supersaturated with respect to aluminosilicate minerals like sepiolite.

Mn and Fe appeared to be the only nutrients that may be limiting to productivity in the pan at certain times of the year.  $\text{PO}_4^{3-}$  levels recorded in the bulk pan water were high enough to suggest that the pan was at the very least mesotrophic. The very high  $\text{PO}_4^{3-}$  levels in the interstitial waters are likely to be for the most part unavailable to the pan biota as a consequence of the oxidized microzone at the sediment surface interface. Wind is likely to play an important role in the nutrient dynamics of the pan by resuspending the sediment and deepening the oxidized microzone. The possibility of seasonal eutrophication associated with periodically high numbers of avifauna must still be investigated.

On the basis of the water quality variables determined, the pan water appears to be largely unpolluted. Only Pb and Ni have unusually high concentrations and the potential source of these pollutants needs further investigation. With natural baseline levels of potential pollutants in the pan not having been determined in the past, it is difficult to make interpretations as to the significance of current levels. The main significance of the data presented in this chapter is , therefore, that it provides a benchmark against which the results of future monitoring activities can be compared. The subsaline nature of the pan water may provide the pan biota with a certain degree of resistance against pollution.

## 4. THE GEOCHEMISTRY OF BARBER'S PAN SEDIMENTS

### 4.1 Introduction

Chapter two reviewed the available literature on the sediments of saline lakes and pans, while Chapter three consisted of an investigation of the aqueous chemistry of Barber's Pan.

The sediments of freshwater lakes are the sites of major biological activity and microbial degradation of detrital organic matter. They also play an important role in the biogeochemical cycling of nutrients (Wetzel, 1983). Forsberg (1989) states that both organic and inorganic nutrients are continuously being transported to the bottom of lakes by sedimentation. Biological, chemical, physical and mechanical processes, however, act to return some of these nutrients to the water column. An understanding of sediment characteristics is, therefore, imperative to the understanding of nutrient dynamics within a lake and of other interactions which occur at the sediment–water interface.

Barber's Pan is an interesting system in that while originally a deflationary pan formed along palaeodrainage lines, anthropogenic intervention in the early part of this century converted it into an essentially perennial lake. Verster *et al.* (1992) comment on the paucity of data pertaining to southern African pan sediments, noting that very little pedogeomorphic work has been carried out on these features despite their ubiquitous occurrence in the South African landscape.

In the light of the above discussion, the main objective of this chapter is to provide a chemical and mineralogical characterization of the sediments of Barber's Pan. To this end, the chapter encompasses a description of sampling and analytical methods used as well as a comprehensive discussion of the results obtained. Detailed clay mineralogical and chemical analyses were carried out on the surficial sediments of Barber's Pan with similar studies on sediment samples from the Harts River and Leeupan being carried out for comparative purposes. The influence of sediment–water interactions on the availability of phosphate in the pan were also investigated because of the fundamental importance of this nutrient to lake productivity. A preliminary appraisal of sedimentation processes in the pan was also carried out using short cores.

## 4.2 Sediment sampling and analysis

### 4.2.1 Sampling

Sediment samples were collected from Barber's pan, Leeupan and the Harts river inlet (Fig. 32). Three types of sediment samples were collected, namely:

- i) grab samples, using a Van Veen Grab (Fig. 33);
- ii) core samples, using a hand-corer (Fig. 34), and
- iii) grab samples, using a shovel (Fig. 35).

The Van Veen grab (Van Veen, 1936) functions through the lowering to the bed of a pair of hinged jaws that are held apart as the grab is lowered to the bed. Impact with the bed releases a restraining mechanism. Applying tension via the rope attached to the grab causes the jaws to close thereby allowing sampling to occur to a depth of approximately 10 cm. The jaws of the grab are held together firmly during withdrawal. Upon collection, the Van Veen grab samples were emptied into a plastic basin and then transferred into pre-rinsed, screw-top, plastic jars (Fig. 33).

The core samples were obtained by means of hand-corer. This consisted of a length (either 0.50 m or 1 m) of 60 mm diameter PVC pipe. A diver pushed the corer into the sediment by hand, and brought the core to the surface where it was immediately capped at both ends. Freezer facilities were not available at the pan but the cores were maintained in an upright position until frozen in a walk-in freezer at  $-20^{\circ}\text{C}$  on returning to the university (after two weeks). The frozen cores were later opened for examination in the laboratory.

Shovel grab samples simply involved taking several representative shovel fulls of sediment, from a particular location, and packing them into freezer bags which were then sealed.

A total of 17 Van Veen grab samples, 6 cores (two at location 6) and 4 shovel grab samples were collected.

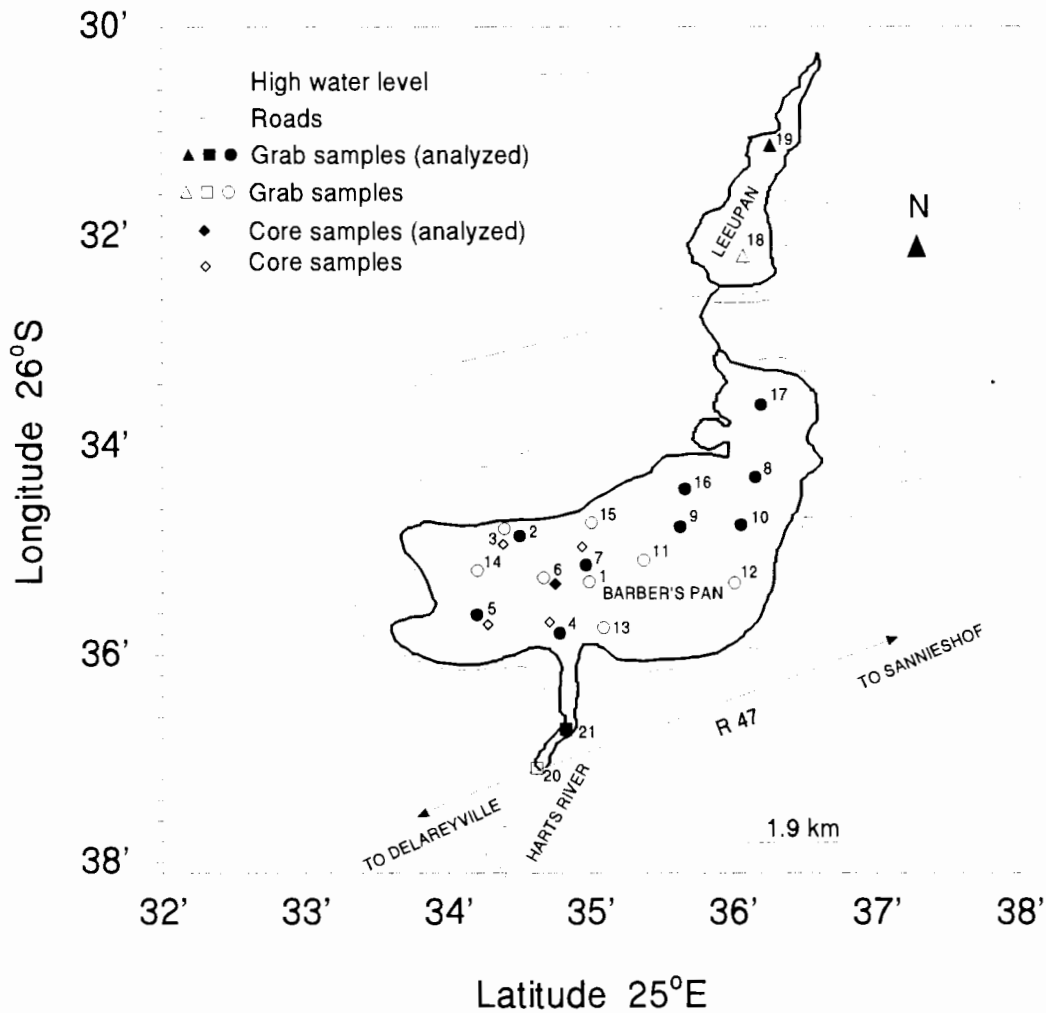
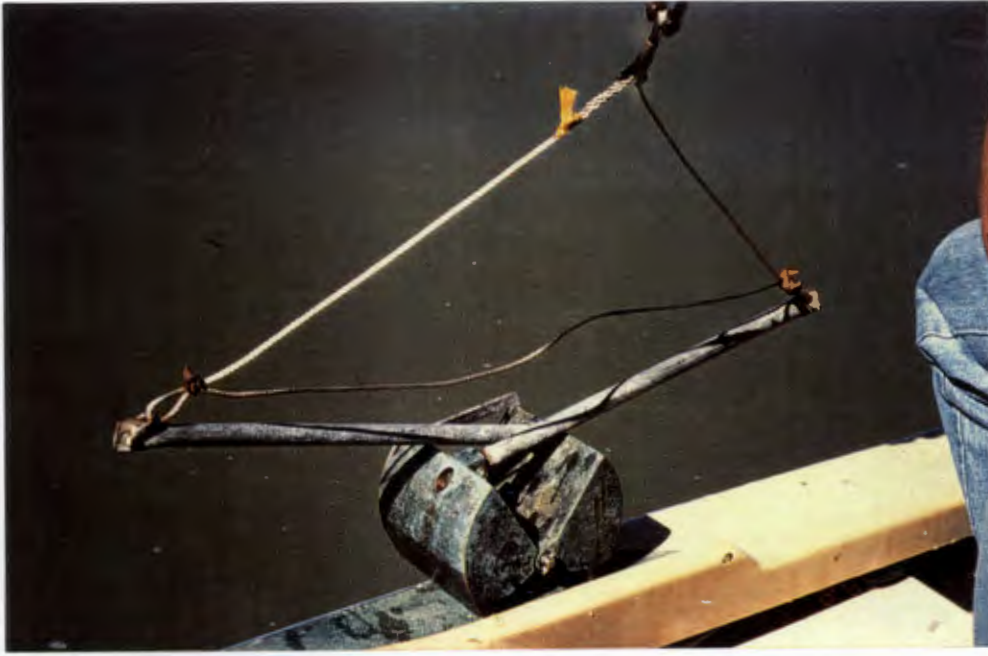


**Figure 32:** A map of the study area showing sites where pan grab and core samples were taken.

#### 4.2.1.1 Barber's Pan

All seventeen of the Van Veen grab samples were collected in Barber's Pan, with the sample sites being distributed evenly across the entire pan. Similarly, all six core samples were taken from Barber's Pan, being distributed across the pan in a similar fashion to the Van Veen samples. Five of the cores taken were 0.50 m in length, while one was 1 m in length. The sample locations were determined by means of a geographical positioning system (GPS).



A



B

**Figure 33:** The Van Veen Grab used for sediment sample collection in Barber's Pan. The grab ready to be lowered to the sediment (A) and being emptied after sample collection (B).



**Figure 34:** The diver preparing to take a core sample from Barber's Pan using a 0.50m PVC hand-corer.



**Figure 35:** A grab sample being taken from Leeupan using a shovel. A lunette associated with Leeupan can be seen in the background.

#### *4.2.1.2 Leeupan*

Leeupan was dry at the time of sampling; as a consequence the two grab samples from the pan were taken by means of a shovel. Leeupan was sampled in order to provide a comparison of the sediments characteristic of an active deflationary pan, subject to the same formative and environmental processes as Barber's Pan, with those of Barber's Pan which no longer experiences significant deflationary episodes.

#### *4.2.1.3 Harts River inlet*

The inlet was also dry at the time of sampling, and two grab samples were taken with a shovel, as for Leeupan. The Harts River was sampled so as to determine the sediment composition of the main sediment input source for Barber's Pan.

### **4.3 Sediment analyses**

Due to time constraints, ten of the seventeen grab samples were selected for analysis, together with one of the shovel samples from Leeupan, and one of the Harts River samples. All of the cores were examined for evidence of stratification, but only the 1 m core sample was subsequently divided into sections and subjected to further analyses.

#### **4.3.1 Organic carbon**

Organic Carbon was determined by means of the Walkley–Black method (Walkley, 1935). Essentially, this is a rapid dichromate oxidation procedure which is widely used in soil investigations as it is simple, rapid, requires minimal equipment and omits heating of the samples. The results obtained cannot, however, be considered strictly quantitative (Nelson and Sommers, 1982).

#### **4.3.2 Carbonate**

The  $\text{CaCO}_3$  content of the sediment samples was determined by means of the "Karbonat–bombe" (Müller and Gastner, 1971), using the method of Birch (1981). This involved treating subsamples of sediment with concentrated HCl which reacted with the

CaCO<sub>3</sub> present in the sample, resulting in the evolution of CO<sub>2</sub>. The volume of CO<sub>2</sub> evolved was measured by a pressure gauge on the "Karbonat Bombe". A calibration curve was prepared using aliquots of CaCO<sub>3</sub> ranging from 0.2 g through to 1.0 g.

### 4.3.3 Clay mineralogy

The clay fraction was isolated from each of the sediment samples by dispersing the samples in a dilute Na<sub>2</sub>CO<sub>3</sub> solution and repeatedly collecting the supernatant after the settling of the > 2µm fraction. The clay collected in this way was then flocculated using NaCl and dialysed against distilled water for 48 hours to remove excess electrolyte. A 2 cm<sup>3</sup> aliquot of the dialysed suspension was pipetted onto a glass slide, to allow the clay particles to settle out with a preferred orientation, and left to dry at room temperature. The clay mineralogy of each sample was then determined by scanning the slides using a Philips PW 1390 X-ray diffractometer fitted with a monochromator, scintillation detector and pulse height selector. A Cobalt tube (CoKα = 1.790 Å) operating at 40 kV and 25 mA was used for the analysis, and the samples were scanned through a range of 5.2 – 40°2θ, with a step size of 0.05°2θ and a counting time of 1 second/step.

An additional two subsamples were taken from the Harts River sediment sample and from Barber's Pan samples 7, 8 and 16. The clay fractions were isolated from these eight subsamples as described above. These were rendered homoionic (after reducing the pH below neutrality) with 0.5M MgCl<sub>2</sub> or 1M KCl, shaken for one hour and then equilibrated overnight. One subsample of each of the four sediments was saturated with K, while the other was saturated with Mg (Whittig and Allardice, 1986). Slides were prepared and scanned as described above. The K saturated slides were first scanned after being air-dried. They were then heated first to 100°C and then to 300°C, being scanned after each treatment. The Mg saturated slides were first air-dried and scanned; they were then glycerol solvated, using a fine aerosol spray of 15% glycerol in water solution in order to facilitate the identification of smectite peaks, prior to being scanned through a range of 5.2 – 20°2θ.

### 4.3.4 Extractable phosphate

Extractable (or available) phosphate was determined by the AMBIC method of van der Merwe *et al.* (1984). The method involves the extraction of available phosphate by means of

$\text{NH}_4\text{HCO}_3 - \text{NH}_4\text{F} - (\text{NH}_4)_2\text{EDTA}$ . The alkaline nature of the extractant ensures its suitability for use on alkaline samples.

The analyses were carried out by the Institute for Soil, Climate and Water of the Agricultural Research Council, Pretoria.

#### **4.3.5 X-ray fluorescence spectrometry (XRFS)**

The 14 sediment samples and 1 m core sample were analyzed for major and trace elements using a Philips PW X'Unique II X-ray spectrometer and a Siemens SRS 303AS X-ray spectrometer.

The samples for XRFS analysis were prepared using the methods described by Willis (1985). This entailed oven-drying the samples at 105°C; they were then crushed to a particle size of -300 mesh (approx. -40 µm) in a carbon-steel vessel, using a Siebtechnik swingmill. Undiluted pressed powder briquettes were prepared for trace element analyses using 6 g of the dried and crushed sample. The briquettes were pressed in a 30 mm die under 7-10 tons of pressure using one drop of mowiol solution (2% Hoechst Mowiol N 70-80 in distilled water) per gram sample as a binding agent and boric acid as backing. Trace elements determined were Co, Mn, Cr, V, Mo, Nb, Zr, Y, Sr, U, Rb, Th, Pb, Zn, Cu, Ni and S. The major element Na (determined as  $\text{Na}_2\text{O}$ ) was also determined on the briquettes.

For major element analyses, fusion discs were prepared. This involved drying 2 g of the crushed sample at 110°C to determine any residual  $\text{H}_2\text{O}$ . The dried sample was then roasted at 1050°C to determine loss on ignition (LOI). The roasted material was used to prepare duplicate fusion discs (0.28 g sample per disc) according to the Norrish and Hutton (1969) technique. The major elements determined (as oxides) were  $\text{SiO}_2$ ,  $\text{TiO}_2$ ,  $\text{Al}_2\text{O}_3$ ,  $\text{Fe}_2\text{O}_3$ , MnO, MgO, CaO,  $\text{K}_2\text{O}$  and  $\text{P}_2\text{O}_5$ .

Analytical conditions for the XRF analysis were set up as per Willis (1995) (refer to Appendix 8). Calibration was by means of international standard rock reference materials.

#### **4.3.6 Particle–size distribution: pipette method**

The percentage sand, silt and clay was determined for core 4 (1 m in length), which was subdivided (from top to bottom) into six subsamples for this purpose. Additionally, the particle–size distribution of grab samples 4, 7 and the Harts River sample was also determined. The pipette method as described by Gee and Bauder (1989) was used. This form of sedimentation analysis is based on the assumption that spherical particles settle at a velocity that can be calculated from Stokes Law (Kohnke, 1968). The samples were treated with 1M NaOAc (pH 5) to remove carbonate and H<sub>2</sub>O<sub>2</sub> to remove organic matter. No pretreatment for the removal of iron oxides was applied. The samples were then dispersed using Calgon dispersing solution. After dispersion they were wet–sieved through a 0.053 mm sieve to separate the sand fraction from the silt and clay. The silt and clay were placed in a settling cylinder which was made up to 1 L with distilled water. 25 ml aliquots of sample were then extracted at appropriate depths and time intervals (as per Gee and Bauder [1989]) using a Lowy pipette.

### **4.4 Results and discussion of sediment analyses**

#### **4.4.1 Particle–size analysis**

Several problems were encountered during the particle–size determinations. Most notable among these was a tendency for the clay fraction of the samples to flocculate before the required extraction of clay had taken place. Repeated resuspension of the samples in distilled water failed to counter the problem. Time constraints prevented a repeat of the entire procedure, with the consequence that only sand and mud contents are reported in Table 13. Sand was determined gravimetrically and included all particles greater than 0.053 mm. The mud fraction includes all particles less than 0.053mm (i.e. silt and clay).

**Table 13:** Proportions of sand and mud determined in core sample 4, grab samples 4 and 7 and the Harts River sediment sample.

Sample No.	Depth of Core Section (cm)	Sand Fraction (%)	Mud Fraction (%)
Core 4			
-a	0 – 11	11.8	88.2
-b	12 – 29	12.4	87.6
-c	30 – 49	1.9	98.1
-d	50 – 64	3.1	96.9
-e	65 – 80	2.4	97.6
-f	81 – 86	13.6	86.4
Grab Sample 4		79.8	20.2
Grab Sample 7		2.5	97.5
Harts River Sample		29.1	70.9

Horie (1978) states that during lacustrine sedimentary processes, coarse-grained sediments are usually deposited close to shore, but subaqueous gravity flows, slumps and slides may transport coarse and fine material together to deeper waters. He notes that at river mouths sediments frequently have the morphology of an alluvial fan, fan-like delta or delta. Grab sample 4, which was sampled at the Harts River inlet, consisted predominantly of sand-sized particles (Table 13). This is in agreement with the sedimentary pattern described by Horie (1978) and suggests a delta or alluvial fan-like morphology may occur at the Harts River inlet. Grab sample 7, taken from a deeper, central portion of the pan consisted predominantly of clay-sized material, while the Harts River sediment sample had substantially more sand than grab sample 7, but less than grab sample 4. Förstner and Wittmann (1979) state that compared to rivers, where shifts between the processes of erosion and deposition take place within short intervals of time and space, lakes exhibit a more continuous accumulation of sediment materials, particularly in deeper water. They suggest that the general pattern that can be expected is one of decreasing sediment grain sizes from the shore towards the centre of the basin, although currents can still give rise to special conditions.

Core 4, the "1 m" core, was separated into six sections of varying length on the basis of colour and/or visible lithological differences. The actual length of the core was 86 cm, and the

length of each of the six sections is given in Table 13. The core was taken from the central portion of the pan (sampling point 6 on Fig. 32) where the pan depth was recorded as being 4 m. The particle–size analysis revealed significant differences between the six sections into which the core was separated. As can be seen from Table 13, the top 30 cm of the core (sections a and b) were found to have a sand content of about 12 %. The sand content of the middle sections (c, d and e) was substantially lower (between 2–3 %), while the bottom 6 cm (section f) showed an increase in sand content to approximately 14 %. These differences may be indicative of differing episodes of deposition in the pan, with the layers having greater sand proportions possibly being associated with episodic inflow from the Harts River. Alternately, they may indicate periods of differing pan depth, as this would influence the extent of winnowing–out of finer particles by wind and wave action. These and other hypotheses are elaborated upon in section 4.4.4.

#### **4.4.2 Clay mineralogy**

##### *4.4.2.1 Untreated samples*

X–ray diffractograms of the untreated Na–saturated clay fractions extracted from the twelve sediment samples are shown in Figures 36, 37 and 38. The sediments can be divided into three basic groups, namely:

- i) the Barber’s Pan sediment samples;
- ii) the Harts River sediment sample, and
- iii) the Leeupan sediment sample.

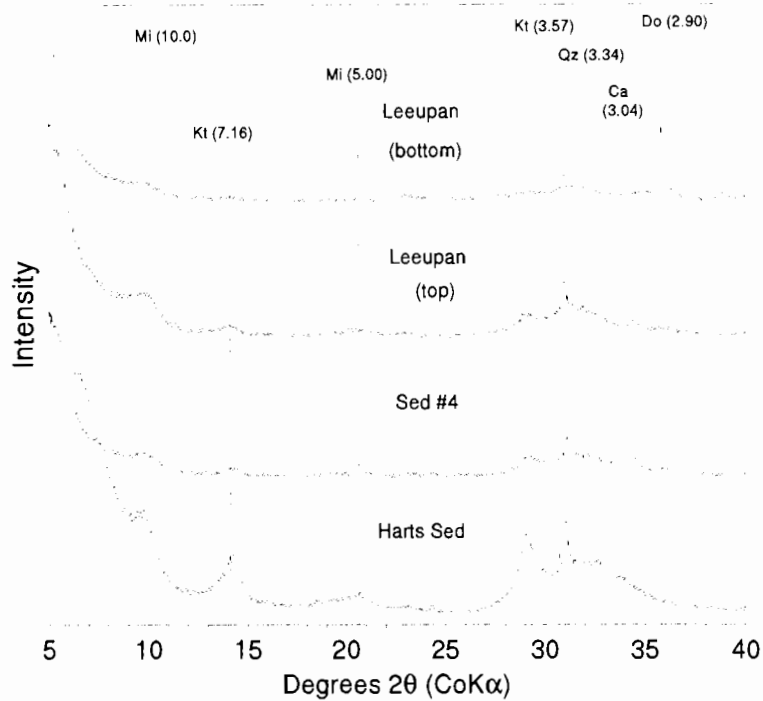


**Figure 36:** X-ray diffractogram of Na-saturated clay fractions extracted from Barber's Pan sediment sample no. 4, Leeupan upper and lower sediment samples and the Harts River sediment sample. Peak locations are shown for calcite (Ca), dolomite (Do), kaolinite (Kt), the mica group minerals (Mi) and quartz (Qz) [*d*-spacings in Å are given in parentheses.]

#### 4.4.2.1.1 Harts River sediment

The Harts River sediment displayed 10,0 Å and 5,00 Å mica peaks, 7.16 Å and 3.57 Å kaolinite peaks, and a 3.34 Å quartz peak (Fig. 36). The diffractogram also suggested the presence of interstratified 2:1 layer silicate material occurring between 10.0 – 18.0 Å (10–5°2θ).

#### 4.4.2.1.2 Barber's Pan sediments

With the exception of sediment sample 4, all of the Barber's Pan samples exhibited remarkably uniform diffraction patterns (Figs 36, 37 and 38). They exhibited the same basic peaks as the Harts River sediment (mica, kaolinite and quartz), with the notable addition of a calcite 3.04 Å peak. As with the Harts River sample, the diffractogram suggested the presence of interstratified 2:1 layer silicate material.

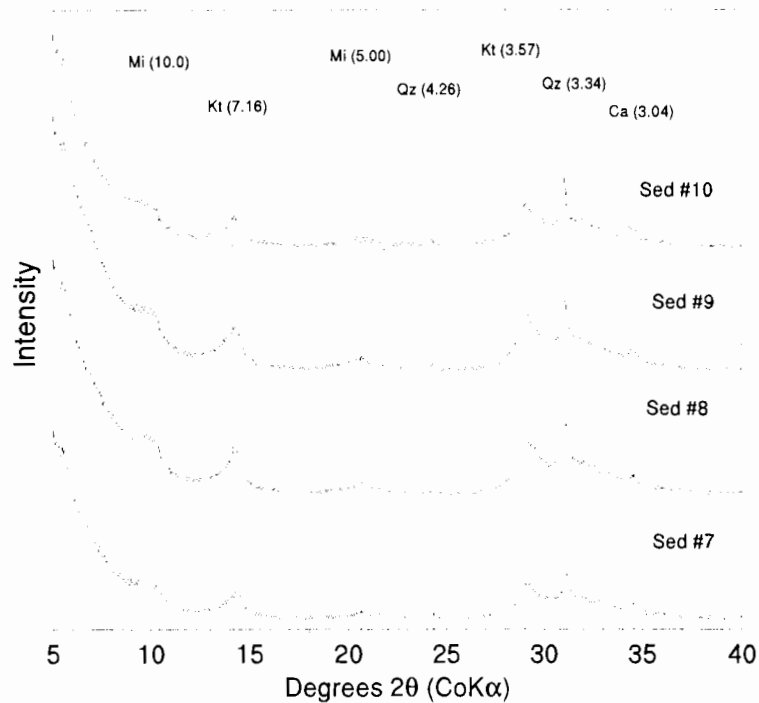


**Figure 37:** X-ray diffractogram of Na-saturated clay fractions extracted from Barber's Pan sediment samples no. 7, 8, 9 and 10. Peak locations are shown for calcite (Ca), kaolinite (Kt), the mica group minerals (Mi) and quartz (Qz) [*d*-spacings in Å are given in parentheses.]

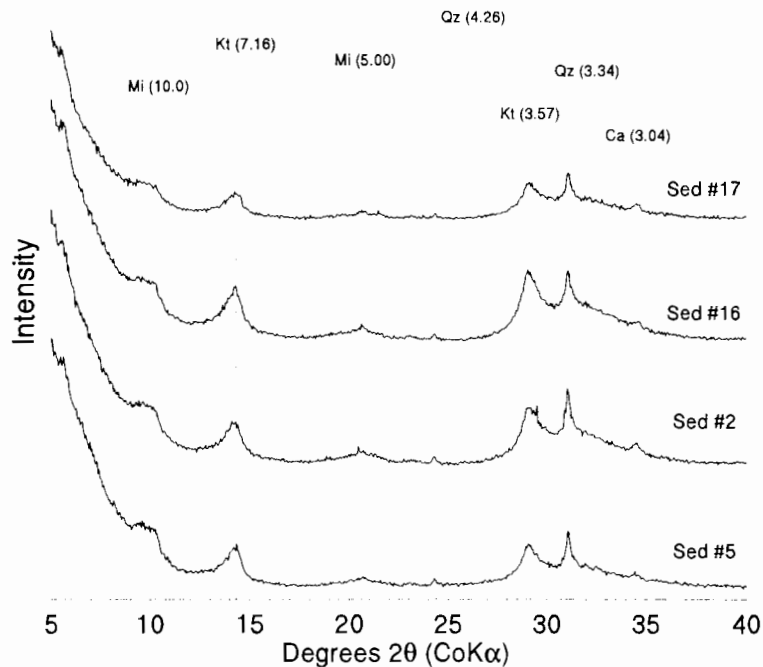


**Figure 38:** X-ray diffractogram of Na-saturated clay fractions extracted from Barber's Pan sediment samples no. 2, 5, 16 and 17. Peak locations are shown for calcite (Ca), kaolinite (Kt), the mica group minerals (Mi) and quartz (Qz) [*d*-spacings in Å are given in parentheses.]

#### 4.4.2.1.3 Leeupan sediment

During sample collection, the Leeupan sediment was visually separated into a lower carbonate-rich horizon, characterized by a very white appearance (Fig.39), underlying a carbonate-poor horizon. The clay fraction of each of these two horizons was extracted and both were subjected to XRD analysis. The upper layer (referred to as Leeupan {top} in Fig. 36) was found to resemble Barber's Pan sediment sample 4, exhibiting mica, kaolinite, quartz and calcite peaks, together with a suggestion of interstratified 2:1 layer silicate material; but having mica and kaolinite peaks far less intense than those observed for the other Barber's Pan samples.

The lower layer (referred to as Leeupan {bottom} in Fig. 36) showed only a very intense 2.90 Å dolomite peak, with a small quartz peak and possibly some interstratified 2:1 layer silicate material.

Determination of the carbonate content of the Leeupan samples by means of the "Karbonat bombe" showed the lower dolomitic horizon to consist of 49.6% carbonate, while the upper horizon contained only 16.4 %, confirming the XRD findings.

Enos (1978) records that Coorong Lagoon, Australia and Deep Springs Lake, California are modern environments where the direct precipitation of dolomite may be taking place. He describes the Coorong as a series of shallow, ephemeral lakes isolated from the ocean but containing essentially sea water that is modified by annual cycles of runoff and evaporation and by carbonate precipitation. Dolomite is found in lakes with high Mg/Ca ratios, high pH and very slow sedimentation rates. Deep Springs Lake, on the other hand, is a shallow playa whose spring fed water bears little relation to sea water. In this environment, dolomite formation has been attributed to the extremely slow, direct precipitation of a Ca-rich precursor which is modified to dolomite by diffusion of Mg inward and Ca outward through the outer 100 Å of the crystal.



**Figure 39:** Dolomite layer in Leeupan.

Dolomite within the sediments of Lake Hayward, a permanent hypersaline lake on the coast of southwestern Australia, is formed diagenetically from pore water derived from evaporated lake water. Dolomitizing conditions within the sediments are thought to be enhanced by a high Mg/Ca ratio in the pore water, bacterial sulphate reduction and the slightly elevated temperatures of the pore water (Rosen *et al.*, 1992).

Shaw (1988) records that calcretes frequently occur beneath pans, often to great depths. As discussed in Chapter three, the bulk water of Barber's Pan is highly alkaline ( $\text{pH} > 9$ ) and likely to be supersaturated with respect to carbonate minerals. It has a high Mg/Ca ratio (Table 9), even when fairly dilute, which increases during evaporative concentration. MINTQA2 predicted that the bulk pan water was supersaturated with respect to both dolomite and calcite. The saturation index for dolomite was, however, predicted as being far greater than that of calcite suggesting that the precipitation of dolomite would be favoured over that of calcite. Bacterial sulphate reduction appears to be taking place in the sediments. These conditions are very similar to those described by Enos (1978) and Rosen *et al.* (1992). Although Leeupan was dry at the time of sampling, it is likely that it has a water composition similar to Barber's Pan brine when it contains water, and that it undergoes the same sequence of evaporative concentration, differing only in that it desiccates completely.

Vasconcelos *et al.* (1995) observed the precipitation of poorly ordered Ca–dolomite and high–Mg–calcite, in association with sulphate–reducing bacteria from the *Desulfovibrio* group, within the upper 15 cm of an anoxic black sludge layer forming the upper sediment of a small (1.9 km<sup>2</sup>), shallow–water (< 2m), coastal lagoon in Brazil. To confirm their observations, they carried out a bacterial culture experiment using samples of the black sludge from the lagoon to simulate the dolomite–producing process observed in the lagoon. They propose that evidence for the microbial mediation was observed in secondary electron images produced by a scanning electron microscope (SEM), which showed subspherical nanobacteria embedded in the surface of the dolomite.

The presence of sulphate in potentially dolomitizing fluids inhibits the precipitation of dolomite. Sulphate reduction in Lake Hayward is, therefore, likely to enhance dolomitization (Rosen *et al.*, 1992).

Vasconcelos *et al.* (1995) also record that Nadson (1928) reported the production of small amounts of authigenic carbonate in a similar bacterial culture experiment in which he used sulphate reducing bacteria from anoxic surface sediments in a Russian salt lake.

A similar process may be responsible for the production of the dolomitic layer observed in the Leeupan sample. The notable release of H<sub>2</sub>S from the Barber’s Pan sediment samples and the development of black mottles (discussed in 3.3.3) suggests the precipitation of iron sulphides and hence the presence of sulphur–reducing bacteria in the pan sediments.

Vasconcelos *et al.* (1995) further showed the dolomite produced through microbial mediation to have an X–ray diffraction pattern in which the major peak, *d*(104) reflection, occurred at 2.90 Å (30.79° 2θ). This position is shifted slightly from the major peak of ideal dolomite, which occurs at 2.89 Å (30.99° 2θ). The dolomite band in the Leeupan sediment sample was similarly found to have its major peak occurring at 2.90 Å (30.79° 2θ).

#### 4.4.2.2 *Treated samples*

In order to distinguish between the possible interstratified 2:1 layer silicates observed in the diffractograms of the untreated clay samples, additional slides were prepared from the Harts

River sediment and Barber's Pan sediment samples 7, 8 and 16, using the method described in section 4.3.3.

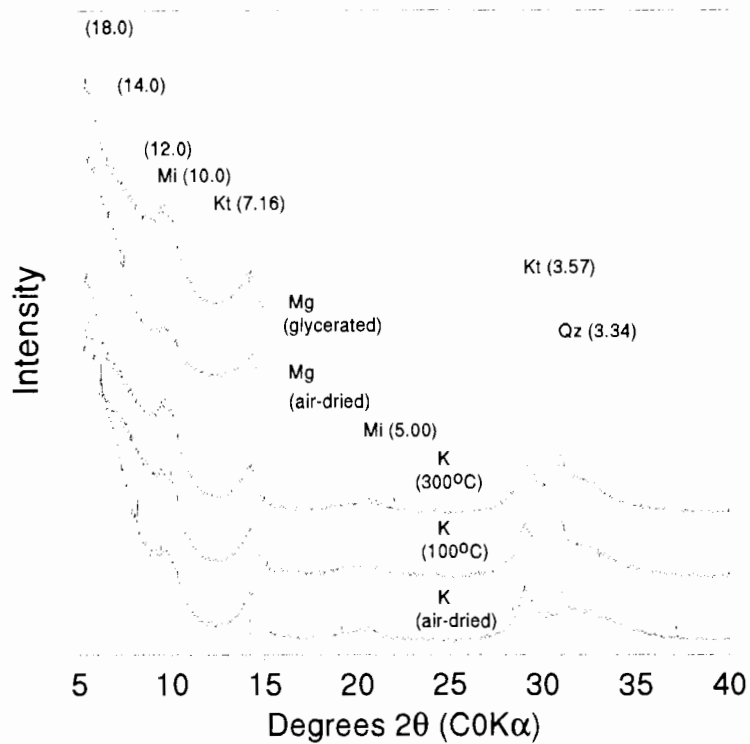
#### 4.4.2.2.1 Mg-saturation and glyceration

The best method of distinguishing the smectite group from other 14 Å clay minerals (i.e. chlorite and vermiculite) is to render the clay homoionic with either Mg<sup>2+</sup> or K<sup>+</sup>, then either solvate it (with glycerol or glycol) or heat it and observe any shifts in the 001 spacing. This is because the expansive nature of smectites is affected by the nature of adsorbed ions and molecules (Bühmann *et al.*, 1985). Borchardt (1989) notes that if the XRD conditions are not carefully controlled, the basal spacings of smectite may vary from 10 to 20 Å, making interpretation difficult or impossible.

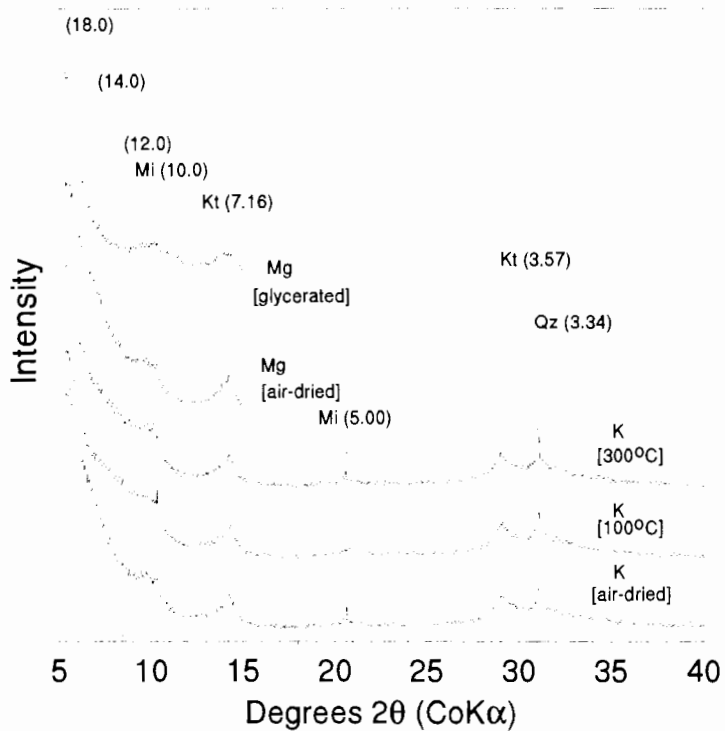
All Mg-saturated smectites give a 15 Å peak at 54% relative humidity, while beidellite gives a 14 Å peak after glycerol solvation from the vapour, whereas montmorillonite expands to 18 Å. The presence of chloritic interlayers may sometimes impede the expansion of montmorillonite in glycerol (Borchardt, 1989).

Examination of the diffraction patterns obtained from the Mg-saturated and glycerated slides (Figs 40 and 41) reveals a definite tendency for the clay to expand towards 18 Å upon glyceration, with the affected portion of the diffractogram (12 – 18 Å) assuming a more concave appearance. This increased concavity is accompanied by the sharpening of the 10 Å mica peak as the clay moves towards 18 Å. The shift towards 18 Å with glyceration suggests the presence of smectite.

Broad shouldered peaks should always be regarded as an indication of an interstratification as must peak positions other than 16.9 Å after glycol solvation, when an interstratification with smectite as the major component can be assumed (Bühmann, 1986). The presence of peaks between 10.0 Å–18 Å in all four of the Mg-saturated and glycerated clay samples (Figs 40 and 41) are therefore indicative of a random smectite–mica interstratification.

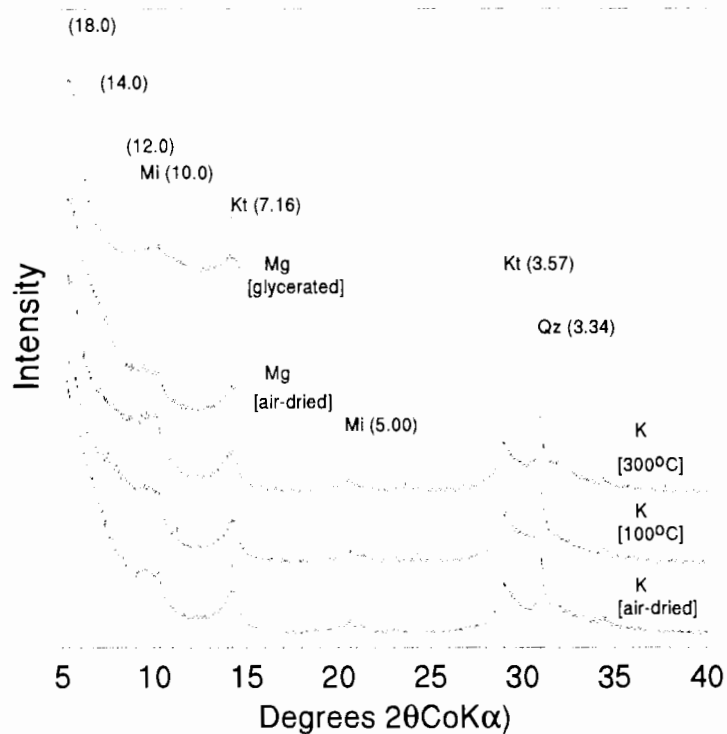


A

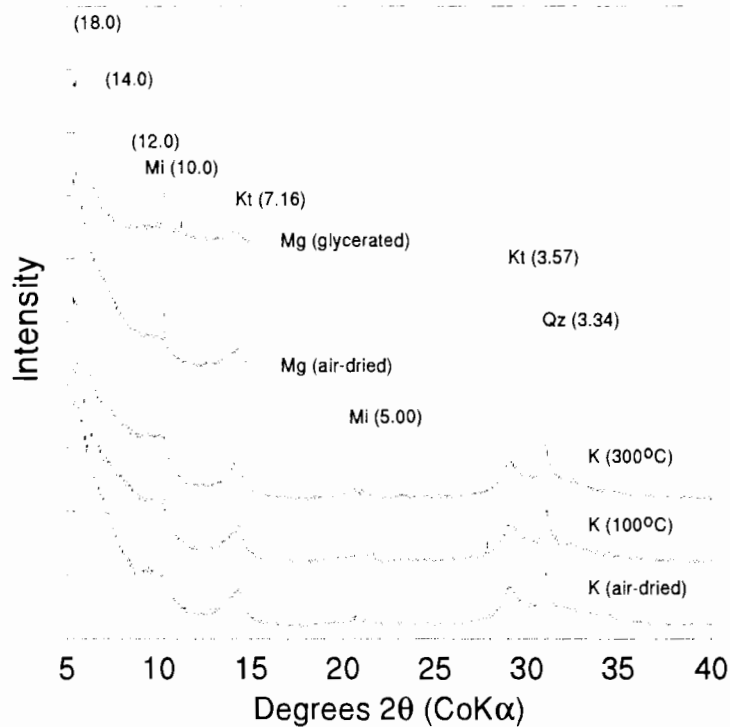


B

**Figure 40:** X-ray diffractograms of Harts River sediment (A) and Barber's Pan sediment sample no. 7 (B) clay fraction pretreated by K-saturation and heating or by Mg-saturation and glycerol solvation. Peak locations are shown for kaolinite (Kt), the mica group minerals (Mi) and quartz (Qz) [ $d$ -spacings in Å are given in parentheses.]



A



B

**Figure 41:** X-ray diffractograms of Barber's Pan sediment sample nos. 8 (A) and 16 (B) clay fraction pretreated by K-saturation and heating or by Mg-saturation and glycerol solvation. Peak locations are shown for kaolinite (Kt), the mica group minerals (Mi) and quartz (Qz) [*d*-spacings in Å are given in parentheses.]

The XRD patterns of the mica group minerals are characterized mainly by two intense peaks in the region of 10 Å and 3.3 Å and a relatively weaker peak at 5 Å. Generally, the appearance of a peak at 10 Å for Mg-saturated specimens indicates the presence of mica group minerals. All three of the main mica peaks remain unaltered upon glycerol solvation (Fanning *et al.*, 1989). All four Mg-saturated samples show distinctive 10 Å and 5 Å peaks. The presence of the 5 Å peak rather than the 3.3 Å peak may indicate the presence of muscovite, as the 5 Å line is relatively strong in the case of muscovite (which has an aluminous octahedral sheet) (Fanning *et al.*, 1989).

The possible presence of chloritic interstratification is indicated by the range of peaks between 10 – 18 Å. Barnhisel and Bertsch (1989) state that chlorite has a *d*-spacing of 14.0–14.4 Å, depending upon the species; with substitutions of Al<sup>3+</sup> for Si<sup>4+</sup> in the tetrahedral sites and Fe<sup>2+</sup> for Mg<sup>2+</sup> or Al<sup>3+</sup> in octahedral sites being largely responsible for this range in *d*-spacing. They further note that the 14.0–14.4 Å *d*-spacings are not significantly affected by ionic saturation or solvation with glycerol.

The identification of chlorite in the presence of smectite can be accomplished by saturating the specimen with Ca<sup>2+</sup> or Mg<sup>2+</sup> and adding glycerol or ethylene glycol. The latter treatment expands smectite to about 17.0 to 18.0 Å, while chlorite remains unaffected (Barnhisel and Bertsch, 1989). As discussed above, examination of Figures 40 and 41 shows that a definite shift towards 18 Å is visible in the Mg-saturated samples after glyceration. The diffractograms, however, also show the continued presence of material between 14.0–14.4 Å, suggesting that chlorite may be present.

#### 4.4.2.2.2 K-saturation and heat treatment

A K-saturation treatment will result in a partial collapse of smectite to around 12 Å when x-rayed at room temperature (25 °C) in the absence of either glycerol or ethylene glycol, if the smectite does not contain appreciable amounts of hydroxy interlayers. Upon heating to 100 °C, the K-saturated smectite should collapse to about 10 Å if no hydroxy interlayers are present (Barnhisel and Bertsch, 1989). From Figures 40 and 41 it can be seen that the K-saturated samples do not show any significant collapse towards 10 Å following heat treatment. This serves as further confirmation of the presence of chloritic interlayers.

Differentiation between chlorite and vermiculite can be accomplished with K-saturation. Vermiculite, containing little or no hydroxy interlayering, will collapse to 10 Å upon K-saturation at room temperature. On this basis, the persistence of a 14 Å peak after K-saturation and heat treatment of 300 °C, and subsequently at 500 °C, confirms the presence of chlorite, while the collapse to 10 Å upon heating confirms the presence of vermiculite and/or smectite (Barnhisel and Bertsch, 1989). With the exception of the Harts River sediment (Fig. 40), the K-saturated samples (Figs 40 and 41) do not show any significant collapse towards 10 Å with heat treatment up to 300°C, confirming the likely presence of chlorite. The K-saturated Harts River sediment appears to show a slight sharpening of the 10 Å peak following heating up to 300°C, which may indicate the possible presence of vermiculite or smectite.

Vermiculites, as well as chlorites and smectites have basal diffraction lines in the 14 to 15 Å region. Because the interlayer H<sub>2</sub>O layers in vermiculite are influenced by the cations in interlayer positions, different basal spacings result with different saturating cations. This property is useful in determining if a 14.0 or 15.0 Å diffraction line is caused by vermiculite or some other clay mineral. Magnesium saturated vermiculites have an 002 diffraction line near 14.3 Å, and upon K-saturation this spacing collapses to 10.2 Å.

This process may, however, be complicated by hydroxy-Al interlayers in vermiculites, which tend to increase the temperature at which a K-saturated vermiculite will collapse (Douglas, 1989). There does not appear to be any indication of a collapse from 14.3 to 10.2 Å in any of the K-saturated samples (Figs 40 and 41); suggesting the absence of vermiculite in the samples.

#### 4.4.2.3 General discussion of Barber's Pan clay mineralogy

The fibrous Mg-silicate clays sepiolite and palygorskite are known to occur in arid environments (discussed in section 3.3.2.6). The main x-ray diffraction maxima of palygorskite occur at 10.4 – 10.5 Å, with moderate reflections occurring at 6.4 and 5.4 Å. Sepiolite gives a strong x-ray diffraction line at 12.1 Å, with other reflections occurring at 4.5, 3.8 and 4.34 Å (Singer, 1989; Elprince *et al.*, 1979). The presence of a peak at 10 Å and of interstratified material between 10–14 Å suggests the possible presence of these minerals in the Barber's Pan, Leeupan and Harts River sediment samples. The 10 Å peaks in the

samples were attributed to mica. Elprince *et al.* (1979) noted that palygorskite occurring in a mixed assemblage with mica was readily detected by a diminution of the 10–10.5 Å peak when heated to 550°C. Singer (1989) states that after heat treating palygorskite at 300°C a new spacing appears at 9.2 Å. Heating sepiolite at 250°C for one hour decreases the intensity of the reflections at 12.2, 4.5, 3.8 and 3.4 Å and causes new reflections to appear at 10.4 and 8.2 Å. Heating the K-saturated samples to 300°C did not cause any significant collapse of the 10 Å peak, nor did it bring about the generation of any new reflections. Glycerol solvation, however, confirmed the presence of smectite, which have a close association with palygorskite (Elprince *et al.*, 1979), in the sediments.

Alteration of minerals like smectite and precipitation from solution are both mechanisms which have been proposed to explain the pedogenic formation of palygorskite (Singer, 1989). The stability diagram for the palygorskite/smectite system developed by Elprince *et al.* (1979) (Fig. 19) shows palygorskite stability to be favoured over that of smectite as pH and the activities of Mg or Si increase. The bulk pan water was found to have high concentrations of Mg and a very alkaline pH. Levels of Si in interstitial water were also high. Saturation indices calculated by MINTEQA2 (section 3.3.2.6) predicted that the bulk pan water was supersaturated with respect to crystalline sepiolite following evaporative concentration, suggesting that this mineral may well occur. Palygorskite was not included in the MINTEQA2 thermodynamic database and hence no saturation index was calculated. Plotting Mg and Si values of the bulk pan water against pH (Fig. 19), however, suggested that palygorskite could form at the expense of smectite. It is, therefore, possible that traces of sepiolite and palygorskite are associated with the interstratified smectitic–chloritic material occurring in the pan sediments.

The clay fraction of the Barber's Pan, Leeupan and Harts River sediments were found to contain quartz, kaolinite, mica and interstratified chloritic–smectitic material. The pan sediments also contained calcite, which the Harts River sediment did not. Barber's Pan, Leeupan and Etosha Pan have been classified as occurring in the same geographical region on the basis of climate. The clay mineralogy of Etosha Pan is well documented, consisting predominantly of an interstratified illite–smectite material with kaolinite as an additional mineral. Significant amounts of sepiolite, palygorskite and quartz have also been recorded in the clay fraction (Verster *et al.*, 1992).

Verster *et al.* (1992) state that powder calcrete is a common feature of the Barber's Pan margin and Goudie (1983) records that sepiolite and palygorskite have been widely noted as clay minerals associated with calcretes. Sepiolite has also been associated with small, randomly distributed authigenic dolomite rhombs (Goudie, 1983).

Mineralogical and chemical analyses of the fine fractions from in and around Lake Abert (an alkaline, saline lake in Oregon, U.S.A.) showed that detrital rock debris had weathered to produce a range of layer silicate minerals from montmorillonite to montmorillonite/illite and montmorillonite/intergrade smectite interstratifications. In Lakes Albert and Manyara in East Africa, smectites in the sediments were illitized by the incorporation of potassium ions released by the transformation of K, Na-zeolite to analcime. This was accompanied by Mg being added to the layer silicate. The enhancement of K and Mg in Lake Abert was attributed to similar changes, although zeolite transformation did not appear to be important (Jones and Weir, 1983).

Barber's Pan is underlain by amygdaloidal lava of the Ventersdorp system (section 1.1.2). Whitten and Brooks (1971) report that amygdaloidal cavities are frequently filled with zeolites, calcite or quartz. Amygdales are abundant in and around the pan (Fig. 42). It is, therefore, possible that a certain degree of zeolite transformation, as described above, may be occurring in the pan.

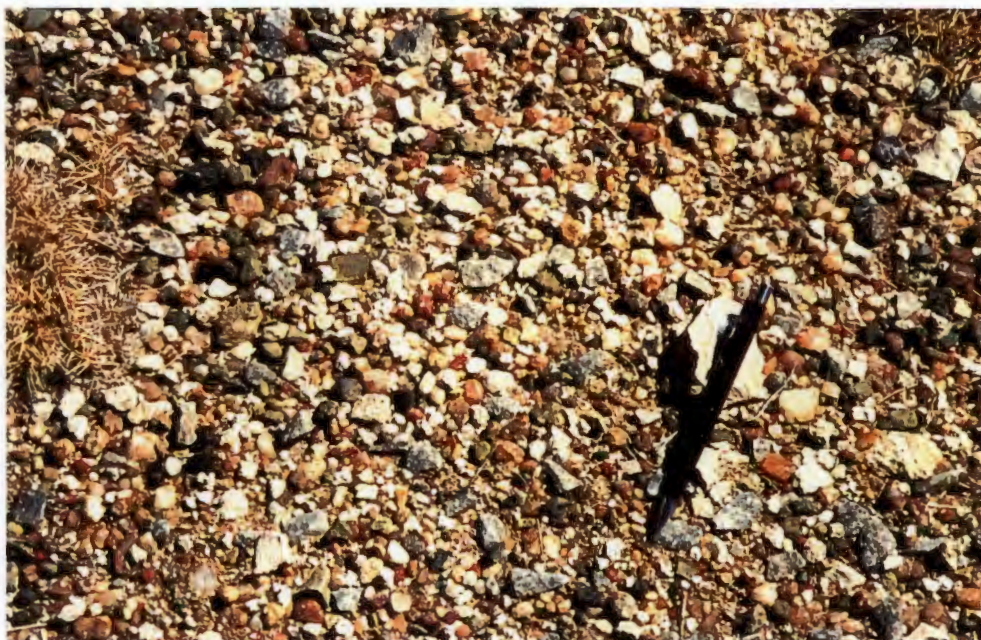


**Figure 42:** Amygdales at the edge of Barber's Pan.

### 4.4.3 Chemical composition of the sediments

Grain-size exercises a determining influence on elemental concentrations with numerous studies showing a general increase of elemental concentrations from coarse to fine grained fractions (Förstner and Wittman, 1979). In comparing grab sample 4, the very sandy inlet sample with grab sample 7, the clay rich central sediment sample, a definite enrichment in metal concentrations can be seen in sample 7 relative to sample 4 (Table 13). Similar patterns of decreasing metal concentrations with increasing grain-size are likely to account for the lower concentrations of most elements in the littoral sediment samples (e.g. samples 5, 10f and 17). These samples have high concentrations of  $\text{SiO}_2$  and Zr, which are likely to be associated with the resistate minerals comprising the sand fraction.

The fate of the major elements during sedimentation has been well documented. Silica concentrates largely in the resistate sediments and alumina in the hydrolysates (essentially the clay minerals). Iron and manganese are associated with the oxidates, while calcium and magnesium concentrate in the carbonates. A large proportion of the sodium present remains in solution, or with evaporative concentration precipitates as various evaporite minerals, particularly halite. Potassium tends to be absorbed by the clays, forming minerals such as illite and glauconite. Far less is known about the fate of minor elements during sedimentation with many factors being associated with their transport and deposition. These include: ionic potential, pH, the oxidation potential of the medium, colloidal properties, and adsorption (Mason and Moore, 1982).

In the light of the above discussion and on the basis of the mineralogical data obtained (section 4.4.2), the  $\text{SiO}_2$  content can be interpreted as reflecting the quartz distribution within Barber's Pan, CaO the carbonate mineral distribution and  $\text{Al}_2\text{O}_3$  the mud/clay mineral fraction. The elemental concentrations (major and trace) determined by means of XRFS for the sediments samples analyzed are tabulated in Appendix 5. The results of organic carbon and carbonate determinations are tabulated in Appendix 6.

In Leeupan, a significant portion of the MgO is associated with dolomite, while in the remainder of the pan sediments the MgO is likely to form part of the clay minerals, particularly chlorite and smectite (as described by Willis [1985] in the Bot River estuary).

This was confirmed by comparing the weight percent CO<sub>2</sub> evolved from the sample (Karbonat bombe) against the weight percent CaO and MgO. The CO<sub>2</sub> evolved equates to the CO<sub>3</sub> content of the sample. Every 1 % CO<sub>2</sub> recalculated to CaCO<sub>3</sub> is equivalent to 1.27 % CaO (Weast, 1975). If all the CaO is present in the sample as CaCO<sub>3</sub>, then the ratio of CaO/CO<sub>2</sub> would be close to 1.27. In the case of both Leeupan samples, the ratio was substantially lower (Table 14) implying that insufficient CaO is present to combine with all the CO<sub>2</sub>. The shortfall is made up by MgO. Several of the sediment samples showed a CaO/CO<sub>2</sub> ratio greater than 1.27 (Table 14). A CaO/CO<sub>2</sub> ratio greater than 1.27 indicates an excess of Ca over that present as CaCO<sub>3</sub>. This "excess" Ca is most likely to be present in the clay minerals or in the form of apatite. A certain amount of the Ca may also be present as gypsum, although MINTEQA2 predicted that the pan water was undersaturated with respect to this mineral.

**Table 14:** The CaO/CO<sub>2</sub> and MgO/CO<sub>2</sub> ratios for the sediments sampled.

Sample No.	CaO/CO <sub>2</sub>	MgO/CO <sub>2</sub>
Harts River	1.73	2.19
Leeupan (top)	1.07	0.91
Leeupan (bottom)	0.85	0.7
Sediment No. 2	3.82	0.71
Sediment No. 4	1.27	0.42
Sediment No. 5	2.00	0.41
Sediment No. 7	1.62	0.89
Sediment No. 8	1.40	0.32
Sediment No. 9	1.43	0.80
Sediment No. 10c	1.34	0.07
Sediment No. 10f	1.35	0.13
Sediment No. 16	1.27	0.70
Sediment No. 17	2.56	0.49

K<sub>2</sub>O and Rb showed a linear relationship. The two points recorded for Leeupan, however, fell on a distinctly different slope to that of Barber's Pan (Fig. 43A). Al<sub>2</sub>O<sub>3</sub>, Fe<sub>2</sub>O<sub>3</sub>, and organic carbon all showed very similar distributions (Fig. 43B, C and D) with Al<sub>2</sub>O<sub>3</sub> and Fe<sub>2</sub>O<sub>3</sub> having a particularly close correlation. Although the correlation coefficient calculated for MnO and

Al<sub>2</sub>O<sub>3</sub> was not significant, a plot of these two oxides showed a certain degree of correlation. TiO<sub>2</sub>, K<sub>2</sub>O, P<sub>2</sub>O<sub>5</sub>, V, Cu and Ni were closely correlated with Al<sub>2</sub>O<sub>3</sub> and Fe<sub>2</sub>O<sub>3</sub>, but less well correlated with organic carbon. Cr, Nb, Y, Rb, Th, Pb, Zn and Ni were closely correlated with Al<sub>2</sub>O<sub>3</sub>, Fe<sub>2</sub>O<sub>3</sub> and organic carbon. S and Co showed correlations with Al<sub>2</sub>O<sub>3</sub> and Fe<sub>2</sub>O<sub>3</sub>. MnO and CaO showed some degree of association (correlation coefficients for all the grab sample data are tabulated in Appendix 7).

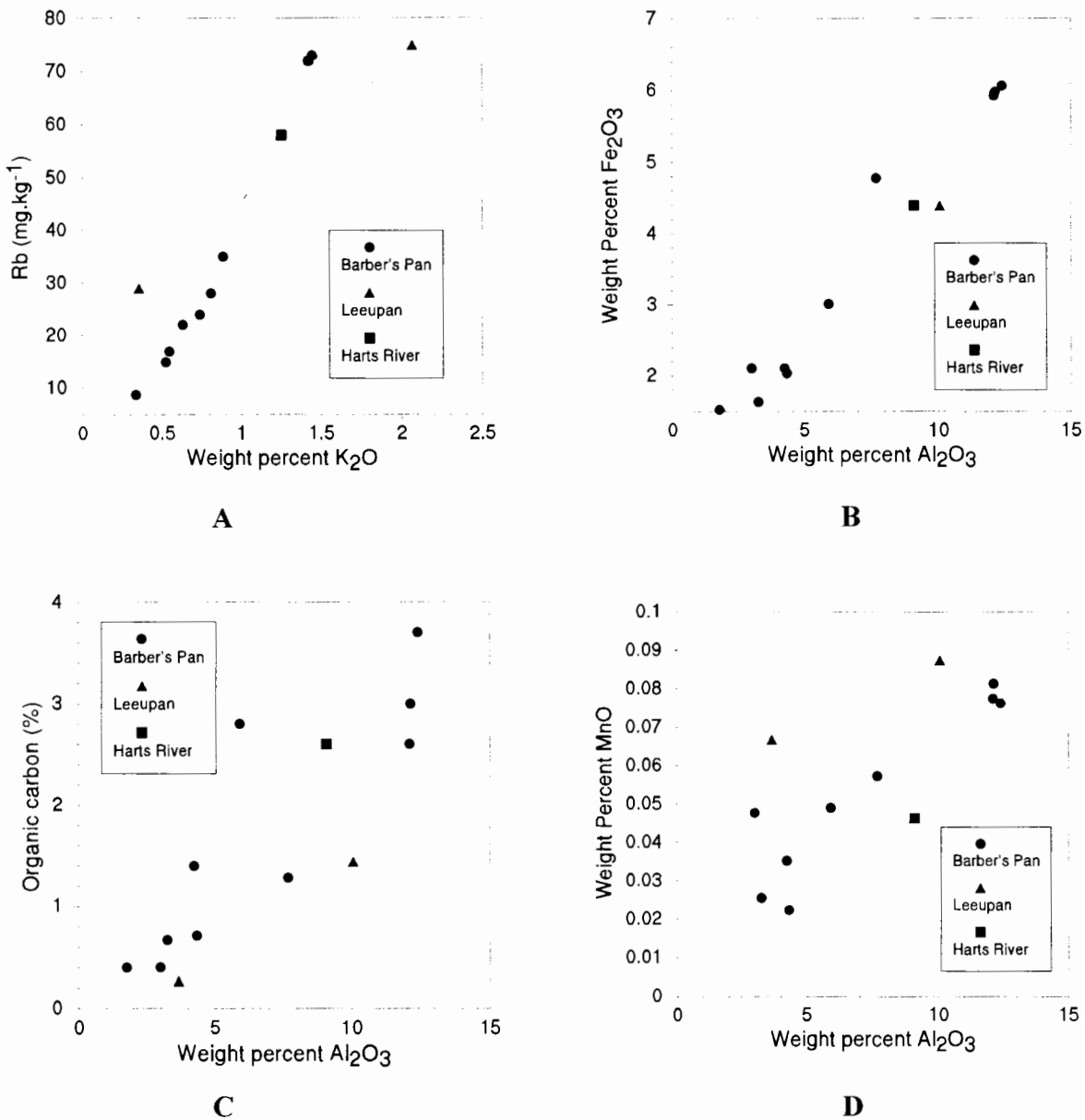


**Figure 43:** Plots of the relationships between K and Rb (A), Al<sub>2</sub>O<sub>3</sub> and Fe<sub>2</sub>O<sub>3</sub> (B), Al<sub>2</sub>O<sub>3</sub> and organic carbon (C) and Al<sub>2</sub>O<sub>3</sub> and MnO (D) in the Barber's Pan, Harts River and Leeupan sediments.

From the particle size analysis, sediment sample no. 4 (Harts River inlet sample) and the Harts River sediment contained the most sand. These two samples were also comprised

predominantly of  $\text{SiO}_2$ . Other  $\text{SiO}_2$  rich samples ( 2, 5, 8, 10f ) were those associated with the shallow littoral zones of the pan and sample no. 17, which was associated with a shallow, sandy, cove. Zr was closely correlated with  $\text{SiO}_2$ , with the highest concentrations also occurring in the littoral zone sediments. It is likely that the Zr is present as zircon, one of the most resistant minerals. Finer mud particles are likely to have been winnowed out of the littoral zone and coves during periods of high winds and strong wave action, particularly when water levels were low, as described by Anderson (1972) and recorded by Willis (1985) in the Bot River estuary. As discussed in section 1.1.3, strong winds have played an essential role in the formation of Barber's Pan, and Göldner (1967) noted that prevailing winds play a very important role in the agitation and movement of suspended particles in the water.

Sediment no. 10 provided very interesting results. Upon collection it was seen to be composed of two very distinct fractions, namely a gravel component and a finer, sandy component. During sample preparation it was separated into two fractions by sieving through a 2 mm nylon-mesh sieve. The coarser ( $> 2\text{mm}$ ) fraction (sample 10c) was found to be composed largely of  $\text{SiO}_2$  and CaO, and had a  $\text{CaCO}_3$  content of 56 %. Its CaO/ $\text{CO}_2$  ratio was slightly greater than 1.27, suggesting that most of the CaO was present as  $\text{CaCO}_3$ . Sample 10c is, therefore, likely to be a siliceous calcrete. Goudie and Thomas (1985) record that lunettes associated with pans in the Delareyville area of the western Transvaal, where Barber's Pan is situated (Fig. 35), are composed of single ridges containing multiple layers of aeolian sediment interspersed with calcrete layers. Some of the pans in the area have lunettes composed largely of calcrete. Termed calunettes, these dunes appear to be associated with areas underlain by (or close to) Ventersdorp lavas. The calcrete making up sample 10c may well be from, or associated with, such a lunette. Alternately, it may be part of an amygdale. These are abundant along the pan shore (Fig. 42), and Whitten and Brooks (1971) record that calcite is commonly one of the minerals that fill amygdaloidal cavities.

Adsorption processes may remove many ions from natural waters, with clay minerals showing a marked adsorptive capacity (Mason and Moore, 1982). In the Bot River estuary, Willis (1985) found that the highest trace element associations, with the exception of Sr, occurred in the central muds. He attributed this phenomenon to the association of the trace elements with the clay minerals or organic matter in the mud fraction. In the Barber's Pan sediments, there is a strong association between  $\text{Al}_2\text{O}_3$  and several trace elements as discussed above. Figure 44 depicts the strong association between Zn, Cu, Ni and Cr, and  $\text{Al}_2\text{O}_3$  as examples.

The highest Al<sub>2</sub>O<sub>3</sub> concentrations are recorded in the deeper, more central, pan sediments (samples 7, 8 and 9). Particle–size analysis of sample no. 7 determined that it consisted of 97.5 % mud (<0.053mm).

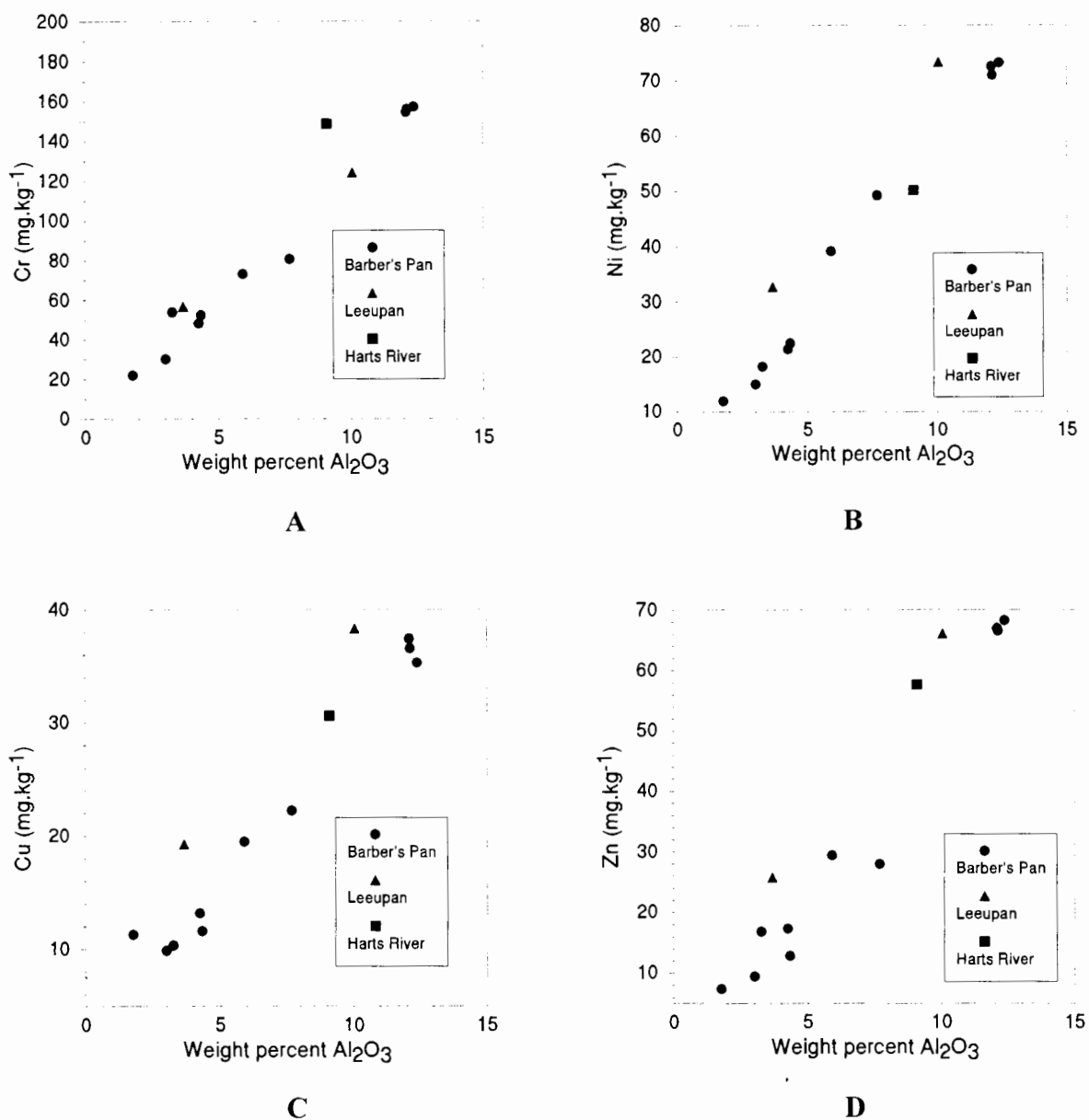


**Figure 44:** Plots of the relationships between Al<sub>2</sub>O<sub>3</sub> and Cr (A), Al<sub>2</sub>O<sub>3</sub> and Ni (B), Al<sub>2</sub>O<sub>3</sub> and Cu (C) and Al<sub>2</sub>O<sub>3</sub> and Zn (D) in the Barber's Pan, Harts River and Leeupan sediments.

With the exception of two anomalous points (5 and 10c), a good correlation was observed between Ca and Sr (Fig. 45) This is expected, with Sr being readily able to substitute for Ca in CaCO<sub>3</sub> minerals (Wehmiller, 1972). The Sr concentration determined for sample no. 5 was 4x higher than the average Sr concentration recorded for the other samples. Sample 10c contains less Sr than expected for the concentration of CaO present, suggesting that less Sr

substitution for Ca took place in the  $\text{CaCO}_3$  material making up the calcrete sample than in the other samples. This supports the earlier contention that the calcrete making up sample 10c was not precipitated within the pan but rather originated from a calcite amygdale, calunette or other, similar calcrete deposit.

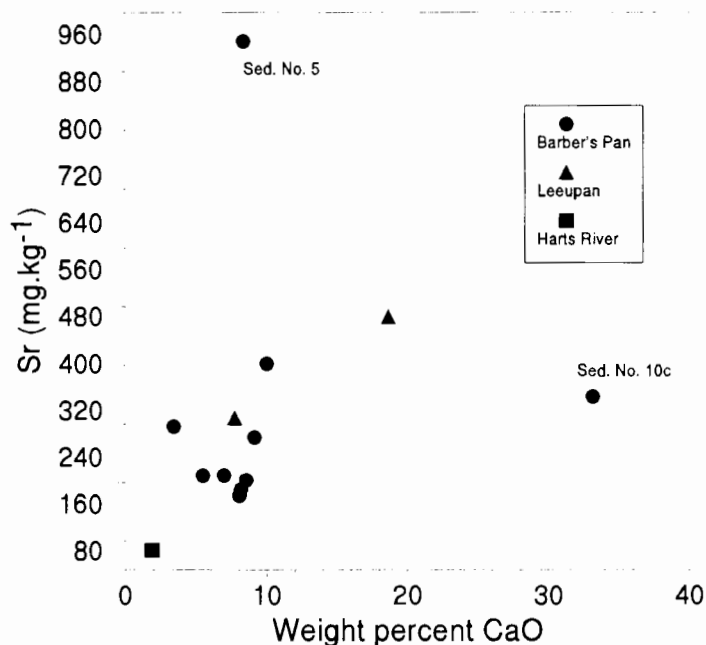


**Figure 45:** Plot of the relationship between Ca and Sr in the Barber's Pan, Harts River and Leeupan sediments.

Förstner and Wittman (1979) state that with respect to the direct association of metal – organic species to sedimentary material, the association with clay minerals is of particular significance. They further record that Curtis (1966) proposed a simplified scheme explaining the positive association between organic carbon and the metals Cr, Cu, Mn, Mo, Ni, U, and V, in a sediment. According to this scheme, positive correlation occurs when metal ions interact in solution with dissolved organic matter that is in turn concentrated by adsorption onto particulates like the clay minerals.

This may account for the correlation observed between organic carbon and  $\text{Al}_2\text{O}_3$  in the sediments sampled, as well as the correlation between organic carbon and certain trace metals.

A number of studies investigating the interaction between heavy metals and carbonates have shown that coprecipitation of the metals with carbonate minerals may be an important mechanism for the removal of these metals from solution (Förstner and Wittman, 1979). Jenne

(1976) [cited in Förstner and Wittman, 1979] proposed that the precipitation of heavy metals with carbonates is important where carbonates occur as a major component in soil or in the fine grained fraction of fluvial sediments and when trace elements are present in high enough concentration to saturate other elemental sinks. In the sediment samples examined here, no correlation was observed between the heavy metals and either MgO or CaO. An interesting case discussed by Förstner and Wittmann (1979) is the situation where an alkaline water body comes into contact with, and becomes mixed in, river water with "normal"  $\text{Ca}^{2+}$  and  $\text{HCO}_3^-$  under neutral pH conditions. Under these circumstances the pH will increase with the consequence that the solubility product of  $\text{CaCO}_3$  is drastically reduced and  $\text{CaCO}_3$  is precipitated in the mixing zone, carrying heavy metals with it. In Barber's Pan, a similar situation is likely to occur when the pan receives periodic inflows of water from the Harts River.

Fe- and Mn-hydroxides and oxides constitute significant sinks for heavy metals in aquatic systems, when under oxidizing conditions. This is because they can readily sorb or coprecipitate cations and anions; even low percentages of  $\text{Fe}(\text{OH})_3$  and  $\text{MnO}_2$  exerting a controlling influence on the heavy metal distribution of an aquatic system (Förstner and Wittman, 1979). It has been proposed that hydrous oxides of Fe and Mn provide the principal control on the fixation of trace elements in soils and freshwater sediments (Adriano, 1986). A strong correlation was observed between  $\text{Fe}_2\text{O}_3$  and several heavy metals (discussed above) as well as with other trace elements, with Fig. 46 serving as an example of these associations. The positive association between free-iron oxides and clay content has already been discussed.

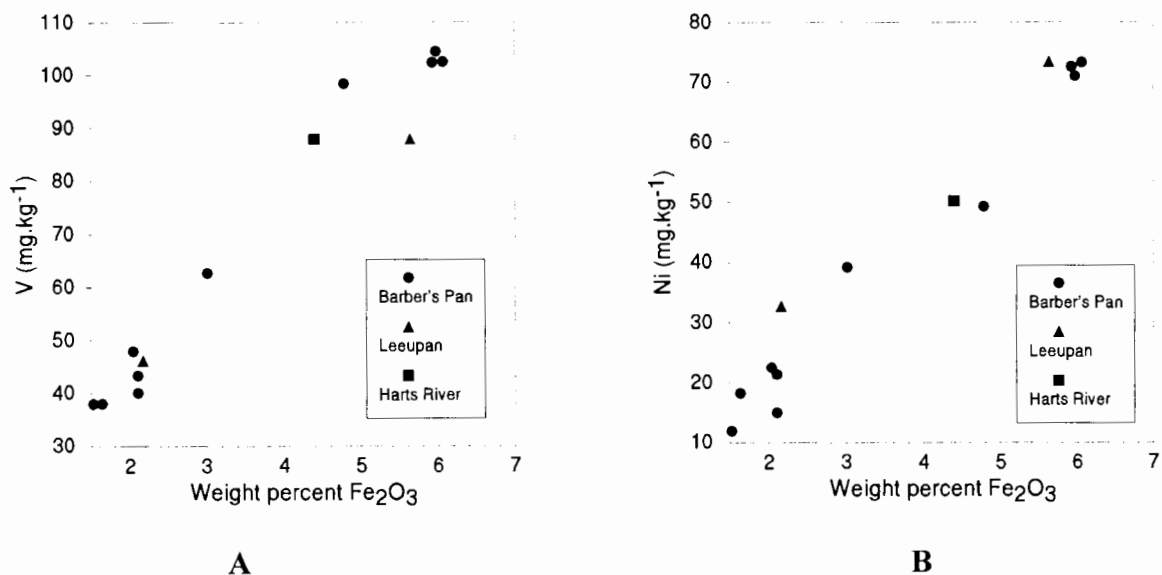


**Figure 46:** Plots of the relationships between  $\text{Fe}_2\text{O}_3$  and V (A) and  $\text{Fe}_2\text{O}_3$  and Ni (B) in the Barber's Pan, Harts River and Leeupan sediments.

Correlations were also observed between the distributions of S in the sediments and the distributions of  $\text{Al}_2\text{O}_3$ ,  $\text{Fe}_2\text{O}_3$ ,  $\text{TiO}_2$ ,  $\text{P}_2\text{O}_5$ , Co, Cr, V, Nb, Rb, Th, Zn, Cu and Ni. The sulphur may be incorporated into, or associated with, organic matter in the sediments (although organic carbon and sulphur did not show a significant correlation) which was concentrated in the central muds along with many of the trace elements as discussed above. The likely presence of iron sulphides in Barber's Pan has already been discussed (section 3.3.3). Förstner and Wittmann (1979) state that inorganic precipitation may account for trace metal incorporation within iron sulphides, and discuss trace element enrichment in iron sulphides within Black sea sediments. They also mention trace element enrichment in unstable iron sulphides of the hydrotroilite type which form finely dispersed black muds, and are instantly oxidized under aerobic conditions. Schwertmann and Taylor (1989) note that the presence of  $\text{Fe}^{3+}$  in layer structured double hydroxy salts known as green rusts (dark green–blue mixed  $\text{Fe}^{3+}$ – $\text{Fe}^{2+}$  hydroxides), which may be phases in the formation of other common Fe–oxides, gives the sheets making up these salts a positive charge that is balanced by anions such as  $\text{CO}_3^{2-}$ ,  $\text{Cl}^-$  and  $\text{SO}_4^{3-}$  which may occupy the interlayer region between the octahedral sheets. Some of the  $\text{Fe}_2\text{O}_3$  and S present in the sediments of Barber's Pan may be associated in this way, accounting for the correlation between S and some of the trace elements.

#### 4.4.4 Chemistry of the core sample

The XRFS analyses of core sample 4 (tabulated in Appendix 5) revealed a very interesting trend of changing chemical composition with depth. With the exception of SiO<sub>2</sub>, MgO, CaO, P<sub>2</sub>O<sub>5</sub>, U, K<sub>2</sub>O and Sr all the elements determined showed a trend of increasing concentration with depth until a depth of 80 – 86cm (portion 4f of the core) was reached. Examples of this trend are given in Figures 47 and 48. In the deepest portion of the core (80 – 86cm), however, the concentrations of these elements showed a sharp decrease.

The concentration of K<sub>2</sub>O increased gradually with depth through the entire length of the core. The concentrations of U showed very erratic behaviour with depth. This can be attributed to analytical error since three of the six portions of the core had U levels below the detection limits of the x-ray spectrometer, while the remainder approached these limits. P<sub>2</sub>O<sub>5</sub> gradually decreased in concentration with depth. The concentrations of MgO and SiO<sub>2</sub> remained essentially constant with depth (increasing slightly) until the deepest portion of the core (80 – 86cm) where their concentrations showed a sharp increase. CaO showed decreasing concentration with depth until the deepest portion of the core at which point its concentration also rose sharply. Sr, being able to substitute for Ca in CaCO<sub>3</sub>, mirrored CaO in its behaviour with depth. The concentrations of MgO, CaO, Al<sub>2</sub>O<sub>3</sub> and Fe<sub>2</sub>O<sub>3</sub> with depth are plotted in Figure 49.

Increases in the concentrations of metals in sediment cores have been attributed to temporal variation of atmospheric deposition, catchment runoff, effluent inflow and the dumping of metals released by human activities. Superimposed onto this are early diagenetic processes, such as metal chelation by organic matter, scavenging by iron and manganese oxides and redox reactions, which often produce decreasing or increasing metal concentrations with depth. Irregular patterns may be the consequence of diagenetic processes being overwhelmed by the input of sediments of different chemical composition (Bifano and Mogollón, 1995).

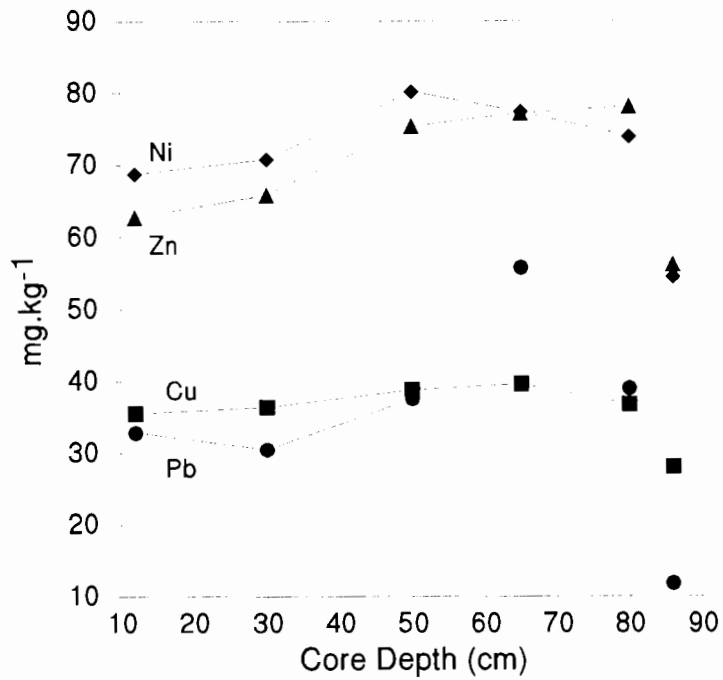


**Figure 47:** A plot of the concentrations of Pb, Cu, Ni and Zn with increasing depth in the core sample from Barber's Pan.

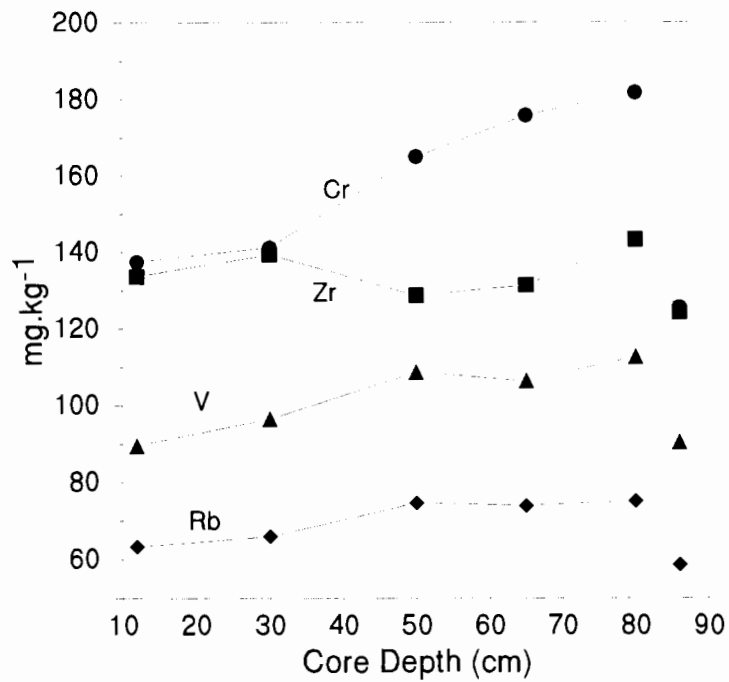


**Figure 48:** A plot of the concentrations of Cr, Zr, Rb and V with increasing depth in the core sample from Barber's Pan.

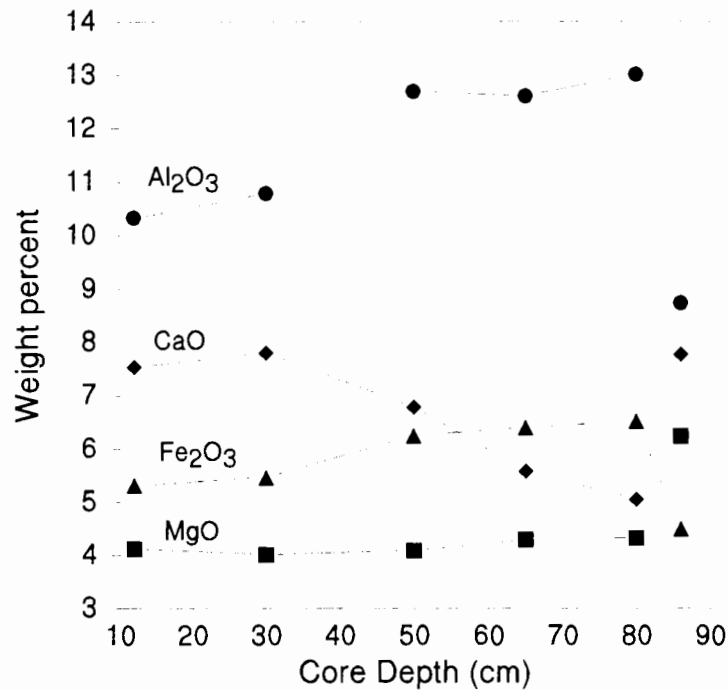


**Figure 49:** A plot of the concentrations of CaO, MgO, Al<sub>2</sub>O<sub>3</sub> and Fe<sub>2</sub>O<sub>3</sub> with increasing depth in the core sample from Barber's Pan.

Resuspension of the sediments by wind is likely to play an important role in Barber's Pan and may account for the irregular pattern (with depth) exhibited by some of the elements determined.

This enrichment of Ca, Mg and Si in the deepest portion of the core, accompanied by the depletion of other elements in this portion may be interpreted in one of two ways. It may be an artifact of the sample collection, storage, transportation and preparation procedures followed, or it may represent a calcareous layer associated with the last period that the pan was completely desiccated.

Once collected the core samples were sealed in the 60 mm diameter PVC corers used for collection by capping them at both ends. They were then transported to the Department of Geological Sciences, University of Cape Town, where they were frozen at a temperature of  $-20^{\circ}\text{C}$  in a walk-in freezer. During collection it was observed that the pan sediments were largely made up of a very fluid mud. This suggests that some mixing may have taken place with particles migrating within the core before it was frozen. Heavier, sand-sized particles, could, therefore, have settled out at the bottom of the core. The top sections of the core (4a and b) still contained higher proportions of sand-sized particles than the central portions (4c,

d and e), suggesting that extensive settling had not taken place. A period of two–weeks elapsed from the time of collection to the time of freezing. In this period some diagenetic reactions may have occurred as a consequence of changing redox conditions. The cores were, however, tightly sealed after collection and could thus be considered as fairly air–tight. Furthermore, no concentration of elements likely to be affected by changing redox conditions (e.g. Fe and Mn) had accumulated at either end of the core where any oxidation (and consequent precipitation) would have taken place.

In the light of the above discussion, the sequence of elemental concentrations observed in the core is likely to be genuine, in which case the increased concentrations of Si, Ca and Mg in the deepest portion may well represent the period when the pan was last dry (or virtually dry). The Ca and Mg are likely to be associated with calcite and/or dolomite, while the increased Si concentration could be attributed to deflational aeolian processes removing the finer clay material and leaving residual quartz and dolomite, or siliceous calcrete particles. On unvegetated pan surfaces wind action entrains surface materials, mainly fine sands and small pellets of clay of equivalent dimension (resulting from salt efflorescence and the breakdown of clay flakes produced by the desiccation of clay surfaces [Fig. 50]). Winnowing out of the finer material from fractures separating surface plates also occurs. Removal of these fine sediments can lead to lag deposits of gravel, silcrete fragments or crustal remains (Shaw and Thomas, 1989). Clay pellets deflated through aeolian action may accumulate on the pan margin forming a transverse dune or lunette. In chemically–evolved salt lake systems  $\text{CaCO}_3$  or  $\text{CaSO}_4$  may be present in deflating surface sediments contributing significant material to surrounding lunettes (Torgersen *et al.*, 1986). Lunettes (Fig. 35) were observed associated with both Barber's Pan and Leeupan and Goudie and Thomas (1985) (section 4.4.3) record the presence of calunettes in the area.

Removal of the clay material by aeolian deflation would account for the decreased concentrations of many of the other elements in portion 4f of the core, since the adsorptive properties of clays tend to allow many ions to be removed from solution by adsorption onto clay minerals. Adsorption and coprecipitation of ions with Fe– and Mn–oxides is another important mechanism whereby ions are removed from solution. This was discussed in section 4.4.3.



**Figure 50:** Breakdown of clay flakes and the removal of finer material by deflation from the surface of Leeupan

The lacustrine deposits of Florisbad Pan, Orange Free State, (which was classified as falling within the same geographical region as Barber's Pan on the basis of climatic data) were found to be composed of clayey, silty and sandy layers with two interlayered carbonate-rich deposits (Verster *et al.*, 1992). The clay layers were interpreted as representing lake floor sediments deposited during high water levels in the pan, while the carbonate layers reflect deposition under shallow water conditions during water regression. The chemical composition of core portions 4a and 4f can be seen to resemble that of the upper Leeupan sediment (Leeupan {top}), which was dry at the time the core samples were taken and was being subjected to aeolian deflation. The Leeupan sediment was undoubtedly deposited under shallow water conditions, while section 4a of the core represents the top layer of Barber's Pan sediment which is being deposited during a period of evaporative concentration. MINTEQA2 predicted that, at present, the bulk pan water is supersaturated with respect to carbonate minerals such as calcite and dolomite (section 3.3.2.6)

The gradual increase in the concentration of the majority of the elements with increasing depth within the core (up to but excluding section 4f) is likely to be a function of the increasing clay content and increased concentrations of Fe and Mn. As with the grab samples (section 4.4.3) the  $\text{Al}_2\text{O}_3$ ,  $\text{Fe}_2\text{O}_3$  and MnO concentrations in the core were closely associated

(Fig. 49 depicts the relationship between  $\text{Al}_2\text{O}_3$  and  $\text{Fe}_2\text{O}_3$  but does not include  $\text{MnO}$  due to scale considerations). The majority of the other elements were, in turn, closely correlated with  $\text{Al}_2\text{O}_3$ ,  $\text{Fe}_2\text{O}_3$  and  $\text{MnO}$  (Fig. 51 showing some of the elemental associations with  $\text{Al}_2\text{O}_3$ ). The ability of aluminosilicates and Fe- and Mn-oxides to scavenge other elements through adsorption and coprecipitation was discussed in section 4.3.3. Sr was associated with Ca, as was observed in the grab samples (section 4.3.3). This may be attributed to the substitution of Ca by Sr in carbonate minerals as discussed in section 4.3.3. Fig. 52 shows the relationship between K and Rb in the core. The relationship is linear as expected, with the exception of the point reflecting the relationship between these two elements in section 4f of the core.

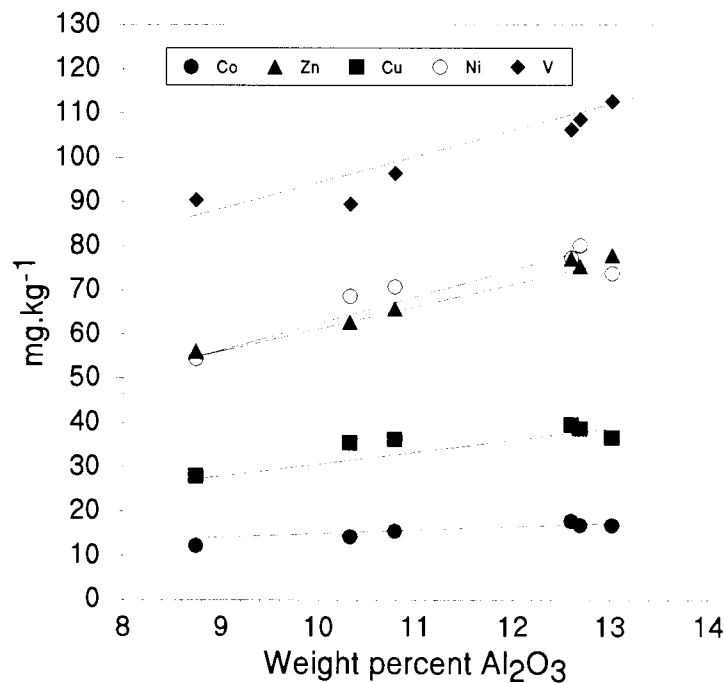


**Figure 51:** A plot of the concentrations of Co, Zn, Cu, Ni and V against  $\text{Al}_2\text{O}_3$  showing their relationship in the core sample from Barber's Pan.

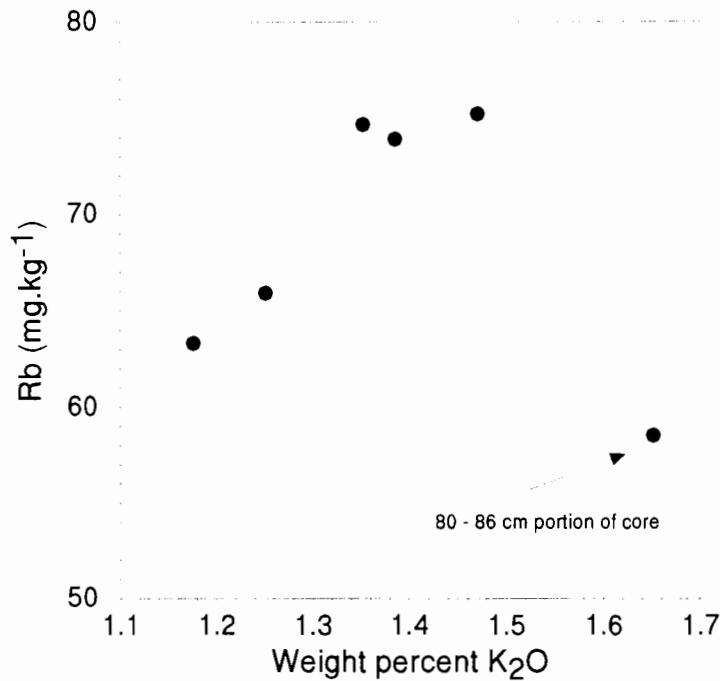


**Figure 52:** A plot of the K against Rb showing their relationship in the core sample from Barber's Pan.

#### 4.4.5 Sedimentation rates in Barber's Pan

In order to make conclusive deductions as to the effect of the Smuts diversion on sedimentation rates in the pan, it would be necessary to take a further series of cores, penetrating down to the original pan sediment or if possible the underlying pan limestone. Verster *et al.* (1992) record that the thickness of sediment in Barber's Pan and Leeupan is 3 and 4m respectively. If this is the case the cores taken during the present study can be seen to be grossly inadequate. Considering these depths, it is suggested that a mechanical vibracorer as used by Baxter and Davies (1994) be used to obtain the cores. They state that this technique is widely believed to be the best method of deriving long, undisturbed cores from fluvial or deltaic sediments.

Any of a variety of dating techniques can then be used to make accurate determinations of the rates of sedimentation in the pan over time. Radioactive carbon (C-14) dating can be used to evaluate the age of organic material in sediments (Wetzel, 1983), while the CaCO<sub>3</sub> content can provide information as to variations in lake levels, particularly when correlated with diatom and C-14 stratigraphy (Eugster and Kelts, 1983). The recent sediments can be dated using <sup>210</sup>Pb or <sup>137</sup>Cs isotopes. Remnant magnetism is an important non-destructive

dating technique that can be considered, while magnetic susceptibility would be useful in evaluating the probable sources of sedimented materials (Wetzel, 1983).

Yuretich and Cerling (1983) successfully determined sedimentation rates in Lake Turkana, Kenya, using  $^{210}\text{Pb}$  and palaeomagnetic records. Baxter and Davies (1994) used pollen analysis to determine sedimentation rates and identify a sequence of rapid changes within the riparian and aquatic vegetation of Verlorenvlei, Western Cape.

#### **4.4.6 Phosphate – sediment interactions**

Olsen and Sommers (1982) regard values of  $11 \text{ mg.kg}^{-1}$  and greater of phosphorus (as extracted by  $\text{NH}_4\text{HCO}_3$ ) as being indicative of very high concentrations of phosphorus on a soil basis (i.e. when extracted from the soil, in relation to the requirements of plants growing in that soil). Extractable phosphate concentrations for the Barber's Pan, Leeupan and Harts River sediment samples are given in Table 15. The values were obtained by means of a standard soil extraction technique devised for estimating the availability of phosphorus to plants from alkaline soils (refer to 4.3.4). The Harts River sediment sample and sample no. 4 (river mouth) were both found to have very low available phosphorus concentrations, while the deeper, more central sediments (7, 9 and 16) were found to be relatively enriched in available phosphorus. The lower available phosphorus concentrations of the Harts River sediment and the shallower, edge sediments in the pan may well be associated with differing particle size distribution (discussed in section 4.4.3), these samples having a greater proportion of sand – sized particles. The deeper, central sediments consisted predominantly of clay – sized material and contained greater amount of organic matter. Adsorption of phosphate onto clay minerals and the phosphorus content of the organic matter are likely to account for the increased extractable phosphorus concentrations in the central sediments. The interstitial water was found to be strongly enriched in phosphate relative to the bulk pan water, having on average a 36x greater concentration.

Sediments act as reservoirs for phosphorus in natural systems with the phosphate concentration in waters overlying sediments being buffered by solubility and adsorption or ion exchange equilibria at the sediment – water interface. Although the nature of this phosphate control is not fully understood, there is, however, agreement that chemical interactions of phosphate with  $\text{Fe}^{3+}$ , Al in clays and  $\text{Ca}^{2+}$  are relevant (Stumm and Morgan, 1970).

The average pH of the bulk pan water was found to be 9.2 while that of the interstitial water was recorded as 8.4. Studies investigating the effect of pH on the ability of oxidized lake sediment to remove inorganic phosphate from water have shown that in the pH range 4.5 – 6.5 phosphate tends to be bound to the solid phase by Fe and Al,

**Table 15:** Concentrations of extractable phosphorus in the Barber’s Pan, Leeupan and Harts River sediment samples (extraction was by means of the AMBIC method of Van der Merwe *et al.* [1984]).

Sample No.	Extractable Phosphorus (mg.kg <sup>-1</sup> )
Harts River	4.6
Leeupan	
Top	28.2
Bottom	19.0
Barber’s Pan	
2	8.4
4	1.0
5	17.6
7	26.9
8	8.3
9	26.8
10	2.4
16	24.2
17	0.7

either by precipitation or adsorption. Very little becomes sorbed between pH 7 – 9. At higher pH values the tendency for phosphate to precipitate is progressively enhanced. This is probably related to the progressively decreasing solubility of apatite (Stumm and Morgan, 1970).

Modelling the mineral solubility equilibria in the pan using MINTEQA2 suggested that hydroxyapatite and fluorapatite were the minerals controlling the solubility of phosphate in the pan water (section 3.3.2.6). Both the bulk and interstitial water were predicted to be supersaturated with respect to phosphate implying the precipitation of both fluorapatite and hydroxyapatite. The lower pH values of the interstitial waters together with the likely reducing

environment encountered in the sediments could well increase the solubility of the precipitated phosphate minerals, promoting their dissolution and thereby increasing the concentration of  $\text{PO}_4^{3-}$  in these waters.

Exchanges across the sediment interface are regulated by mechanisms associated with mineral–water equilibria, sorption processes (particularly ion exchange), oxygen–dependent redox interactions, and the activities of bacteria, fungi, plankton and invertebrates. The most conspicuous regulatory features of the sediment boundary are the mud–water interface and the oxygen content of this interface (Wetzel, 1983). Stumm and Morgan (1970) record that the sediment–water interface separates two very different domains, since in all but the upper few millimetres of sediment, exchange is governed by motions on molecular scales with correspondingly low diffusion rates. In the water, exchange is regulated by much higher and more variable rates of turbulent diffusion.

Oxygen penetration into the sediments is governed by the rate of oxygen supply to the sediments and by their oxygen demand per unit volume. In the case of superficial sediments turbulent mixing is also an important factor, and the importance of an oxidized microzone to chemical exchanges from the sediments, particularly those of phosphorus, has been demonstrated by several studies (Wetzel, 1983).

The ability of sediments to retain phosphorus beneath an oxidized microzone at the interface is related to several interacting factors. Most sediment phosphorus is inorganic (e.g. apatite or phosphate adsorbed onto clays and ferric hydroxides) and, additionally, phosphate coprecipitates with iron, manganese and calcium. The rate of transfer across the sediment–water interface depends upon the state of the microzone, with the oxidized layer forming an efficient trap for iron and manganese, as well as for phosphate. In this way it can greatly reduce the transport of materials into the water and scavenge materials such as phosphate from the water (Wetzel, 1983).

Barber's Pan is relatively shallow, with the greatest depth recorded during the sampling period being 4.2m. The shallow nature of the pan together with the strong winds which regularly occur in the area (Milstein, 1975) suggest that turbulent mixing of the superficial sediments is likely to be a frequent occurrence. As a consequence the superficial sediments are likely to be well oxygenated, with a significant oxidized microzone at the sediment–water interface.

Rogers *et al.* (1989) record that in Rolfes pan, Elandsfontein, the release of phosphorus into the water column appears to be inhibited by an oxidized microzone. In Barber's Pan the sediments can, therefore, be seen to act as a sink for phosphorus, with very little being released back into the water as a consequence of an oxidized microzone. The high alkalinity and resulting supersaturation with carbonates is also likely to reduce the solubility of much of the  $\text{PO}_4^{3-}$  remaining in solution, stimulating it to precipitate/coprecipitate in the forms discussed above.

The release of phosphorus from sediments is also highly dependent on the speciation of the phosphorus present in the sediments. Ca-bound phosphorus has slow release rates, while phosphorus bound to Fe and Al is easily released under anaerobic conditions and at high pH levels (Forsberg, 1989). MINTEQA2 predicted that phosphorus in the bulk pan water of Barber's Pan would largely be present as  $\text{MgPO}_4^-$  and  $\text{HPO}_4^-$ . Ca-bound phosphorus was predicted as comprising only 5% of the soluble phosphorus. This is likely to be attributable to the relative enrichment of Mg over Ca in the pan water.

A number of studies have, however, shown that this classical theory of an oxidized microzone at the sediment surface is not sufficient to explain the behaviour of phosphorus in the sediments of all lakes (Pettersson, 1984). A study by Twinch and Peters (1984) suggested that aerobic phosphate release from marginal sediments may be an important source of phosphate to plankton in the shallow zones of oligotrophic lakes, where a combination of algal demand and well-mixed water maintains low ambient phosphate concentrations in water directly overlying the sediments. They state that under such conditions the sediment-water phosphate gradient can favour a slow but steady flux into the overlying water. In contrast to anaerobic phosphate release, aerobic phosphate release is not usually detectable from field monitoring of epilimnetic phosphate concentrations because of the low concentrations and well mixed conditions.

A further important consideration is the apparent resistance of shallow lakes to eutrophication (in terms of algal growth) until a critical point is reached. This is thought to be related to the large surface area/volume ratio and littoral/pelagic zone ratios of shallow lakes which can increase the extent of the oxidized microzone, decreasing the release of phosphate into the water column (Rogers *et al.*, 1989). In Barber's Pan, low levels of  $\text{PO}_4^{3-}$  in the bulk pan

water contrast with very high levels in the interstitial water and sediments, suggesting that this is indeed the case in the pan.

#### 4.5 Conclusions

The sediments of Barber's Pan were found to consist predominantly of mud-sized particles ( $< 0.053\text{mm}$ ). The shallower sediments on the pan fringe were found to contain a greater proportion of sand-sized ( $> 0.053\text{mm}$ ) particles than the deeper, central sediments. Wind and wave action are likely to be responsible for the removal of finer clay-sized material from the edge to the central sediments. The clay mineralogy of Barber's Pan can be described as interstratified chloritic-smectitic material with mica, kaolinite, quartz and calcite also present. The same clay minerals were identified in the Harts River sediment with the exception of calcite which was not present. The mineralogy of the Leeupan sediment was found to have two distinct components. An upper layer which closely resembled that of Barber's Pan and a lower layer consisting predominantly of dolomite. A microbially mediated process may be responsible for the formation of this dolomite layer. Traces of sepiolite and palygorskite could also be present in the clay fractions of all the sediments sampled.

The carbonate content of the Barber's Pan sediments was high and the deeper, central sediments contained substantial quantities of organic matter. Elemental associations in the sediments analyzed appeared to conform to well documented relationships. Trace elements were associated predominantly with  $\text{Al}_2\text{O}_3$ ,  $\text{Fe}_2\text{O}_3$  and organic matter. CaO was associated with carbonates and MgO with the mud fraction. Calcrete was observed in one of the edge sediments of Barber's Pan. In Leeupan, a substantial amount of the MgO was associated with the dolomite layer, the remainder with the mud fraction. Al was thought to be concentrated in the clay minerals and Fe in the oxidates. Adsorption of trace elements by the clay minerals and organic matter accounts for the correlation observed between these three components. Adsorption and coprecipitation of trace elements by iron oxides probably accounts for the correlation between  $\text{Fe}_2\text{O}_3$  and the trace elements.  $\text{SiO}_2$  and Zr were associated with resistant minerals such as quartz and zircon and showed elevated concentrations in the shallow edge sediments, which were found to have a greater proportion of sand-sized particles.

The core sample analyzed showed an interesting trend of changing chemical composition with depth. Most elements increased in concentration with depth until the deepest portion, at which

point their concentrations showed a sharp decrease. In contrast, MgO, CaO and SiO<sub>2</sub> concentrations increased sharply in the deepest portion of the core. This was accompanied by an increase in the proportion of the sand-sized fraction. Two possible explanations for this trend were invoked. It could either be attributed to the sampling, storage, transport and preparation procedures, or it could represent the sediments that had accumulated on top of a calcareous layer formed when the pan was last completely desiccated. In the latter case, aeolian deflation could account for the removal of finer mud-sized material (increasing the proportion of sand-sized particles) and the precipitation of carbonates during evaporative concentration would account for the calcareous layer. A further series of longer cores are, however, required to make conclusive deductions as to the present sedimentation rates in the pan and the effect of the Smuts diversion on these rates. The superficial sediments of Leeupan and central, superficial sediments of Barber's Pan were found to be enriched in extractable phosphorus. In Barber's Pan the oxidation of the superficial layers of the sediments through perturbation by wind action is, however, likely to make this pool of phosphorus largely unavailable to the pan biota by trapping it beneath an oxidized microzone.

## 5. CONCLUSIONS AND RECOMMENDATIONS

The objectives of this thesis were outlined in a number of key questions posed in the introduction. These questions together with answers obtained during this study are discussed below.

1. *In the past it was stated that the pan was one of the least contaminated, large bodies of water in the then Transvaal Province. Is this statement still valid ?*

Although by no means comprehensive, this study established the levels of several potential pollutants in the pan water. Without natural background levels for comparison it was difficult to assess the present water quality, particularly from the point of view of the biota utilizing the pan. Despite this limitation an assessment of water quality was attempted through the comparison of the levels of the various water quality variables determined in the bulk pan water with several recognized water quality standards. On this basis, the pan appears to be largely unpolluted. Elevated levels of Pb and Ni are of concern, however. Pb in particular was substantially elevated relative to the recognized water quality standards used for comparison. Considering the relatively isolated location of the pan, the most likely source of these heavy metals appears to be boating activities.

The levels of extractable phosphorus in the sediment were found to be very high, as were levels of  $\text{PO}_4^{3-}$  in the interstitial water. These high levels of phosphorus are unlikely to present a eutrophication problem, however, as they are largely unavailable to the pan biota as a consequence of the oxidized microzone at the sediment–water interface (discussed below). Bulk pan water levels were depleted in  $\text{PO}_4^{3-}$  relative to the interstitial waters. The present solute concentrations of the bulk pan water allow Barber's Pan to be classified as a subsaline system (Hammer, 1986). Increased salinity is generally thought to provide biota with some protection against heavy metals as a consequence of increased speciation interactions, while elevated (alkaline) pH values tend to influence chemical speciation by decreasing the solubility of these elements through the formation of unavailable hydrated hydroxides (Dallas and Day, 1993). The very alkaline pH and elevated salinity of the pan water are, therefore, likely to provide the pan biota with a degree of protection from potential pollutants.

The concentrations of biocides (i.e. herbicides and pesticides) and other organic pollutants in the pan water were not determined and hence no attempt has been made to quantify the potential impact of these pollutants on the pan ecosystem. Considering their potentially severe impact it is imperative that their concentrations and hence potential impacts on the pan be determined in the near future.

It must also be borne in mind that the evaluation of the status of certain pollutants in the pan presented in this thesis is by no means comprehensive and is intended to serve primarily as a baseline against which the results of future monitoring actions can be compared. Investigational and research projects cannot yield data suitable for long term trend analysis in time and space, and intensive baseline studies have comparative value but are limited in terms of their ability to provide early warning of adverse trends (Mackay, 1993). To make accurate evaluations of the pan water quality, long-term statistically valid data is required. To this end it is recommended that a long-term monitoring programme for Barber's Pan be designed and implemented.

In addition to monitoring the physical and chemical characteristics of the pan water, land use in the greater catchment area of the pan should be investigated with major land users and potential polluters being identified. Pollutant loads in the catchment should then be calculated.

2. *How do the prevailing chemical conditions within the pan influence the distribution and bioavailability of phosphate ( $\text{PO}_4^{3-}$ ) and other nutrients in the pan ?*

MINTEQA2 predictions showed the predominant species of soluble inorganic phosphate in the pan water to be  $\text{MgPO}_4^-$  and  $\text{HPO}_4^{2-}$ . Hydroxyapatite and fluorapatite were predicted to be the minerals controlling phosphate solubility. Vivianite did not appear to play a significant role in phosphate solubility in the pan, most probably as a consequence of the high pH and high concentrations of  $\text{HCO}_3^-$  in the pan water.

Concentrations of soluble inorganic phosphate ( $\text{PO}_4^{3-}$ ) in the pan water did not appear to be limiting, but were substantially lower than levels recorded in the interstitial waters. The higher concentrations of  $\text{PO}_4^{3-}$  in the interstitial waters and large amounts of extractable phosphorus in the superficial sediments are attributable to the action of an oxidized microzone at the sediment-water interface. Strong winds are frequently recorded at Barber's Pan. These winds

are likely to bring about significant resuspension of the sediment, increasing the penetration of oxygen into the pan sediments. This action serves to maintain the oxidized microzone, trapping phosphorus in the anaerobic sediments below. MINTEQA2 predicted that the bulk and interstitial pan waters were supersaturated with respect to hydroxyapatite and fluorapatite. Precipitation of these minerals from the water column would contribute to the depletion of the  $\text{PO}_4^{3-}$  in the bulk pan water. MINTEQA2 also predicted that the bulk pan water was supersaturated with respect to several carbonate minerals (e.g. calcite and dolomite).

The high pH of the pan water may act to inhibit the growth of vegetation in the littoral zone, minimizing the potential impacts of this vegetation on nutrient dynamics within the pan. Previous research (Milstein, 1975) showed the benthic population of Barber's Pan to be rather poor. The benthos are, therefore, also unlikely to exert a major influence on nutrient dynamics in the pan. A potentially significant influence on phosphorus and nitrogen dynamics in the pan, that needs to be investigated, is the input of guano from resident and migrant waterfowl. This input may contribute to seasonal or episodic eutrophication in the pan. No such eutrophication has, however, been recorded to date.

Mn and Fe appear to be the only nutrients which may become limiting during certain periods. Mn concentrations in the bulk pan water found to be very low. The high pH and likely supersaturation of the water with carbonate minerals is likely to limit the solubility of Fe and Mn, with coprecipitation removing substantial quantities of these nutrients to the sediment. As with phosphorus, the oxidized microzone at the sediment surface may well limit their subsequent release. The pan sediments can thus be seen to act predominantly as a sink for nutrients, with very small quantities being released back into circulation from the sediment.

To gain a more complete understanding of nutrient dynamics in the pan the aquatic vegetation needs to be comprehensively classified so that the nutrient uptake and release of these plants can be quantified. Investigations into the populations of fish, plankton and benthos were carried out in the 1960's. A re-evaluation of these populations and their nutrient requirements is also necessary. The possible role of the macrophyte *Chara sp.* in the dynamics of Ca in the pan must be investigated by determining the presence and abundance of these plants in the pan and quantifying their Ca utilization.

3. *Anthropogenic intervention in 1918 changed Barber's Pan from a intermittently dry, wind-blown pan to a shallow, perennial lake. Can any effects of this change be detected in the pan's sediments, and what implications do they hold for the pan's future ?*

Conclusive deductions as to the effect of the Smuts diversion on sedimentation rates could not be made on the basis of the single 86cm core analyzed. The depth of the sediments in Barber's Pan are in the region of 3–4m (Verster *et al.*, 1992). A vibracorer (Baxter and Davies, 1994) is, therefore, likely to be the best method to obtaining long, undisturbed cores which are a prerequisite for the accurate determination of sedimentation rates in the pan. Time constraints prevented such intensive core sampling during the present study. It is therefore recommended that vibracores be obtained from both Leeupan and Barber's Pan in the near future. Care should be taken to ensure that these cores penetrate through to the parent material. A variety of dating techniques can then be applied to make accurate determinations of the sedimentation rates in Barber's Pan (with Leeupan providing comparative data for an active deflationary pan).

Results from the single core sample analyzed do suggest that substantial amounts of material have been deposited into the pan since the Smuts diversion. The pan sediment in the core sample appeared to be well mixed (most probably as a consequence of wind and wave action) although two different layers were distinguishable; the deepest portion constituting one and the remainder of the core the other. When compared with the upper portions of the core, the deepest layer was enriched in CaO, MgO and SiO<sub>2</sub> and had a higher proportion of sand-sized particles. Trace element concentrations were also depleted relative to the remainder of the core. This stratification within the core may be an artifact of the sampling, storage, transport and preparation procedures or it may be attributable to the deposition of sediment subsequent to the last deflationary period (when the pan was completely dry). The increased proportion of sand sized particles and depletion of trace element concentrations in the deepest layer may indicate the effects of aeolian deflation and carbonate deposition during the final desiccation stage and subsequent period of deflation when the pan was completely dry. The sediment in the remainder of the core (above the bottom layer) consisted predominantly of mud-sized particles suggesting that no substantial removal of the fine fraction had taken place.

A lack of data pertaining to natural background levels of elements in the pan sediments and their well mixed nature, made interpretations as to the possible anthropogenic enrichment of

certain elements difficult. The extensive chemical characterization of the sediments does, however, provide a benchmark against which future studies can be compared as well as providing a geochemical fingerprint for the pan sediments.

## 6. REFERENCES

Acocks, J.P.H. 1988. Veld Types of South Africa, 3rd Edition. Memoirs of the Botanical Survey of South Africa No. 57. Botanical Research Institute.

Adriano, D.C. 1986. Trace Elements in the Terrestrial Environment. Springer-Verlag, Berlin.

Al-Droubi, A., Fritz, B., Gac, J. and Tardy, Y. 1980. Generalized residual alkalinity concept; application to prediction of the chemical evolution of natural waters by evaporation. American Jnl. Science, Vol.280, June: pp. 560 - 572.

Allanson, B.R., Hart, R.C., O'Keefe, J.H. and Robarts, R.D. 1990. Inland Waters of Southern Africa: an Ecological Perspective. Kluwer Academic Publications, Dordrecht.

Allison, J.D., Brown, D.S. and Novo-Gradac, K.J. 1991. MINTEQA2/PRODEFA2, A Geochemical Assessment Model for Environmental Systems. EPA/600/3-91/021. Environmental Protection Agency, Athens, GA.

American Public Health Association. 1985. Standard methods for the examination of waste and wastewater. (16th Edition). APHA, AWWA and APCF Joint Publication. Washington DC.

Arakel, A.V., Jacobson, G. and Lyons, W.B. 1990. Sediment-water interaction as a control on geochemical evolution of playa lake systems in the Australian arid interior. Hydrobiologia, No. 197: pp. 1- 2.

Anderson, F.E. 1972. Resuspension of estuarine sediments by small amplitude waves. Jnl.of Sedimentary Petrology, No. 42: pp. 602-607.

Ashton, P.J. and Schoeman, F.R. 1983. Limnological studies on the Pretoria Salt Pan, a hypersaline maar lake. 1. Morphometry, physical and chemical features. Hydrobiologia, No. 99: pp. 61 - 73.

Barnhisel, R.I. and Bertsch, P.M. 1989. Chlorites and hydroxy-interlayered vermiculite and smectite. In: Dixon, J.B. and Weed, S.B. (Eds.) Minerals in Soil Environments. Am. Soil Sci. Soc. Madison, Wisconsin.

Baumann, A., Forstner, U. and Rodhe, R. 1975. Lake Sala: water chemistry, mineralogy and geochemistry of sediments in an Ethiopian rift lake. Geol.Rund. No. 64: pp. 593 - 609. Cited in: Hammer, U.T. 1986. Saline Lake Ecosystems of the World. Junk Publishers, Dordrecht.

Baxter, A.J. and Davies, B.R. 1994. Palaeoecological insights for the conservation of aquatic ecosystems in dryland environments: a case study of Verlorenvlei system, South Africa. Aquatic Conservation: Marine and Freshwater Ecosystems. Vol. 4: pp. 119.1 - 119.17.

Berner, R. A. 1971. Principles of Chemical Sedimentology. McGraw-Hill, New York.

Bifano, C. and Mogollón, J.L. 1995. Metallic contaminant profiles in sediment cores from Lake Valencia, Venezuela. Environmental Geochemistry and Health, Vol 17. No. 3: pp. 113 - 118.

Birch, G.F. 1981. The Karbonat-Bombe: a precise, rapid and cheap instrument for determining calcium carbonate in sediments and rocks. Trans.geol.Soc.S.Afr., No. 84: pp. 199-203.

Bowler, J.M. 1986. Spatial variability and hydrological evolution of Australian lake basins: an analogue for Pleistocene hydrologic change and evaporite formation. Palaeogeography, Palaeoclimatology, Palaeoecology, No. 54: pp. 21 - 41.

Borchardt, G. 1989. Smectites. In: Minerals in Soil Environments. Dixon, J.B. and Weed, S.B. (Eds.) Am. Soil Sci. Soc. Madison, Wisconsin.

Bühmann, C. 1986. The Investigation of 2:1 Layer Silicate Clays in Selected Southern African Soils. PhD Thesis, University of Natal, Pietermaritzburg (Unpublished).

Bühmann, C., Fey, M.V. and de Villiers, J.M. 1985. Aspects of the X-ray identification of swelling clay minerals in soils and sediments. S. African Jnl. Science, Vol. 81: pp 505-509.

Combrinck, J.J. 1966. 'n Kwantitatiewe en Kwalitatiewe Onderzoek van die Plankton van Barberspan. M.Sc Thesis, Potchefstroom University (Unpublished).

Curtis, C.D. 1966. The incorporation of soluble organic matter into sediments and its effect on trace element assemblages. In: Advances in Organic Chemistry. Hobson, G.D. and Louis, M.C. (Eds.) Pergamon Press, Oxford. Cited in: Förstner, U. and Wittman, G.T.W. 1979. Metal Pollution in the Aquatic Environment. Springer-Verlag, Berlin.

Dallas, H.F. and Day, J.A. The Effect of Water Quality Variables on Riverine Ecosystems: A Review. Water Research Commission, Pretoria.

Day, J.A. 1993. The major ion chemistry of some southern African saline systems. Hydrobiologia, No. 267: pp. 37 - 59.

de Bruijn, H. 1971a. Pans in the western Orange Free State. Ann. Geol. Surv. South Africa. Vol. 9: pp. 121 -124.

de Bruijn, H. 1971b. 'n Geologiese Studie van die Panne in die Westelike Oranje-Vrystaat. M.Sc. Thesis. University of the Orange Free State, Bloemfontein (Unpublished).

De Dekker, 1988. Biological and sedimentary facies of Australian salt lakes. pp. 237-270. In: Gray, J. (Ed.) Palaeolimnology - Aspects of Freshwater Palaeoecology and Biogeography. Elsevier, Amsterdam.

Doner, H.E. and Lynn, W.C. 1989. Carbonate, halide, sulphate, and sulphide minerals. In: Minerals in Soil Environments. Dixon, J.B. and Weed, S.B. (Eds.) Am. Soil Sci. Soc. Madison, Wisconsin.

Douglas, L.A. 1989. Vermiculites. In: Dixon, J.B. and Weed, S.B. (Eds.) Minerals in Soil Environments. Am. Soil Sci. Soc. Madison, Wisconsin.

Drever, J.I. 1988. The Geochemistry of Natural Waters. (2nd Ed.). Prentice Hall, New Jersey.

Drever, J.I. and Smith, C.L. 1978. Cyclic wetting and drying of the soil zone as an influence on the chemistry of groundwater in arid terrains. American Jnl. Science, Vol. 278, December: pp. 1448 -1454.

Elprince, A.M., Mashhady, A.S. and Aba-Husayn, M.M. 1979. The occurrence of pedogenic palygorskite (attapulgitite) in Saudi Arabia. Soil Science, Vol. 128. No. 4: pp. 211 - 219.

Enos, P. 1978. Dolomite, dolomitization. In: Fairbridge, R.W. and Bourgeois, J. (Eds.) The Encyclopedia of Sedimentology. Dowden, Hutchinson and Ross Inc., Pennsylvania.

Eugster, H.P. 1980. Geochemistry of Evaporitic Lacustrine Deposits. Ann. Rev. Earth Planet. Sci., No. 8: pp. 35 - 63.

Eugster, H.P. and Hardie, L.A. 1978. Saline lakes. In: Lerman, A (ed) Lakes: Chemistry, Geology and Physics. Springer – Verlag, New York.

Eugster, H.P. and Jones, B.F. 1979. Behaviour of major solutes during closed-basin brine evolution. American Jnl. Science, Vol. 279, June: pp. 609 - 631.

Eugster, H.P. and Kelts, K. 1983. Lacustrine chemical sediments. pp. 321 - 368. In: Goudie, A.S. and Pye, K. (Eds.) Chemical Sediments and Geomorphology - Precipitates and Residua in the Near-Surface Environment. Academic Press, London.

Fanning, D.S., Keramidas, V.Z. and El-Desoky, M.A. 1989. Micas. In: Dixon, J.B. and Weed, S.B. (Eds.) Minerals in Soil Environments. Am. Soil Sci. Soc. Madison, Wisconsin.

Farkas, T. 1962. Contribution to the bird fauna of Barberspan. Ostrich, Supplement No. 4: pp 3-8.

Farkas, T. 1962. Contribution to the bird fauna of Barberspan. Ostrich, Supplement No. 4: pp. 1-39.

Fergusson, J.E. 1990. The Heavy Elements: Chemistry, Environmental Impact and Health Effects. Pergamon Press, New York.

Forsberg, C. 1989. Importance of sediments in understanding nutrient cyclings in lakes. Hydrobiologia, No. 176/177: pp. 263-277.

Förstner, U. and Wittman, G.T.W. 1979. Metal Pollution in the Aquatic Environment. Springer-Verlag, Berlin.

Gales, P.M., Reddy, K.R. and Graetz, D.A. 1992. Mineralization of sediment organic matter under anoxic conditions. J. Environ. Qual., Vol. 21: pp. 394 - 400.

Garrels, R.M. and MacKenzie, F.T. 1967. The origin of the chemical compositions of some springs and lakes. Am. Chem. Adv. Chem., No. 67: pp. 222 - 242.

Gee, G.W. and Bauder, J.W. 1989. Particle size analysis. In: Klute, A. (Ed.) Methods of Soil Analysis :Physical and Mineralogical methods. Part 2 (2nd Ed.) Am.Soc.Agron. Madison, Wisconsin.

Geldenhuis, J.N. 1982. Classification of pans of the western Orange Free State according to vegetation structure, with reference to avifaunal communities. S.Afr.J. Wildlife Research, Vol. 12: pp. 55 - 62.

Göldner, H.J. 1967. 'n Populasie Studie van varswatervisse in Barberspan, Wes-Transvaal. M.Sc. Thesis, University of Potchefstroom (Unpublished).

Goudie, A.S. 1991. Pans. Progress in Physical Geography, Vol. 15, No. 3: pp. 221 -237.

Goudie, A.S. 1983. Calcrete. In: Goudie, A.S. and Pye, K. (Eds.) Chemical Sediments and Geomorphology - Precipitates and Residua in the Near-Surface Environment. Academic Press, London.

Goudie, A.S. and Thomas, D.S.G. 1985. Pans in southern Africa with particular reference to South Africa and Zimbabwe. Zeitschrift für Geomorphologie, Vol. 29. No. 1: pp. 1 - 19.

Goudie, A.S. and Wells, G.L. 1995. The nature, distribution and formation of pans in arid zones. Earth Science Reviews, Vol. 38, No. 1: pp. 1 - 69.

Green, J.T. 1995. An Assessment of Pans as Landscape Features in the North West Province using Remote Sensing Techniques. M.Sc. Thesis, University of the Witwatersrand, Johannesburg (Unpublished).

Hammer, U.T. 1986. Saline Lake Ecosystems of the World. Junk Publishers, Dordrecht.

Handford, R.C. 1982. Sedimentology and evaporite genesis in a Holocene continental-sabkha playa basin- Bristol Dry Lake, California. Sedimentology, No. 29: pp. 239 - 253.

Hardie, L.A. and Eugster, H.P. 1970. The evolution of closed-basin brines. Mineral Soc. Am. Spec. Publ. No. 3: pp. 273 - 290.

Hardie, L. A., Smoot, J.P., and Eugster, H.P. 1978. Saline lakes and their deposits: a sedimentological approach. pp. 7 - 42. In: Matter, A. and Tucker, M.E. (Eds.) Modern and Ancient Lake Sediments. Blackwell Scientific Publications, London.

Harmse, J.T., Olivier, P.G. and Goudie, A.S. 1990. A Bibliography on Pans and Related Deposits. Rand Afrikaans University Press, Johannesburg.

Holdren, G.C. and Armstrong, D.E. 1980. Factors affecting phosphorus release from intact lake sediment cores. Environmental Science and Technology, Vol. 14. No. 1: pp. 79 - 87.

Horie, S. 1978. Lacustrine Sedimentation. In: Fairbridge, R.W. and Bourgeois, J. (Eds.) The Encyclopedia of Sedimentology. Dowden, Hutchinson and Ross Inc., Pennsylvania.

Hudec, P.P. and Sonnenfeld, P. 1974. Hot Brines on Los Roques, Venezuela. Science, Vol. 185: pp. 440 - 442. Cited in: Wetzel, R.G. 1983. Limnology. (2nd Ed.) Saunders College Publishing, Fort Worth.

Hsü, K.J. and Siegenthaler, C. 1969. Preliminary experiments on hydrodynamic movement induced by evaporation and their bearing on the dolomite problem. Sedimentology, No. 12: pp. 11 - 25. Cited in: Hardie, L. A., Smoot, J.P., and Eugster, H.P. 1978. Saline lakes and their deposits: a sedimentological approach. pp. 7 - 42. In: Matter, A. and Tucker, M.E. (Eds.) Modern and Ancient Lake Sediments. Blackwell Scientific Publications, London.

Hutchinson, G.E. 1937. A contribution to the limnology of arid regions. Trans. Connecticut Acad. Arts Sci. No. 33: pp. 47 - 132. Cited in: Hammer, U.T. 1986. Saline Lake Ecosystems of the World. Junk Publishers, Dordrecht.

Jansson, M. 1984. Nitrate as a catalyst for phosphorus mobilization in sediments. pp. 387 - 390. In: Sly, P. (Ed.) Sediment and Water Interactions. Springer-Verlag, New York.

Jenne, E.A. 1976. Trace element sorption by sediments and soils - sites and processes. In: Chappell, W. and Petersen, K. (Eds) Symposium on Molybdenum. Vol. 2, New York. Cited In: Förstner, U. and Wittman, G.T.W. 1979. Metal Pollution in the Aquatic Environment. Springer-Verlag, Berlin.

Jones, B.F., Eugster, H.P. and Rettig, S.L. 1977. Hydrochemistry of the Lake Magadi Basin, Kenya. Geochim. Cosmochim. Acta, Vol. 41: pp. 53 - 72.

Jones, B.F. and Weir, A.H. 1983. Clay minerals of Lake Abert, an alkaline, saline lake. Clays and Clay Minerals, Vol. 31. No. 3: pp. 161 - 172.

Kempster, P.L., Hattingh, W.H.J. and Van Vliet, H.R. Summarized Water Quality Criteria. Department of Water Affairs and Forestry, Pretoria.

Kilham, P. 1984. Sulphate in African inland waters: sulphate to chloride ratios. Verh. Internat. Verein. Limnol, Vol. 22, July: pp. 296 - 302.

Kilham, P. and Cloke, P.L. 1990. The evolution of saline lake waters: gradual and rapid biogeochemical pathways in the Basotu Lake District, Tanzania. Hydrobiologia, No. 197: pp. 35 - 50.

Knesl, O. 1994. Management Recommendations for Barber's Pan Nature Reserve: Monitoring Report - 1994. Report WS 8/8/1/76, July 1994; Tvl. Chief Directorate for Nature and Environmental Conservation (Unpublished).

Kohnke, H. 1968. Soil Physics. McGraw-Hill Book Company, New York.

Last, W.M. and Schweyen, T.H. (1983). Sedimentology and geochemistry of saline lakes of the great plains. pp. 245 - 263. In: Saline Lakes - Proceedings of the 2nd International Symposium on Athalassic (Inland) Saline Lakes, Held in Saskatchewan, Canada, June 1982. Junk Publishers, The Hague.

Langbein, W.B. 1961. Salinity and hydrology of closed lakes. U.S. Geol. Survey. Prof. Paper. No. 412: pp. 1 - 20.

Lijklema, L. 1994. Nutrient dynamics in shallow lakes: effects of changes in loading and role of sediment-water interactions. Hydrobiologia, No. 275/6: pp. 335 - 348.

Lindsay, W.L. 1979. Chemical Equilibria in Soils. Wiley-Interscience, New York.

Lindsay, W.L., Vlek, P.L.G. and Chien, S.H. 1989. Phosphate minerals. In: Dixon, J.B. and Weed, S.B. (Eds.) Minerals in Soil Environments. Am. Soil Sci. Soc. Madison, Wisconsin.

Lowenstein, T.K. and Hardie, L.A., 1985. Criteria for the recognition of salt-pan evaporites. Sedimentology, No. 32: pp. 627 - 644.

Lumsdon, D.G. and Evans, L.J. 1995. Predicting chemical speciation and computer simulation. In: Ure, A.M. and Davidson, C.M. (Eds) Chemical Speciation in the Environment. Blackie Academic and Professional, London.

Mabbutt, J.A. 1977. Desert Landforms. MIT Press, Cambridge. Cited in: Shaw, P.A. and Thomas, D.S.G. 1989. Playas, pans and salt lakes. pp. 184 -205. In: D.S.G. Thomas (Ed.) Arid Zone Geomorphology, Belhaven Press, London.

Mackay, H. 1993. Pollution in the St. Lucia lake and estuary system: past, present and future. In: Taylor, R.H. (Ed.) 1993. Proceedings of the Workshop on Water Requirements for Lake St. Lucia. Department of Environment Affairs, Pretoria.

Marchant, R. and Williams, W.D. 1977. Organic content of some saline lake sediments in western Victoria. Aust. J. Freshwater Res. No. 28: pp. 269 - 275.

Marshall, T.R. and Harmse, J.T. 1992. A review of the origin and propagation of pans. S.A. Geographer, Vol. 19, Nos. 1 and 2: pp. 9-21.

Mason, B. and Moore, C.B. 1982. Principles of Geochemistry. (4th Ed). John Wiley and Sons, New York.

Mertz, W. 1981. The essential trace elements. Science, Vol. 213: pp. 1332-1338.

Milstein, P. le S. 1975. The biology of Barberspan, with special reference to the avifauna. Ostrich, Supplement No. 10: pp. 1-25.

Müller, G. and Gastner, M. 1971. The "Karbonat-Bombe", a simple device for the determination of the carbonate content in sediments, soils and other minerals. N.Jb.Mineral, No. 10: pp. 466-469.

Murphy, J. and Riley, J.P. 1962. A modified single solution method for the determination of phosphate in natural waters. Anal. Chim. Acta, Vol. 27: pg 31.

Nadson, G.A. 1928. Archiv. Hydrobiol, No. 19: pp. 154-164. Cited in: Vasconcelos, C., McKenzie, J.A., Bernasconi, S., Djordje, G. and Albert, A.J. 1995. Microbial mediation as a possible mechanism for natural dolomite formation at low temperatures. Nature, 21 September, Vol. 377: pp. 220-222.

Neev, D. and Emery, K.D. 1967. The Dead Sea. Depositional processes and environments of evaporites. Israel Geol. Surv. Bulletin. No. 41. Cited in: Hammer, U.T. 1986. Saline Lake Ecosystems of the World. Junk Publishers, Dordrecht.

Nelson, D.W. and Sommers, L.E. 1982. Total organic carbon, organic carbon, and organic matter In: Page, A.L. (Ed.) Methods of Soil Analysis. Part 2. Am.Soc.Agron. Madison, Wisconsin.

Nordstrom, D.K. and Munoz, J.L. 1994. Geochemical Thermodynamics. 2nd ed. Blackwell Scientific Publications, Oxford.

Norrish, K. and Hutton, J.T. 1969. An accurate X-ray spectrographic method for the analysis of a wide range of geological materials. Geochim. Cosmochim. Acta, Vol.33: pp. 431-453.

Olsen, S.R. and Sommers, L.E. 1982. Phosphorus. In: Page, A.L. (Ed.) Methods of Soil Analysis. Part 2. Am.Soc.Agron. Madison, Wisconsin.

Patrick, R. 1978. Effects of trace metals in aquatic ecosystems. American Scientist, Vol 66: pp. 185 - 192.

Pettersson, K. 1984. The fractional Composition of phosphorus in lake sediments of different characteristics. pp. 149 - 156. In: Sly, P. (Ed.) Sediment and Water Interactions. Springer-Verlag, New York.

Potts, P.J. 1987. A Handbook of Silicate Rock Analysis. Ch. 5. pp: 153 - 197. Blackie, London.

Plummer, L. N. 1992. Geochemical modelling of water-rock interaction: past, present and future. In: Kharaka, Y.K. and Maest, A.S. Water-Rock Interaction: Low Temperature Environments. Proceedings of the 7th International Symposium on Water-Rock Interaction (Vol. 1). A.A. Balkema, Rotterdam.

Prescott, G.W. 1969. The Algae: A Review. Nelson, New York.

Rai, D. and Kittrick, 1989. J.A. Mineral equilibria and the soil system. In: Dixon, J.B. and Weed, S.B. (Eds.) Minerals in Soil Environments. (2nd Ed.) Soil Science Society of America, Wisconsin.

Rogers, K.H., Ellery, W.N., Winternitz, N.L. and Dohmeier, R. 1989. Physical, chemical and biotic responses to decreasing water depth in a highveld pan following wet and dry summers. sthn. Afr. J. aquat. Sci., Vol. 15 No. 1: pp. 67 - 90.

Rosen, M.R., Turner, J.V. and Coshell, L. 1992. Water-rock interaction in the formation of diagenetic dolomite in a non-marine, coastal evaporitic basin, Lake Hayward, Western Australia. In: Kharaka, Y.K. and Maest, A.S. Water-Rock Interaction: Low Temperature

Environments. Proceedings of the 7th International Symposium on Water-Rock Interaction (Vol. 1). A.A. Balkema, Rotterdam.

Renaut, R.W. 1990. Recent carbonate sedimentation and brine evolution in the saline lake basins of the Cariboo Plateau, British Columbia, Canada. Hydrobiologia, No. 197: pp. 67 - 81.

Schwertmann, U. and Taylor, R.M. 1989. Iron Oxides. In: Dixon, J.B. and Weed, S.B. (Eds.) Minerals in Soil Environments. (2nd Ed.) Soil Science Society of America, Wisconsin.

Seaman, M.T., Ashton, P.J. and Williams, W.D. 1991. Inland salt waters of southern Africa. Hydrobiologia, No. 210: pp. 75 - 91.

Silberbauer, M.J. and King, J.M. 1991. The water chemistry of selected wetlands in the southwestern Cape Province, South Africa. sthn. Afr. J. aquat. Sci., No. 17: pp. 82 - 88.

Shaw, P.A. 1988. Lakes and Pans. In: Moon, B.P. and Dardis, G.F. (Eds.) The Geomorphology of Southern Africa. Southern Book Publishers, Johannesburg, South Africa.

Shaw, P.A. and Thomas, D.S.G. 1989. Playas, pans and salt lakes. pp. 184 - 205. In: D.S.G. Thomas (Ed.) Arid Zone Geomorphology. Belhaven Press, London.

Singer, A. 1989. Palygorskite and sepiolite group minerals. In: Dixon, J.B. and Weed, S.B. (Eds.) Minerals in Soil Environments. (2nd Ed.) Soil Science Society of America, Wisconsin.

Sposito, G. 1989. The Chemistry of Soils. Oxford University Press, Oxford.

Stumm, W. and Morgan, J.J. 1980. Aquatic Chemistry. An Introduction Emphasizing Chemical Equilibria in Natural Waters. J. Wiley and Sons, New York.

Talling, J.F. and Talling, I.B. 1965. The chemical composition of African lake waters. Int.Revue ges.Hydrobiol., Vol. 50. No. 3: pp. 412 - 463.

Taylor, R.H. 1993. Biological responses to changing salinity. In: Taylor, R.H. (Ed.) 1993. Proceedings of the Workshop on Water Requirements for Lake St. Lucia. Department of Environment Affairs, Pretoria.

Timms, B.V. and Brand, G.W. 1973. A limnological survey of the basin lakes, Nalangil, Western Victoria, Australia. Aust. Soc. Limnol. Bull. No. 5: pp. 32-40. Cited in: Hammer, T.U. 1986. Saline Lake Ecosystems of the World. Junk Publishers, Dordrecht.

Thomas, G.P. and Goldstone, L.C. 1994. Advances in Environmental Inorganic Analysis. International Laboratory. Vol. 13, September: pp. 13 - 14.

Thomas, D.S.G., Nash, D.J., Shaw, P.A. and Van der Post, C. 1986. Present day lunette cycling at Witpan in the arid southwestern Kalahari desert. Catena, Vol. 20: pp. 515 - 527.

Torgersen, T., De Deckker, P., Chivas, A.R. and Bowler, J.M. 1986. Salt lakes: a discussion of processes influencing palaeoenvironmental interpretation and recommendations for future study. Palaeogeography, Palaeoclimatology, Palaeoecology, No. 54: pp. 7 - 19.

Twinch, A.J. and Ashton, P.J. 1983. Nutrient cycling in wetlands. J. Limnol.Soc.sth.Africa, Vol. 9. No. 2: pp. 104 - 109.

Twinch, A.J. and Breen, C.M. 1980. Advances in Understanding Phosphorus Cycling in Inland Waters - Their Significance to South African Limnology. South African National Scientific Programmes Report No. 42, Pretoria.

Twinch, A.J. and Peters, R. H. 1984. Phosphate exchange between littoral sediments and overlying water in an oligotrophic north-temperate lake. Can.J.Aquat.Sci., Vol.41: pp. 1609 - 1617.

Ure, A.M. and Davidson, C.M. 1994. Introduction to speciation. In: Ure, A.M. and Davidson, C.M. (Eds.) Chemical Speciation in the Environment. Blackie Academic and Professional, London.

Van Veen, J. 1936. Onderzoekingen in de Hoofden. Algemeene Landsdukkerij, 'S-Gravenhage.

Van Vliet, H.R.P., Kempster, P.L., Sartory, D.P., Gerber, F.A. and Schoonraad, I.J. 1988. Analytical methods manual. Hydrological Research Institute Report No. TR136. South African Department of Water Affairs, Pretoria.

Van der Merwe, A.J., Johnson, J.C. and Ras, L.S.K. 1984. An  $\text{NH}_4\text{HCO}_3\text{-NH}_4\text{F-(NH}_4\text{)}_2\text{-EDTA}$  method for the determination of extractable P, K, Ca, Mg, Cu, Fe, Mn, and Zn in soils. SIRI Inf. Bull. B2/2.

Vasconcelos, C., McKenzie, J.A., Bernasconi, S., Djordje, G. and Albert, A.J. 1995. Microbial mediation as a possible mechanism for natural dolomite formation at low temperatures. Nature, 21 September, Vol. 377: pp. 220-222.

Verhagen, B. Th. 1991. On the nature and genesis of pans - a review and ecological model. Paleoecology of Africa, No. 21: pp. 179 - 194. Cited in: Marshall, T.R. and Harmse, J.T. 1992. A review of the origin and propagation of pans. S.A. Geographer, Vol. 19. Nos. 1 and 2: pp. 9 -21.

Verster, E., van Deventer, P.W. and Ellis, F. 1992. Soils and associated materials of some pan floors and margins in southern Africa: a review. S.A. Geographer, Vol. 19, Nos. 1 and 2: pp. 35 -47.

Viner, A.B. 1975. Non-biological factors affecting phosphate recycling in the waters of a tropical eutrophic lake. Verh.Internat.Verein.Limnol., No. 19: pp. 1404 - 1415.

Von Backström, J.W. 1963. The geology of Barberspan and environs. Fauna and Flora, No. 14: pp. 24-31.

Walkley, A. 1935. An examination of methods for determining organic carbon and nitrogen in soils. J.Agr.Sci., No. 25: pp. 598-609.

Ward, R.C. 1975. Principles of Hydrology. MacGraw–Hill, London.

- Weaver, C.E. 1989. Clays, Muds, and Shales. Developments in Sedimentology No. 44. Elsevier, Amsterdam.
- Weaver, R.M., Syers, J.K. and Jackson, M.L. 1968. Determination of silica in citrate-bicarbonate-dithionite extracts of soils. Soil Sci. Soc. Am. Proc. Vol. 32: pp. 497 - 501.
- Weast, R.C. (Ed.) 1975. Handbook of Chemistry and Physics. (56th Ed.) CRC Press, Ohio.
- Wehmiller, J. 1972. Strontium: element and geochemistry. Fairbridge, R.W. (Ed.) The Encyclopedia of Geochemistry and Environmental Sciences. Van Nostrand Reinhold Company, New York.
- Wetzel, R.G. 1983. Limnology. (2nd Ed.). Saunders College Publishing, Fort Worth.
- Whitten, D.G.A. and Brooks, J.R.V. 1971. Dictionary of Geology. Penguin, London.
- Wild, A. and Jones, L.H.P. 1988. Mineral nutrition of crop plants. In: Wild, A. (Ed.) Russell's Soil Conditions and Plant Growth. 11th Ed. Longman Scientific and Technical, New York.
- Williams, W.D. 1964. A contribution to lake typology in Victoria, Australia. Verh. int. Ver. Limnol., No. 15: pp. 158 - 163. Cited in: Hammer, U.T. 1986. Saline Lake Ecosystems of the World. Junk Publishers, Dordrecht.
- Willis, J.P. 1985. The bathymetry, environmental parameters and sediments of the Bot river estuary, S.W. Cape Province. Trans. Roy. Soc. S. Afr., Parts 3 and 4.
- Willis, J.P. 1995. Instrumental Parameters and Data Quality for Routine Major and Trace Element Determinations by WDXRFS. Information Circular No. 14, Department of Geological Sciences, University of Cape Town (Unpublished).
- World Health Organisation (WHO) 1984. Guidelines for Drinking-Water Quality: Vol 1. - Recommendations. WHO, Geneva.

Wood, W.W. and Osterkamp, W.R. 1987. Playa-lake basins on the Southern High Plains of Texas and New Mexico: part II. A hydrologic model and mass-balance arguments for their development. Geol. Soc. America Bulletin., Vol. 99: pp. 224 - 230.

Yuretich, R.F. and Cerling, T.E. 1983. Hydrogeochemistry of Lake Turkana, Kenya: Mass balance and mineral reactions in an alkaline lake. Geochim. Cosmochim. Acta, Vol.47: pp. 1099 - 1109.

## 7. APPENDICES

### 7.1 APPENDIX 1: On-site water analyses

**TABLE 1:** Analysis of Barber's Pan bulk pan water (Sampling locations are recorded on Figure 14).

Location (on Figure 14)	Water depth (m)	Probe depth (m)	pH	Temperature (°C)	EC (mS/cm)	Salinity (‰)
1	4.3	1	9.5	11.3	1.83	1.3
		2	9.5	11.2	1.84	1.3
		3	9.6	11.2	1.84	1.3
		4.05	9.6	11.2	1.85	1.3
2	3.2	1	9.7	11.1	1.97	1.4
		2	9.7	10.9	1.97	1.4
3	0.3	0.2	9.6	9.3	1.67	1.2
4	3.1	0.25	9.6	13.7	2.1	1.4
		1	9.6	13.0	2.1	1.4
		2	9.5	12.7	2.1	1.4
5	3.8	0.25	9.6	14.8	2.1	1.3
		1	9.6	11.4	2.0	1.4
		2	9.6	11.2	2.0	1.4
		3	9.6	11	2.0	1.4
6	4	0.25	9.7	12.6	2.04	1.4
		1	9.7	11.7	2.0	1.4
		2	9.6	11.5	2.0	1.4
		3	9.6	11.4	2.0	1.4
7	4.2	0.25	9.8	13.8	2.1	1.4
		1	9.7	11.4	2.0	1.4
		2	9.7	11.2	2.0	1.4
		3	9.7	11.2	2.0	1.4
8	2.9	0.3	9.0	12.5	1.8	1.2
		1	9.0	12.2	2.0	1.4
		2	9.0	10.8	2.0	1.4
9	4.1	0.25	9.4	13.1	1.9	1.3
		1	9.4	12.1	2.0	1.4
		2	9.4	11.4	2.0	1.4
		3	9.4	11.0	2.0	1.4

## 7.2 APPENDIX 2: Calculation of concentration factor for Barber's Pan

Calculation of Concentration factor for Barber's Pan using concentrations from the DWA database:

		Date Recorded
Initial Cl <sup>-</sup> concentration:	199 mg.dm <sup>-3</sup>	18th December 1982
Final Cl <sup>-</sup> concentration:	2601 mg.dm <sup>-3</sup>	8th February 1988
Concentration factor:	13	
Initial Na <sup>+</sup> concentration:	187 mg.dm <sup>-3</sup>	18th December 1982
Final Na <sup>+</sup> concentration:	2380 mg.dm <sup>-3</sup>	8th February 1988
Concentration factor:	12.7	
Expected Concentration:	2444.09 mg.dm <sup>-3</sup>	
Expected Concentration Factor:	13	
Actual Concentration Factor:	12.7	
Initial SO <sub>4</sub> <sup>2-</sup> concentration:	28 mg.dm <sup>-3</sup>	18th December 1982
Final SO <sub>4</sub> <sup>2-</sup> concentration:	145 mg.dm <sup>-3</sup>	8th February 1988
Expected Concentration:	365.96 mg.dm <sup>-3</sup>	
Expected Concentration Factor:	13	
Actual Concentration Factor:	5	

The expected concentration of SO<sub>4</sub><sup>2-</sup> is far lower than would be the case if it were behaving as a conservative ion like Na<sup>+</sup>, suggesting that S is being removed from the pan water in some form.

7.3 APPENDIX 3: Department of Water Affairs and Forestry database (NO<sub>3</sub><sup>-</sup> + NO<sub>2</sub><sup>-</sup> as N and PO<sub>4</sub><sup>3-</sup> as P. All values in Mg/L unless stated otherwise).

APPENDIX 3: Department of Water Affairs and Forestry water quality monitoring data for Barber's Pan

DATE	TIME	LEVEL	EC	TDS	pH	Na	Mg	Ca	F	Cl	N	SO <sub>4</sub>	PO <sub>4</sub>	CACO <sub>3</sub>	Si	K	NH <sub>4</sub>
		M	mS/M	MG/L													
720314	1145	9.693	101.1		8	179.6	24.3	19.3	0.45	154	0	16.8		250.4	0.69	23.73	0.03
820724	1800	10.26	124	860	8.33	173.6	37.2	20.2	0.78	186.8	0.14	30.8	0.015	316.6	0.91	24.8	0
820828	900	10.21	122	864	8.38	175.5	38.9	20.9	0.74	188	0.07	32.2	0.003	313.5	1.15	24.83	0.25
820925	1700	10.09	125.5	898	7.9	181.8	42	19.2	0.6	187.9	0.15	31	0.008	336.1	1.54	23.53	0.07
821018	1200	10	123.3	875	9	182.2	38.8	19.5	0.63	186.8	0.02	32.5	0.074	320	1.92	19.23	0.05
821129	1215	9.89	100	706	7.8	136.6	35	21.6	0.41	143.6	0.27	22.2	0.028	267.7	0.79	25.99	0.03
821218	1805	10	129	869	8.4	187.2	34.3	14.4	0.54	198.9	0.16	28.1	0.01	310.4	0.46	23.19	0.02
830122	1800	9.9	128.4	908	1.14	191.4	43.1	22.1	0.58	197.5	0.06	35.4	0.001	323.8	0.67	25.23	0.05
830430	1730	0	143	948	9.2	196.7	45.1	15.5	0.72	213.8	0.02	30.9	0.003	344.4	0.91	27.62	0.01
830501	1730	0	154	1022	8.4	207.4	48.1	19.9	0.77	231	0	33.8	0	371.8	1.18	26.73	0.04
830829	1030	0	152	1148	8.5	256.1	46.4	18	0.66	233	0.35	90.8	0.009	389.3	0	36.54	0.07
831026	1545	0	168	1181	8.5	255.4	53.6	19.3	0.73	258	0.52	45.4	0.065	417.5	1.1	36.64	0.03
840528	800	7.61	191.2	1337	8.22	292.1	61.4	14.3	0.84	314.1	0.33	25.9	0.019	483.7	1.25	45.57	0.02
840701	800	7.545	209.8	1279	9.01	319.7	50.6	14.7	1.18	333.6	0.33	48.7	0.029	380.3	1.34	45.94	0.03
841029	800	7.16	213.7	1576	8.59	358.9	73.5	14.2	1.06	372.7	0.03	57.5	0.013	534.9	0.34	38.7	0.04
841129	730	6.98	190.1	1388	8.85	301.2	66.4	7.2	1.12	381.8	0.02	84.6	0.02	416	2.34	51.11	0.05
841230	830	6.78	247.6	1711	9.13	408	71.4	5.6	1.14	429.9	0.02	56.3	0.006	563.7	1.21	0	0.07
850201	700	6.64	215	1744	8.4	424.8	82.3	12	1.04	443.1	0.02	67.3	0.018	584.7	1.56	54.72	0.02
850305	800	6.45	253	1684	9.09	365.1	70.5	12.9	1.13	445.5	0.02	93	0	525.4	0.59	225.92	0.07
850414	815	6.27	342.8	2396	8.92	475	82	15.5	1.22	526.1	0.26	454.3	0.027	504.3	1.51	86.99	0.08
850624	1000	6.05	298.3	2179	9.01	490.3	83.8	46.5	0.01	498	0.38	335.5	0.009	521.4	1.43	60.42	0.12
850728	830	5.985	291.2	1911	8.4	492.8	74.3	8.3	1.22	564.1	0.02	68.3	0	526.3	1.45	61.67	0.06
850825	900	5.9	325.8	2155	7.5	510.2	90.1	19.7	1.17	521.5	1.17	78.8	0.08	710.7	0.93	68.56	0.03
850930	800	6.73	320	2319	8.2	556.3	93.6	14.4	1.35	570.8	0.31	104.3	0.021	744.7	2.75	70.14	0.08
851103	830	5.59	350.1	2380	8.66	590.3	86.6	14.3	1.33	572	1.44	96.9	0.119	772	0.87	80.24	0.04
851130	800	5.4	358.4	2459	7.9	612.9	83.9	36.5	1.35	623	0	167.2	0.022	700	0.98	79.01	0.04
851229	830	5.3	330.2	2886	9.09	662.2	108.5	14.7	1.5	680.7	0.28	94.3	0.021	1020	1.87	80.73	0.13
860126	815	5.17	384	2829	4.46	663.9	112.1	7.6	1.44	710	2.09	97.4	0.199	940	1.18	101.55	0.09
860331	1600	4.97	412.8	3200	8.87	758.7	119	9.8	1.54	800.2	0.05	104.6	0.035	1070	2.07	90.41	0.04
860430	1430	4.85	428.8	3297	9.09	779	114.3	14.6	1.46	856.9	0.62	120.3	0.029	1080	1.9	95.86	0.14
860629	800	4.69	457.6	3014	9.4	811.8	12	15.6	1.48	449.1	0.34	163.5	0.04	1200	1.81	102.73	0.06
860727	800	4.62	470.4	3678	9.2	893.7	115.5	16.4	1.21	913.5	0.01	146.9	0.018	1220	3.03	111.36	0.08
860831	800	4.525	492.8	3800	8.9	920.8	140.8	8.8	1.56	982.8	1.55	114.9	0.065	1240	1.8	109.8	0.21
860928	815	4.41	518.4	3934	9.39	938.1	137.9	9.3	1.77	996.5	0.04	118	0.09	1330	2.52	119.98	0.04
861026	1600	4.33	537.6	4213	9	1032.1	146.3	17.6	1.6	1054.6	0	109.4	0.028	1420	2.84	93.51	0.21
861130	800	4.74	430.1	3280	9.71	801.6	105.6	8.3	2.39	827.4	0	124.3	0.086	1080	2.37	95.54	0.06
870104	720	4.73	441.6	3540	9.34	816.7	113.1	45.1	1.32	845	0.03	98.4	0.02	1250	3.12	101.89	0.27
870201	530	4.53	480	3601	9.5	880.7	118.9	14.4	1.18	925.2	0.02	94.4	0.204	1200	2.15	110.36	0.07
870329	700	4.47	509.4	4043	9.3	969.6	118.1	20.9	1.29	999.9	0.02	139.8	0.078	1380	1.97	123.75	0.08
870427	830	4.27	584.3	4356	9.55	1055.7	135.5	9.5	1.21	1103.8	0.05	121.4	0.035	1480	3.34	129.72	0.11
870701	1000	4.1	611.2	4660	9.4	1192.5	128.4	12	1.29	1235.7	0.22	142.9	0.037	1490	3.59	169.54	0.15
870803	800	4.025	640	4978	9.34	1274.7	149.1	14.9	1.36	1337.5	0.04	140.7	0.076	1550	3.25	147.01	0.16
870901	800	3.93	640	5297	9.2	1364.6	161.7	17.4	1.42	1407.3	0.01	124.2	0.151	1700	2.7	140.13	0.17
871004	800	3.95	620	5128	9.3	1301.4	157.1	15.2	1.36	1385.1	0.03	148.3	0.104	1623			

APPENDIX 3 cont.: Department of Water Affairs and Forestry water quality monitoring data for Barber's Pan

DATE	TIME	LEVEL M	EC mS/M	TDS	pH	Na	Mg	Ca	F	Cl	N	SO4	PO4	CACO3	Si	K	NH4
871102	830	4.84	664	5422	9.55	1436.4	149.5	18.4	1.36	1485.6	0.01	157.5	0.169	1650	2.46	160.89	0.29
871130	700	3.68	788.3	5956	8.84	1581.7	155.4	16.2	1.22	1668.3	0.03	187.1	0.326	1790	0.94	161.68	0.62
871207	700	3.66	854.9	6452	9.36	1730	167	11.1	1.43	1850.4	0.17	231.8	0.261	1867	1.54	181.04	0.66
871228	730	3.62	911.4	6759	9.16	1808.7	124	30.5	0.75	1968.5	0.03	260.9	0.193	1950	1.33	186.85	0.52
880104	732	3.56	876.9	7851	9.75	2024.4	141	10.4	1.01	2184.6	0.03	295.4	0.017	2260	1.33	437.03	1.01
880111	730	3.52	873.9	6555	9.26	1831.5	138.7	3.3	0.77	1853.2	0.04	206.3	0.127	1910	1.22	191.45	0.04
880118	730	3.53	920	7469	9.62	2063.3	155.1	13.1	0.93	2148.1	0.04	173.4	0.29	2215	1.21	212.07	0.63
880125	730	3.53	950	7640	9.62	2111	152	13.1	0.73	2285.7	0.04	106.6	0.17	2256	1.32	218.55	0.49
880201	730	3.45	1037.6	7910	9.32	2243.5	126.4	7.3	0.67	2441.8	0.04	195.6	0.147	2185	1.76	229.86	0.05
880208	730	3.38	1080	8757	9.5	2379.6	177.9	15	0.75	2601	0.02	144.6	0.32	2630	1.62	228.99	1.1
880215	730	3.4	950	7606	9.68	2109.9	152.2	15	0.71	2219.9	0.04	97.9	0.21	2300	1.57	203.69	1.3
880222	745	4.02	720	5907	9.15	1556.2	141.3	11.3	0.88	1671.8	0.02	134	0.12	1830	2.22	159.76	0.16
880229	715	4.42	464	3417	9.09	890.3	80.3	11.3	0.62	950.6	0.02	47.4	0.1	1100	3.17	95.02	0.08
880307	732	4.715	437.1	3181	9.2	836	75	11.3	0.6	877.8	0.02	72.5	0.09	1000	3.35	88.42	0.1
880321	700	7.33	164	1042	8.84	275.7	26.8	8	0.36	294.3	0.1	31.5	0.09	305.1	4.29	32.43	0.08
880328	715	7.51	151	981	9.07	247.4	25.2	7.6	0.28	274.3	0.02	30.8	0.087	300.7	4.13	27.83	0.09
880404	815	7.8	153	1013	8.5	261.7	17.6	20.9	0.3	280.1	0.04	28.2	0.063	307.5	4.91	29.02	0.12
880404	818	7.5	154	1008	8.9	266.5	29.1	9.7	0.21	271.2	0.02	27.3	0.059	310.2	4.86	25.11	0.02
880411	730	7.49	152	994	8.8	258.4	29.1	9.5	0.3	265	0.02	30.1	0.083	303.9	4.45	30.77	0.28
880418	1130	7.49	154	980	8.7	243.8	29.1	9.2	0.42	273.1	0.08	29.4	0.097	304.8	4.58	22.24	0.32
880425	715	7.56	154	992	8.5	249.8	30.7	9.9	0.31	271.8	0.09	30.1	0.065	307.6	4.75	23.38	0.34
880502	730	7.53	156	1022	8.37	259.9	28.7	10.2	0.3	268.5	0.13	26.6	0.042	324.4	4.52	31.15	0.26
880509	730	7.51	156	1029	8.39	257.8	28.8	9.7	0.42	271.1	0.15	28	0.065	329.2	4.86	30.45	0.28
880516	734	7.48	156	1023	8.42	253.8	29.6	9.7	0.36	269.5	0.21	27.9	0.091	327.9	4.95	30.96	0.35
880523	725	7.46	156	1038	8.51	257.6	30.2	9.9	0.36	275.4	0.17	27.8	0.039	331.1	4.7	31.74	0.12
880530	1630	7.44	160.5	1060	8.37	271.5	30.2	10.5	0.44	280.1	0.13	22.2	0.042	338	4.88	32.33	0.13
880606	716	7.42	161.3	1080	8.86	275.4	31	10.4	0.46	286.2	0.19	23.9	0.078	342.2	5.19	33.94	0.12
880613	725	7.44	159.8	1069	8.49	271.5	30.8	10.1	0.59	283	0.17	25.5	0.068	339	4.95	33.39	0.11
880620	738	7.37	163.6	1080	8.72	269.5	31.3	10.3	0.49	292.3	0.2	24.8	0.067	342.7	4.95	32.56	0.05
880627	725	7.36	156.3	1115	8.14	275.1	29.7	11.1	0.48	312.4	0.21	27.6	0.083	349	4.63	32.11	0.14
880704	817	7.34	156.6	1135	7.91	281.3	29.7	10.1	0.64	322.1	0.26	28.3	0.099	350.7	5.02	33.8	0.19
880708	825	7.255	169	1132	8	285.6	33.8	9.4	0.6	304.2	0.25	27.4	0.085	357	4.91	34.45	0.22
880711	825	7.32	164	1105	8.09	283.5	31.2	10.5	0.34	299.7	0.25	28.3	0.069	340.5	4.79	34.58	0.08
880718	830	7.34	159.3	1146	8.05	283.2	31.4	10.5	0.47	322.3	0.3	27.9	0.11	357.1	5.02	33.43	0.12
880725	855	7.29	168	1124	7.9	284	33.2	10.3	0.4	295.2	0.32	28.4	0.075	358.1	4.91	34.19	0.07
880801	825	7.275	168	1140	7.9	285.8	34	9.7	0.41	307.5	0.26	29.8	0.057	358.1	4.76	34.45	0.14
880815	715	7.235	171	1142	8	287.4	34.5	9.8	0.51	303.8	0.24	28.4	0.092	361.7	5.21	34.99	0.21
880822	845	7.215	172	1158	8	287.4	34.2	11.6	0.34	306.4	0.25	31	0.086	370.3	4.92	33.47	0.19
880829	840	7.19	173	1169	8.2	287.3	34.2	11.3	0.41	310.3	0.22	30.5	0.076	376.1	4.99	34.56	0.13
880905	900	7.17	174	1160	8.34	291.4	34.4	11.3	0.58	299.6	0.09	32.2	0.095	373.7	5.07	34.49	0.14
880912	800	7.14	178	1195	8.5	295.5	35.6	12.3	0.43	308.9	0.04	30.4	0.098	391.6	5.46	34.14	0.1
880919	820	7.135	163.2	1192	8.5	300.9	33.8	12.1	0.42	318.6	0.04	29.6	0.118	377.2	5.41	36.03	0.1
880926	815	7.11	178	1192	8.5	300.5	34.1	11.3	0.54	316.2	0.05	28.8	0.087	380.2	5.73	36.26	0.15
881003	800	7.07	166.4	1213	8.75	304.4	35.7	11.9	0.49	321.6	0.01	29.2	0.098	386.9	5.5	37.05	0.08
881011	800	7.03	168.3	1230	8.7	307.5	36.2	12.4	0.5	327	0.01	30.1	0.109	391.7	5.59	37.83	0.03
881017	730	7.01	187.6	1256	8.99	313.9	36.3	13	0.47	330.1	0.03	28	0.083	407.5	5.36	37.11	0.11

APPENDIX 3 cont.: Department of Water Affairs and Forestry water quality monitoring data for Barber's Pan

DATE	TIME	LEVEL	EC	TDS	pH	Na	Mg	Ca	F	Cl	N	SO4	PO4	CACO3	Si	K	NH4
		M	mS/M							MG/L							
881024	730	7.05	189.3	1260	9.04	314	37.1	13.2	0.49	328.8	0.07	28.5	0.076	410.3	4.71	36.82	0.07
881031	700	7.07	166.4	1260	9.1	321.9	36.5	10.6	0.49	332.6	0.03	30.4	0.076	400.7	4.63	38.99	0.04
881107	730	7.16	173.5	1242	9.13	305.8	37.3	13.4	0.48	323.8	0.03	26.9	0.091	407.8	4.63	36.54	0.07
881114	720	7.14	201.6	1254	8.9	311.4	38.1	13.4	0.52	332.9	0.05	29.4	0.086	400.6	3.81	37.53	1.11
881121	730	7.12	204.2	1256	8.99	309.7	37.2	12.6	0.73	326.8	0.04	29.7	0.091	400.7	3.8	37.75	9.95
881128	730	7.07	206.1	1254	9.1	308.6	38.5	13.2	0.61	334.2	0.04	28.7	0.092	402.6	3.88	37.43	1.45
881205	745	7.06	207.5	1270	9.24	310.2	38.9	13.4	0.57	336.5	0.03	28.7	0.087	412.3	4.11	37.92	0.82
881214	743	7.04	201.4	1259	8.49	313.2	38.9	11.4	0.59	319.6	0.01	28.9	0.074	417.1	3.66	36.98	0.2
881219	730	7.03	202.9	1271	8.66	319.5	39.2	10.8	0.66	324.7	0.03	28.2	0.07	418	4.07	37.36	0.1
890103	800	7.02	166.4	1268	8.67	324.4	38.7	13.1	0.48	323.9	0.05	25.6	0.078	413	3.67	37.83	0.1
890109	730	7.06	166.4	1251	8.5	320.6	35.9	12.3	0.55	326.3	0.03	25.1	0.088	403.1	2.89	37.89	0.1
890116	720	7.5	161.2	1180	8.59	286.6	34.1	11.9	0.49	302	0.03	22.6	0.082	399.1	3.35	35.11	0.11
890123	816	7.54	166	1133	8.4	274	32.8	13.1	0.46	288.6	0.02	21.5	0.093	383.6	4.05	34.27	0.1
890130	845	7.51	168	1139	8.59	280.1	33.2	12.3	0.5	291.6	0.01	21	0.091	381.1	4.2	35.11	0.05
890206	730	7.57	163.2	1164	8.31	279.3	35.3	13.3	0.41	322.4	0.03	22.3	0.099	375	4.66	33.62	0.15
890213	730	7.97	159.1	1120	8.25	266.4	34.3	13.3	0.44	300	0.03	21.6	0.065	367.8	4.66	34.53	0.16
890220	730	8.515	141.1	956	8.23	227.4	31.6	13.3	0.38	240.9	0.01	18.4	0.07	322.8	3.86	29.81	0.07
890226	730	9.23	134.1	896	7.92	211.1	29.1	14.4	0.34	220.5	0.01	16.7	0.056	307.2	5.3	28.64	0.08
890306	725	9.67	97.1	773	8.38	170.5	24.2	14.9	0.33	186.4	0.02	24.4	0.05	269.4	6.29	23.88	0.05
890313	713	9.67	99.7	795	8.27	173.9	25.1	16.1	0.34	191.2	0.01	25	0.04	277.3	6.73	24.7	0.06
890320	720	9.665	96.5	739	8.34	166.3	23.7	14.9	0.35	174.7	0.02	12.8	0.04	264.5	6.38	23.48	0.08
890328	720	9.66	96.2	779	8.46	169.8	25.1	16.2	0.34	188.1	0.01	22.5	0.05	272.3	6.37	24.47	0.05
890403	720	9.66	97.5	734	7.48	163.6	24.6	16.3	0.34	167.7	0.01	9.8	0.055	269.4	6.07	23.37	0.06
890408	730	9.875	102.3	747	8.89	161.8	25	16.5	0.43	170.3	0.04	10.6	0.04	278	3.32	22.9	0.06
890410	720	9.635	101.4	771	7.38	172	25.7	17.6	0.37	173	0.02	7.9	0.036	286.9	4.65	24.21	0.03
890417	800	9.615	105.1	802	8.52	176	26.7	18.4	0.36	183.9	0.01	8.8	0.027	297.3	2.67	24.82	0.04
890424	730	9.595	98.7	752	8.53	164.2	25.1	16.6	0.35	175.2	0.02	8.3	0.046	277.2	4.31	24.04	0.05
890501	730	9.62	101.3	744	8.93	162.3	24.7	16.7	0.39	171.9	0.02	9.5	0.044	274.3	4.3	23.42	0.07
890515	800	10.24	110.5	823	8.66	179.4	27.4	20.6	0.38	184.7	0.03	9.4	0.041	309	4.46	24.5	0.07
890522	730	10.256	98.6	747	8.87	160.6	25.3	18.4	0.38	167.9	0.03	10.2	0.032	279	3.07	23.47	0.04
890529	720	10.25	98.7	736	8.66	159.3	25.4	20.2	0.34	172.9	0.04	9	0.031	266.3	3.2	23.3	0.07
890605	900	10.225	98.3	696	8.84	149.2	24.1	18	0.41	164	0	12.9	0.039	249.9	3.19	22	0.08
890612	835	10.215	98.4	702	8.82	150.8	24.8	19.2	0.37	165.4	0.01	12.2	0.031	251.6	2.7	22.73	0.05
890619	930	10.19	98.7	732	9.02	159.3	26.3	19.8	0.36	170.6	0	12.2	0.026	262.4	2.2	23.3	0.06
890626	940	10.18	93.2	742	8.99	156.5	25.7	18.3	0.39	164.1	0.05	17.4	0.021	276.3	2.58	22.69	0.05
890703	930	10.16	90.4	714	8.84	149.8	25	17.6	0.39	157.6	0.04	17.1	0.036	265.9	2.17	22.3	0.05
890710	910	10.145	92.1	735	8.84	154.7	25.9	18.9	0.39	160.8	0.03	16.8	0.031	274.5	1.84	22.83	0.04
890717	840	10.13	91.3	747	8.88	155.8	26.4	18.9	0.39	163.2	0.02	17.2	0.039	280.3	1.76	22.99	0.04
890724	840	10.1	106.4	724	8.68	152.4	24.3	17.9	0.37	154.7	0.05	10.7	0.03	279.1	1.47	22.43	0.07
890807	905	10.06	104.8	737	8.82	156.1	25.5	17.3	0.36	161.1	0.04	11.4	0.034	279.9	1.83	23.42	0.1
890814	835	10.04	105.7	741	8.75	156.1	25.7	18.7	0.38	161.8	0.07	9.2	0.036	283.4	2	23.31	0.08
890821	935	10.02	95.6	736	8.66	155.2	26.4	19.7	0.36	154.2	0.12	6.2	0.028	287.3	1.45	22.57	0.12
890829	920	10.01	94.1	730	8.59	154.1	25.7	19.3	0.36	153.6	0.04	7.4	0.027	283.8	1.3	22.74	0.08
890831	1440	10.08	103.9	721	8.64	152.4	24.7	18.5	0.37	160.3	0.05	10.6	0.031	271.4	2.18	22.81	0.13
890904	850	9.965	94.9	733	8.74	154.1	26	18.6	0.39	158.4	0.03	8.7	0.03	282	1.37	22.62	0.06
890911	810	9.93	95.1	739	8.75	156.2	26.6	18.8	0.38	156.3	0.04	8.4	0.03	286.3	0.99	22.95	0.07

APPENDIX 3 cont.: Department of Water, Affairs and Forestry water quality monitoring data for Barber's Pan

DATE	TIME	LEVEL		pH	Na	Mg	Ca	F	MG/L							NH4
		M	M/S/M						TDS	EC	Cl	N	SO4	PO4	CACO3	
890918	900	9.89	96.2	8.54	159.7	27.1	20.6	0.35	161.8	0.06	20	0.036	283.8	2.46	23.87	0.11
890925	836	9.85	96.8	8.79	164.4	27.7	20.4	0.38	167.7	0.04	20.8	0.032	287.3	1.38	24.36	0.04
891009	710	9.77	99.6	8.7	162.3	27.8	20.2	0.37	165.1	0.04	19.2	0.028	289.1	2.36	24.36	0.04
891016	700	9.74	93.7	8.67	163.8	27.3	20.8	0.37	170	0.007	10.2	0.024	290.5	3.73	23.4	0.033
891020	720	9.81	98.8	8.83	164.4	28	20	0.38	166.4	0.04	19	0.027	288.2	1.52	24.42	0.07
891023	723	9.72	94	8.87	165.9	27.7	20.3	0.38	187.2	0.007	11.9	0.024	292.1	2.24	23.95	0.061
891030	700	9.67	105.3	8.81	171.1	28.4	19.9	0.37	183	0.016	8.4	0.02	297.3	1.89	24.62	0.043
891106	710	7.64	93	9.58	172.5	28.4	12.8	0.42	180.5	0.008	8.2	0.017	278.3	1.32	23.76	0.032
891113	715	9.65	101.9	9.03	168.3	28.7	16.6	0.42	171.3	0.01	11.7	0.016	290.7	0.57	23.96	0.07
891120	730	9.65	103.5	8.74	169.4	28.6	16.6	0.43	178.3	0.01	11.7	0.03	291.7	0.49	25.8	0.12
891127	730	9.57	102	9.55	177.7	29.9	12	0.42	178.2	0.01	9.4	0.01	285.2	0.21	24.87	0.05
891204	920	9.55	104	9.57	177.2	29.7	12.9	0.4	179.8	0.03	10.1	0.014	289	0.35	23.53	0.05
891211	730	9.51	106.3	9.34	177.2	28.4	12	0.38	184.1	0.01	10.2	0.007	290.3	0.74	24.51	0.03
891218	700	9.455	105.5	9.39	176.1	28.7	15.5	0.39	181.7	0	10.1	0.009	294.2	1.25	23.96	0.04
891227	700	9.41	108.2	9.43	182.5	29.4	12	0.43	191.4	0	10.6	0.004	300.1	0.59	25.04	0.04
900102	710	9.38	101.3	9.75	189.4	30.1	11.3	0.49	199	0.009	9	0.021	295.9	1.26	9.92	0.123
900108	711	9.33	97.4	9.16	182.8	29.2	12.6	0.51	193.2	0.003	11.4	0.016	290.8	1.12	12.44	0.05
900122	710	9.29	98.9	9.2	187.2	29.1	11.8	0.51	196.2	0.024	9.4	0.017	295.5	0.67	3.8	0.052
900129	700	9.29	98.2	8.79	183.3	30.4	14.6	0.52	192	0.337	10.2	0.027	302.2	1.27	5.83	0.022
900205	715	9.23	105.3	8.71	186.5	31.2	12.9	0.45	195.7	0.011	9.3	0.02	314.1	0.52	27.7	0.033
900212	715	9.21	105.8	8.12	183.5	30.3	13.3	0.45	192.6	0.076	9.7	0.014	308.7	1.6	27.74	0.026
900219	715	9.21	105.1	9.23	187.7	30.2	10.6	0.46	201.7	0.012	9.9	0.009	300.4	0.52	28.17	0.035
900226	715	9.17	107.6	9.2	188.4	31.8	11.4	0.47	201.6	0.012	9.8	0.01	311.1	0.62	25.71	0.012
900318	1645	9.165	109	9.61	189.2	31.1	13.6	0.52	195.1	0.002	10.2	0.012	313.7	1.07	27.64	0.051
900325	1700	9.185	108	9.68	188	29.8	12.4	0.54	201.7	0.006	10.1	0.012	300.9	0.42	27.84	0.029
900401	1545	9.17	103.1	9.06	184.9	29.2	13	0.45	199.5	0.044	13.6	0.018	302	0.56	27.61	0.044
900408	1615	9.14	106.8	9.34	185.5	29.8	13	0.48	198.7	0.029	13.1	0.014	305.2	0.34	27.94	0.045
900417	720	9.1	107.3	9.17	187.2	30.1	12.9	0.51	200.1	0.024	12.3	0.011	308	0.19	28.4	0.066
900423	700	9.07	109	9.04	190.4	31.3	13.8	0.51	203.6	0.026	11.9	0.015	316.3	0.16	28.5	0.061
900430	700	9.49	116.6	8.91	189.4	31	13.8	0.49	207.8	0.046	15	0.014	313.6	0.85	27.34	0.067
900507	716	9.115	105.7	9	194.6	31.7	13.8	0.46	196.1	0.018	12	0.006	319	0.53	27.37	0.067
900515	728	9.11	115.4	8.79	195.6	32.5	14.7	0.52	198.6	0.019	11.6	0.01	325.3	0.56	28.59	0.101
900521	745	9.1	101.7	8.75	194.3	31.9	15.4	0.54	195	0.02	11.3	0.008	326.8	0.75	27.85	0.098
900528	740	9.075	104	8.78	190.6	31.3	16.9	0.6	202	0.039	10	0.01	321.9	0.71	28.28	0.114
900604	740	9.06	104.6	8.7	192.6	32.8	17	0.52	206.9	0.016	9.9	0.013	320.3	0.55	28.92	0.099
900611	720	9.03	117.6	8.83	195.6	32.8	18	0.51	216.5	0.013	9.6	0.008	326.9	0.23	29.58	0.129
900618	830	9.01	117.5	8.62	196.5	33	18.9	0.53	222.8	0.012	9.4	0.009	331.9	0.42	30.1	0.199
900625	843	8.99	109.9	8.79	197.7	35	16.5	0.4	210.6	0.027	17.3	0.013	331.3	0.78	28.48	0.158
900702	835	8.97	107.6	8.93	198.5	35.5	16.5	0.42	210.3	0.026	17.8	0.014	338.4	0.66	28.93	0.129
900709	828	8.96	109.7	8.72	197.9	35.5	17.4	0.42	214.5	0.051	16.9	0.033	343.8	0.95	29.64	0.26
900716	845	8.94	108.4	8.7	193.9	36.3	17.1	0.43	215.6	0.031	18.2	0.025	347.2	0.74	28.08	0.163
900820	910	8.85	121.6	8.91	199.4	32.5	17.1	0.52	216.4	0.055	13.8	0.071	317.5	4.47	28.66	0.081
900827	859	8.82	117.9	9.08	193.6	33.5	16.7	0.52	219.7	0.037	13.1	0.015	329.3	1.38	29.18	0.063
900903	940	7.78	122	9.94	226.6	34.7	19	0.55	220	0.043	14.1	0.057	367.8	1.72	30.19	0.157
900910	932	8.75	122.5	9.08	220.4	33.2	17.9	0.53	217.4	0.045	15.2	0.028	349.3	1.4	29.78	0.078
900917	942	8.73	121.2	8.94	200.9	32.7	16.2	0.56	219.8	0.025	13.5	0.023	351.2	2.34	29.29	0.057

APPENDIX 3 cont.: Department of Water Affairs and Forestry water quality monitoring data for Barber's Pan

DATE	TIME	LEVEL M	EC mS/M	TDS	pH	Na	Mg	Ca	F	Cl	N	SO4	PO4	CACO3	Si	K	NH4
900924	920	8.69	119	960	9.04	205.2	34.1	18	0.46	219.6	0.082	13.5	0.014	360.5	2.26	28.98	0.106
901001	730	8.67	119.5	966	8.94	204.5	35.1	17.7	0.53	225.4	0.015	11.4	0.02	362.6	3.02	29.43	0.089
901008	709	8.62	121.6	971	8.86	205	35	17.6	0.53	227.5	0.014	11.8	0.034	363.6	3.02	29.66	0.121
901015	745	8.61	127.9	987	8.77	212.1	36.4	19	0.54	228.1	0.034	15.3	0.03	364.8	4.48	30.48	0.153
901022	745	8.55	145	1004	9.01	219.1	35.9	18.6	0.59	237.5	0.035	17.9	0.019	363.2	2.59	31.38	0.031
901029	745	8.52	146	1008	9.07	218.1	36.3	18.7	0.61	239.7	0.037	19	0.02	363.8	2.13	31.38	0.033
901105	1030	8.5	148	1021	9.29	228.9	37.2	18.1	0.45	236.1	0.031	16	0.024	370.1	2.62	32.48	0.057
901112	715	8.438	143	1011	8.97	220.5	35.5	18.4	0.55	235.9	0.035	19.1	0.023	367.6	2.59	32.29	0.05
901119	815	8.38	144	1025	8.93	224.6	36.1	18.4	0.56	240.7	0.063	19.8	0.021	370	2.54	33.06	0.054
901126	720	8.32	145	1062	7.99	231.7	36.8	16.4	0.56	242.3	1.108	20.1	0.014	388.8	2.26	34.68	0.025
901203	740	8.28	148	1055	8.7	234.6	36.1	15.3	0.45	237.7	0.014	19.2	0.008	391.4	2.35	34.34	0.026
901210	730	8.25	153	1064	9.02	236.3	39.4	14	0.5	241.5	0.56	18.2	0.04	390.4	2.77	35.06	0.04
901224	730	8.168	156	1080	8.73	239.3	40.1	15.3	0.56	246.2	0.22	18.6	0.011	396.5	0.88	35.4	0.03
910107	730	8.07	145	1094	8.04	241.8	35	12.4	0.55	249.7	0.03	19.4	0.022	409.1	0.38	35.84	0.06
910114	745	8.06	164	7.84													
910121	720	8.095	163	1101	8.01	241.6	35.7	12.9	0.57	255.8	0	19.9	0.019	408.6	0.65	36.24	0.07
910128	840	8.17	159	7.98													
910204	748	8.8	123.7	1058	8.26	227.4	41.9	16.3	0.54	236	0.122	17.2	0.014	396.4	0.63	34.43	0.01
910211	735	9.505	145	8.39													
910218	745	9.99	106.7	786	8.26	167.5	31.6	16.1	0.46	172.5	0.217	10.6	0.05	295.5	3.51	25.77	0.024
910226	740	10.19	85.3	8													
910304	740	10.19	107.5	767	8.16	159.5	28.4	16.4	0.53	163.7	0.67	11.7	0.03	293.1	3.92	26.12	0.022
910311	740	10.16	102.7	8.14													
910318	743	10.28	106.4	746	8.76	155.7	27.1	16.3	0.52	159.4	0.273	11.2	0.013	286.6	3.17	25.53	0.019
910325	803	10.33	103.6	8.07													
910408	814	10.34	86.5	735	8.83	150	28.2	17.7	0.39	152.8	0.529	8.8	0.011	289.7	3.17	21.71	0.018
910415	750	10.31	105.2	8.09													
910422	745	10.27	100.9	747	8.35	151	28.8	18.5	0.4	156.3	0.511	8.3	0.01	295	2.98	21.97	0.02
910506	747	10.21	103.9	752	8.88	155.3	29	17.2	0.45	154.4	0.035	9.5	0.031	294.9	2.95	25.76	0.142
910513	748	10.17	108.1	8.8													
910520	745	10.15	107.7	777	8.75	159	30.4	18.9	0.46	160.5	0.068	9.8	0.021	305.1	2.46	25.73	0.132
910527	944	10.12	107.3	765	8.97	158	29.2	18.5	0.44	150.4	0.04	11	0.038	305.3	3.2	24.82	0.06
910603	810	12.1	104.5	787	8.74	159.7	30	20.1	0.38	164	0.023	12.6	0.033	306.9	2.52	25.96	0.134
910612	758	10.05	105.7	8.86													
910617	755	10.06	106.8	802	8.73	164.1	31.2	21.9	0.47	164.6	0.01	11.6	0.036	313	2.6	26.51	0.033
910624	725	10.07	106.4	8.83													
910701	1035	10.06	106.6	797	8.95	157.2	29.8	20	0.45	161	0.054	10.4	0.024	321.7	2.82	25.78	0.173
910715	800	10.01	107.7	815	8.97	160.3	30.6	20.4	0.47	164.7	0.04	10.5	0.019	328.9	2.77	26.24	0.08
910722	758	10	96.2	818	8.9	160.9	31.3	20.8	0.47	164.2	0.065	10.5	0.021	330.8	2.97	26.41	0.096
910729	750	9.98	97.1	796	8.64	159.4	30.7	20.1	0.42	163.9	0.025	11.2	0.023	315.4	2.71	25.83	0.125
910805	830	9.95	110.3	795	8.44	159.3	30.2	19.4	0.53	164.9	0.02	11.7	0.037	314	2.66	25.95	0.058
910812	810	9.93	113	826	8.85	167.4	31.2	20	0.49	168.1	0.013	14.8	0.03	326.1	3.03	26.23	0.14
910819	808	9.91	107.9	814	8.64	165.1	32.2	19.6	0.6	167	0.342	12.8	0.034	318.3	2.59	27.11	0.036
910826	804	9.87	115.6	823	8.95	161.1	30.6	20	0.4	167.7	0.067	14.4	0.033	330.2	2.86	25.92	0.141
910902	700	9.26	118.7	848	8.82	165.3	31.7	20.4	0.45	174	0.011	16.1	0.029	338.8	2.9	27.07	0.073
910909	700	9.81	117.2	842	8.78	164.4	31.6	20.5	0.46	170.7	0.05	15.3	0.041	337.2	2.84	27.18	0.174

APPENDIX 3 cont.: Department of Water Affairs and Forestry water quality monitoring data for Barber's Pan

DATE	TIME	LEVEL M	EC mS/M	TDS	pH	Na	Mg	Ca	F	Cl	N	SO4	PO4	CACO3	Si	K	NH4
910916	700	9.78	116.8	839	8.9	163.3	31.3	20.3	0.46	170.9	0.036	15.8	0.029	336.2	2.61	26.48	0.148
910923	700	9.76	116.5	813	8.94	166	29.9	20.6	0.51	171.5	0.007	8.6	0.021	318.3	3.17	27.69	0.081
910930	700	9.82	111.6	809	9.02	164.8	29.9	20.9	0.52	171.5	0.009	8.8	0.016	315.4	3.19	27.97	0.073
911007	730	9.73	113.6	822	8.96	168.7	30.5	21.4	0.52	173.9	0.007	8.8	0.02	320	3.17	28.06	0.05
911014	736	9.7	109.7	823	8.93	166.1	30.5	21.3	0.53	174.9	0	9	0.018	321.9	2.83	27.97	0.093
911021	1000	9.72	113.6	850	8.88	165.9	33	20.5	0.47	171	0.024	11.2	0.022	344.6	2.45	27.33	0.05
911026	800	9.7	114.1	859	8.93	167.1	33.3	20.4	0.51	176.1	0.024	11.3	0.028	346.9	1.87	27.48	0.096
911028	730	9.57	110.8	871	9.02	177.2	33.4	21	0.43	182.1	0.02	11.1	0.025	341.8	0.45	28.4	0.019
911104	720	9.675	121.4	875	9.05	170.5	35.7	20.5	0.52	183.3	0.01	11.8	0.022	348	0.49	28.05	0.05
911111	720	9.64	123.8	891	8.98	172.8	35.5	20.8	0.53	182.8	0.015	11.8	0.037	358.3	0.56	29.15	0.081
911118	730	9.41	118	867	8.94	175.2	33.8	20.8	0.42	181.4	0.012	11.9	0.02	340.7	0.34	28.09	0.016
911202	730	9.81	112.3	883	9.08	179.6	34	19.9	0.42	184.3	0.006	11.2	0.019	347.8	0.55	28.9	0.041
911209	740	9.48	119.5	885	9.13	178.8	34.7	19.9	0.43	184.7	0.01	11.3	0.019	349.1	0.53	29.04	0.033
911217	750	9.44	119.1	890	9.09	185.2	36.1	18.3	0.44	187.3	0.039	12.3	0.027	344.5	0.91	30.12	0.048
911223	745	9.425	124.8	869	8.78	177.9	34.6	17.5	0.46	182.2	0	12	0.018	340	0.95	29.84	0.03
911230	745	9.37	124.8	876	8.99	183.8	35.3	14.8	0.53	185.1	0.001	11.9	0.02	339	1.13	30.9	0.03
920106	730	9.34	114.7	880	9.07	186.3	35.4	16	0.42	189.4	0.006	11.8	0.035	336.2	1.42	30.62	0
920113	742	9.29	116.7	881	8.98	183.6	34.5	15.4	0.5	188.6	0.04	11.9	0.039	341.3	1.8	29.71	0.033
920127	750	9.19	121.3	915	8.24	188.5	35.9	14.4	0.57	194.7	0.107	12.1	0.023	358.6	1.55	30.9	0.073
920203	754	9.13	113.3	913	8.7	188.5	35.8	14.3	0.58	196.3	0.015	12.2	0.023	356.2	1.97	31.18	0.025
920217	740	9.028	118.2	961	8.54	198.7	37.5	16.2	0.51	205.1	0	22.1	0.01	367.6	1.4	33.06	0.011
920224	825	9.01	125.4	950	8.75	195	36.6	14.2	0.49	205.5	0	22.9	0.008	363.2	0.47	32.48	0.019
920302	735	8.928	125.9	956	8.82	195.8	37.1	15.5	0.48	206.5	0.024	22.5	0.009	365.5	0.52	32.65	0.031
920309	750	8.91	128.3	974	8.46	204.5	38.1	13.7	0.62	207.4	0.005	19.6	0.013	374.5	0	33.51	0.099
920315	755	8.875	127.3	997	8.11	206.7	39.1	15.1	0.61	210.9	0	18.7	0.009	387	0.09	34.09	0.083
920323	755	8.86	129.4	994	8.32	206.7	39.2	15.8	0.6	211.5	0	18.8	0.011	383.3	0.28	34.21	0.102
920330	715	8.815	145	1004	8.45	205.8	39.3	16	0.67	213.4	0	18.5	0.011	390.3	0.62	34.35	0.071
920406	750	8.795	140	992	8.73	203.7	39.7	16.2	0.52	215.7	0.007	17.8	0.011	380.2	0.69	34.32	0.037
920413	730	8.76	147	1006	8.95	206.8	40	15.6	0.75	220.2	0.252	18	0.024	384.7	0.99	34.73	0.041
920420	740	8.74	144	1024	8.87	207.7	40.6	16.3	0.71	227.9	0.272	18.1	0.04	390.5	0.91	34.97	0.034
920427	820	8.701	142	1014	9.11	210.9	40.5	16	0.54	222.9	0.008	17.3	0.018	386.3	0.97	34.4	0.074
920810	800	0	156	1084	9.22	218.1	43.7	17.6	0.55	233.5	0.025	19.8	0.029	421.7	1.04	36.72	0.045
920817	800	0	153	1115	9.27	222.4	44.7	18	0.61	239.4	0.04	20.1	0.047	436	1.08	37.9	0.069
920824	800	0	157	1107	9.22	220	43.6	17.9	0.63	237	0.013	20	0.022	435.5	1.2	37.11	0.068
920831	800	0	158	1103	9.26	221.4	44.6	17.8	0.61	242.1	0.019	19.7	0.039	426.2	1.26	37.28	0.051
920928	1100	0	167	1197	9.14	262.4	47.5	17.3	0.76	254.8	0.014	24.6	0.032	451.8	1.22	38.66	0.044
921005	800	0	163	1190	9.13	258.4	47.4	17.4	0.91	249.5	0.044	24.2	0.022	454	1.1	38.72	0.046
921012	1030	0	162	1181	8.98	257	47.8	17.6	0.93	255.1	0.012	24.2	0.02	442.7	1.3	38.69	0.014
921019	1000	0	164	1214	9.18	263.4	47.3	17.7	0.8	251.9	0.03	26.2	0.021	465.2	0.95	39.11	0.04
921026	800	0	163	1208	9.05	249	47.6	16.3	0.64	261.8	0.04	24.1	0.025	466.5	0.97	39.35	0.052
921102	800	8	164	1215	9.16	252.3	48.1	17.3	0.74	262.7	0.036	25	0.073	466.6	1.2	39.13	0.227
921109	800	8.19	155	1146	8.94	238.8	43.1	15.8	0.7	244	0.16	26.6	0.035	437	1.1	42.67	0.285
921118	706	8.5	159	1133	9.08	236.2	43.4	16.4	0.68	240.1	0.042	23	0.03	436.7	0.71	40.18	0.117
921125	851	8.63	148	1073	9.02	223.3	42.2	16.6	0.69	236.6	0.03	28.8	0.026	399.7	1.01	37.43	0.049
921203	933	8.55	143	1075	9.07	223.5	41.2	16.6	0.62	228.3	0.024	25.6	0.03	412	0.37	36.94	0.091
921209	1440	8.52	149	1065	9.08	225.2	41.3	15.4	0.66	230.6	0.038	30.2	0.028	396.8	0.31	37.17	0.051

APPENDIX 3 cont.: Department of Water Affairs and Forestry water quality monitoring data for Barber's Pan

DATE	TIME	LEVEL M	EC mS/M	TDS	pH	Na	Mg	Ca	F	Cl	N	SO4	PO4	CACO3	Si	K	NH4
MG/L																	
921217	800	8.45	146	1076	9.17	228.1	42.2	17.1	0.73	229.1	0.024	24.2	0.018	406.7	0.48	38.29	0.074
930104	1100	8.54	157	1126	9.16	232.8	42.9	15.8	0.64	248.7	0.053	24.5	0.066	428.3	0.93	38.17	0.034
930202	1000	8.3	156	1303	8.62	249.7	58.2	26.3	0.84	252.6	0.07	10.7	0.022	541.2	1.91	43.94	0.648
930301	800	8.2	167	1197	9.34	261	44.7	15.1	0.68	268.8	0.033	25.6	0.053	442.6	0.83	41.57	0.059
930401	900	8.12	147	1209	9.24	253.5	45.7	15.7	0.81	253.8	0.028	22.3	0.014	472.8	1.59	40.66	0.04
930514	825	8	161	1217	9.09	257.7	48.2	15.3	0.5	257.4	0.03	23.5	0.023	470	1.62	41.22	0.077
930601	823	7.89	171	1264	9.03	264.4	47.1	17.1	0.64	259.1	0.104	24.2	0.025	500	0.98	40.67	0.062
930810	1038	7.73	174	1294	9	285.7	52.9	18.4	0.8	273.7	0.036	24.9	0.018	487.4	1.35	42.73	0.046
930930	815	7.53	155	1375	8.92	292.1	54.5	15.7	0.79	293.8	0.084	29	0.03	527.1	1.47	45.86	0.098
931029	745	8.65	165	1397	9.05	291.4	56.8	13	0.67	288.5	0.1	29.5	0.038	550	1.57	45.47	0.123
931130	815	7.75	178	1431	9.05	324.1	56	15.5	0.91	305.1	0.067	31.9	0.019	530	1.93	50.37	0.046
931230	745	7.85	180	1400	9.03	312.5	54	13.7	0.81	288	0.059	25	0.035	539.3	1.09	48.15	0.125
940129	815	7.95	180	1334	9.07	295	51.1	14.1	0.79	284.6	0.003	29.2	0.009	503.4	1.08	45.35	0.027
940225	745	8.65	133	1047	8.88	228	43.9	10.4	0.62	218.5	0.026	35.7	0.025	387.5	1.4	37.14	0.011
940430	920	7.68	135	1035	9	221.1	41.8	14.5	0.64	222	0.035	19.3	0.031	391.3	0.74	38.01	0.059
940527	800	8.42	150	1129	9.08	231.4	45.3	15	0.66	227.3	0.051	33.7	0.055	440	1.19	38.49	0.092
940630	745	8.33	156	1115	8.54	243.1	47.9	15.4	0.76	242.8	0.054	21	0.025	413.2	0.35	39.33	0.154
940730	745	2.39	169	1217	9.02	245.5	50.8	17.7	0.81	261.4	0.048	18.4	0.051	477.7	0.57	39.43	0.081
940831	900	1.28	144	1111	9.17	231.2	43.2	14.7	0.75	233.9	0.075	21.7	0.03	432.1	0.96	38.42	0.042
940930	745	8.79	163	1190	8.98	249.6	45.5	17.4	0.65	252.8	0.038	25.6	0.024	457.2	1.24	40.5	0.035
941026	845	8.64	153	1255	9.03	248.1	47.1	18.3	0.85	256.3	0.033	32.4	0.048	496	7	46.33	0.08
941228	745	5.69	182	1325	9.09	285.6	51.9	17.1	0.67	271.2	0.154	34.8	0.015	506.6	0.79	45.13	0.026
950205	830	7	179	1311	9.13	298.4	48.3	11.2	0.73	288.1	0.116	40.3	0.095	468.9	1.28	51.61	0.285
950227	745	2.3	185	1442	9.2	304.8	53.4	15.1	0.83	295.5	0.059	30.3	0.038	568.8	3.51	47.92	0.044
950329	745	1.935	191	1415	9.23	310.2	52.1	13.3	0.8	297.4	0.076	30.9	0.036	542.3	1.64	48.73	0.055
950601	745	7	207	1566	9.22	337	55.3	14.5	0.77	325.3	0.116	72	0.036	582.6	0.82	49.68	0.025

7.4 APPENDIX 4: An example of a MINTEQA2 print out

```

-----
PART 1 of OUTPUT FILE
AIX MINTEQA2 v3.10  DATE OF CALCULATIONS: 20-NOV-95  TIME:  9:24: 3
0Barber's Pan Bulk Water Sample 5 (20/11/1995)

-----
Temperature (Celsius): 11.25
Units of concentration: MG/L
Ionic strength to be computed.
If specified, carbonate concentration represents total inorganic carbon.
Do not automatically terminate if charge imbalance exceeds 30%
Precipitation is allowed only for those solids specified as ALLOWED
in the input file (if any).
The maximum number of iterations is: 40
The method used to compute activity coefficients is: Davies equation
Intermediate output file

-----
330 0.000E+00 -9.23 Y
180 3.683E+02 -1.98 Y
732 3.621E+01 -3.42 Y
140 3.568E+02 -2.98 Y
770 1.050E+00 -4.84 Y
600 3.930E-01 -5.72 Y
540 8.000E-02 -5.87 Y
950 6.500E-02 -6.00 Y
460 7.230E+01 -2.53 Y
30 1.210E+00 -4.35 Y
231 1.000E-03 -7.80 Y
150 1.650E+01 -3.39 Y
500 3.660E+02 -1.80 Y
410 7.190E+01 -2.74 Y
280 4.080E-01 -5.14 Y
580 1.530E-02 -7.28
0 H2O has been inserted as a COMPONENT
3 1
330 9.2300 .0000
0 INPUT DATA BEFORE TYPE MODIFICATIONS
0 ID NAME ACTIVITY GUESS LOG GUESS ANAL TOTAL
330 H+1 5.888E-10 -9.230 0.000E+00
180 Cl-1 1.047E-02 -1.980 3.683E+02
732 SO4-2 3.802E-04 -3.420 3.621E+01
140 CO3-2 1.047E-03 -2.980 3.568E+02
770 H4SiO4 1.445E-05 -4.840 1.050E+00
600 Pb+2 1.905E-06 -5.720 3.930E-01
540 Ni+2 1.349E-06 -5.870 8.000E-02
950 Zn+2 1.000E-06 -6.000 6.500E-02
460 Mg+2 2.951E-03 -2.530 7.230E+01
30 Al+3 4.467E-05 -4.350 1.210E+00
231 Cu+2 1.585E-08 -7.800 1.000E-03
150 Ca+2 4.074E-04 -3.390 1.650E+01
500 Na+1 1.585E-02 -1.800 3.660E+02
410 K+1 1.820E-03 -2.740 7.190E+01
280 Fe+2 7.244E-06 -5.140 4.080E-01
580 PO4-3 5.248E-08 -7.280 1.530E-02
2 H2O 1.000E+00 .000 0.000E+00

0 Charge Balance: UNSPECIATED
0 Sum of CATIONS= 2.472E-02 Sum of ANIONS = 2.306E-02
0 PERCENT DIFFERENCE = 3.465E+00 (ANIONS - CATIONS)/(ANIONS + CATIONS)

```

## PART 4 of OUTPUT FILE

AIX MINTEQA2 v3.10 DATE OF CALCULATIONS: 20-NOV-95 TIME: 9:24: 4

PERCENTAGE DISTRIBUTION OF COMPONENTS AMONG  
TYPE I and TYPE II (dissolved and adsorbed) species

+PO4-3				
+	48.6	PERCENT BOUND IN SPECIES #4605800	MgPO4 -	
+	13.8	PERCENT BOUND IN SPECIES #4605802	MgHPO4 AQ	
+	1.4	PERCENT BOUND IN SPECIES #1505800	CaHPO4 AQ	
+	4.8	PERCENT BOUND IN SPECIES #1505801	CaPO4 -	
+	30.6	PERCENT BOUND IN SPECIES #3305800	HPO4 -2	
+Cl-1				
+	100.0	PERCENT BOUND IN SPECIES # 180	Cl-1	
+SO4-2				
+	84.0	PERCENT BOUND IN SPECIES # 732	SO4-2	
+	10.5	PERCENT BOUND IN SPECIES #4607320	MgSO4 AQ	
+	1.6	PERCENT BOUND IN SPECIES #1507320	CaSO4 AQ	
+	3.4	PERCENT BOUND IN SPECIES #5007320	NaSO4 -	
+CO3-2				
+	7.5	PERCENT BOUND IN SPECIES # 140	CO3-2	
+	4.6	PERCENT BOUND IN SPECIES #4601400	MgCO3 AQ	
+	1.3	PERCENT BOUND IN SPECIES #4601401	MgHCO3 +	
+	84.4	PERCENT BOUND IN SPECIES #3301400	HCO3 -	
+H4SiO4				
+	90.1	PERCENT BOUND IN SPECIES # 770	H4SiO4	
+	9.9	PERCENT BOUND IN SPECIES #3307700	H3SiO4 -	
+Pb+2				
+	52.7	PERCENT BOUND IN SPECIES #6001400	Pb(CO3)2-2	
+	46.6	PERCENT BOUND IN SPECIES #6001401	PbCO3 AQ	
+Ni+2				
+	56.1	PERCENT BOUND IN SPECIES #5401401	NiCO3 AQ	
+	43.8	PERCENT BOUND IN SPECIES #5401402	Ni(CO3)2-2	

+Zn+2				
+	6.4	PERCENT BOUND IN SPECIES #9503301	Zn(OH)2 AQ	
+	8.7	PERCENT BOUND IN SPECIES #9501401	ZnCO3 AQ	
+	84.2	PERCENT BOUND IN SPECIES #9501402	Zn(CO3)2-2	
+Mg+2				
+	86.9	PERCENT BOUND IN SPECIES # 460	Mg+2	
+	9.1	PERCENT BOUND IN SPECIES #4601400	MgCO3 AQ	
+	2.6	PERCENT BOUND IN SPECIES #4601401	MgHCO3 +	
+	1.3	PERCENT BOUND IN SPECIES #4607320	MgSO4 AQ	
+Al+3				
+	84.4	PERCENT BOUND IN SPECIES # 303302	Al(OH)4 -	
+	15.5	PERCENT BOUND IN SPECIES # 303303	Al(OH)3 AQ	
+Cu+2				
+	2.1	PERCENT BOUND IN SPECIES #2311400	CuCO3 AQ	
+	1.2	PERCENT BOUND IN SPECIES #2311401	Cu(CO3)2-2	
+	96.6	PERCENT BOUND IN SPECIES #2313301	Cu(OH)2 AQ	
+Ca+2				
+	84.1	PERCENT BOUND IN SPECIES # 150	Ca+2	
+	1.6	PERCENT BOUND IN SPECIES #1501400	CaHCO3 +	
+	12.8	PERCENT BOUND IN SPECIES #1501401	CaCO3 AQ	
+	1.5	PERCENT BOUND IN SPECIES #1507320	CaSO4 AQ	
+Na+1				
+	99.5	PERCENT BOUND IN SPECIES # 500	Na+1	
+K+1				
+	99.9	PERCENT BOUND IN SPECIES # 410	K+1	
+Fe+2				
+	88.4	PERCENT BOUND IN SPECIES # 280	Fe+2	
+	10.4	PERCENT BOUND IN SPECIES #2803300	FeOH +	
+	1.2	PERCENT BOUND IN SPECIES #2807320	FeSO4 AQ	
+H2O				
+	3.7	PERCENT BOUND IN SPECIES #3300020	OH-	
+	83.5	PERCENT BOUND IN SPECIES # 303302	Al(OH)4 -	
+	11.5	PERCENT BOUND IN SPECIES # 303303	Al(OH)3 AQ	

```

+H+1
+          1.6      PERCENT BOUND IN SPECIES #4601401   MgHCO3 +
+          101.3    PERCENT BOUND IN SPECIES #3301400   HCO3 -
1

```

---

PART 5 of OUTPUT FILE

---

AIX MINTEQA2 v3.10    DATE OF CALCULATIONS: 20-NOV-95    TIME: 9:24: 4

-----  
 ----- EQUILIBRATED MASS DISTRIBUTION -----  
 -----

0 IDX	NAME	DISSOLVED		SORBED		PRECIPITATED	
		MOL/KG	PERCENT	MOL/KG	PERCENT	MOL/KG	PERCENT
580	PO4-3	1.613E-07	100.0	0.000E+00	.0	0.000E+00	.
180	Cl-1	1.040E-02	100.0	0.000E+00	.0	0.000E+00	.
732	SO4-2	3.774E-04	100.0	0.000E+00	.0	0.000E+00	.
140	CO3-2	5.953E-03	100.0	0.000E+00	.0	0.000E+00	.
770	H4SiO4	1.094E-05	100.0	0.000E+00	.0	0.000E+00	.
600	Pb+2	1.899E-06	100.0	0.000E+00	.0	0.000E+00	.
540	Ni+2	1.364E-06	100.0	0.000E+00	.0	0.000E+00	.
950	Zn+2	9.956E-07	100.0	0.000E+00	.0	0.000E+00	.
460	Mg+2	2.978E-03	100.0	0.000E+00	.0	0.000E+00	.
30	Al+3	4.490E-05	100.0	0.000E+00	.0	0.000E+00	.
231	Cu+2	1.576E-08	100.0	0.000E+00	.0	0.000E+00	.
150	Ca+2	4.122E-04	100.0	0.000E+00	.0	0.000E+00	.
500	Na+1	1.594E-02	100.0	0.000E+00	.0	0.000E+00	.
410	K+1	1.841E-03	100.0	0.000E+00	.0	0.000E+00	.
280	Fe+2	7.315E-06	100.0	0.000E+00	.0	0.000E+00	.
2	H2O	1.816E-04	100.0	0.000E+00	.0	0.000E+00	.
330	H+1	4.961E-03	100.0	0.000E+00	.0	0.000E+00	.

```

0 Charge Balance: SPECIATED
0 Sum of CATIONS = 2.367E-02 Sum of ANIONS 1.706E-02
0 PERCENT DIFFERENCE = 1.624E+01 (ANIONS - CATIONS)/(ANIONS + CATION)
0 EQUILIBRIUM IONIC STRENGTH (m) = 2.407E-02
0 EQUILIBRIUM pH = 9.230
0 DATE ID NUMBER: 951020
0 TIME ID NUMBER: 9240400
1

```

---

PART 6 of OUTPUT FILE

---

AIX MINTEQA2 v3.10    DATE OF CALCULATIONS: 20-NOV-95    TIME: 9:24: 4

0 Saturation indices and stoichiometry of all minerals

0 ID #	NAME	Sat. Index	Stoichiometry in [brackets]					
2003000	ALOH3(A)	-.492	[ 1.000]	30	[ 3.000]	2	[ -3.000]	3
6003000	ALOHSO4	-8.139	[ -1.000]	330	[ 1.000]	30	[ 1.000]	7
			[ 1.000]	2				
6003001	AL4(OH)10SO4	-1.530	[-10.000]	330	[ 4.000]	30	[ 1.000]	7
			[ 10.000]	2				
6041000	ALUM K	-21.731	[ 1.000]	410	[ 1.000]	30	[ 2.000]	7
			[ 12.000]	2				
6041001	ALUNITE	-3.977	[ 1.000]	410	[ 3.000]	30	[ 2.000]	7
			[ 6.000]	2	[ -6.000]	330		
6015000	ANHYDRITE	-2.969	[ 1.000]	150	[ 1.000]	732		

5015000	ARAGONITE	.897	[ 1.000]	150	[ 1.000]	140		
5046000	ARTINITE	-1.455	[ -2.000]	330	[ 2.000]	460	[ 1.000]	1
			[ 5.000]	2				
2003001	BOEHMITE	1.272	[ -3.000]	330	[ 1.000]	30	[ 2.000]	
2046000	BRUCITE	-2.092	[ 1.000]	460	[ 2.000]	2	[ -2.000]	3
5015001	CALCITE	1.087	[ 1.000]	150	[ 1.000]	140		
2077000	CHALCEDONY	-1.317	[ -2.000]	2	[ 1.000]	770		
8646000	CHRYSOTILE	2.791	[ -6.000]	330	[ 3.000]	460	[ 2.000]	7
			[ 1.000]	2				
8246000	CLINOENSTITUTE	-1.435	[ -1.000]	2	[ 1.000]	460	[ 1.000]	7
			[ -2.000]	330				
2077001	CRISTOBALITE	-1.221	[ -2.000]	2	[ 1.000]	770		
2003002	DIASPORE	3.101	[ -3.000]	330	[ 1.000]	30	[ 2.000]	
8215000	DIOPSIDE	-.678	[ -2.000]	2	[ 1.000]	150	[ 1.000]	4
			[ 2.000]	770	[ -4.000]	330		
5015002	DOLOMITE	2.933	[ 1.000]	150	[ 1.000]	460	[ 2.000]	1
6046000	EPSOMITE	-4.362	[ 1.000]	460	[ 1.000]	732	[ 7.000]	
8646003	SEPIOLITE(C)	-.659	[ -.500]	2	[ 2.000]	460	[ 3.000]	7
			[ -4.000]	330				
7015003	HYDRAPATITE	2.430	[ 5.000]	150	[ 3.000]	580	[ 1.000]	
			[ -1.000]	330				
8046000	FORSTERITE	-3.789	[ -4.000]	330	[ 2.000]	460	[ 1.000]	7
2003003	GIBBSITE (C)	1.268	[ -3.000]	330	[ 1.000]	30	[ 3.000]	
3003000	AL2O3	-1.287	[ 2.000]	30	[ 3.000]	2	[ -6.000]	3
8628000	GREENALITE	8.223	[ -6.000]	330	[ 3.000]	280	[ 2.000]	7
			[ 1.000]	2				
6015001	GYPSUM	-2.616	[ 1.000]	150	[ 1.000]	732	[ 2.000]	
4150000	HALITE	-5.460	[ 1.000]	500	[ 1.000]	180		
5015003	HUNTITE	2.381	[ 3.000]	460	[ 1.000]	150	[ 4.000]	1
5046001	HYDRMAGNESIT	-3.271	[ 5.000]	460	[ 4.000]	140	[ -2.000]	3
			[ 6.000]	2				
8450000	MAGADIITE	-13.358	[ -1.000]	330	[ -9.000]	2	[ 1.000]	5
			[ 7.000]	770				

1

ID #	NAME	Sat. Index	Stoichiometry in [brackets]					
5046002	MAGNESITE	1.360	[ 1.000]	460	[ 1.000]	140		
6028000	MELANITERITE	-6.632	[ 1.000]	280	[ 1.000]	732	[ 7.000]	
6050001	MIRABILITE	-5.699	[ 2.000]	500	[ 1.000]	732	[ 10.000]	
3050000	NATRON	-5.467	[ 2.000]	500	[ 1.000]	140	[ 10.000]	
5046003	NESQUEHONITE	-1.035	[ 1.000]	460	[ 1.000]	140	[ 3.000]	
8646001	PHLOGOPITE	-20.247	[ -10.000]	330	[ 1.000]	410	[ 3.000]	4
			[ 1.000]	30	[ 3.000]	770		
2077002	QUARTZ	-.777	[ -2.000]	2	[ 1.000]	770		
8646004	SEPIOLITE(A)	-2.560	[ -.500]	2	[ 2.000]	460	[ 3.000]	7
			[ -4.000]	330				
5028000	SIDERITE	1.309	[ 1.000]	280	[ 1.000]	140		
2077003	SIO2 (A, GL)	-1.828	[ -2.000]	2	[ 1.000]	770		
2077004	SIO2 (A, PT)	-2.155	[ -2.000]	2	[ 1.000]	770		
8646002	TALC	2.537	[ -4.000]	2	[ 3.000]	460	[ 4.000]	7
			[ -6.000]	330				
6050002	THENARDITE	-7.324	[ 2.000]	500	[ 1.000]	732		
5050001	THERMONATR	-7.558	[ 2.000]	500	[ 1.000]	140	[ 1.000]	
8215001	TREMOLITE	7.566	[ -8.000]	2	[ 2.000]	150	[ 5.000]	4
			[ 8.000]	770	[ -14.000]	330		
7028001	VIVIANITE	-1.951	[ 3.000]	280	[ 2.000]	580	[ 8.000]	
4123100	MELANOTHALLI	-20.855	[ 1.000]	231	[ 2.000]	180		
5023100	CUCO3	-6.571	[ 1.000]	231	[ 1.000]	140		
2023100	CU(OH) 2	-3.316	[ -2.000]	330	[ 1.000]	231	[ 2.000]	
4123101	ATACAMITE	-7.549	[ -3.000]	330	[ 2.000]	231	[ 3.000]	
			[ 1.000]	180				
6023100	ANTLERITE	-12.910	[ -4.000]	330	[ 3.000]	231	[ 4.000]	
			[ 1.000]	732				

6023101	BROCHANTITE	-14.096	[ -6.000]	330	[ 4.000]	231	[ 6.000]
			[ 1.000]	732			
6023102	LANGITE	-16.950	[ -6.000]	330	[ 4.000]	231	[ 7.000]
			[ 1.000]	732			
2023101	TENORITE	-2.295	[ -2.000]	330	[ 1.000]	231	[ 1.000]
6023103	CUOCUSO4	-23.276	[ -2.000]	330	[ 2.000]	231	[ 1.000]
			[ 1.000]	732			
7023100	CU3(PO4)2	-22.543	[ 3.000]	231	[ 2.000]	580	
7023101	CU3(PO4)2,3W	-24.274	[ 3.000]	231	[ 2.000]	580	[ 3.000]
6023104	CUSO4	-20.003	[ 1.000]	231	[ 1.000]	732	
6023105	CHALCANTHITE	-13.661	[ 1.000]	231	[ 1.000]	732	[ 5.000]
2023102	DIOPTASE	-5.956	[ -2.000]	330	[ 1.000]	231	[ 1.000] 7
4195000	ZNCL2	-20.495	[ 1.000]	950	[ 2.000]	180	
5095000	SMITHSONITE	-2.512	[ 1.000]	950	[ 1.000]	140	
5095001	ZNCO3, 1H2O	-2.098	[ 1.000]	950	[ 1.000]	140	[ 1.000]
2095000	ZN(OH)2 (A)	-2.742	[ -2.000]	330	[ 1.000]	950	[ 2.000]
2095001	ZN(OH)2 (C)	-2.492	[ -2.000]	330	[ 1.000]	950	[ 2.000]
2095002	ZN(OH)2 (B)	-2.042	[ -2.000]	330	[ 1.000]	950	[ 2.000]
2095003	ZN(OH)2 (G)	-2.002	[ -2.000]	330	[ 1.000]	950	[ 2.000]
2095004	ZN(OH)2 (E)	-1.792	[ -2.000]	330	[ 1.000]	950	[ 2.000]
4195001	ZN2(OH)3CL	-7.061	[ -3.000]	330	[ 2.000]	950	[ 3.000]
			[ 1.000]	180			
4195002	ZN5(OH)8CL2	-12.514	[ -8.000]	330	[ 5.000]	950	[ 8.000]
			[ 2.000]	180			

ID #	NAME	Sat. Index	Stoichiometry in [brackets]				
6095000	ZN2(OH)2SO4	-10.299	[ -2.000]	330	[ 2.000]	950	[ 2.000]
			[ 1.000]	732			
6095001	ZN4(OH)6SO4	-11.784	[ -6.000]	330	[ 4.000]	950	[ 6.000]
			[ 1.000]	732			
2095005	ZNO(ACTIVE)	-1.602	[ -2.000]	330	[ 1.000]	950	[ 1.000]
2095006	ZINCITE	-2.207	[ -2.000]	330	[ 1.000]	950	[ 1.000]
6095002	ZN3O(SO4)2	-36.523	[ -2.000]	330	[ 3.000]	950	[ 2.000] 7
			[ 1.000]	2			
7095000	ZN3(PO4),4W	-15.826	[ 3.000]	950	[ 2.000]	580	[ 4.000]
8295000	ZNSIO3	1.127	[ -2.000]	330	[ -1.000]	2	[ 1.000] 9
			[ 1.000]	770			
8095000	WILLEMITE	-2.100	[ -4.000]	330	[ 2.000]	950	[ 1.000] 7
6095003	ZINCOSITE	-16.198	[ 1.000]	950	[ 1.000]	732	
6095004	ZNSO4, 1H2O	-12.315	[ 1.000]	950	[ 1.000]	732	[ 1.000]
6095005	BIANCHITE	-10.750	[ 1.000]	950	[ 1.000]	732	[ 6.000]
6095006	GOSLARITE	-10.432	[ 1.000]	950	[ 1.000]	732	[ 7.000]
4160000	COTUNNITE	-8.810	[ 1.000]	600	[ 2.000]	180	
4160002	PHOSGENITE	-7.259	[ 2.000]	600	[ 2.000]	180	[ 1.000] 1
5060000	CERRUSITE	.012	[ 1.000]	600	[ 1.000]	140	
2060000	MASSICOT	-4.729	[ -2.000]	330	[ 1.000]	600	[ 1.000]
2060001	LITHARGE	-4.525	[ -2.000]	330	[ 1.000]	600	[ 1.000]
2060002	PBO, .3H2O	-4.205	[ -2.000]	330	[ 1.000]	600	[ 1.330]
5060001	PB2OCO3	-4.422	[ -2.000]	330	[ 2.000]	600	[ 1.000]
			[ 1.000]	140			
6060000	LARNAKITE	-4.613	[ -2.000]	330	[ 2.000]	600	[ 1.000] 7
			[ 1.000]	2			
6060001	PB3O2SO4	-7.025	[ -4.000]	330	[ 3.000]	600	[ 1.000] 7
			[ 2.000]	2			
6060002	PB4O3SO4	-10.457	[ -6.000]	330	[ 4.000]	600	[ 1.000] 7
			[ 3.000]	2			
7060001	CLPYROMORPH	1.546	[ 5.000]	600	[ 3.000]	580	[ 1.000] 1
7060002	HXPYROMORPH	-8.818	[ -1.000]	330	[ 5.000]	600	[ 3.000] 5
			[ 1.000]	2			
5060002	PB3O2CO3	-7.697	[ -4.000]	330	[ 3.000]	600	[ 1.000] 1
			[ 2.000]	2			
7060003	PLUMBGUMMITE	-2.885	[ -5.000]	330	[ 1.000]	600	[ 3.000]

7060004	HINSDALITE	-16.896	[ 2.000]	580	[ 6.000]	2		
			[ -6.000]	330	[ 1.000]	600	[ 3.000]	
7060005	TSUMEBITE	-5.290	[ 1.000]	580	[ 1.000]	732	[ 6.000]	
			[ -3.000]	330	[ 2.000]	600	[ 1.000]	2
8260000	PBSIO3	-3.876	[ 1.000]	580	[ 6.000]	2		
			[ -1.000]	2	[ -2.000]	330	[ 1.000]	6
			[ 1.000]	770				
8060000	PB2SIO4	-8.134	[ -4.000]	330	[ 2.000]	600	[ 1.000]	7
6060003	ANGLESITE	-5.574	[ 1.000]	600	[ 1.000]	732		
2060004	PB(OH)2 (C)	.129	[ -2.000]	330	[ 1.000]	600	[ 2.000]	
4160003	LAURIONITE	-3.125	[ -1.000]	330	[ 1.000]	600	[ 1.000]	1
			[ 1.000]	2				
4160004	PB2(OH)3CL	-2.520	[ -3.000]	330	[ 2.000]	600	[ 3.000]	
			[ 1.000]	180				
5060003	HYDCERRUSITE	-.346	[ -2.000]	330	[ 3.000]	600	[ 2.000]	1
			[ 2.000]	2				

1

0	ID #	NAME	Sat. Index	Stoichiometry in [brackets]				
	2060005	PB2O(OH)2	-8.650	[ -4.000]	330	[ 2.000]	600	[ 3.000]
	6060004	PB4(OH)6SO4	-8.215	[ -6.000]	330	[ 4.000]	600	[ 1.000]
				[ 6.000]	2			7
	5054000	NICO3	-6.496	[ 1.000]	540	[ 1.000]	140	
	2054000	NI(OH)2	-.639	[ -2.000]	330	[ 1.000]	540	[ 2.000]
	6054000	NI4(OH)6SO4	-17.889	[ -6.000]	330	[ 4.000]	540	[ 1.000]
				[ 6.000]	2			7
	2054001	BUNSENITE	-4.216	[ -2.000]	330	[ 1.000]	540	[ 1.000]
	7054000	NI3(PO4)2	-18.443	[ 3.000]	540	[ 2.000]	580	
	6054001	RETGERSITE	-11.056	[ 1.000]	540	[ 1.000]	732	[ 6.000]
	6054002	MORENOSITE	-10.671	[ 1.000]	540	[ 1.000]	732	[ 7.000]
	8054000	NI2SIO4	-2.562	[ -4.000]	330	[ 2.000]	540	[ 1.000]
	8450001	ANALCIME	.678	[ 1.000]	500	[ 1.000]	30	[ 2.000]
				[ -1.000]	2	[ -4.000]	330	
	8603000	HALLOYSITE	1.284	[ 2.000]	30	[ 2.000]	770	[ 1.000]
				[ -6.000]	330			
	8603001	KAOLINITE	4.710	[ 2.000]	30	[ 2.000]	770	[ 1.000]
				[ -6.000]	330			
	8415000	LEONHARDITE	13.329	[ -1.000]	2	[ -16.000]	330	[ 2.000]
				[ 8.000]	770	[ 4.000]	30	
	8450002	LOW ALBITE	-.006	[ 1.000]	500	[ 1.000]	30	[ 3.000]
				[ -4.000]	330	[ -4.000]	2	
	8450003	ANALBITE	-1.012	[ 1.000]	500	[ 1.000]	30	[ 3.000]
				[ -4.000]	330	[ -4.000]	2	
	8641000	MUSCOVITE	8.867	[ 1.000]	410	[ 3.000]	30	[ 3.000]
				[ -10.000]	330			7
	8641001	ANNITE	15.688	[ 1.000]	410	[ 3.000]	280	[ 1.000]
				[ 3.000]	770	[ -10.000]	330	
	8415001	ANORTHITE	-1.504	[ 1.000]	150	[ 2.000]	30	[ 2.000]
				[ -8.000]	330			7
	8603002	PYROPHYLLITE	3.278	[ 2.000]	30	[ 4.000]	770	[ -4.000]
				[ -6.000]	330			
	8415002	LAUMONTITE	.174	[ 1.000]	150	[ 2.000]	30	[ 4.000]
				[ -8.000]	330			7
	8415003	WAIKAKITE	-4.686	[ 1.000]	150	[ 2.000]	30	[ 4.000]
				[ -8.000]	330	[ -2.000]	2	
	5023101	MALACHITE	-5.709	[ 2.000]	231	[ 2.000]	2	[ 1.000]
				[ -2.000]	330			1
	5023102	AZURITE	-10.459	[ 3.000]	231	[ 2.000]	2	[ 2.000]
				[ -2.000]	330			1
	7060006	PBHPO4	-5.819	[ 1.000]	600	[ 1.000]	580	[ 1.000]
	7060007	PB3(PO4)2	-6.163	[ 3.000]	600	[ 2.000]	580	
	2015000	LIME	-19.694	[ -2.000]	330	[ 1.000]	150	[ 1.000]
	2015001	PORTLANDITE	-9.020	[ -2.000]	330	[ 1.000]	150	[ 2.000]

2028000	WUSTITE	.735	[ -2.000]	330	[ .947]	280	[ 1.000]
2046001	PERICLASE	-7.175	[ -2.000]	330	[ 1.000]	460	[ 1.000]
3028001	HERCYNITE	4.768	[ -8.000]	330	[ 1.000]	280	[ 2.000]
			[ 4.000]	2			
3046000	SPINEL	-2.181	[ -8.000]	330	[ 1.000]	460	[ 2.000]
			[ 4.000]	2			
8215002	WOLLASTONITE	-3.947	[ -1.000]	2	[ -2.000]	330	[ 1.000]
			[ 1.000]	150			7

ID #	NAME	Sat. Index	Stoichiometry in [brackets]					
8215003	P-WOLLSTANIT	-4.853	[ -1.000]	2	[ -2.000]	330	[ 1.000]	7
			[ 1.000]	150				
8015001	CA-OLIVINE	-15.105	[ -4.000]	330	[ 1.000]	770	[ 2.000]	1
8015002	LARNITE	-16.687	[ -4.000]	330	[ 1.000]	770	[ 2.000]	1
8015007	CA3SIO5	-38.410	[ -6.000]	330	[ 1.000]	770	[ 3.000]	1
			[ 1.000]	2				
8015003	MONTICELLITE	-6.668	[ -4.000]	330	[ 1.000]	770	[ 1.000]	1
			[ 1.000]	460				
8015005	AKERMINITE	-15.086	[ -1.000]	2	[ -6.000]	330	[ 2.000]	7
			[ 2.000]	150	[ 1.000]	460		
8015004	MERWINITE	-22.501	[ -8.000]	330	[ 2.000]	770	[ 1.000]	4
			[ 3.000]	150				
8441000	KALSILITE	-1.589	[ -4.000]	330	[ 1.000]	770	[ 1.000]	
			[ 1.000]	410				
8441001	LEUCITE	.065	[ -2.000]	2	[ -4.000]	330	[ 2.000]	7
			[ 1.000]	30	[ 1.000]	410		
8441002	MICROCLINE	1.215	[ -4.000]	2	[ -4.000]	330	[ 3.000]	7
			[ 1.000]	30	[ 1.000]	410		
8441003	H SANIDINE	.700	[ -4.000]	2	[ -4.000]	330	[ 3.000]	7
			[ 1.000]	30	[ 1.000]	410		
8450004	NEPHELINE	-2.185	[ -4.000]	330	[ 1.000]	770	[ 1.000]	
			[ 1.000]	500				
8015006	GEHLENITE	-14.761	[ -10.000]	330	[ 2.000]	30	[ 1.000]	7
			[ 2.000]	150	[ 3.000]	2		

7.5 APPENDIX 5: Total elemental concentrations for the sediment samples determined by x-ray fluorescence spectrometry

Table 1: Major element concentrations determined for the grab samples ( in weight percent).

Sample No.	SiO <sub>2</sub>	TiO <sub>2</sub>	Al <sub>2</sub> O <sub>3</sub>	Fe <sub>2</sub> O <sub>3</sub>	MnO	MgO	CaO	Na <sub>2</sub> O	K <sub>2</sub> O	P <sub>2</sub> O <sub>5</sub>	H <sub>2</sub> O	CO <sub>2</sub>	LOI <sup>1</sup>
Harts River	68.46	0.559	9.10	4.39	0.046	2.39	1.89	0.48	1.25	0.070	0.77	1.1	9.8
Leeupan (top)	46.91	0.508	10.06	5.64	0.087	6.58	7.74	1.98	2.07	0.090	0.96	7.2	9.5
Leeupan (bottom)	26.22	0.203	3.66	2.17	0.067	15.3	18.67	1.89	0.36	0.081	-0.46	21.8	10.5
2	83.86	0.355	4.33	2.04	0.022	0.64	3.42	1.42	0.55	0.038	-0.09	0.9	3.5
4	78.40	0.258	3.25	1.64	0.025	1.83	5.46	0.47	0.63	0.074	-0.33	4.3	3.2
5	67.04	0.528	7.69	4.78	0.057	1.70	8.36	0.97	0.74	0.110	-0.11	4.2	4.1
7	43.75	0.582	12.10	5.93	0.077	4.51	8.19	0.43	1.43	0.169	1.15	5.1	16.7
8	63.72	0.437	5.90	3.01	0.049	2.07	9.11	0.58	0.88	0.086	-0.12	6.5	7.7
9	43.41	0.584	12.13	5.98	0.081	4.82	8.55	0.51	1.45	0.163	0.11	6.0	16.3
10 (coarse)	32.07	0.138	1.77	1.52	0.114	1.64	33.17	0.14	0.33	0.078	-0.06	24.7	3.8
10 (fine)	73.82	0.320	3.00	2.11	0.048	0.94	10.0	0.56	0.52	0.054	0.02	7.5	1.56
16	44.06	0.592	12.40	6.07	0.076	4.43	8.04	0.43	1.42	0.174	-0.47	6.3	16.7
17	73.97	0.372	4.24	2.11	0.035	1.33	6.98	0.81	0.81	0.054	-0.11	2.7	7.0

Explanatory Notes for Table 1: <sup>1</sup> - LOI = Loss on Ignition at 1050°C - CO<sub>2</sub>

**Table 2:** Ca and K are in weight percent and trace element concentrations determined for the grab samples (in mg.kg<sup>-1</sup>).

Sample No.	Ca	K	Co	Mn	Cr	V	Mo	Nb	Zr	Y	Sr	U	Rb	Th	Pb	Zn
Harts River	1.35	1.04	16.0	403	148.7	87.9	0.6	9.3	220	17	83	1.9	58	5.9	14	57.7
Lecupan (top)	5.53	1.72	17.6	693	124.2	87.9	0.7	7.9	115	14	311	1.9	75	6.9	8.7	66.1
Lecupan (bottom)	13.35	0.30	9.1	501	57.0	46.2	<0.5	2.8	56	5.8	483	5.1	29	2.6	4	25.8
2	2.45	0.46	7.0	170	52.5	48	0.7	3.7	186	10	296	1.7	17	2.5	4.4	12.9
4	3.9	0.52	5.5	226	54.0	38.1	<0.5	3.6	179	8	212	<1.2	22	2.2	3.3	16.9
5	5.97	0.61	14.0	446	80.8	98.3	0.7	4.2	163	16	951	<1.4	24	<2.0	7.7	28.0
7	5.85	1.19	14.9	596	154.6	102.3	1.3	9.1	112	18	188	2	72	8.3	12	67.0
8	6.51	0.73	11.6	394	73.2	62.7	0.8	5.6	154	12	277	<1.3	35	3.7	6	29.0
9	6.12	1.20	15.5	633	155.9	104.4	0.9	8.7	108	18	204	2.3	73	6.9	11	66.68
10 (coarse)	23.71	0.28	4.2	868	22.2	38.0	0.6	1.5	41	10	347	<1.6	8.8	<2.2	4	7.3
10 (fine)	7.15	0.43	5.9	364	30.5	43.3	0.8	2.8	115	9.9	403	<1.3	15	2.9	5.5	9.4
16	5.756	1.18	15.9	598	157.3	102.5	0.9	8.8	107	18	177	<1.3	72	6.4	12	68.3
17	4.99	0.67	7.0	262	48.4	40.0	0.25	4.9	225	9.9	212	1.89	28	3.1	5.1	17.3

**Table 2 continued:** Trace element concentrations determined for the grab samples (in mg.kg<sup>-1</sup>; S concentrations in weight percent).

Sample No.	Cu	Ni	S (Wt. %)
Harts River	30.6	50.2	0.14
Leeupan (top)	38.4	73.4	0.22
Leeupan (bottom)	19.3	32.7	0.2
2	11.6	22.6	0.07
4	10.4	18.3	0.07
5	22.2	49.3	0.18
7	37.4	72.6	0.26
8	19.5	39.2	0.22
9	36.6	71.0	0.30
10 (coarse)	11.3	11.9	0.06
10 (fine)	9.9	15.0	0.05
16	35.3	73.3	0.27
17	13.2	21.4	0.09

**Table 3:** Major element concentrations determined for core sample 4 (in weight percent).

Sample No.	SiO <sub>2</sub>	TiO <sub>2</sub>	Al <sub>2</sub> O <sub>3</sub>	Fe <sub>2</sub> O <sub>3</sub>	MnO	MgO	CaO	Na <sub>2</sub> O	K <sub>2</sub> O	P <sub>2</sub> O <sub>5</sub>	H <sub>2</sub> O	LOI <sup>1</sup>
4a	49.30	0.526	10.33	5.32	0.066	4.13	7.54	0.43	1.18	0.157	1.94	19.43
4b	51.29	0.559	10.79	5.47	0.070	4.02	7.81	0.44	1.25	0.147	0.80	17.48
4c	48.54	0.632	12.69	6.26	0.076	4.09	6.78	0.50	1.35	0.137	1.41	17.84
4d	49.07	0.635	12.61	6.40	0.083	4.30	5.59	0.65	1.39	0.110	2.03	17.36
4e	52.17	0.651	13.02	6.52	0.074	4.33	5.06	0.82	1.47	0.090	1.74	14.36
4f	54.89	0.461	8.74	4.51	0.062	6.25	7.77	0.55	1.65	0.090	0.42	14.69

<sup>1</sup> Explanatory Notes for Table 3: <sup>1</sup> - LOI = Loss on Ignition at 1050°C - CO<sub>2</sub>

**Table 4:** Ca and K in weight percent and trace element concentrations determined for core sample 4 ( in mg.kg<sup>-1</sup>).

Sample No.	Ca	K	Co	Mn	Cr	V	Mo	Nb	Zr	Y	Sr	U	Rb	Th	Pb	Zn
4a	5.39	0.98	14.4	520.5	137.4	89.63	0.98	8.2	133.6	16.2	189.1	1.89	63.3	6.8	32.9	62.7
4b	5.58	1.04	15.6	553.7	141.2	96.5	1.03	8.4	139.3	17.6	183.8	<1.2	65.9	6.9	30.5	65.8
4c	4.85	1.12	17.0	603.1	165.0	108.0	0.81	9.5	128.7	18.9	158.2	1.51	74.7	8.1	37.6	75.4
4d	4.0	1.15	17.9	645.6	175.9	106.0	1.18	10.2	131.4	18.6	136.3	<1.2	73.9	7.1	55.7	77.2
4e	3.61	1.22	16.9	573.6	181.7	112.0	1.21	10.6	143.3	19.2	138.1	<1.2	75.2	8.6	39.0	78.0
4f	5.55	1.37	12.4	525.4	125.5	90.6	0.63	7.1	124.2	13.9	215.9	1.76	58.5	6.2	11.8	56.1

**Table 4 continued:** Trace element concentrations determined for core sample 4 ( in mg.kg<sup>-1</sup>; S concentrations in weight percent).

Sample No.	Cu	Ni	S (Wt. %)
4a	35.6	68.7	0.27
4b	36.4	70.8	0.27
4c	38.8	80.2	0.2
4d	39.6	77.3	0.28
4e	36.8	73.9	0.46
4f	28.1	54.4	0.21

**7.6 APPENDIX 6: Results of organic carbon and carbonate determinations in the sediment samples**

**Table 1:** Percent organic carbon and carbonate determined in the grab samples.

Sample No.	% CaCO <sub>3</sub> per g sample	% Organic Carbon
Harts River	2.5	2.6
Leeupan (top)	16.4	1.4
Leeupan (bottom)	49.6	0.3
2	2.0	0.7
4	9.7	0.7
5	9.5	1.3
7	11.5	2.6
8	14.8	2.8
9	14.6	3.0
10 (coarse)	56.2	0.4
10 (fine)	17.0	
16	14.4	3.7
17	6.2	1.4

**Table 2:** Percent carbonate determined in core sample 4. Organic carbon was not determined.

Sample No.	% CaCO <sub>3</sub> per g sample
4a	18.0
4b	14.0
4c	11.0
4d	9.8
4e	8.9
4f	14.0

7.7 APPENDIX 7: Correlation matrix for XRFs grab sample data. Only significant correlations are tabulated (figures in bold;  $P < 0.0001$ ; underlined:  $P < 0.001$ ; normal font:  $P < .01$ . In all cases  $n = 13$ ).

	Si	Ti	Al	Fe	Mn	Mg	Ca	Na	K	P	Co	Cr	V	Mo	Nb	Zr	Y	Rb	Th	Pb	Zn	Cu	Ni		
Ti		<b>1</b>																							
Al		<b>.93</b>	<b>1</b>																						
Fe		<b>.91</b>	<b>.98</b>	<b>1</b>																					
Mn	<b>-.87</b>				<b>1</b>																				
Mg	<b>-.71</b>					<b>1</b>																			
Ca	<b>-.66</b>		<b>-.64</b>		<b>.69</b>		<b>1</b>																		
Na					<b>.59</b>			<b>1</b>																	
K		<b>.80</b>	<b>.86</b>	<b>.86</b>					<b>1</b>																
P		<b>.64</b>	<b>.83</b>	<b>.82</b>				<b>.57</b>		<b>1</b>															
Co		<b>.89</b>	<b>.93</b>	<b>.94</b>				<b>.87</b>	<b>.66</b>	<b>.66</b>	<b>1</b>														
Cr		<b>.89</b>	<b>.97</b>	<b>.93</b>				<b>.85</b>	<b>.77</b>	<b>.92</b>	<b>1</b>														
V		<b>.92</b>	<b>.96</b>	<b>.98</b>				<b>.77</b>	<b>.81</b>	<b>.94</b>	<b>.91</b>	<b>1</b>													
Mo		<b>.64</b>	<b>.67</b>	<b>.68</b>				<b>.66</b>	<b>.66</b>	<b>.58</b>	<b>.58</b>	<b>.68</b>	<b>1</b>												
Nb		<b>.90</b>	<b>.94</b>	<b>.87</b>				<b>.89</b>	<b>.66</b>	<b>.97</b>	<b>.97</b>	<b>.84</b>	<b>.56</b>	<b>1</b>											
Zr	<b>.84</b>				<b>-.80</b>		<b>-.78</b>								<b>1</b>										
Y		<b>.92</b>	<b>.91</b>	<b>.91</b>				<b>.74</b>	<b>.75</b>	<b>.84</b>	<b>.88</b>	<b>.94</b>	<b>.74</b>	<b>.85</b>	<b>1</b>										
Rb		<b>.82</b>	<b>.94</b>	<b>.91</b>				<b>.93</b>	<b>.74</b>	<b>.89</b>	<b>.88</b>	<b>.83</b>	<b>.95</b>	<b>.95</b>	<b>.77</b>	<b>1</b>									
Th		<b>.72</b>	<b>.85</b>	<b>.80</b>				<b>.87</b>	<b>.67</b>	<b>.75</b>	<b>.94</b>	<b>.71</b>	<b>.64</b>	<b>.90</b>	<b>.90</b>	<b>.72</b>	<b>.94</b>	<b>1</b>							
Pb		<b>.88</b>	<b>.90</b>	<b>.87</b>				<b>.76</b>	<b>.67</b>	<b>.86</b>	<b>.98</b>	<b>.88</b>	<b>.62</b>	<b>.92</b>	<b>.92</b>	<b>.85</b>	<b>.81</b>	<b>1</b>							
Zn		<b>.84</b>	<b>.96</b>	<b>.94</b>				<b>.91</b>	<b>.77</b>	<b>.93</b>	<b>.95</b>	<b>.89</b>	<b>.57</b>	<b>.95</b>	<b>.82</b>	<b>.99</b>	<b>.91</b>	<b>.89</b>	<b>1</b>						
Cu		<b>.83</b>	<b>.96</b>	<b>.96</b>				<b>.90</b>	<b>.78</b>	<b>.95</b>	<b>.94</b>	<b>.91</b>	<b>.59</b>	<b>.90</b>	<b>.82</b>	<b>.97</b>	<b>.88</b>	<b>.86</b>	<b>.99</b>	<b>1</b>					
Ni		<b>.87</b>	<b>.97</b>	<b>.98</b>				<b>.89</b>	<b>.81</b>	<b>.95</b>	<b>.81</b>	<b>.94</b>	<b>.62</b>	<b>.88</b>	<b>.84</b>	<b>.95</b>	<b>.83</b>	<b>.83</b>	<b>.97</b>	<b>.98</b>	<b>1</b>				
S		<b>.71</b>	<b>.85</b>	<b>.85</b>				<b>.68</b>	<b>.85</b>	<b>.84</b>	<b>.81</b>	<b>.82</b>		<b>.73</b>	<b>.67</b>	<b>.83</b>	<b>.70</b>	<b>.65</b>	<b>.85</b>	<b>.87</b>	<b>0.90</b>	<b>1</b>			
CO <sub>2</sub>	<b>-.75</b>	<b>-.65</b>			<b>.65</b>		<b>.95</b>																	<b>1</b>	
OrgM	<b>.79</b>	<b>.78</b>	<b>.71</b>	<b>.71</b>				<b>.68</b>	<b>.58</b>	<b>.83</b>	<b>.79</b>	<b>.69</b>		<b>.85</b>	<b>.78</b>	<b>.75</b>	<b>.71</b>	<b>.81</b>	<b>.74</b>	<b>.69</b>	<b>.67</b>			<b>1</b>	

**7.8 APPENDIX 8: Instrumental parameters and data quality for routine major and trace element determinations by WDXRFS.**



**DEPARTMENT OF GEOLOGICAL SCIENCES**  
**UNIVERSITY OF CAPE TOWN**

---

**INSTRUMENTAL PARAMETERS AND DATA  
QUALITY FOR ROUTINE MAJOR AND TRACE  
ELEMENT DETERMINATIONS BY WDXRFS**

**J P WILLIS**

---

**INFORMATION CIRCULAR No. 14**

## MAJOR ELEMENTS

Nine major elements, Fe, Mn, Ti, Ca, K, P, Si, Al and Mg (with Ni and Cr when Ni and Cr concentrations exceed ~2000 ppm) are determined using fusion disks prepared according to the method of Norrish and Hutton (1969). The disks are analyzed on a Philips PW1480 wavelength dispersive XRF spectrometer with a Mo/Sc x-ray tube. Fe, Mn and Ti are measured with the tube at 100 kV, 25 mA. The other elements are determined with the tube at 40 kV, 65 mA. Peak only measurements are made on the elements Fe through Mg. Sodium is determined using powder briquettes, the x-ray tube at 40 kV, 65 mA, and with backgrounds measured at  $-2.00$  and  $+2.00^\circ 2\theta$  from the peak position. Analytical conditions are given in Table 1.

Fusion disks made up with 100% Johnson Matthey Specpure  $\text{SiO}_2$  are used as blanks for all elements except Si. Fusion disks made up from mixtures of Johnson Matthey Specpure  $\text{Fe}_2\text{O}_3$  and  $\text{CaCO}_3$  are used as blanks for Si. Intensity data are collected using the Philips X40 software. Matrix corrections are made on the elements Fe through Mg using the de Jongh model in the X40 software. Theoretical alpha coefficients used in the de Jongh model for all other elements on the analyte element are calculated using the Philips on-line ALPHAS programme.  $\text{Na}_2\text{O}$  is not included in the matrix corrections in de Jongh model, and no matrix corrections are made to the sodium intensities.

**Table 1. Analytical conditions for determination of major elements using a Philips PW1480 WDXRF spectrometer.**

Element/line	Collimator	Crystal	Detector	PHS LWL UPL	Counting time (s)	Concentration range *	RMS	No. of standards
FeK $\alpha$	F	LiF(220)	FL	16 70	150	0 - 17	0.118	14
MnK $\alpha$	F	LiF(220)	FL	15 70	150	0 - 0.22	0.005	14
TiK $\alpha$	F	LiF(200)	FL	28 70	150	0 - 2.75	0.020	14
CaK $\alpha$	F	LiF(200)	FL	36 70	20	0 - 12.5	0.037	14
K K $\alpha$	F	LiF(200)	FL	36 70	50	0 - 15.5	0.057	14
P K $\alpha$	C	GE(111)	FL	25 75	100	0 - 0.36	0.008	14
SiK $\alpha$	C	PE(002)	FL	32 74	100	0 - 100	0.408	14
AlK $\alpha$	C	PE(002)	FL	25 75	80	0 - 17.5	0.136	14
MgK $\alpha$	F	PX-1	FL	30 74	150	0 - 46	0.095	14
NaK $\alpha$	F	PX-1	FL	30 78	200	0 - 9	0.189	15

\* = all concentrations expressed as wt% oxide

$$RMS = \sqrt{\frac{1}{n - k} \sum (Conc_{given} - Conc_{calc})^2}$$

where

- n = no. of standards  
 k = no. of calibration coefficients, *i.e.* 2, the slope and intercept of the calibration line.  
 Conc<sub>given</sub> = recommended concentration for an element in a standard

$\text{Conc}_{\text{calc}}$  = concentration of an element calculated from the best-fit calibration line

First order calibration lines, with intercept, are calculated using all data points, including blanks. Calibration plots for  $\text{Fe}_2\text{O}_3$ ,  $\text{CaO}$ ,  $\text{SiO}_2$  and  $\text{MgO}$  are given in Figures 1 - 4.

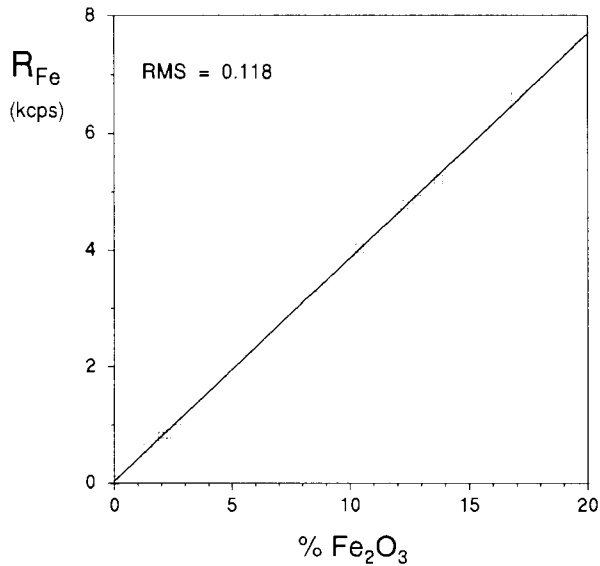


Figure 2. Calibration plot for  $\text{Fe}_2\text{O}_3$  using "Norrish" fusion disks.

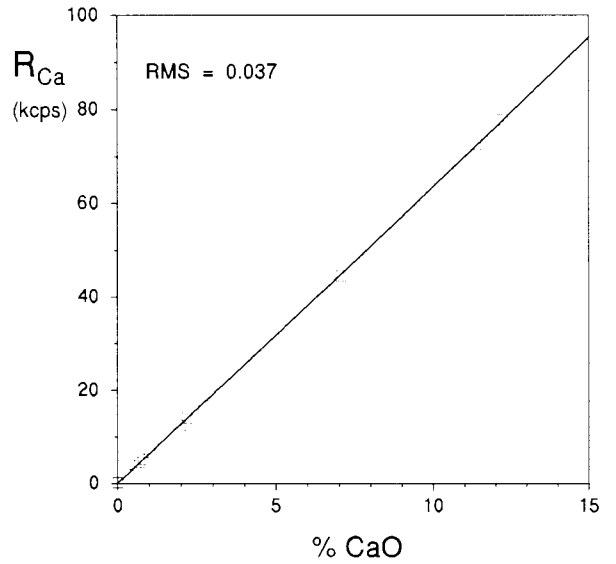


Figure 3. Calibration plot for  $\text{CaO}$  using "Norrish" fusion disks.

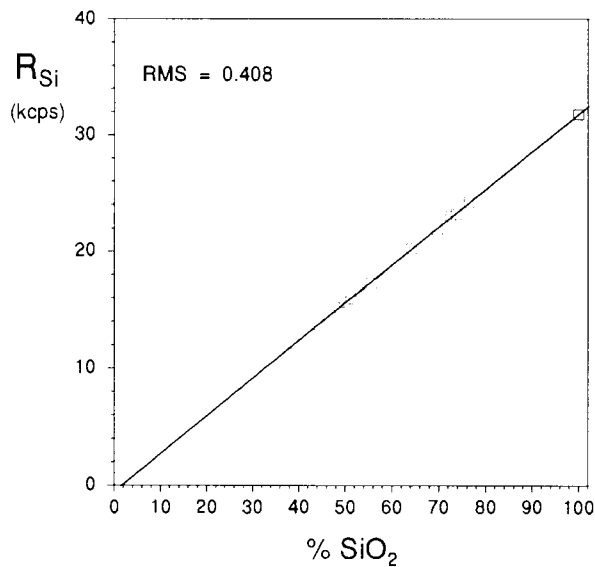


Figure 4. Calibration plot for  $\text{SiO}_2$  using "Norrish" fusion disks.

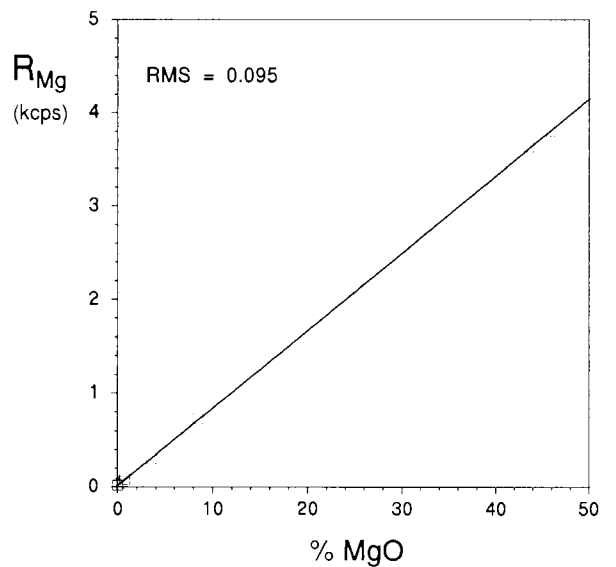


Figure 5. Calibration plot for  $\text{MgO}$  using "Norrish" fusion disks.

## TRACE ELEMENTS

Trace elements are determined on powder briquettes using a series of x-ray tubes. Analytical conditions are listed in Tables 2 and 3.

**Table 2. X-ray tubes and tube and x-ray path settings for the determination of trace elements using a Siemens SRS303AS and Philips PW1480 WDXRF spectrometer.**

Spectrometer	Element/line	X-ray tube		X-ray path
		Target	kV - mA	
SRS303AS	RhK $\alpha$ C	Rh	60 45	Vacuum
SRS303AS	MoK $\alpha$	Rh	60 45	Vacuum
SRS303AS	NbK $\alpha$	Rh	60 45	Vacuum
SRS303AS	ZrK $\alpha$	Rh	60 45	Vacuum
SRS303AS	Y K $\alpha$	Rh	60 45	Vacuum
SRS303AS	SrK $\alpha$	Rh	60 45	Vacuum
SRS303AS	U L $\alpha_1$	Rh	60 45	Vacuum
SRS303AS	RbK $\alpha$	Rh	60 45	Vacuum
SRS303AS	ThL $\alpha_1$	Rh	60 45	Vacuum
SRS303AS	PbL $\beta_1$	Rh	60 45	Vacuum
PW1480	ZnK $\alpha$	Au	60 45	Vacuum
PW1480	CuK $\alpha$	Au	60 45	Vacuum
PW1480	NiK $\alpha$	Au	60 45	Vacuum
PW1480	CoK $\alpha$	W	50 55	Vacuum
PW1480	MnK $\alpha$	W	50 55	Vacuum
PW1480	CrK $\alpha$	W	50 55	Vacuum
PW1480	V K $\alpha$	W	50 55	Vacuum
PW1480	BaL $\alpha_1$	Cr	50 55	Vacuum
PW1480	ScK $\alpha$	Cr	50 55	Vacuum

**Table 3. Instrumental conditions for determination of trace elements using a Siemens SRS303AS and Philips PW1480 WDXRF spectrometer.**

Element /line	Collimator	Crystal	Detector	PHS		Counting time (s)	Background position(s) relative to peak position		Concentration range *
				LWL	UPL				
RhK $\alpha$ C	F	LiF(220)	SC	0.6	1.5	200			
MoK $\alpha$	F	LiF(200)	SC	0.7	1.7	160	-0.8	+0.65	0 - 5.2
NbK $\alpha$	F	LiF(200)	SC	0.5	1.6	160			0 - 268
ZrK $\alpha$	F	LiF(200)	SC	0.5	1.6	160			0 - 1210
Y K $\alpha$	F	LiF(200)	SC	0.5	1.6	160	-0.61	+0.54	0 - 143
SrK $\alpha$	F	LiF(200)	SC	0.5	1.6	160	+0.60		0 - 440
U L $\alpha_1$	F	LiF(200)	SC	0.5	1.6	160			0 - 15
RbK $\alpha$	F	LiF(200)	SC	0.5	1.6	160	+0.53		0 - 530
ThL $\alpha_1$	F	LiF(200)	SC	0.5	1.6	160			0 - 51
PbL $\beta_1$	F	LiF(200)	SC	0.4	1.4	160	+1.27		0 - 40
ZnK $\alpha$	F	LiF(220)	FS	20	80	200	-1.08	+4.24	0 - 235
CuK $\alpha$	F	LiF(220)	FS	20	80	200	+4.44		0 - 227
NiK $\alpha$	F	LiF(220)	FS	20	80	200	+2.52		0 - 630
CoK $\alpha$	F	LiF(220)	FL	15	75	200	+1.00		0 - 116
MnK $\alpha$	F	LiF(220)	FL	15	75	200	-2.30	+4.70	0 - 1700
CrK $\alpha$	F	LiF(220)	FL	15	75	200	-4.10	+2.90	0 - 465
V K $\alpha$	F	LiF(220)	FL	13	67	200	+3.40		0 - 640
BaL $\alpha_1$	F	LiF(200)	FL	25	75	200	-5.20		0 - 2680
ScK $\alpha$	F	LiF(200)	FL	25	75	200	-2.78		0 - 54

\* = all concentrations expressed as part per million (ppm or mg.kg<sup>-1</sup>)

The RhK $\alpha$  Compton peak is used to determine the mass absorption coefficients of the specimens at the RhK $\alpha$ C wavelength (Figure 5) and the calculated values are used to correct for absorption effects on the Mo, Nb, Zr, Y, Sr, U, Rb, Th, Pb, Zn, Cu and Ni analyte wavelengths. Primary and secondary mass absorption coefficients for the Co, Mn, Cr, V, Ba and Sc analyte wavelengths are calculated from major element compositions using the tables of Heinrich (1986). Mass absorption coefficient corrections are made to the net peak intensities, (gross peak intensities corrected for dead time losses, background and spectral overlap), to correct for absorption differences between standards and specimens. No corrections are made for enhancement, which could be small but significant (<~5% relative) for the elements Cr, V, Ba and Sc in certain specimens, depending on their concentrations of Fe, Mn and Ti.

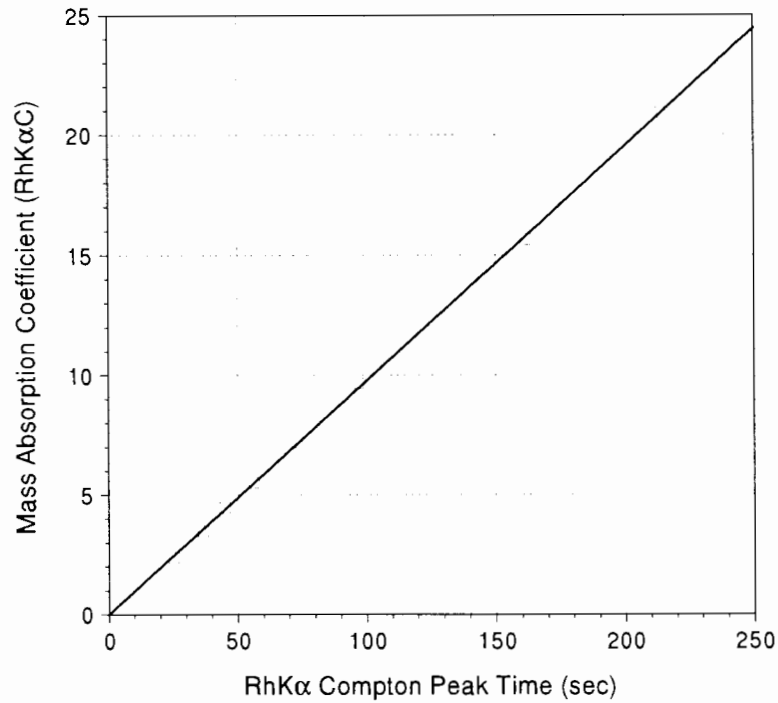


**Figure 5. Calibration line for determination of mass absorption coefficients at the RhK $\alpha$ C wavelength. RhK $\alpha$ C peak time is the time required to accumulate 400 000 counts on the RhK $\alpha$ C peak using the fixed count method.**

Measured intensity data are processed through the computer program TRACE to correct gross peak intensities for background and spectral overlap and to make mass absorption coefficient corrections according to the methods outlined in Duncan *et al.* (1984). First order calibration lines with zero intercept are calculated using six or more international rock standard reference materials (SRMs) for each element. The one standard deviation ( $1\sigma$ ) error due to counting statistics and the lower limit of detection is calculated for each element in each specimen.

Table 4 lists the given and calculated concentrations for selected elements in a number of rock SRMs, which gives an indication of the accuracy of the trace element data. Table 5 lists the one standard deviation counting error and lower limit of detection for each of the elements in an acidic (low Fe, Ca and Mg, high Si) rock and in a mafic (high Fe, Ca and Mg, low Si) rock. Because of the difference in mass absorption coefficients between the two types of specimen the counting error and lower limit of detection will be slightly higher in mafic rock specimens. The two examples given cover the range of mass absorption coefficients found in the majority of geological rock, soil and sediment specimens.

The counting error and lower limit of detection are calculated using the following formulae:

$$1\sigma \text{ error (in ppm)} = \text{Conc} \times \frac{\sqrt{\frac{I_p}{T_p} + \frac{I_b}{T_b}}}{I_n}$$

and

$$LLD \text{ (in ppm)} = \frac{6}{m} \sqrt{\frac{I_b}{T_{total}}}$$

where Conc = calculated concentration in ppm

$m$	=	net peak / concentration
$I_p$	=	gross peak count rate in cps
$I_b$	=	background count rate under the peak in cps
$I_n$	=	$I_p - I_b$ = true <b>net</b> peak count rate in cps
$T_p$	=	counting time for peak in seconds
$T_b$	=	total counting time for background in seconds
$T_{total}$	=	$T_p + T_b$

N.B.  $I_b$  is the calculated background *plus* any corrections for spectral interference, and is equal to  $I_p - I_n$

**Table 4. Given and calculated trace element data (all values in ppm) for some rock SRMs.**

Element	QLO-1		BHVO-1		W-2		STM-1		BIR-1	
	Given	Calc	Given	Calc	Given	Calc	Given	Calc	Given	Calc
Mo	2.6	3.5	1.0	0.8	(0.6	0.5	5.2	3.1	(0.5	<0.8
Nb	10	11	19	19	7.9	7.4	268	267	0.6	0.9
Zr	185	190	179	181	94	95	1210	1220	16	19
Y	24	25	28	28	24	23	46	47	16	17
Sr	336	329	403	395	194	195	700	689	108	109
U	1.9	2.3	0.4	<1.6	0.5	<1.2	9.1	8.8	0.01	<1.2
Rb	74	71	11	9.7	20	20	118	114	0.3	<0.6
Th	4.5	4.0	1.1	1.8	2.2	2.7	31	31	0.03	<1.5
Pb	20	20	2.6	3.1	9.3	8.5	18	17	3	3.1
Zn	61	61	105	106	77	79	235	242	71	69
Cu	29	25	136	139	103	108	(4.6	2.1	126	132
Ni	(5.8	1.8	121	127	70	72	(3	1.7	166	170
Co	7.2	7.6	45	44	44	43	0.9	<1.9	51	52
Mn	720	690	1300	1290	1260	1240	1700	1600	1320	1280
Cr	(3.2	3.6	289	312	93	100	(4.3	3.2	382	404
V	54	44	317	314	262	257	(8.7	<1.6	313	306
Ba	1370	1430	139	138	182	191	560	589	7.0	10
Sc	8.9	10.3	31.8	33.9	35	36	0.6	0.5	44	39

(n.n = value given for information only

**Table 5.** Calculated trace element data,  $1\sigma$  counting error and lower limit of detection (all values in ppm) for two rock specimens having different mass absorption coefficients.

Element	Leeupan (bottom)			Sediment 8		
	Calc	$1\sigma$	LLD	Calc	$1\sigma$	LLD
Mo	0.28	0.2	0.5	0.84	0.2	0.5
Nb	2.8	0.2	0.6	5.6	0.2	0.6
Zr	56	0.3	0.8	154	0.3	0.7
Y	5.8	0.3	0.8	12.5	0.3	0.7
Sr	483	0.5	0.7	277	0.4	0.7
U	5.6	0.5	1.4	0.6	0.4	1.3
Rb	28.8	0.3	0.8	34.9	0.3	0.7
Th	2.6	0.6	1.9	3.7	0.6	1.8
Pb	4.0	0.8	2.3	6	0.7	2.2
Zn	25.8	0.2	0.6	29.4	0.2	0.6
Cu	19.3	0.3	0.8	19.5	0.3	0.8
Ni	32.7	0.4	0.9	39.2	0.4	0.9
Co	8.8	0.5	1.5	12.8	0.6	1.6
Mn	500	1.36	1.4	408	1.2	1.5
Cr	46.6	0.5	1.2	62.6	0.6	1.2
V	43	0.7	1.6	56.7	0.8	1.8
Ba						
Sc						

## REFERENCES

- Duncan, A R, Erlank, A J and Betton, P J (1984) Analytical techniques and database descriptions. *Spec. Publ. geol. Soc. S. Afr.*, **13**, Appendix 1, 389-395.
- Heinrich, K F J (1986) Mass absorption coefficients for electron probe microanalysis. In: *Proc. 11th Int. Congress on X-ray Optics and Microanalysis, London, Canada*, J B Brown and R H Packwood (Eds).